

1990

## Beach Forms Induced by Coastal Structures Forming Embayments in Fetch-Limited Environments

Jian Hua Li

*College of William and Mary - Virginia Institute of Marine Science*

Follow this and additional works at: <https://scholarworks.wm.edu/etd>



Part of the [Ocean Engineering Commons](#), and the [Oceanography Commons](#)

---

### Recommended Citation

Li, Jian Hua, "Beach Forms Induced by Coastal Structures Forming Embayments in Fetch-Limited Environments" (1990). *Dissertations, Theses, and Masters Projects*. Paper 1539617617.

<https://dx.doi.org/doi:10.25773/v5-ys6f-4f09>

This Thesis is brought to you for free and open access by the Theses, Dissertations, & Master Projects at W&M ScholarWorks. It has been accepted for inclusion in Dissertations, Theses, and Masters Projects by an authorized administrator of W&M ScholarWorks. For more information, please contact [scholarworks@wm.edu](mailto:scholarworks@wm.edu).

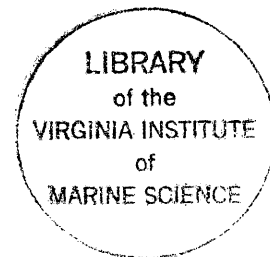
BEACH FORMS INDUCED BY COASTAL STRUCTURES  
FORMING EMBAYMENTS IN FETCH-LIMITED ENVIRONMENTS

A Thesis

Presented to  
The Faculty of the School of Marine Science  
The College of William and Mary in Virginia

In Partial Fulfillment  
of the Requirements for the Degree of  
Master of Arts

by  
Jian Hua Li  
August, 1990



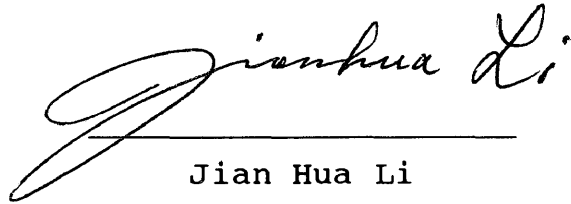
APPROVAL SHEET

This thesis is submitted in partial fulfillment


of

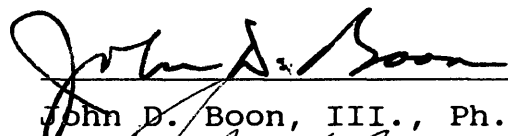
the requirements for the degree of

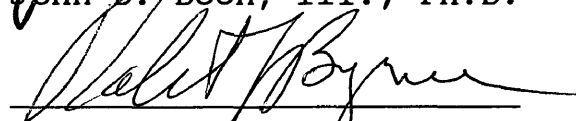
master of arts in Marine Science

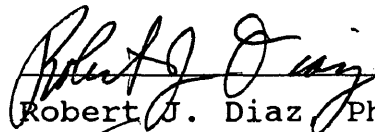
  
\_\_\_\_\_  
Jian Hua Li

Approved, August 1990

  
\_\_\_\_\_  
L. Donelson Wright, Ph.D.  
Committee Chairman/Advisor

  
\_\_\_\_\_  
John D. Boon, III., Ph.D.

  
\_\_\_\_\_  
Robert J. Byrne, Ph.D.

  
\_\_\_\_\_  
Robert J. Diaz, Ph.D.

  
\_\_\_\_\_  
Evon P. Ruzecki, Ph.D.

## DEDICATION

This thesis is dedicated to my wife

## CONTENTS

Acknowledgement.....	v
List of tables.....	vi
List of figures.....	vii
List of symbols.....	ix
Abstract.....	xi
1. Introduction.....	2
2. General background.....	7
2.1. Major previous studies on profiles.....	7
2.2. A brief review on plan beach form models.....	14
3. Data and Methodology.....	21
3.1. Surveys and data sets on beach profiles and photography.....	21
3.2. Data sets on plan-view beach forms.....	28
3.3. Sediment data.....	29
3.4. Methods of wave hindcasting.....	29
3.5. Methods on wave refraction and diffraction.....	32
4. Field site descriptions.....	36
5. Results of profile and sediment analysis.....	44
5.1. Results of field profile measurements.....	44
5.2. Sediment characteristics in the study area.....	60
6. Discussions and Conclusions - Profiles.....	63
6.1. The general characteristics.....	63
6.2. The mechanisms of profile development.....	71
6.3. Beach slope and sediments.....	77
6.4. Profile variations with seasons/wave climate.....	85
6.5. Sediment distributions along profiles.....	85
7. Results of plan-view beach form measurements.....	89
7.1. Circular bay beach forms.....	89
7.2. Spiral bay beach forms.....	93
7.3. Irregular bay beach forms.....	97
8. Discussions and conclusions - plan beach forms.....	99
8.1. General characteristics.....	99
8.2. Plan form and Wave refraction.....	101
8.3. Plan form and Wave diffraction.....	104
8.4. Wave reflection.....	108
9. Future study considerations.....	111
APPENDIX A: Calculations of A, m and $e_r$ .....	112
APPENDIX B: A few of examples of enlarged profiles.....	118
APPENDIX C: Results of bay measurements in Spring'90.....	126
APPENDIX D: Plots of field measured profiles.....	135
REFERENCES CITED.....	183
VITA .....	190

#### ACKNOWLEDGEMENTS

I would like to thank my major professor, Dr. L.D. Wright, for his continuing guidance during the past few years. Great thanks and appreciation are extended to all other members in my advisory committee for their help in this study.

Special thanks to C. Scott Hardaway and George Thomas for their very close corporation in all field data collection. This special thanks also go to Dr. E.P. Ruzecki and Dr. R.J. Diaz for their very careful english correction on the text of this thesis. Finally, thanks to all the others in the Division of Geological and Benthic Oceanography for their continuing friendship and support.

LIST OF TABLES

TABLE	PAGE
1.1. The average erosion rate at study sites.....	4
3.1. Profiling and aerial photography schedule.....	22
3.2. Profiling and aerial photography schedule.....	22
3.3. Wave predictions by various methods.....	31
5.1. Results of slope and sediment analysis.....	45
5.2. Sediment size distribution along bay beaches.....	61
6.1. Surf scaling parameters in the study area.....	69
<del>6.2.</del> Bank erosion history and beach fill.....	78
6.3. Field measured data and Sunamura's parameter.....	84
8.1. Summary table of beach forms.....	100

## LIST OF FIGURES

Figure	Page
1.1. Virginia Chesapeake Bay and its river system.....	5
2.1. Plan of spiral beach, Sandy hook, New Jersey.....	16
2.2. Logarithmic Spiral nomenclature (Yasso, 1965).....	16
2.3. Definition sketch of logarithmic spiral.....	16
2.4. Typical prototype bay showing refracted orthogonals.....	17
2.5. A mathematical simulation of spiral beaches.....	17
3.1. Feature profiling method.....	24
3.2 through 3.8. Base maps with numbered profiles.....	25-27
3.9. Wave diffraction diagram.....	35
4.1. Long term wind roses.....	43
5.1 through 5.17 Plots of beach profiles.....	46-59
6.1. Comparisons of different models.....	65
6.2. Comparisons of different models.....	66
6.3. Reflective beach profile.....	68
6.4. Comparisons of beach profiles.....	70
6.5. Beach slope prediction.....	80-83
6.6. The distribution pattern of sediments.....	87
7.1. Breakwater system and its embayments at CHP.....	90
7.2. Breakwater system and its embayments at HI2.....	90
7.3. Breakwater system and its embayments at DMF.....	91
7.4. Breakwater system and its embayments at WAL.....	91
7.5. Photo showing the breakwaters and embayments at WAL.....	92
7.6. The spiral bay at SUM.....	94
7.7. Photo showing the general spiral bay shape at SUM.....	94
7.8. Breakwater system and its embayments at NPS.....	95
7.9. Headlands and their bays at YTB.....	96
7.10. Photo showing the headlands and bays at YTB.....	96



List of figures continued:

7.11. Headlands and the plan beach forms at HIH.....	98
8.1. Wave refraction in waters with curved shorelines.....	103
8.2. Wave refraction in circular bay.....	105
8.3. Wave refraction in spiral bay.....	105
8.4. Wave diffraction diagram for SUM.....	107
8.5. Wave reflections from breakwaters.....	110

## LIST OF SYMBOLS

- A - Scale factor in Bruun-Dean's model.
- $a_1$  - Incident wave amplitude.
- $\alpha$  - (1). The angle between a radius vector and tangent for a given logspiral, a constant; (2). Wind direction in effective fetch calculation; (3). The angle between wave crest and respective depth contour (wave refraction).
- B - The vertical increase in water depth.
- $\beta_b$  - Nearshore slope angle seaward from breaking waves.
- C - Wave phase speed ( $C=L/T$ ).
- $C_o$  - Wave phase speed in deep water.
- $\epsilon$  - Wave reflectivity or surf-scaling parameter.
- E - Wave energy density.
- e - The base of Napierian logarithms.
- $e_r$  - Root-Mean-Square (RMS) error.
- D - Diameter of a sediment particle.
- $D_{50}$  - Median grain size.
- $D_e$  - The average wave energy dissipation rate.
- $F_g$  - Gravitational force parameter.
- $F_f$  - Fluid force.
- g - Gravitational acceleration.
- $H_b$  - Wave height at breaking.
- h - Water depth.
- $h_{bo}$  - Breaking depth before water level change.
- $h_b$  - Breaking depth after water level change.
- $h_s$  - The depth of effective motion of active profile.
- $h_{do}$  - The original dune height above mean sea level.
- $h_{bo}$  - The original breaking depth before water level rise.
- $H_d$  - Wave height in the region affected by wave diffraction.
- $H_i$  - Incident wave height unaffected by diffraction.
- $H_o$  - Wave height in deep water.
- $H_r$  - Reflected wave height.
- $h_s$  - Water depth at the tip of a spur (wave diffraction).

Symbol List Continued:

- $H_t$  - Transmitted wave height.
- $k$  - A constant relating wave height to water depth within fully developed surf zone ( $H_b/h_b=0.78$ ).
- $k'$  - Wave diffraction coefficient.
- $L$  - The active beach width; Wave length.
- $L_o$  - Wave length in deep water.
- $L_s$  - Width between wave rays.
- $M_1$  - Beach face slope ( $M_1=\tan\beta$ ).
- $M_2$  - Nearshore profile slope.
- $m$  - Shape factor in Bruun-Dean's model.
- $P$  - Percentage of compatible beach material; Wave energy flux.
- $Q$  - The quantity of total water transport.
- $Q_{sx}$  - The quantity of longshore sediment transport.
- $R$  - Shore retreat distance after water level rise.
- $r$  - The length of a radius vector from log spiral center.
- $d$  - Water mass density.
- $S$  - Local sea level.
- $T$  - Wave period.
  
- $\theta$  - The angle of a log-spiral radius.
- $\omega$  - Radial frequency ( $2\pi/T$ ).
- $U$  - Horizontal rate of change of profile.
- $\mu$  - A sand fraction ( refer to LeBlond 1972).
- $V$  - The rate of change of profile vertically.
- $X_f$  - Projected distance in effective fetch calculation.
- $X$  - Power of the spiral equation.
- $x$  - Distance waterward from beach.
- $k_r$  - Reflection coefficient.

## ABSTRACT

The present study is focused on the descriptions of beach forms in plan and profile around breakwaters and headlands in fetch-limited environments.

Profiles in the study area show a two-segment characteristic: The upper segment is the beach face, being best predicted by a linear model,  $h=M_1x$  or  $h=x\tan\beta_1$ , where  $h$  is water depth;  $M_1$  ( $\tan\beta_1$ ) is the beach face slope with an average value of 0.12;  $x$  is the distance waterward from upper beach berm. The lower segment is from beach toe waterward, being best predicted either by the formula:  $h=Ax^m+0.64$ , with an average of  $A$  of 0.56, and  $m$  of 0.15, or by a linear model,  $h=M_2x+0.11$  or  $h=x\tan\beta_2+0.11$ , with  $M_2=0.01$ , where  $M_2$  ( $\tan\beta_2$ ) is the lower profile slope.

Plan beach forms are generally recognized as four groups: 1). Circular bay beach forms; 2). Spiral bay beach forms; 3). Straight beach forms; 4). Irregular beach forms. Circular bay beach forms are commonly found at those sites of closely spaced breakwaters without significant seasonal storm waves incident obliquely from a particular direction. Spiral bay forms are related to headland construction and storm waves from particular oblique directions. Straight beach form is insignificant at the study sites, only a small section with straight form is found at one of the seven study sites.

BEACH FORMS INDUCED BY COASTAL STRUCTURES  
FORMING EMBAYMENTS IN FETCH-LIMITED ENVIRONMENTS

## 1. INTRODUCTION

Shoreline erosion widely occurs either due to natural forces or human intervention such as mining of beach materials, modification of inlets, and channel dredging. In order to reduce the shoreline recession and property losses, various methods of shoreline protection have been adopted like the construction of attached or detached breakwaters, headlands, beach nourishment, and combinations of structure and nourishment. In response to the construction of various structures in shoreline protection, a variety of beach forms are evolved: spiral bay beaches, circular bay beaches and tomboloes behind breakwaters. All of these beach forms and structures combine to protect the shoreline. Therefore, knowledge of beach forms around coastal structures would be helpful not only in the design of structure construction along beaches, but also in understanding beach processes in the vicinity of structures (structures refer to breakwaters and manmade headlands in all of the text below).

With the increasing utilization of shoreline protection measures described above, more and more private and public breakwaters or headlands have been constructed in recent years to stabilize shorelines. For example, more than 30 detached and attached breakwaters and headlands were installed in a section less than 20 kilometers, from Hog Island to Waltrip, in the James River within past five years. This

shoreline stabilization is achieved through the combination of structures and stabilized bay beaches between them. However, most of the stabilized bay beaches are not really "stable", i.e. not in a static equilibrium due to the time-varying situations of the overall dynamic state in the littoral zone. The equilibrium association between beaches, structures and natural forces is dynamically shifting from one state to another. Beach forms are always changing with time, especially with seasonal wave climate.

The study areas are located in the tributary systems of the lower Chesapeake Bay: the James, York, and Potomac Rivers. They are typical shallow, fetch limited, low energy environments with terraces of different widths. These river systems together with the main body of Chesapeake Bay are the products of late Pleistocene sea level rise that started approximately 15,000 - 18,000 years ago. The estuaries developed as drowned valleys of the old Susquehanna River valley systems as sea level rose into the bay basin systems nearly 10,000 years ago (Schubel et al., 1972). The topographic features of the youthful river valley systems are still retained such as the meandering outline, triangular cross-section, and the gradual widening to the mouth areas.

Shoreline erosion has been severe around Chesapeake Bay including the study areas. Byrne and Anderson (1977) indicated that over  $2.1 \times 10^8 \text{ m}^3$  material was eroded from only the Virginia portion of Chesapeake Bay between 1850 and 1950. Summarized results from various studies of erosion rates within Chesapeake Bay estimate a net loss of nearly 27,900 acres ( $1.1 \times 10^8 \text{ m}^2$ ) over the same period. The sand derived from this erosion is the primary source for the estuarine beaches. The flank

areas and channels receive most of the silt and clay fractions (Hobbs, Byrne, et. al., 1981). Table 1.1, based on information from Byrne and Anderson (1978), shows the average shore erosion rate in the reaches containing the study sites.

Table 1.1. The average erosion rate at study sites

SITE	HIH	HI2	CHP	DMF	WAL	NPS	SUM
RATE (ft/year)	2.5	1.7	1.2	1.6	1.6	1.5	5.0

Eight sites with breakwaters and headlands were selected as the study sites (Figure 1.1), which represent different fetch exposures and shore orientations. The following abbreviations are used for each study site throughout the text:

DMF - Drumonds field, James River, James City County.

CHP - Chippokes State Park, James River, Surry County.

HIH - Hog Island Headlands, James River, Surry County.

HI2 - Hog Island Breakwaters, James River, Surry County.

NPS - National Park Service beach site, York river, York County.

YTB - York Town Bays, York River, York County.

SUM - Summerille Beach site, Potomac River, Northumberland County.

(This site was not formally selected as a study site as other seven locations due to its overall different physical characteristics. Its selection is only for some comparisons of plan spiral beach forms).

WAL - Waltrip, James River, James City county.

At each site, there is at least one breakwater or headland present. All breakwaters are manmade, and installed between 1985 and 1987 (detailed descriptions in Chapter 4). Three headlands are manmade at



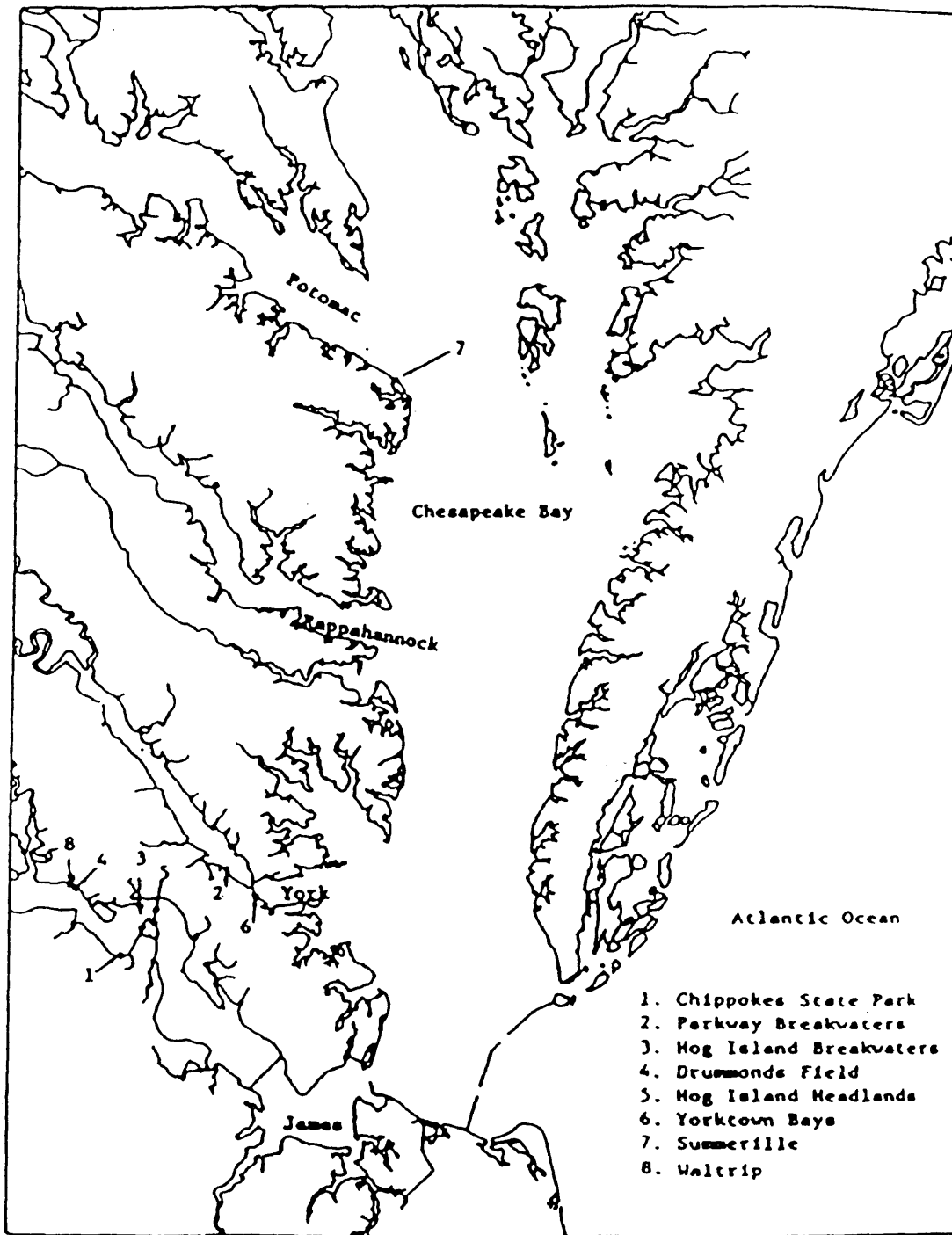


Figure 1-1. Virginia Chesapeake Bay and its river system with study sites arrow-pointed.

sites SUM and HIH, four headlands are the combination of artificial and nature at YTB.

The objective of this research is to investigate the three dimensional beach forms around manmade coastal breakwaters and headlands: plan beach forms and profiles. Although some basic physical mechanisms behind the beach forms are to be discussed in this study, these discussions are limited. The focus of this study is the beach "forms" in plan and profile.

## 2. GENERAL BACKGROUND

There have been a number of field and laboratory studies on the general characteristics of equilibrium beach profiles and plan forms. It is useful to review briefly these studies as a general background of this study.

### 2.1. Major Previous Studies On Profiles

An early qualitative analysis of a number of mechanisms which shape the loose granular materials into an equilibrium beach profile was presented by Fenneman (1902). He observed that the resulting profile is concave upwards near to shore and concave downward in the seaward portion of the subaqueous terrace. He concluded that the waves tend to transport material onshore and the return flow ("undertow") currents are regarded as the primary agents in shaping the equilibrium profile. He also concluded that due to the increase of flow cross-section (depth) offshore, the offshore slope will decrease until the transported material is deposited on the platform on which the wave-built terrace is constructed.

Bruun (1954) developed an empirical equation between water depth,  $h$ , and distance,  $X$ , from the shoreline and scale factor  $A$ ,

$$h = A X^{2/3} \quad (2-1)$$

based on the analysis of beach profiles measured at different places, two mechanisms were proposed: (1). the onshore component of shear stress is uniform, and the onshore component of the gradient of wave energy

flux is constant, which lead to an empirical formula (2-1). (2). the loss of wave energy is due only to bottom friction and the loss per unit area is constant. Using a nonlinear wave theory incorporated friction factor results determined in laboratory studies, Bruun found a somewhat more detailed equation for beach profiles

$$h = (A'/T^{4/9})(X^{2/3}) \quad (2-2)$$

where A is a scale factor, and T the wave period.

Bruun (1985) also briefly summarized the mechanisms of the development of storm (winter) and swell (summer) profiles: during the storm the point of incipient motion will be located far offshore while the point of equilibrium will be found closer to shore. Consequently, materials will move offshore. Conversely, during a (low) swell condition the point of the incipient motion will be close to shore while the oscillating equilibrium will be located further out. Consequently, materials will move onshore. This was supported by Bratteland and Bruun (1975) and Cart, Liu and Mei (1973).

Eagleson et al.(1963) developed a model for the equilibrium profile seaward of the break zone based on considerations of a balance between gravitational force,  $F_g \sin(\alpha)$ , and the fluid force on sediment particles,  $F_f$ , in a plane parallel to the beach. He concluded that in the case of equilibrium beach profile under the action of a given deep-water incident wave,  $F_g = F_f$  will be obtained at all points on the sand beach. He developed the theory based on the earlier considerations of the mechanics of wave induced bed motion of single spherical particles on plane, roughened, impermeable beaches. A reasonably good agreement was found by comparison of model predictions with experimental

results.

A beach response model was developed by Edelman(1968) based on actual surveys of pre- and poststorm beach profiles along the coast of Holland. He found that the equilibrium profile relative to the instantaneous sea level was approximately constant and can be expressed by a uniform slope depending on the sediment characteristics. He defined the depth of effective motion to be given by the breaking depth. Then a balance is established between material deposited out to the breaking depth on the uniform slope and the materials eroded to a landward limit of the instantaneous water level on the eroded profile. The slope was found to be approximately 1:40 for Edelman's measurements.

Dean (1977) proposed a more comprehensive form of the Bruun (1954) model based on over 500 beach profiles along the Atlantic and Gulf of Mexico shorelines. He considered that there are both "constructive" and "destructive" forces physically presented in the surf zone which tend to transport sand onshore and offshore, respectively. Three destructive forces were recognized: (1).uniform longshore shear stress; (2).turbulence resulting from uniform wave energy dissipation per unit plane area; (3). turbulence resulting from uniform wave energy dissipation per unit water volume. The model has the form:

$$h = A X^m \quad (2-3)$$

in which A is a scale factor depending on the stability characteristics of the bed materials, m is a shape factor, found to be 2/3.

Swart (1974) developed numerical models to describe beach profiles. He divided the beach profile into three zones:

1. The backshore above the limit of wave runup. If wind-blown

sediment transport is neglected, there is no transport in this zone.

2. Developing zone (D-profile), where a combination of bed-load and suspended load transport takes place. The dividing point of these two zones is the highest point waves can reach. The position of this point was determined empirically as

$$h_o = 7650 D_{50} [1 - \exp(-1.000143 H_{max}^{0.488} T^{0.93} / D_{50}^{0.786})] \quad (2-4)$$

where  $H_{max}$  is the maximum wave height in the spectrum equal to twice the significant wave height,  $T$  is the wave period,  $D_{50}$  is the median particle diameter.

3. Transition area, seaward of D-profile and landward of a point where sediment is initiated by wave action. Bed-load is normally the only transport in this zone. The point dividing these two low zones was determined empirically by

$$h_m = 0.0063 L_o \exp(4.347 H_o^{0.473} / T^{0.894} D_{50}^{0.093}) \quad (2-5)$$

where  $h_m$  is the depth of the D-profile;  $H_o$ ,  $L_o$  and  $T$  are deep water wave parameters;  $D_{50}$  is the median grain size.

Swain (1989) proposed a series of detailed steps/methods to calculate beach profiles based almost completely on Swart's theory stated above. These calculations were focused on the finding of the equilibrium curve termed W-curve, which was supported by his model testing.

Dean (1990) theoretically modified his previous work on equilibrium beach profile modeling. One of the most obvious improvements is the addition of a gravity effect to the turbulence effect near the shore. When the distance offshore and water depth are very small,

$$x = h/m(1/A^{3/2})h^{3/2} \rightarrow x = h/m \text{ or } h = M_1 x; \text{ when } h \text{ is large,}$$

$x=A^{-3/2}h^{3/2}$  or  $h=Ax^{2/3}$ , which is the original model form.

Byrne and Anderson (1978) carried out a systematical survey of shoreline erosion of Virginia Chesapeake Bay and its tributaries. In this study, they not only made detailed statistics on 2,366 miles of shoreline erosion, but also proposed major factors that control the beach processes in FETCH-LIMITED environment. These major factors are:

- 1). The intensity of wave action and the exposure to strong tidal currents.
- 2). The character of sediments at the site and the degree of protection offered by vegetative cover, specifically marsh grass, at the shoreline.
- 3). The supply of sand moving along the shoreline from other eroding areas or from streams along the shoreline.
- 4). The gradient or slope of the fastland adjacent to the shoreline and the slope of the nearshore bottom.

They further pointed out that the dominant erosion agent is the waves generated by LOCAL WIND ACTION. The growth and height of the waves is controlled by: fetch size; wind speed; the duration of wind and the depth of water. It is obvious that these are the most important factors when discussing wave conditions in fetch limited environment.

They particularly noticed another phenomenon in fetch-limited environment: the water elevation raised by local wind set-up and storm surge within the estuary during storm time. These storm effects can be further enhanced in conjunction with the spring tides, resulting in severe beach erosion. Therefore, the shoreline changes are greatly influenced by the local weather patterns. The northeast storms during

the fall, winter and early spring generate local waves that attack the western shore of the bay and tributary shorelines with a fetch to the northeast and east. The winds and low pressure along the coast line have an additional, indirect effect on the bay system. The storms force additional water into the bay. This local "wind tide" or storm surge may be one or two feet above the normal tide level.

Boon and Green (1988) performed field measurements on two Caribbean islands. They found that the two dimensional nearshore profiles can be well represented by Dean's (1977) model,  $h = Ax^m$ . Based on the least squares curve fitting of observed profile data, they found an average value for the curvature,  $m = 1/2$ , yielding a more concave and therefore steeper profile in inshore than Bruun and Dean's average value,  $m = 2/3$ . They also suggested an interesting surrogate for the beach face slope,  $\tan(\text{Beta})$ , on HIGHLY concave beaches to be  $A^{1/m}$ , where A and m have the same definitions as in Dean's model. An important result of their work is the correlation analysis, which connected the beach slopes closely with the most important physical and environmental factors such as wave height and period, sediment size and gravitational acceleration, g.

According to Wright et al. (1979), the linear, steep beach face and the linear gentler nearshore profile are one of the major morphological characteristics of reflective beaches. The reflectivity is determined mainly by the incident wave amplitude near the breaker point, wave period, the acceleration of gravity and the beach slope, this can be expressed:

$$\epsilon = a_1 \omega^2 / g \tan^2 \beta_1 \quad (2-7)$$

$\epsilon$  is referred to as the reflectivity or surf-scaling parameter. When



$\epsilon < 1.0$ , waves completely reflect with negligible dissipation; when  $\epsilon < 2.0$ – $2.5$ , low dissipation and strong reflection occur; when  $\epsilon > 2.5$ , then waves begin to plunge, dissipating energy; when  $\epsilon > 20$ , then spilling breakers occur; when  $\epsilon$  ranges from 30 to over 100, spilling breakers and approximately saturated surf zones occur across which bores decay progressively to become very small by the time they reach the subaerial beaches.

They identified a number of distinct morphological "states" or "stages" associated with various wave and tide regimes (1879; 1982a,b,c; 1983; 1984). They have been able to integrate many seemingly disparate hydrodynamic and morphological factors into coherent models, emphasizing the role of antecedent conditions in determining morphological states. In their summary papers, Wright and Short (1984) have replaced the original, somewhat confusing terminology with dissipative and reflective domains separated by four intermediate domains:

(1). Dissipative domain extreme. This is characterized by flat shoaling slope and wide surf zone. The surf scaling parameter has values ranging from 20 to 200. Nearshore topography was characterized by multiple parallel bars.

(2). Reflective domain extremes. The beach gradients are invariably steep ( $\text{Beta} > 6^\circ$ ), with no nearshore bars. The values of surf scaling parameter are less than 2.5. Leaky or trapped mode gravity edge waves dominate the secondary fluid motions in the narrow breaker zone, leading to the formation of subharmonic or synchronous beach cusps.

(3). Intermediate domains. These incorporate elements of both the

reflective and dissipative domains, coupling of waves and morphology becomes important. Intermediate states may arise as a consequence of tidal changes (Wright et al. 1982b), especially across beach profiles with separate sand and gravel elements. Four intermediate types in this domain are recognized: Longshore bar-trough; rhythmic bars; transverse (welded) bars and low tide terrace.

Sunamura (1984) summarized the previous studies on beach slopes and proposed two formulas to try to give a quantitative predictions of beach slopes:

(1). For laboratory beach slope

$$\tan\beta_1 = 0.013/(H/D^{0.5}g^{0.5}T)^2 + 0.15 \quad (2-8)$$

(2). For field beach slope

$$\tan\beta_1 = 0.12/(H/D^{0.5}g^{0.5}T)^{0.5} \quad (2-9)$$

He pointed out that the beach slopes predicted based on laboratory data are always higher than those based on field data for a given value of the dimensionless parameter, which indicates the laboratory beaches are high energy beaches, why it is high in energy is at present unknown (Sunamura, 1984, p244).

## 2.2. A Brief Review on Plan Beach Models

Yasso (1965), proposed the "headland-bay" beach conception which was defined as a beach lying in the lee of a headland subjected to a predominant direction of wave attack. He concluded that the erosion caused by refraction, diffraction and reflection of waves into the shadow zone behind the headland were the mechanisms leading to the formation of a seaward concave plan shape. The tidally induced currents have no direct effect on the formation of the plan headland bay beaches.

He suggested the formula,

$$r = e^{0\cot\alpha} \quad (2-10)$$

as an approximation to the plan form of the headland-bay beach in considering the fact that the radius of the curvature from the headland increases with distance (see Fig.2.1 and 2.2).

Silvester (1972) pointed out that the crenelate shaped bays are the rule rather than the exception on shorelines where sedimentary beaches exist between headlands. There exists a particular relationship between the advance direction of swell or resultant energy vector and the orientation, such that the straight tangent section is down coast and the curved portion is upcoast. This curved portion at upcoast is a logarithmic spiral (Figs.2.3,4) when the bay is fully stable. The constant,  $\alpha$ , in the equation

$$r_2/r_1 = e^{0\cot\alpha} \quad (2-11)$$

has a specific relationship to the approach angle of waves, to the headland alignment. Wave refraction and diffraction are involved when waves sculpture the curved beach in the lee of the upcoast headland. He also proposed a particular ratio,  $a/b$ , to identify stable bays, where  $a$  is the distance of the bay indentation,  $b$  is the distance between structures at the open side of a bay.

LeBlond (1972) studied spiral bay beaches from a somewhat different aspect. This study is a mathematical simulation of the development of spiral bay beaches using the theory of wave induced longshore currents. In order to relate sand transport to longshore current, he assumed that the volume rate of sand transport,  $T$ , is proportional to the total water transport,  $Q$ , in the surf zone times a "sand fraction",  $\mu$ ,

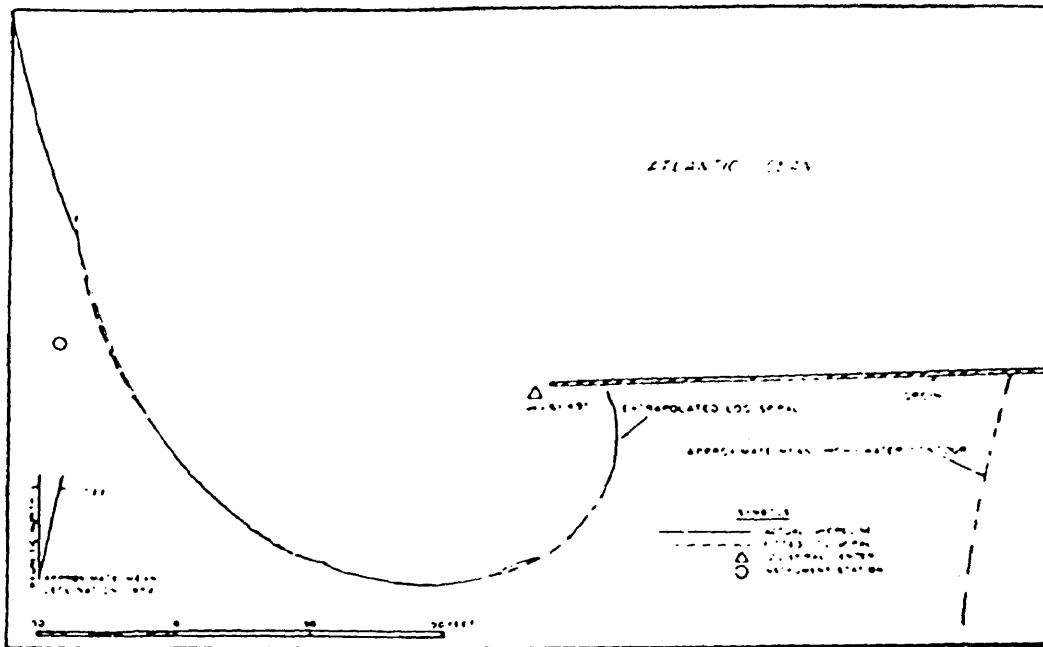


Fig.2.1. Plan of spiral beach, Sandy Hook, New Jersey, and fitted logarithmic spiral (after Yasso, 1965).

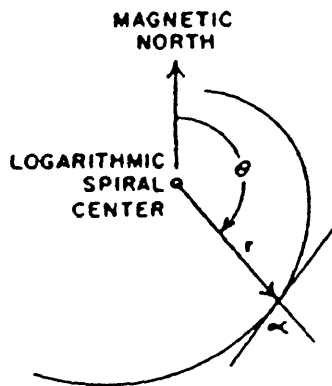


Fig.2.2. Logarithmic spiral nomenclature (after Yasso 1965).

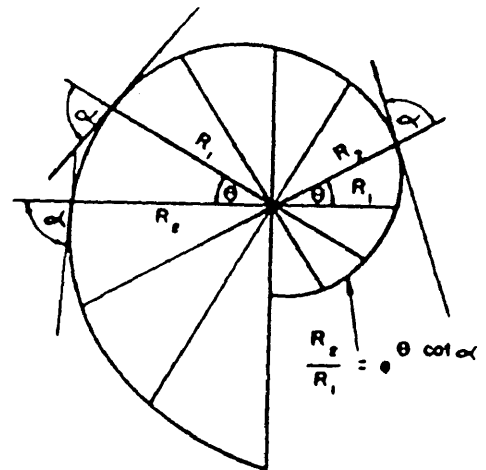


Fig.2.3. Definition sketch of logarithmic spiral (after Yasso, 1965).

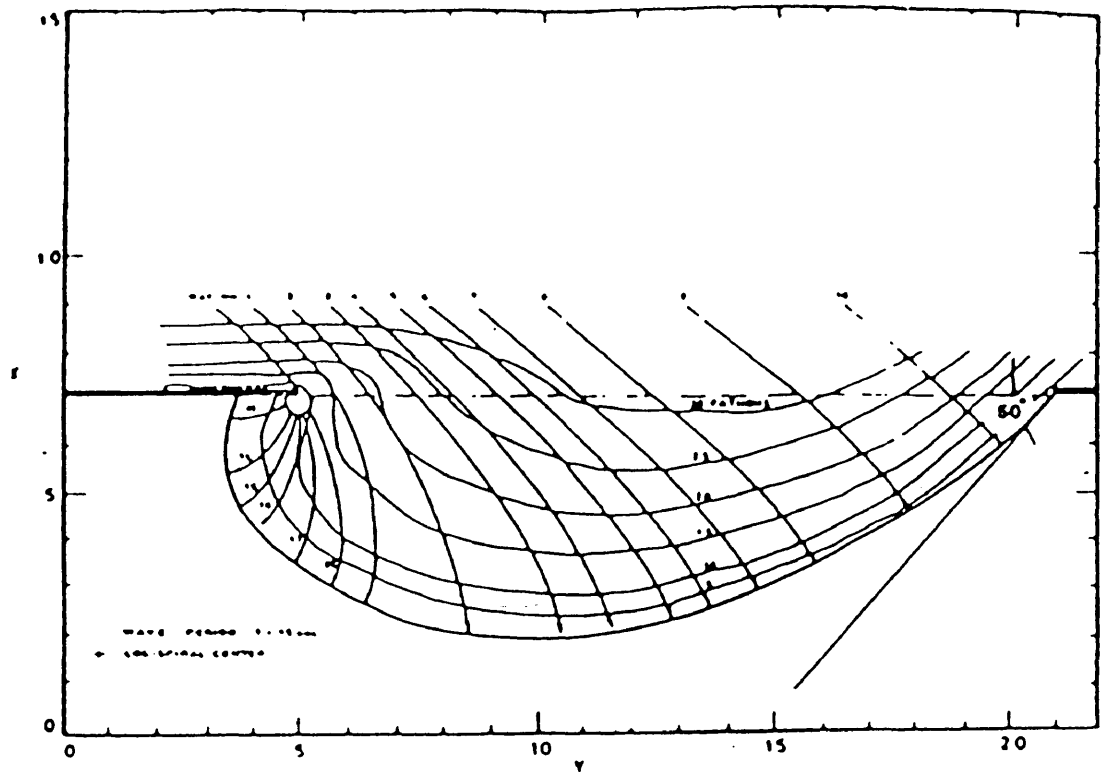


Fig.2.4. Typical prototype bay showing refracted orthogonals (after Silvester, 1972).

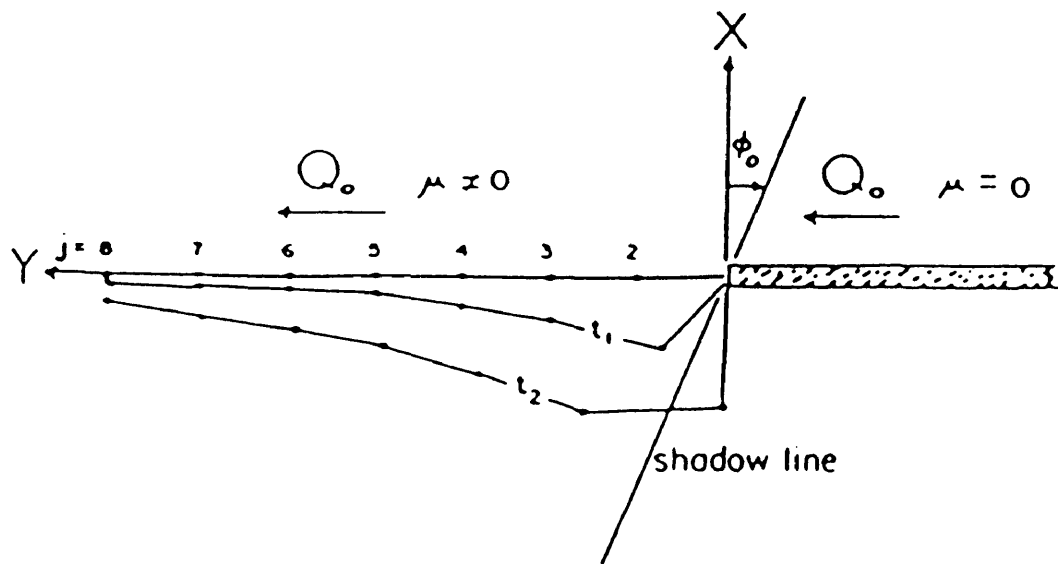


Fig.2.5. The initial linear beach configuration and qualitative estimates of some consecutive shapes (after LeBlond, 1972).

$$T = Q(\mu) \quad (2-12)$$

Therefore, sand transport is an integral property of the surf zone. With the erosion occurring from the initial linear shoreline, the sand transport divergence is large and positive at the origin (see Fig 2.5) because of the sand fraction discontinuity. The beach will gradually deform as shown in Figure 2.5.

Hsu and Silvester (1989) argued that the previous methods for determining the bay-beach planimetric shape using the logarithmic spiral principle apply mainly to the shadow zone behind the upcoast headland, not to the entire bay periphery, and do not have a fixed center. In order to solve this problem, they proposed a new method utilizing arcs from the point of wave diffraction to the shoreline, whose lengths and angles to the wave crest line are related to those of the control line.

In summary, the theoretical and empirical relationships presented in the previous studies are valuable to help explain some of the phenomena found in our fetch-limited study areas. It is seen that almost all relationships rely heavily on the empirical parameters and constants, which implies the difficulty in explaining the complex natural phenomena with theory. It can be said that a successful explanation on the natural phenomena is not at all easier than a precise calculation of the orbits of a sophisticated satellite or missile. It is just like what Komar (1976) said on wave prediction that the "state of the art" is largely a matter of accumulation or collecting of data. This is also very true in developing models on beach forms.

On beach profiles at present level, the new Bruun-Dean (1990) model,  $h=M^1x$  (beach face) and  $h=Ax^m$  (lower profile), is of great

reference in describing beach profiles. This model is actually a new version or improvement of the earlier Bruun-Dean (1977) single curve model,  $h=Ax^m$ . The old model has proven to work reasonably well with  $m=2/3$  (Bruun, 1954; Dean, 1977), and  $m=1/2$  (Boon and Green, 1988) in open ocean conditions. Boon's data were collected from beaches with carbonate dominated materials of a different environment. It would be expected that the new model would also work in fetch-limited, low energy level areas though some improvements are needed in explanation on the mechanisms of the nearshore profile development. This is because the origination of Bruun-Dean's model was based on profiles formed under fully dissipative wave conditions, the turbulence scale and nearshore circulation patterns are somewhat different from those in the fetch-limited environment. However, a rigorous improvement on the mechanisms is beyond the ability of the author for the purpose of this study.

At present, the quantitative predictions of beach slope are still remote based on the controlling physical parameters in the nearshore region (Komar, 1976; Sunamura, 1984) though the qualification of relationships between the controlling parameters and the slope has been attempted since early 70's. This is because of the complexity of the nearshore processes. However, the most important factors affecting beach slopes have been identified by many researchers (e.g. Byrne, 1978, Sunamura, 1984, Boon, 1988 and Wright et al., 1979, 1982, 1983, 1984). These factors are: (1). Sediment characteristics; (2). Wave properties such as wave height, period and length; (3). Tide range and stages; (4). Longshore current velocities; (5). Water table (ground water level).

The equation 2-9 proposed by Sunamura would represent a useful model in predicting beach slopes based on a number of important environmental parameters.

On plan beach forms, less modeling has been done than profiles, especially for beach forms between structures. Most modeling work has been concentrated on spiral bay beaches, and there are still severe arguing on the spiral bay beach predictions. This can be seen from Hsu and Silvester (1989) paper. On regular or irregular circular bay beach modeling, there has been few studies in the literature.

Yasso's spiral bay beach model gave a bright preliminary idea in simulating spiral bay beaches though some weak points exist as pointed by Hsu and Silvester (1989). Hsu and Silvester did not use a particular logarithmic equation to simulate the plan bay shape, but use the empirical parameters based on field and laboratory data, or hind-forecast analysis. The advantage of their method is that it provides a better fit to the natural headland bay beaches. The disadvantage is that the diffraction point and the critical point down beach where the wave orthogonal is determined are often difficult to determine. Any small error in determining the locations of these two points can lead to large variations in predicted bay shape. And they did not propose a formula to generalize their method which would result in a difficulty in simulating by computers.



### 3. DATA AND METHODOLOGY

#### 3.1. Surveys and Data Sets of Beach Profiles and Photography

Field data used in this study are part of an ongoing shoreline study of Chesapeake Bay. It is a cooperative project between the Commonwealth of Virginia and the Norfolk District of the U.S. Army Corps of Engineers. The study area and sites in this thesis are generally the same as those in the project (Fig.1.1).

The field data collection involved quarterly and after-storm shore profiling and low level aerial photography as well as sediment sampling and laboratory grain size analysis (Tables 3.1 and 3.2).

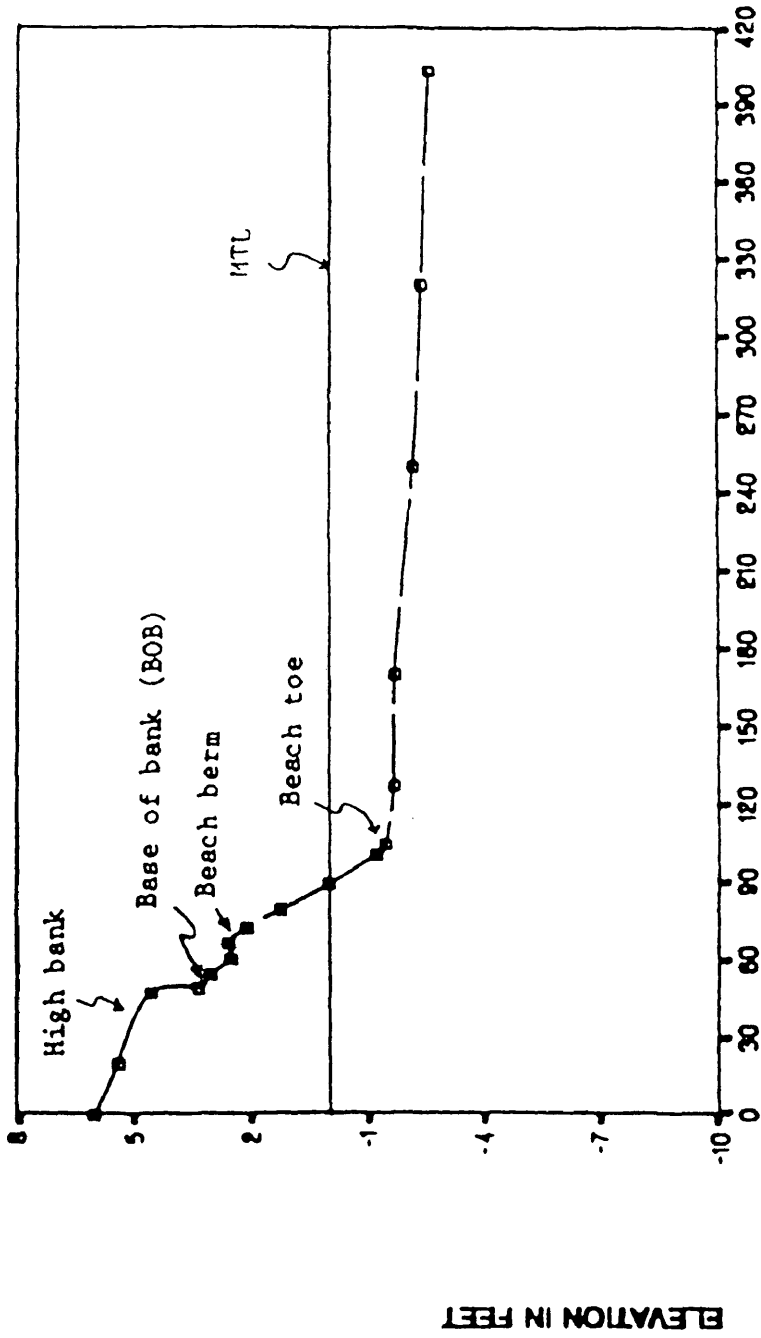
The detailed arrangements of structures and profiles at each site are presented in Figures 3.2 through 3.8. The baselines in these figures were established using a transit. The spacings between profiles along baselines are determined based on site situations. The more concerned areas have smaller spacings so that beach changes can be more accurately measured. From the baselines, profile lines were determined and surveys were performed using a rod and level. The feature profiling method is used (Fig.3.1): at any perceived break along a profile, a point is set up for measuring. The square symbols in figure 3.1 are such points. In addition to these perceived breaking points, some more points are usually added in certain critical section such as the one connecting the beach face and offshore profile. When a beach face looks



Table 3.2. Profiling and Aerial Photography Schedule by Month and Day

Site	1988						1989					
	Phase I			Phase II			Phase III			Phase IV		
	Jul	Aug	Sep	Oct	Nov	Dec	Jan	Feb	Mar	Apr	May	Jun
<u>CHP</u>												
33 profiles												
baseline - 839 ft												
profiles			21			14			28			8
aerial photos			15			19			29		25	
<u>NPS</u>												
27 profiles												
baseline - 748 ft												
profiles			14			6			17			2
aerial photos			15			19			29		25	
<u>HI2</u>												
61 profiles												
baseline - 1275 ft												
profiles			7		22				16			6
aerial photos			15			19			29		25	
<u>DMF</u>												
35 profiles												
baseline - 1674 ft												
profiles			13			8			30			15
aerial photos			15			19			29		25	
<u>WAL</u>												
17 profiles												
baseline - 447 ft												
profiles			27			20			20		26	
aerial photos			15			19			29		25	
<u>HIH</u>												
30 profiles												
baseline - 2400 ft												
profiles			6	20		6			17			8
aerial photos			15			19			29		25	
<u>YB</u>												
21 profiles												
baseline - 357 ft												
profiles			28		17	19			15		23	
aerial photos			15			19			29		25	
<u>SUM</u>												
12 profiles												
baseline - 863 ft												
profiles			2			5			27			5
aerial photos						19			29		25	

# FEATURE PROFILLING METHOD



DISTANCE FROM BASE LINE IN FEET

Fig.3.1. A diagram showing the feature profiling method used in this study. The data used in this diagram was taken on Dec. 1988, at National Park Service beach, York River.

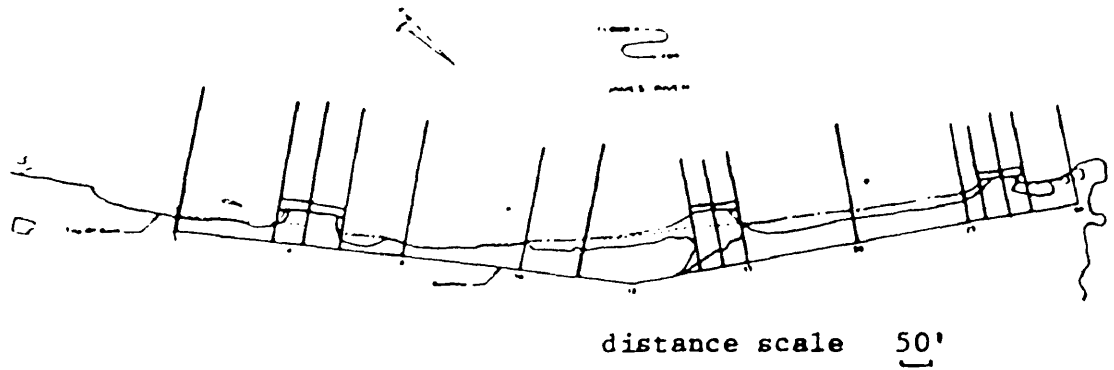


Fig.3.2. Hog Island Headlands, Base map with some profiles numbered.

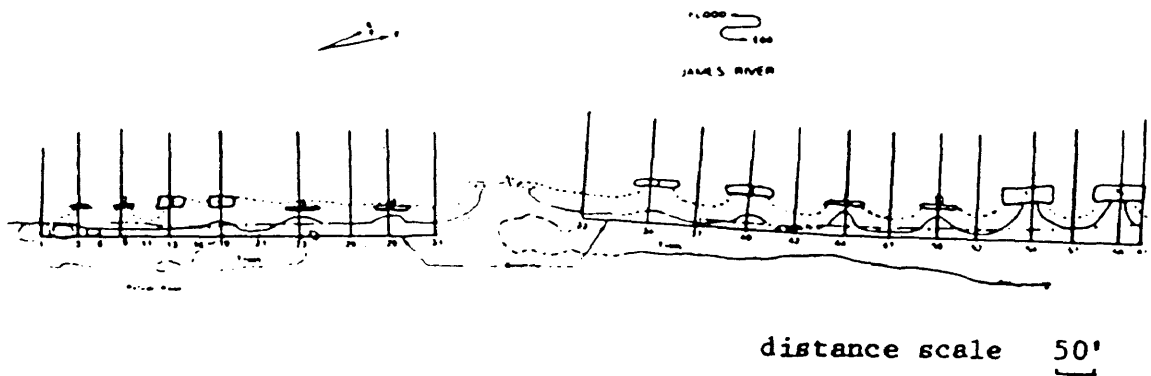


Fig.3.3. Hog Island Breakwaters, Base map with numbered profiles.

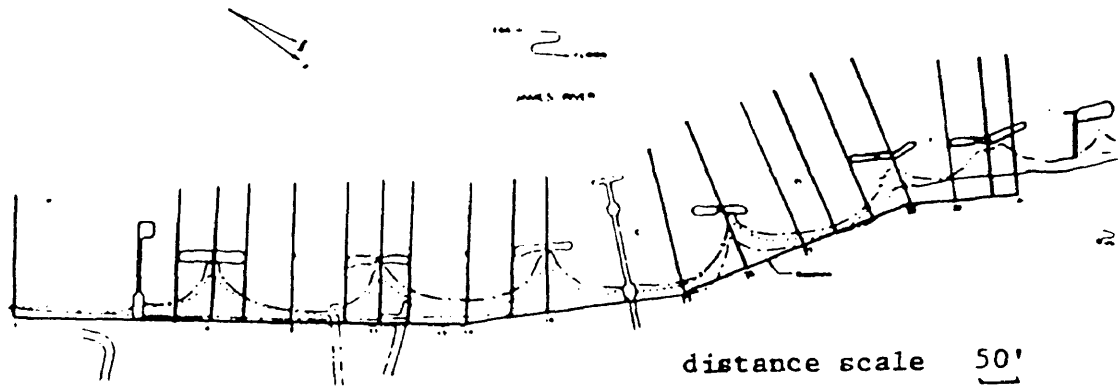


Fig.3.4. Drummonds Field, Base map with numbered profiles.

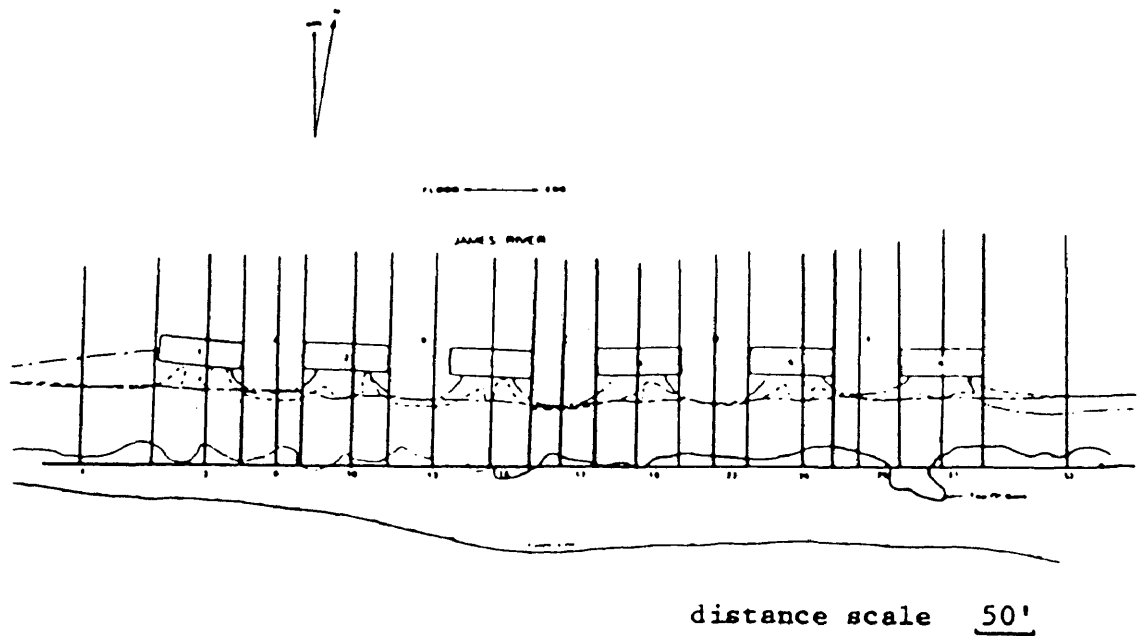


Fig.3.5. Chippokes State Park, Base map with numbered profiles.

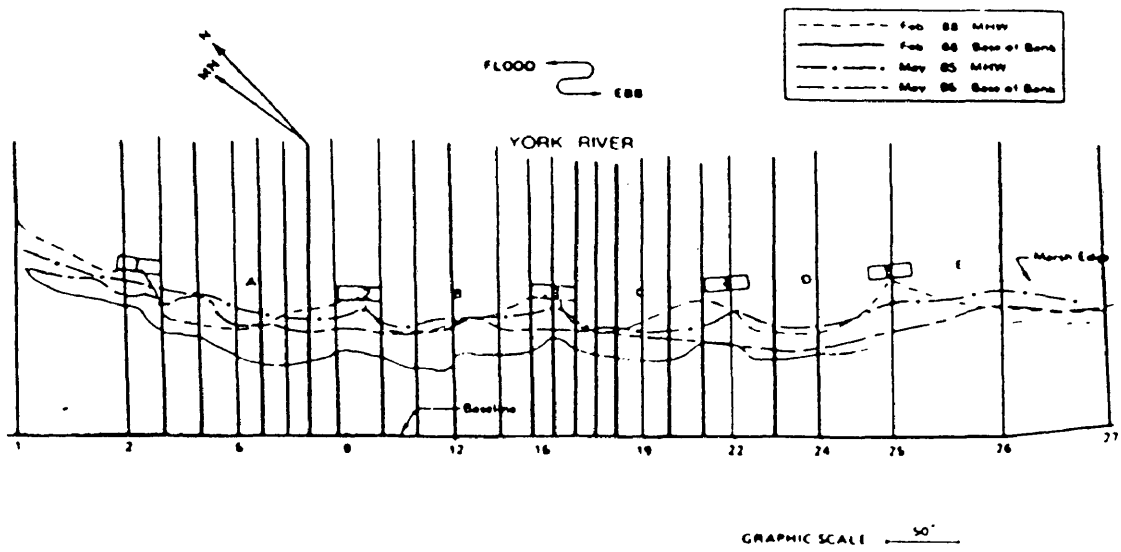


Fig.3.6. Parkway Breakwaters, Base map with numbered profiles.

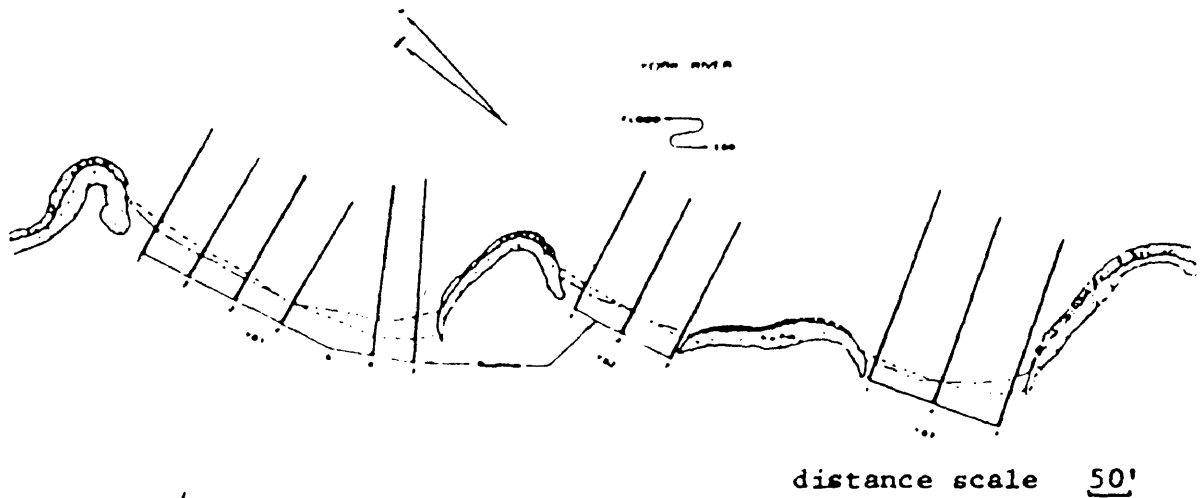


Fig.3.7. York Town Bays, Base map with some numbered profiles.

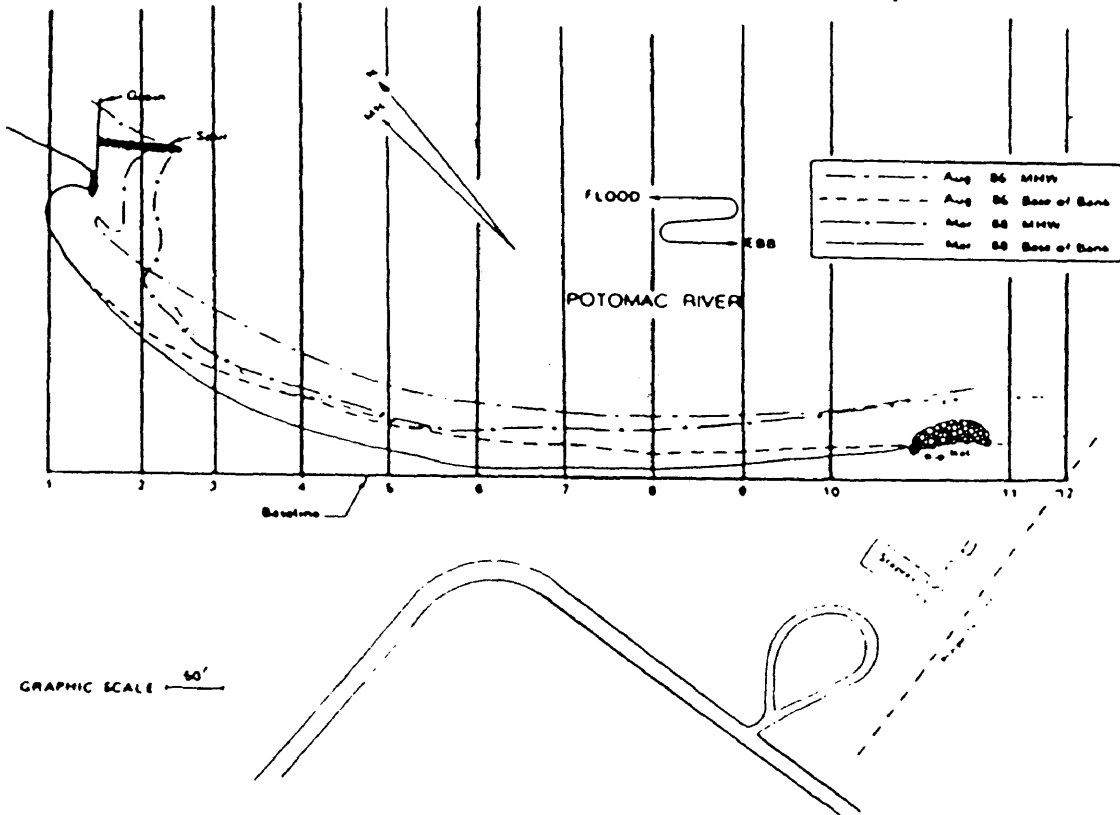


Fig.3.8. Summerille, Base map with numbered profiles.

straight across it, we did not just measure two points at both ends of the beach face, but a series points for the purpose of statistical analysis. Tables 3.1 and 3.2 give the detailed schedule of profiling and aerial photography.

All coastal structures are manmade except the headlands at Yorktown Bays which is a combination of manmade and natural structures. Five sites have breakwaters: HIH, CHP, DMF, WAL and NPS. The breakwaters at CHP, HI2 and NPS were initially set up at or near mean low water (MLW). CHP and NPS had no beach fill added, whereas HI2, DMF and WAL did. Three sites have headland structures: HIH, YTB and SUM. Only the headlands at HIH were constructed for the project. The headlands, their crenelate bays and pocket beaches at both sites SUM and YTB have existed for over ten years.

All profile data are plotted in Appendix B,C AND D.

### 3.2. Data Sets on Plan-view Configurations

The plan-view configurations of shores at each study site were determined by 1). low aerial photography; 2). comparisons of adjacent profiles along with the field pen records on beach features; 3). detailed measurements of plan beach forms on selected bays between breakwaters.

From Table 3.1 and 3.2, it is seen that frequent photography was done according to schedule. The photographs were taken at 500, 1,000 and 2,000 feet, and were used along with the profile data to create a base map for each site against which the general trend of sediment movement could be determined by carefully examining photographs. The variation of beach forms relative to certain fixed targets can be more



easily determined. The comparisons of adjacent profiles were very useful in determining plan-beach forms. For instance, there generally exists a clear slope break at the beach toe for most sites and an upper beach point defining the approximate mean high high water level. These features were hand-recorded while the profile was measured in the field. After these points were connected from adjacent profiles, a clear plan-view of the distribution of the beach face zone would be fairly accurate. Some representative bays were selected to be measured to determine the general pattern of beach slope distribution within a whole bay between structures. Five bays were selected for this purpose: Bay 11 at HI2; Bay 3/C at CHP; Bay A at DMF; Bay 1/A at WAL and Bay 2/B at NPS. For detailed results of analysis on these bay measurements please see Section 5.3.

### 3.3. Sediment Data and Analysis

Surface sediment samples were taken from back shore to offshore along selected profiles at each site. Sediment sampling was done at least three times along the same profiles for each site. Borings on the beach and nearshore were also done to measure the thickness of recently eroded bank materials overlying the older, in situ strata. All sediment samples were analyzed at VIMS sediment laboratory for percent of gravel, sand, clay/silt and other characteristics of sediment such as moment measure mean, standard deviation. The detailed results of sediment analysis are presented in section 5.

### 3.4. Methods of Wave Hindcasting

As pointed out by Komar(1976), in the absence of a satisfactory understanding of the mechanisms of wave generation, semiempirical

approaches should be developed for wave prediction. Development of the "state of the art" is largely a matter of collecting data on winds and waves. As new data accumulates, the relationships must be modified and, so, continue to evolve.

In general, the prediction methods can be classified into two categories: 1). the significant wave method; 2). wave spectrum method. The first method, significant wave method, was proposed by Sverdrup and Munk(1947) and revised later by Bretschneider(1952, 1958). A name of S-M-B method has been used after their names. The second category, the wave spectrum method, was first introduced by Pierson, Neumann and James(1955). This method is commonly called P-N-J method which describes the generated storm waves in terms of the complete spectrum of periods and energies, representing a considerable improvement in wave forecasting techniques. However, the S-M-B method is chosen in this thesis because: (a) only significant wave parameters are concerned in this study; (b) predicted results can be used to compare with field observations of significant wave parameters; (c). this method is easier to use but give a useful reference results. Table 3.3 shows comparisons of some predicted values by various methods.

Based on the known storm conditions such as wind velocity  $U$ , fetch distance  $F$ , and storm duration  $D$ , the significant wave parameters like  $H_{1/3}$ ,  $T_{1/2}$  and  $L_{1/3}$  can be predicted. In practice there are basically two types of procedures to use S-M-B method: 1). computerized S-M-B procedure which is used in this thesis (This procedure gives a faster and more accurate predicted results than the traditional dealing by graphical method). 2). graphical procedure which has been more

traditional (This second procedure is based on the empirical graphs first presented by Bretchneider(1959) and Wiegel(1961). The graphs were formed based on all available data at that time in terms of the dimensionless ratios  $gF/U^2$ ,  $gD/U$ ,  $gH_{1/3}$  and  $gT_{1/3}/U$ . The graphs have been updated and widely used in coastal engineering researches).

Table 3-3. Wave predictions by various methods

WIND SPEED (m/s)	FETCH DISTANCE (km)	SIGNIFICANT WAVE HEIGHT(m)				SIGNIFIC. WAVE PERIOD			
		S-M-B	P-N-J	LIU	DARBYSHIRE	S-M-B	P-N-J	LIU	D.
10	200	2.1	2.4	2.1	1.2-1.4	7	8	7	7
10	1,000	2.7	2.4	3.4	1.2-1.5	11	8	10	7
20	200	5.2	4.3	5.8	4.3-5.2	10	8.5	10	10
20	1,000	8.9	11	9.2	4.6-5.6	15	16	15	11
30	200	8.2	7.9	11	9.7-12	12	10	12	15
30	1,000	15	15	17	11-13	19	15	18	16

Steps of S-M-B method used in this thesis:

1) Determine the size of the effective fetch. This step is particularly important when S-M-B method is to be used in small water bodies such as the tributary estuaries to lower Chesapeake Bay. If the S-M-B method is used in open waters like the ocean, there is not too much concern about the size of effective fetch because the fetch distance is usually "unlimited". However, the small water bodies are often very fetch-limited (Wright, 1985), any error in determining the effective fetch distance can lead to errors in predicting the significant wave parameters. In determining the effective fetches, the distances within  $90^\circ$  are measured symmetrically around the direction of main storm winds. A formula

$$F_{\text{eff}} = \sum X_i \cos(\alpha) / \sum \cos(\alpha) \quad (3-1)$$

is used to determine the effective fetch based on the values measured, where  $X_i$  is distance,  $\alpha$  is the angle between wind direction and any other lines.

2) Divide the whole length of water surface along the wind direction concerned into segments. The water depth within each segment should be relatively evenly distributed. This can be done on a detailed topography map based on the well established depth contours by map surveyor.

3) Take the average of water depths for each segment using a simple formula

$$d = (d_i + d_{i+1})/2 \quad (3-2)$$

4) Input the effective fetch, wind direction, wind speed, surge levels and the average depth for each segment into the computer, or alternatively, look up directly the predicted values of wave parameters on the empirical graphs.

### 3.5. Methods on Wave Refraction and Diffraction

Wave refraction:

Waves are subject to refraction as they enter shallow water. Wave orthogonals keep change directions with decreasing water depth in such a way that the crests tend to parallel the depth contours. The wave refraction is similar to that of light rays. Therefore, the wave refraction can also be described by Snell's law

$$\sin(\alpha_1)/C_1 = \sin(\alpha_2)/C_2 = \text{constant} \quad (3-4)$$

where  $\alpha$  is the angle between wave crest and the respective depth contour.  $C_1$  and  $C_2$  are the successive phase velocities at the two depths. Based on the Airy wave theory,  $C$  can be obtained from:

$$L/L_0 = C/C_0 = \tanh (2\pi h/L) \quad (3-5)$$

From the simple relationship in equation 3-4, it is easily seen that to keep the constant, the two factors,  $a$  and  $C$ , have to change in a similar manner, decreasing as the shore is approached. That is, when  $a$  decreases,  $C$  can not increase.

The method for generating refraction diagrams in the Shore Protection Manual was employed for considering wave refraction patterns. This method is easy to use and able to generate refraction diagrams with reasonable accuracy. It is actually a orthogonal or template method. It uses bottom topography charts of any scale. Underwater contours are drawn on the charts or a tracing paper overlay. The depth intervals chosen depend on the degree of accuracy desired. In tracing contours, small irregularities must be smoothed out, because the bottom features comparably small in respect to the wave length do not affect waves appreciably. For each wave period and direction selected, a separate diagram must be prepared.  $C_1/C_2$  values for each contour interval are then marked between contours.  $C_1$  and  $C_2$  are phase velocities. For further detailed procedures of this method, please refer to S.P.M., volume I, pages 265 - 279.

#### Wave diffraction:

The phenomenon of wave diffraction is very common along coasts with various manmade structures and natural headlands. In this process, wave energy is transferred laterally along wave crests from where the wave height is large to where it is small.

The result of wave diffraction is the re-distribution of wave energy, which is indicated by the variation of wave height. The wave

diffraction is best expressed by the patterns of wave diffraction coefficient,  $K'$ , which is defined as the ratio of a wave height,  $H_d$ , in the area affected by diffraction to the incident wave height,  $H_i$ , in the area unaffected by diffraction:

$$K' = H_d/H_i \quad (3-6)$$

The diagrams for wave diffraction were first systematically presented by Wiegel (1962). These diagrams have been widely used or referenced by coastal engineers and geologists( e.g. Shoreline Protection Manual, Vol.1). Figure 3-9 is only one example of these diagrams. This diagram was constructed in polar coordinate form with arcs and rays centered at the tip of the structure. The unit used for rays is radius-wavelength. One wave length between arcs in this diagram. The predicted wave parameters are only to be used as a very general reference to understand the general wave conditions in the further offshore areas near the study site.

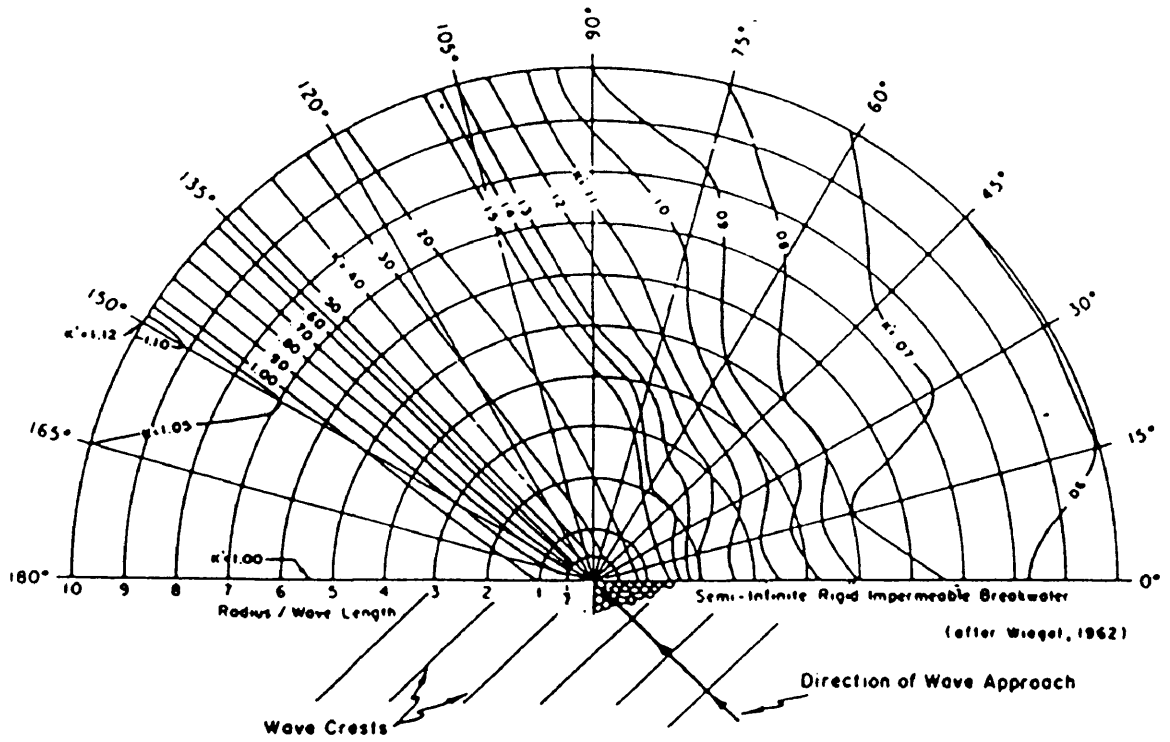


Fig.3.9. Wave diffraction diagram - 135° wave angle.

#### 4. FIELD SITE DESCRIPTIONS

In this section, the following characteristics for each site will be described: a). site exposure direction; b). effective fetch; c). predicted wave characteristics; d). sediment characteristics; e). Morphology and substrate characteristics.

##### Site 1. Hog Island Headlands (HIH)

The site is located within a long shallow embayment between Hog point and Walnut point (Fig.1.1 and Fig.3.2). The shoreline along the embayment generally faces northeast. The effective fetches are 2.1 nautical miles (northeast), and 3.0 nautical miles (southeast). The historical erosion rate was 2.5 feet per year (Byrne and Anderson, 1978). The tide range is 2.1 feet. The bank along the northern section is approximately 10 feet high and is composed of dredged material (mixture of clay/silt, sands and gravels). Proceeding southward the bank's elevation decreases and becomes a low (about 2 feet) clayey fastland. On the northern end of the site, large concrete blocks were placed along 150 feet of shoreline at MLW in the early 1960's. Midway between the blocks and the southern end of the site is a small erosion resistant bank. These features segmented the shore into two segments.

The beach is composed of medium to coarse sand mixed with gravel and pebbles overlying stiff brown clay. The sand was only about 1 foot thick at MHW before construction. Three rock headlands were built at



this site in Oct. 1987. Breakwater 1 has a 150 ft crest length, a 4 ft crest width and is 3.5 ft above MHW. Breakwaters 2 and 3 have the same crest lengths of 100 feet, 4 feet crest width and 2 feet above MHW. Breakwater 1 was placed at -1.0 MLW while breakwaters 2 and 3 were placed at 0.0 MLW. Approximately 2,400 cubic yards of fill was placed on HIH. The mean diameter of the fill material was 0.4 mm (1.23 Phi). The bank behind breakwater 1 was graded and about 1,200 cubic yards of fill was emplaced. About 600 cubic yards of fill was placed behind each of breakwaters 2 and 3. The new beach fill was placed to an elevation of about 3.0 feet above MHW at the backshore.

The shore normal long term wave climate can be implied by the general shoreline orientation and the aerial photographs. Only very slight changes were shown by historical aerial photographs. There are no significant offsets. The predicted wave height for this site can be seen from Table 4.1.

#### Site 2. Hog Island Breakwaters (HI2)

This site is located on the western shore of Hog Island, along the shoreline between Virginia Power's Surry Nuclear Power Plant outfall to a marshland at the north end. The baseline is 1,475 feet long. The shore faces west northwest (Fig.1.1 and 3.2) with effective fetches of 2.4 nautical miles (southwest), and 2.5 nautical miles (northeast). The fast land bank is 3 to 11 feet above MSL and consists of mixed clayey sands and gravels in an earthen dike composed of dredged materials from nearby channels. The historical erosion rate along this reach is approximately 1.7 feet per year (Byrne and Anderson, 1978). There is a gabon revetment in the middle of the site that was built in 1962. This

Table 4.1. Predicted Wave Height for each site

SITE	WAVE HEIGHT (2 ft ABOVE MLW, WIND 20 MPH )						WAVE HEIGHT (4 ft ABOVE MLW, WIND 40 MPH)					
	NEARSHORE (m)			OFFSHORE (m)			NEARSHORE (m)			OFFSHORE (m)		
HIH	0.27 (SE)	0.27 (NE)		0.43 (SE)	0.40 (NE)		0.55 (SE)	0.55 (NE)		0.76 (SE)	0.73 (NE)	
HI2	0.24 (N)	0.24 (NW)	0.24 (SW)	0.34 (N)	0.36 (NW)	0.34 (SW)	0.56 (N)	0.56 (NW)	0.56 (SW)	0.64 (N)	0.73 (NW)	0.62 (SW)
CHP	0.27 (N)	0.27 (NW)	0.27 (NE)	0.38 (N)	0.37 (NW)	0.37 (NE)	0.43 (N)	0.43 (NW)	0.43 (NE)	0.73 (N)	0.70 (NW)	0.72 (NE)
DMF	0.27 (S)	0.27 (SW)	0.27 (W)	0.34 (S)	0.38 (SW)	0.38 (W)	0.55 (S)	0.55 (SW)	0.55 (W)	0.72 (S)	0.73 (SW)	0.76 (W)
NPS	0.28 (N)	0.28 (NE)		0.30 (N)	0.36 (NE)		0.55 (N)	0.55 (NE)		0.75 (N)	0.66 (NE)	
YTB	0.31 (N)	0.31 (NE)	0.31 (E)	0.33 (N)	0.49 (NE)	0.61 (E)	0.64 (N)	0.64 (NE)	0.64 (E)	0.66 (N)	1.04 (NE)	1.37 (E)
SUM	0.31 (N)	0.31 (NE)		0.76 (N)	0.73 (NE)		0.61 (N)	0.55 (NE)		1.62 (N)	1.46 (NE)	

Note: N-north, NW-northwest, NE-northeast, S-south, SE-southeast, SW-southwest, W-west.

gabon headland resulted in two types of shoreline configuration at the site. To the south of the headland, there was a narrow beach (3-5 feet from base of bank to MHW) fronting the steep, wave cut bank. The northern shoreline segment had a narrow beach fronting a low, wooded terrace. Net littoral sediment transport to the south is indicated by the impoundment of sand, wider beaches along the northern segment and the faster erosion at the south end of the middle headland. The beaches are basically composed of sand and gravels.

Twelve breakwaters were installed in June, 1987. Six of them were placed south of the gabon headland, and six placed north. Approximately

1,000 cubic yards of beach fill of same particle size as those used at HIH was placed along the northern section, and 500 cubic yards on the southern section.

#### Site 3. Chippokes State Park (CHP)

Six gaped breakwaters were installed in June, 1987 at this site (Fig.1.1 and 3.4). The site is located between College Run and lower Chippokes Creek. The reach is characterized by high bank (40 feet) and very wide (over 7,000 feet) shallow terrace. The high banked shore faces almost due north and have effective fetches of 3.2 nautical miles (northwest), 3.6 nautical miles (north), and 3.0 nautical miles (northeast). The high banks are composed of a lower unit of shelly, fossiliferous, fine to coarse sand overlain by an upper layer of slightly muddy, fine to medium sand. The beach itself consists of a fine to coarse, well sorted, shelly sand derived from the eroding bluff.

This six breakwater system has a length to gap ratio of 1:1.5. The crest lengths are 50 feet and gaps are 75 feet. The center line of the breakwaters is about 30 feet from the initial MHW line. The crest width of each breakwater is 4 feet. Net transport here is eastward but with seasonal fluctuations and onshore offshore movement.

#### Site 4. Drummonds Field (DMF)

Drummonds Field is a private development located on the north shore of the James River just west of the Jamestown Ferry pier (Fig.1.1 and 3.3). The site faces south southwest. The effective fetches are 2.2 nautical miles (south southeast), 2.8 nautical miles (south west) and 3.8 nautical miles (west). The baseline is about 1,300 feet long. The historical erosion rate is 1.6 feet per year (Byrne and Anderson, 1978).

The 25 ft high bank is composed of a blue grey, very stiff clay overlain by a layer of fine to medium sand. The clay layer is an aquiclude causing intermittent springs to occur along the bank. Bank erosion provided sand to the narrow beach which, in turn, provided little or no buffer to wave action under storm conditions. The net sediment transport was judged to be down river (to the southeast).

The breakwater system was installed in Sep., 1985. The purpose of the system is to provide a stable, protective and recreational beach for this waterfront development. About 10,000 cubic yards of material was placed with the construction of these breakwaters. An additional 3,000 cubic yards of material were added in Apr., 1986. This was placed mostly behind breakwaters 1, 2 and 3. The sediment characteristics can be seen from table 6.1. and 6.2. A Field observation was carried out in Sep., 1985 when Hurricane Gloria hit. The northwest winds of 50-60 mph generated waves of heights 1.5 to 2.0 feet.

#### Site 5. Parkway Breakwaters (NPS)

This site is located along the Colonial Parkway in the Colonial National Historical Park (Fig.1.1 and 3.5), between Sandy Point and the piers at Yorktown Navy Weapons Station. The shore faces northeast with an effective fetches of 2.7 nautical miles (north), and 1.6 nautical miles (northeast). The historical erosion rate along this reach is approximately 1.5 ft/year (Byrne and Anderson, 1978).

Five breakwaters were placed in May 1985 along the crenelate embayment between two low headlands. The upriver headland is the terminal end of a rock revetment with a salt marsh fringe in its lee. The downriver headland is actually made up by a narrow salt marsh

fringe. The distance between the two headlands is about 800 feet along which breakwaters were built. The bank and back shore are characterized by shelly, medium sand. The beach is composed of medium to coarse sand and gravel with abundant shell fragments, which was derived from the low bank. Silty fine sands reside offshore. The general trend of littoral drift is downstream, which is indicated by the offset at the downstream end of the revetment and the northerly facing tangential shore between breakwaters.

#### Site 6. Yorktown Bays (YTB)

This site has three pocket bay beaches located about one mile downriver from the George P. Coleman Bridge at Yorktown, Virginia. They face east northeast with effective fetches of 4.7 nautical miles (northeast), and 7.8 nautical miles (east). However, there is a long distance of 23 nautical miles to the east through the mouth of York River and across Chesapeake Bay. This site represents estuarine beaches which have been relatively stable over a long period of time. Yorktown bays have evolved over the past 50 years. The headlands separating each bay are composed of a highly indurated, shelly marl of the Yorktown Formation. The headlands are interflaves with banks approximately 80 feet above MSL. The bay beaches have been developed in the adjacent drainage. The headlands were hardened with rock revetments in the early 1960s and reinforced in 1979. This created stable headlands and the beaches evolved into their present configuration (Fig.1.1 and 3.6). The three bays at this site are designated by YB1, YB2 and YB3. YB1 is the largest with approximately 400 feet long from the MHW. It has a slightly crenelate shape and the tangential section of the beach faces

east northeast, showing the influences of both the NE winds in winter and the long fetch from the east. The sediments on these beaches are characterized by generally well sorted medium coarse, shelly sand and gravel. The sand has been derived from historical and continued erosion of the adjacent headlands.

#### Site 7. Summerille (SUM)

This site is located on the Potomac River near Smith Point. The shore faces northeast with effective fetches of 15.5 nautical miles (north), and 14.3 nautical miles (northeast). Fig.3.7 depicts the general shape of this crenelate bay. The segment in front of the Summerille House evolved into headlands after the installation of a groin field in 1967. A low sill installed in front of Staples house about 1975 had the effect of slowing the erosion. A bay has evolved between the Staples house and Summerille house. The Staples' was 50 feet offshore in 1978. A short rock revetment was placed in front of Staples. This acts as a small headland. The beach along the embayment averages about 30 feet wide from the base of bank (BOB) to MHW. It is characterized by well sorted, medium sands. This material is derived from erosion of the bay banks and littoral transport which brings sand into the embayment from the north. The general configuration of the bay indicates a northeast wave climate and a littoral transport southward toward Smith Point.

The wind climate can be seen from figure 4.1. The general trends are that during summer seasons, south winds are dominant; while during winter seasons north winds are prevail.

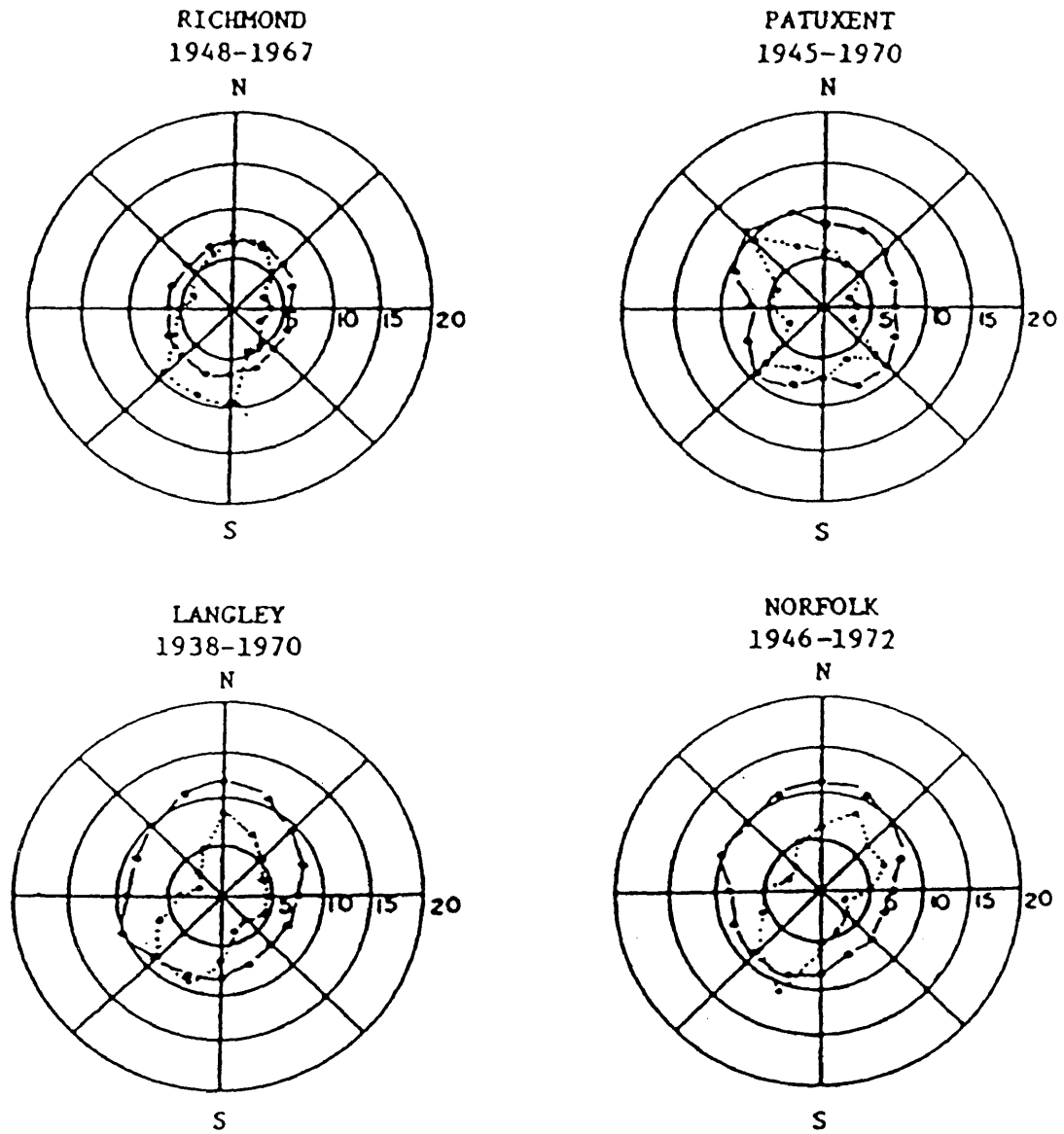


Fig.4.1. Long term wind roses for Richmond, Patuxent, Langley, and Norfolk.  
 ·—· Frequency of occurrence(%)  
 ·—· Average velocity(kts)  
 (Hardaway et al., 1984)

## 5. RESULTS OF PROFILE AND SEDIMENT ANALYSIS

### 5.1. The Analytical Results of Field Profile Measurements

The field profile measurements for more than three years show a general two segment profile character from the beach berm offshore: the upper segment is the beach face, the lower segment is the nearshore segment from beach toe offshore. The analysis below shows the general profile characteristics in the fetch-limited environment around coastal breakwaters and headlands.

The profile characteristics can be seen by plotting the water depth,  $h$ , against the distance offshore,  $x$ , and the statistical analysis. These two parameters are the same as used in Bruun-Dean's 1977 model. Figures 5.1 through 5.17 in this chapter and the figures in Appendixes B, C and D are the results of such analysis.

The selected bays for bay beach face profile analysis are representative of the study area. Once again, the selection of the five bays presented here are the same as those in the Chesapeake Bay Shoreline Study Project selected in advance. More detailed discussions on profiles will be presented in chapter 6.

The results of beach face and nearshore slopes and sediment size analysis are presented in Table 5.1.a and b.



Table 5.1.a. Results of Slope and Sediment Analysis

SITE	BEACH FACE SLOPE	BEACHFACE SEDIMENT		SORTING	NEARSHORE PROFILE SLOPE	NEARSHORE SEDIMENT		SORTING
		SIZE (mm)	( $\phi$ )			SIZE (mm)	( $\phi$ )	
HIH	0.11	0.40	1.32	0.68	0.013	0.19	2.39	0.69
HI2	0.12	0.40	1.32	0.73	0.010	0.21	2.19	0.85
CHP	0.11	0.30	1.73	0.93	0.009	0.18	2.47	0.77
DMF	0.11	0.43	1.29	0.59	0.007	0.22	2.26	0.87
WAL	0.12	0.32	1.62	0.93	0.012	0.12	3.09	0.60
NPS	0.11	0.27	1.88	0.47	0.005	0.20	2.34	0.56
YTB	0.13	0.67	0.55	0.63	0.015	0.32	1.63	0.82
GRAND MEAN	0.116	0.35	1.52	0.72	0.009	0.17	2.46	0.72

NOTE: The grand mean values for beach face and offshore slopes are the average for all seven sites, the mean grain size did not include these from YTB that are almost 50% larger than the average of others.

Table 5.1.b. Bay Beach Slope and Sediment Size

SITE	POSITION	BEACHFACE SLOPE		SEDIMENT FALL '89		BEACHFACE SLOPE		SEDIMENT SPRING '90	
		FALL '89	( $\phi$ )	SIZE	SORT.	SPRING '90	( $\phi$ )	SIZE	SORT.
HI2	Left bay	0.11	1.30	0.52		0.13	1.20	0.79	
	Mid bay	0.12	0.95	0.64		0.15	1.07	1.06	
	Right Bay	0.13	1.40	0.88		0.14	1.09	1.00	
CHP	Left bay	0.11	1.61	0.81		0.12	1.06	0.87	
	Mid bay	0.10	1.57	0.59		0.10	1.98	0.53	
	Right bay	0.11	1.84	0.42		0.09	1.69	0.52	
DMF	Left bay	0.10	1.19	0.60		0.07	1.43	0.93	
	Mid bay	0.13	0.93	0.58		0.12	1.50	0.67	
	Right bay	0.12	1.26	0.52		0.06	0.89	0.75	
WAL	Left bay	0.12	1.88	0.77		0.12	1.87	0.83	
	Mid bay	0.13	1.47	1.12		0.14	1.39	1.09	
	Right bay	0.11	1.86	0.81		0.12	0.76	0.68	
NPS	Spiral	0.16	1.88	0.43		0.16	1.76	0.41	
	Mid bay	0.11	1.92	0.44		0.11	1.74	0.56	
	Tangential	0.07	1.89	0.55		0.09	1.33	0.77	

Note: For the convenience to get a reference on sediment diameter in mm, refer to the following: 0.000  $\phi$  = 1.000 mm; 1.000  $\phi$  = 0.5000 mm; 1.5000  $\phi$  = 0.353 mm; 2.000  $\phi$  = 0.250 mm.

Fig.5.1 NEARSHORE PROFILES AT DMF

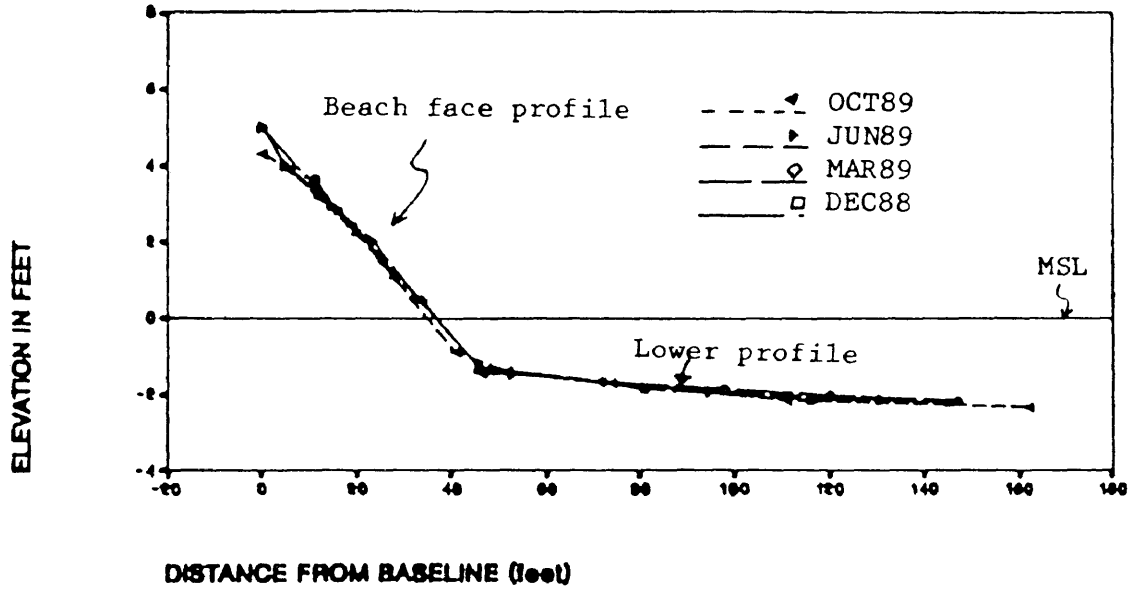


Fig.5.2. NEARSHORE PROFILES AT WAL

PROFILE 7.

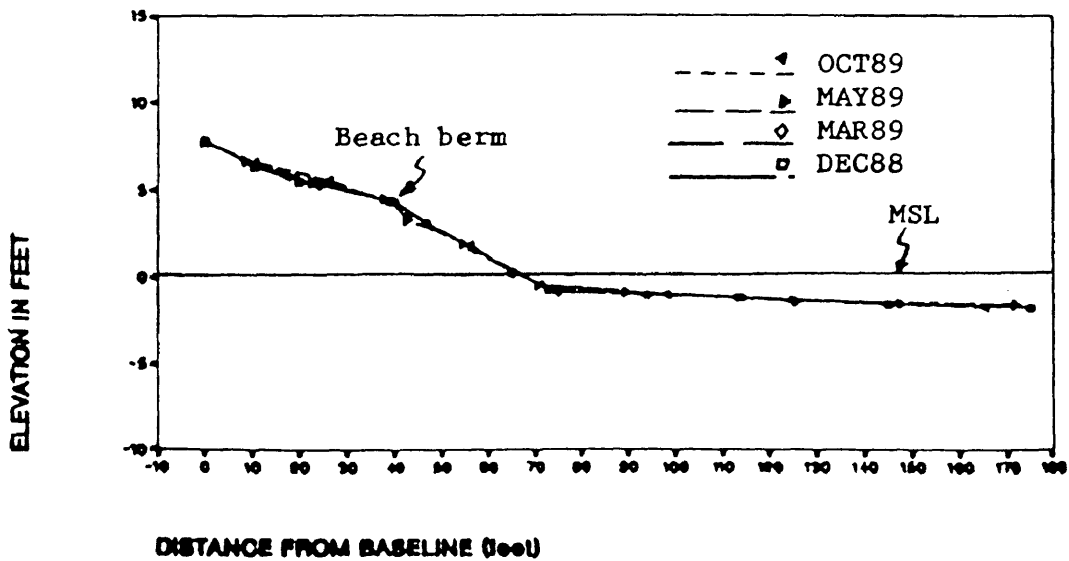


Fig. 5.3. NEARSHORE PROFILES AT NPS

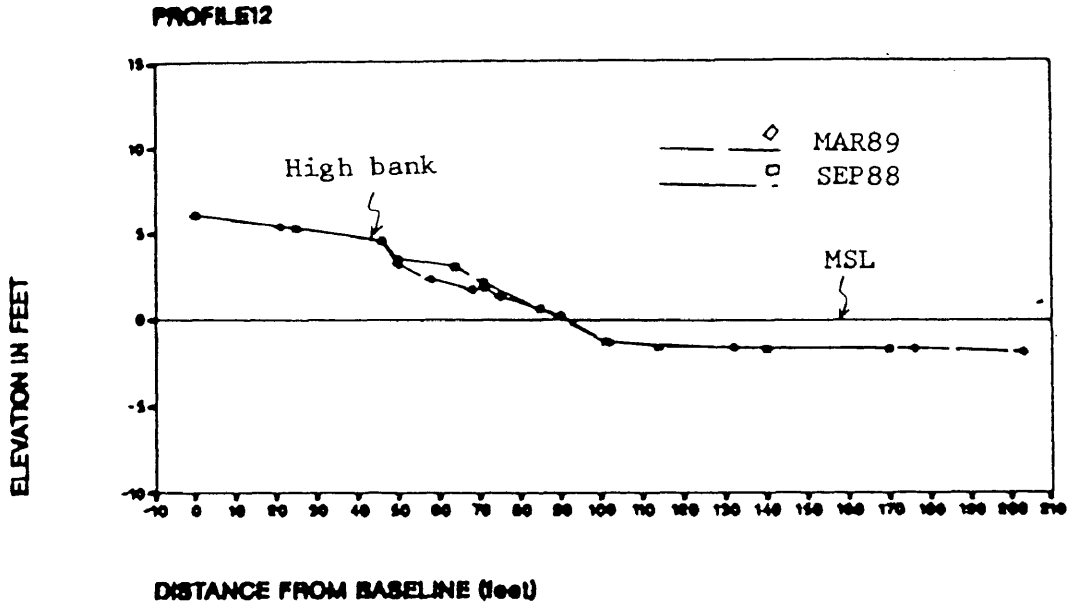


Fig. 5.4. NEARSHORE PROFILES AT NPS

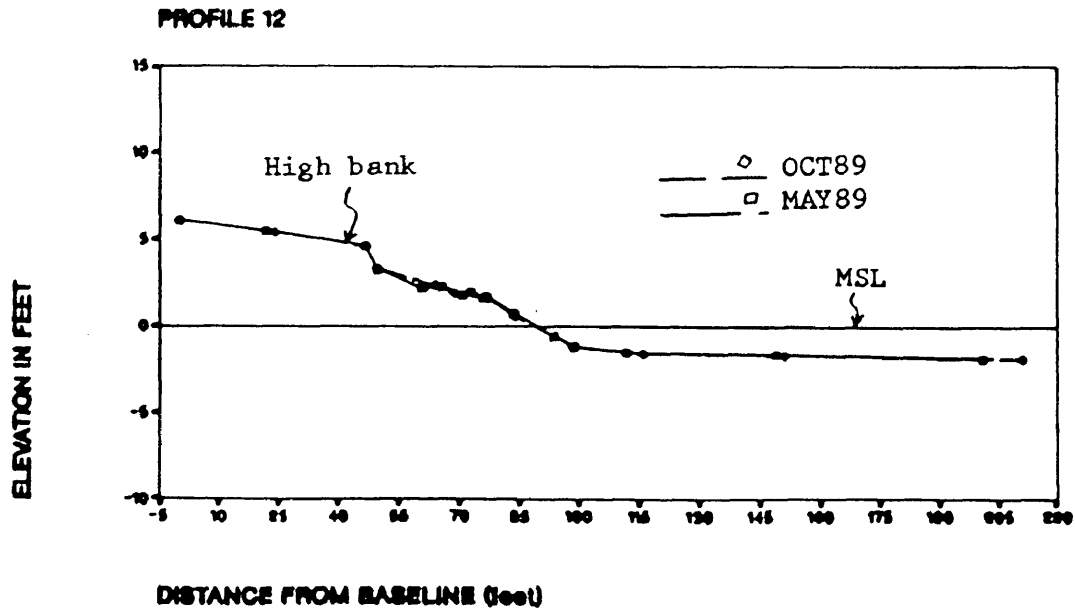


Fig.5.5. NEARSHORE PROFILES AT YTB 1.

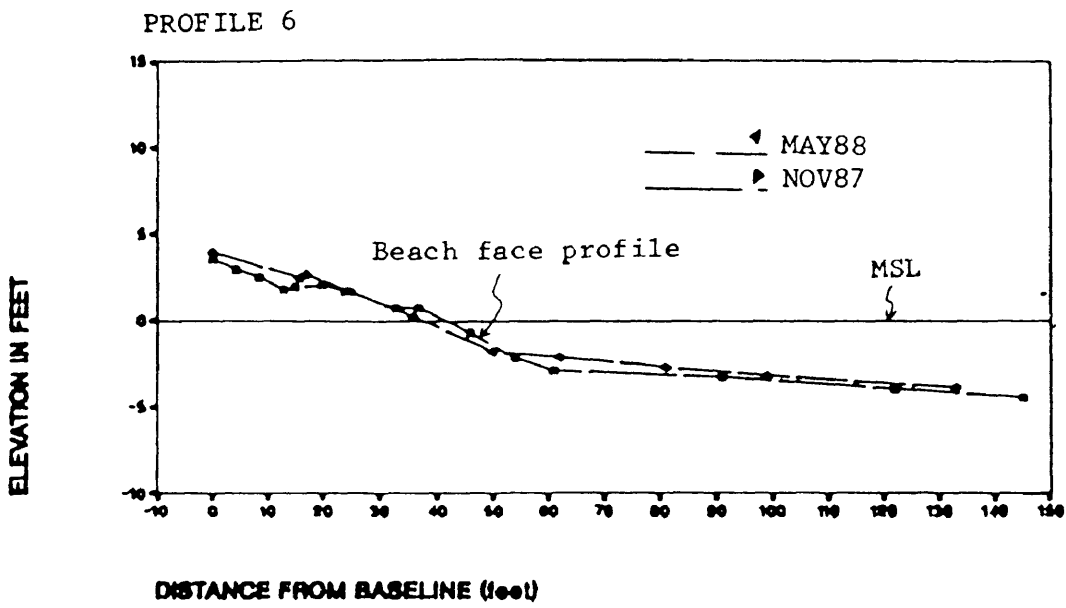
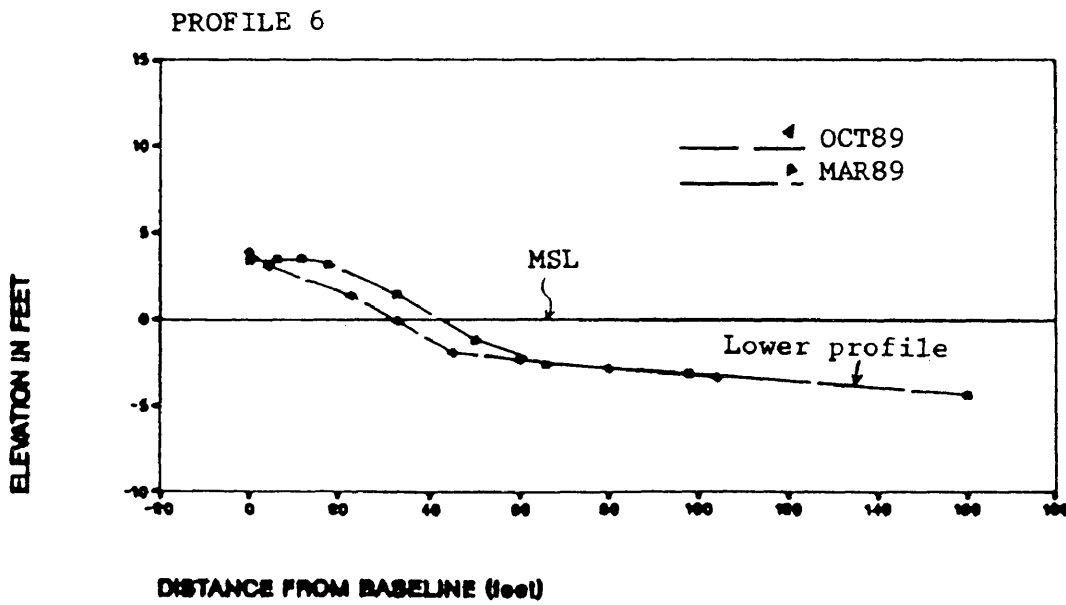


Fig.5.6. NEARSHORE PROFILES AT YTB 1.



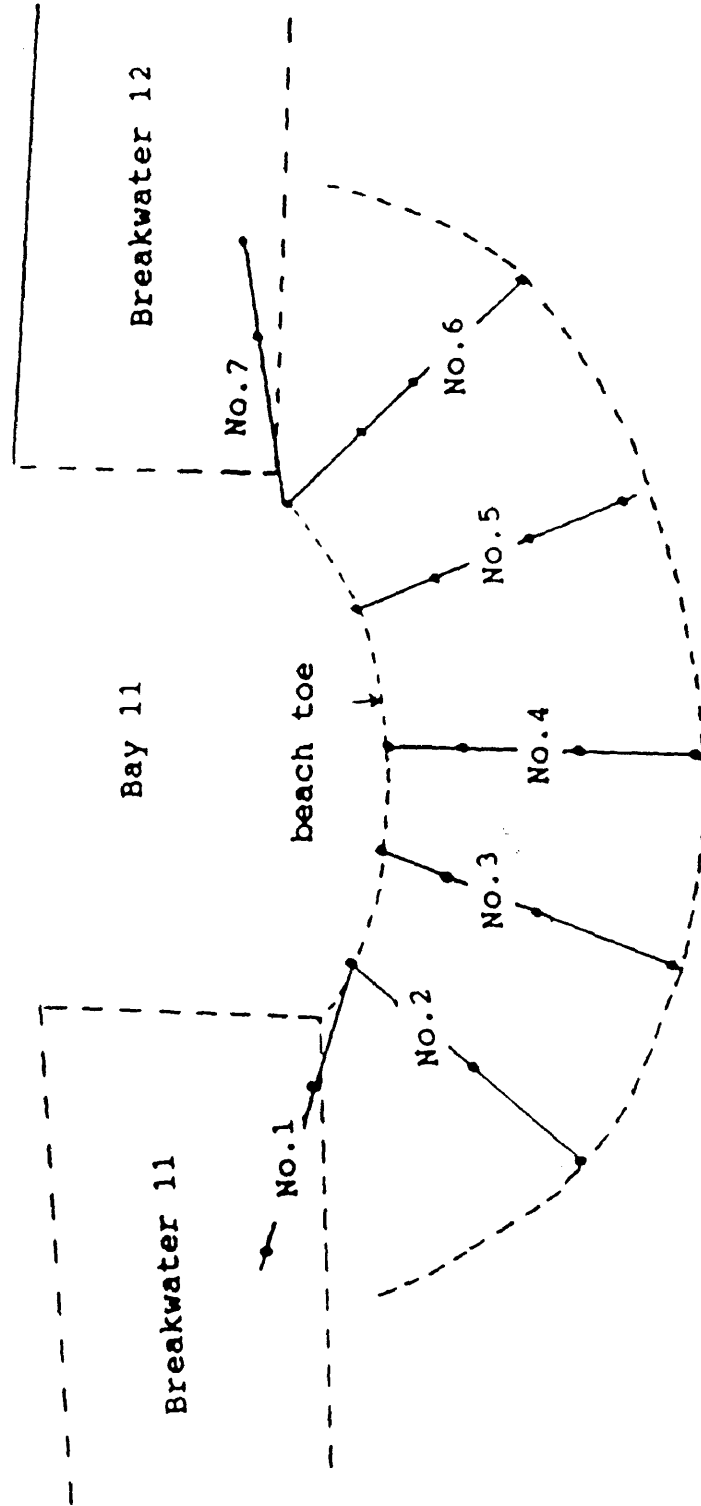
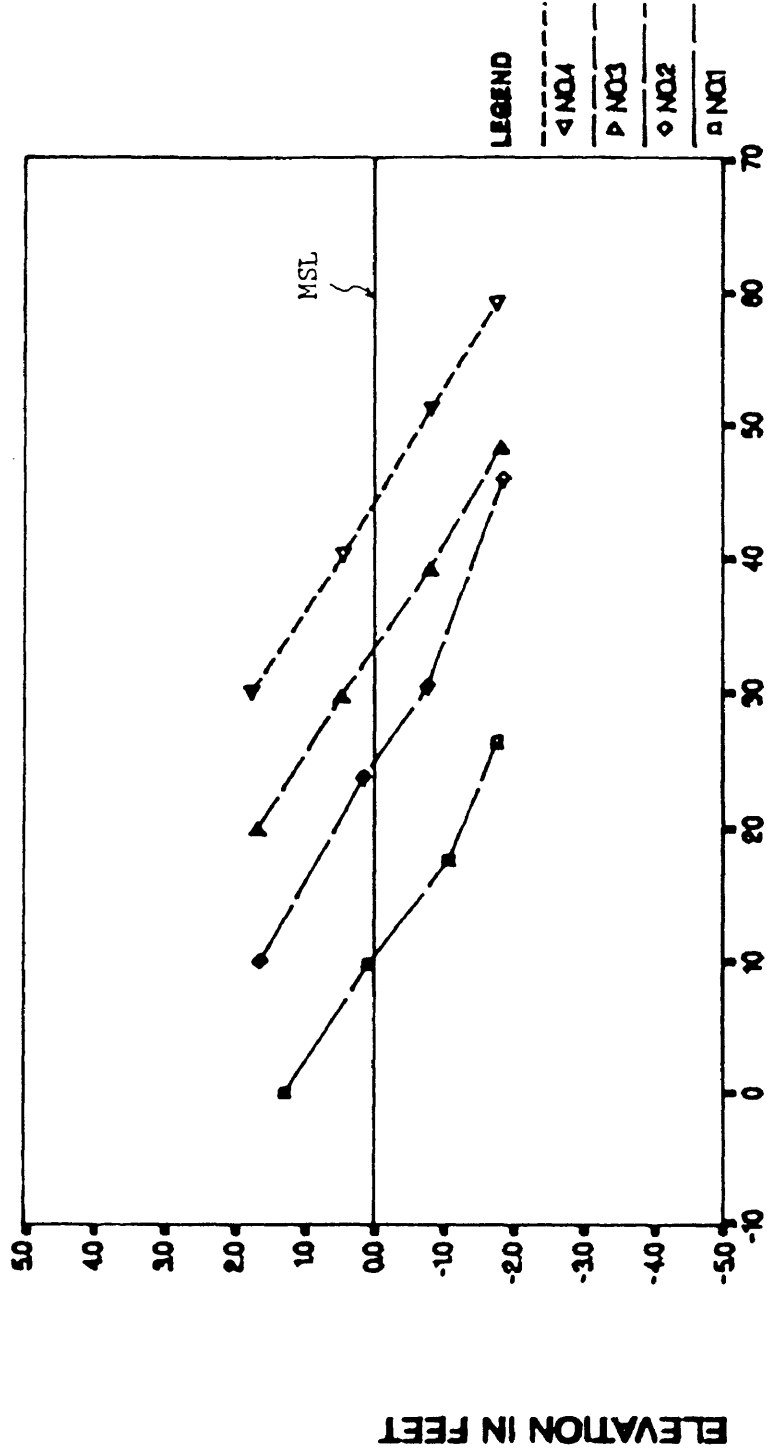


Fig.5.7. A schematic digram showing the measurements on Bay 11 at HI2, Nov.,1989. Profiles No.1 through No.7 corresponde to the slope numbers in Figures 5.8 and 5.9.

Fig. 5.8.

# BEACH FACE PROFILE

H12.



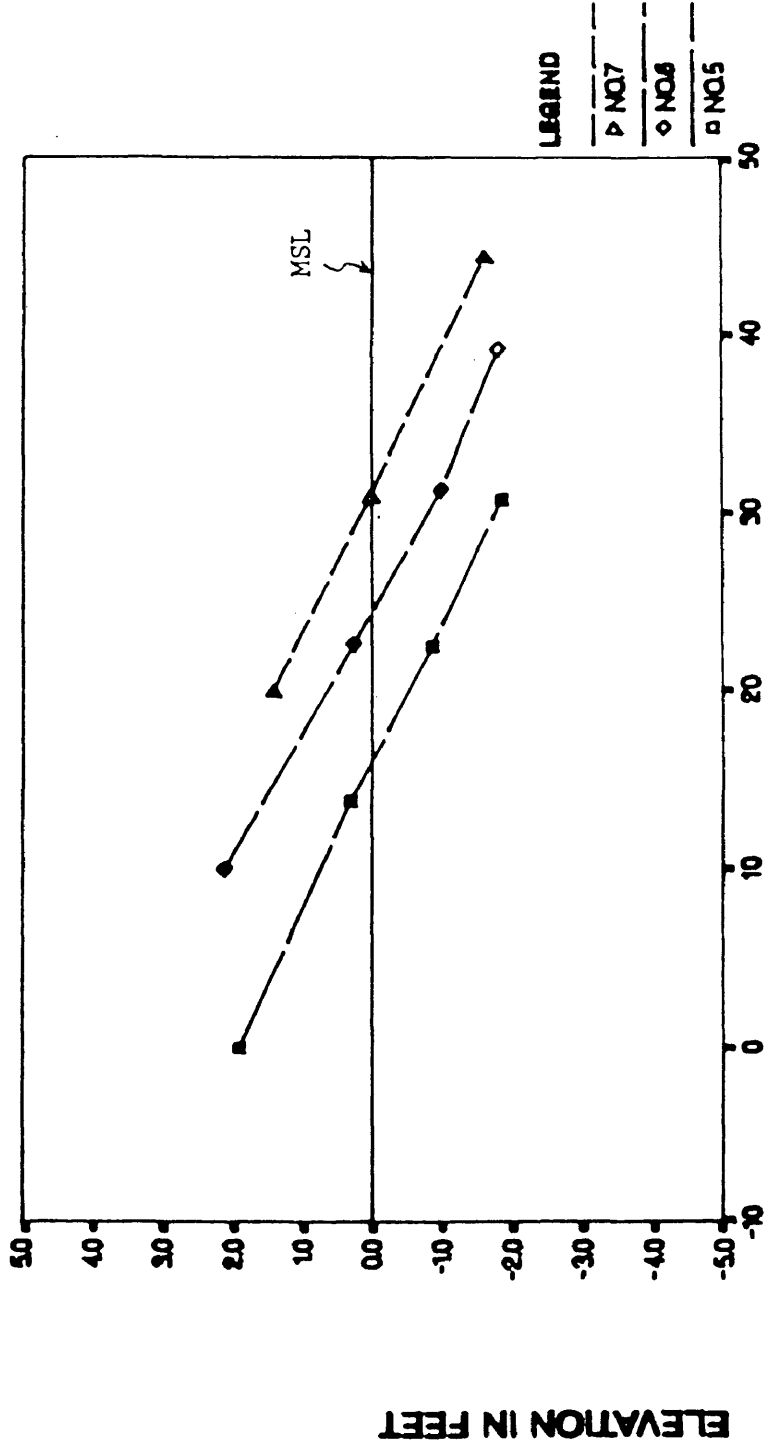
DISTANCE IN FEET

MEASURED IN OCT. 1960

Fig. 5.9.

# BEACH FACE PROFILE

H12, NQ5-8



DISTANCE IN FEET

MEASURED IN OCT. 1980

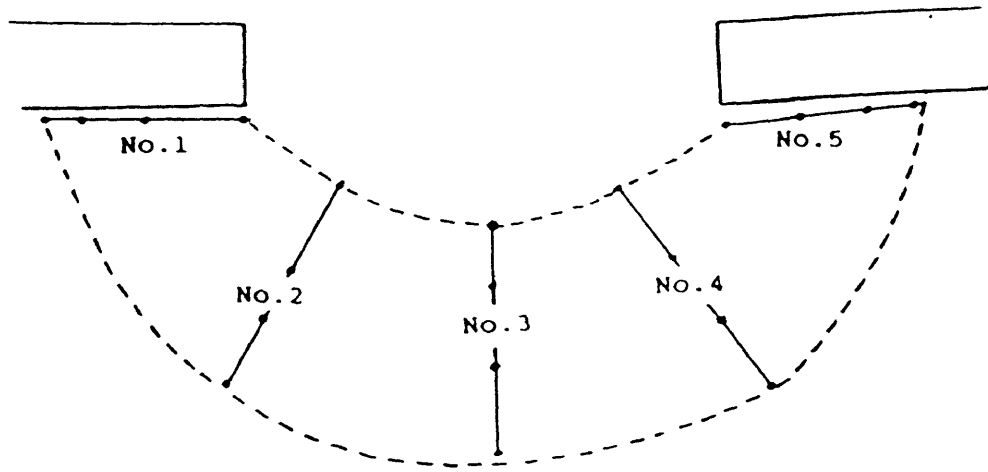
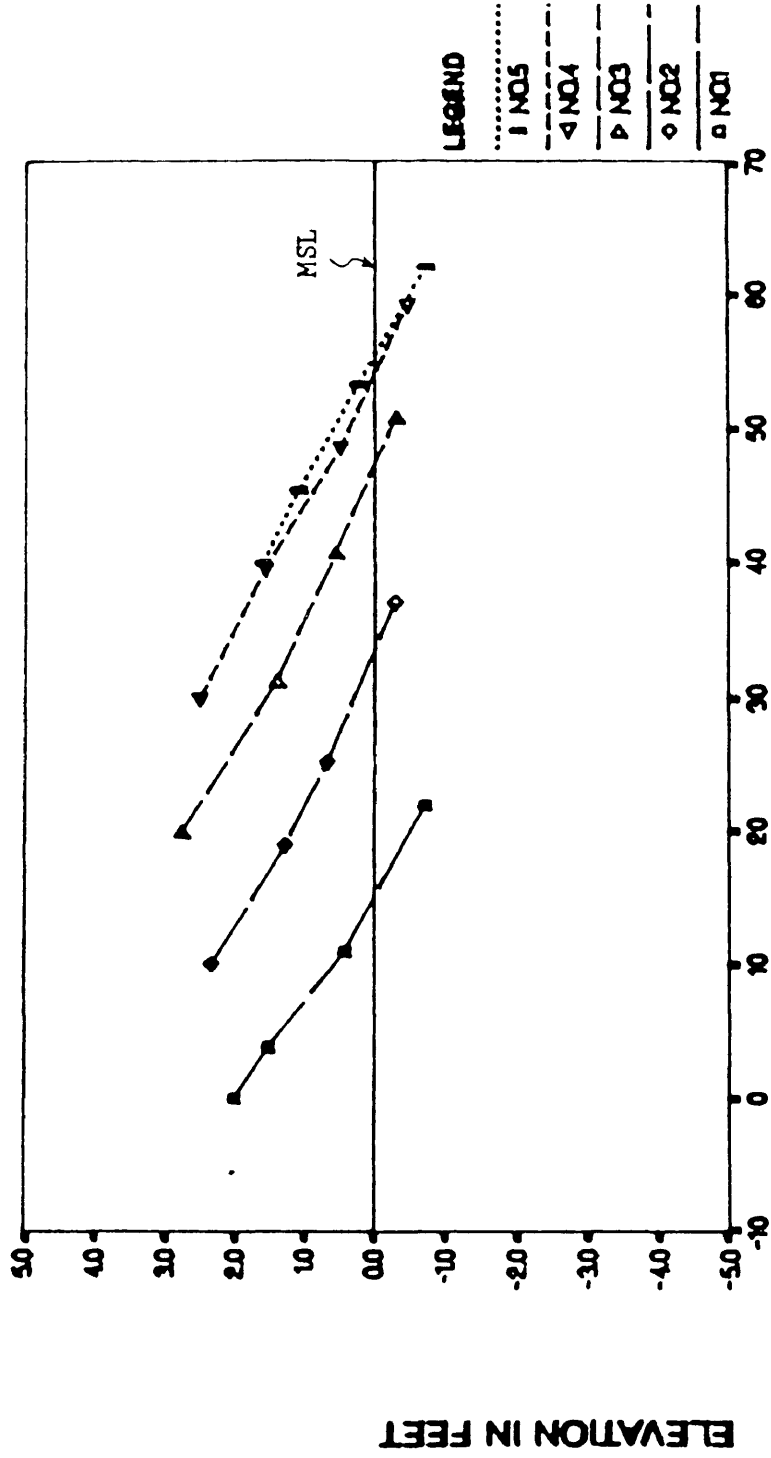


Fig.5.10 A schematic diagram showing the measurements on Bay C, CHP, Oct., 1989. Profiles No.1 through No.5 along bay beaches correspond to the numbers in Fig.5.11.



Fig. 5.11

# BEACH FACE PROFILE CHP, BAY B.



DISTANCE IN FEET

MEASURED IN OCT. 1968

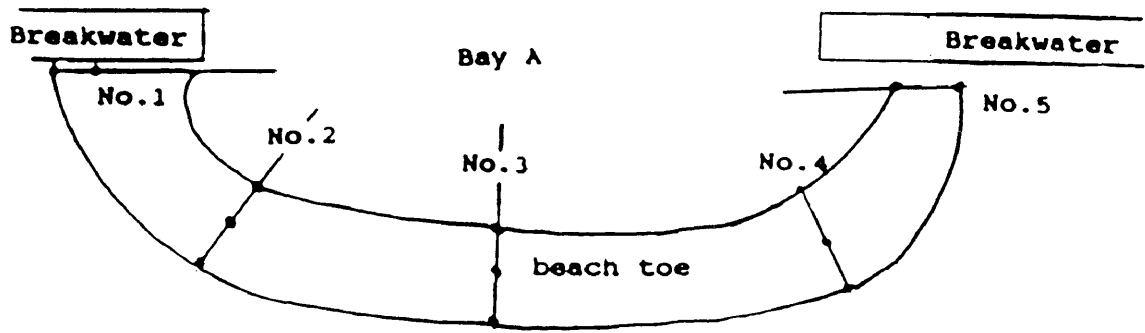
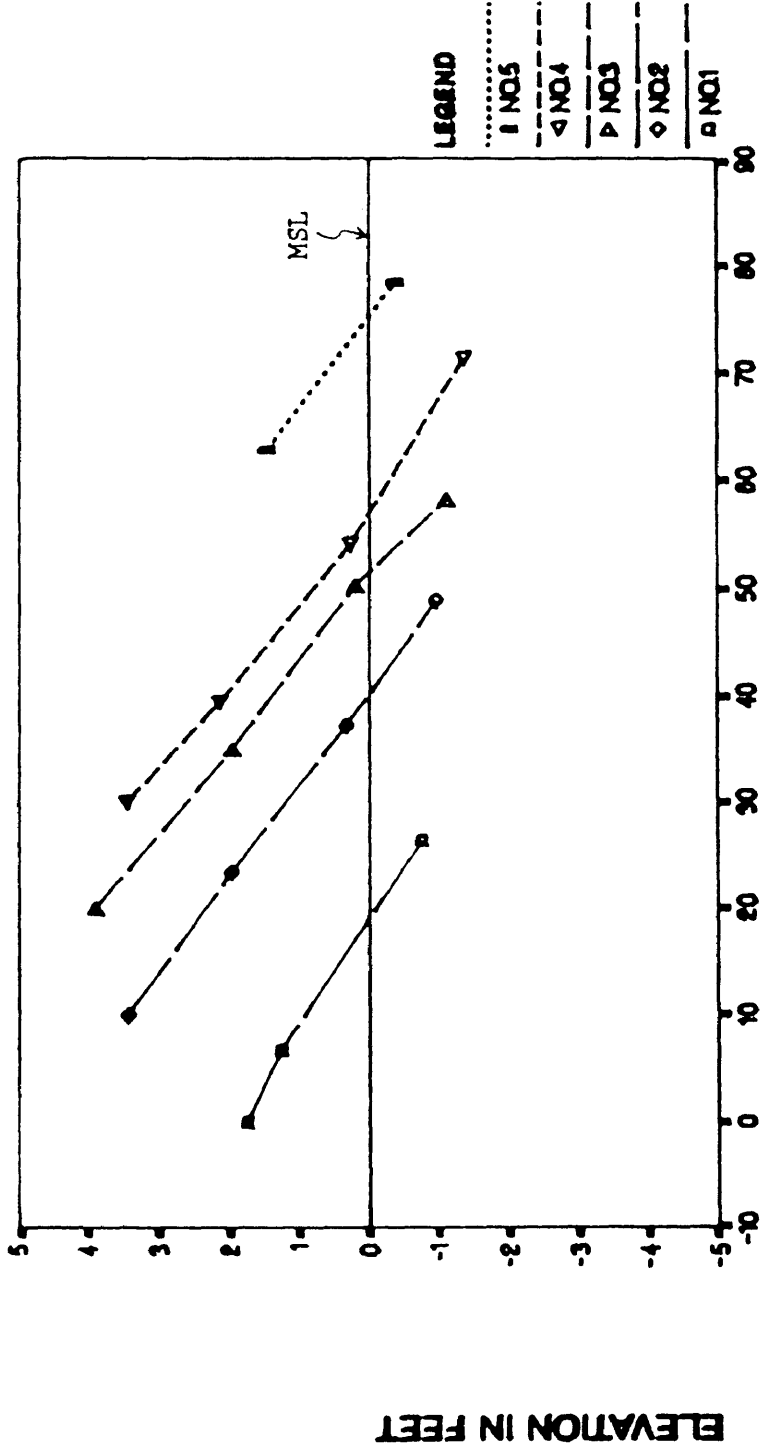


Fig.5.12. A schematic digram showing the measurements on Bay A at DMP, Oct.,1989. Profiles No.1 through No.5 along bay beaches correespond to the numbers in Fig. 5.13.

Fig. 5.13.

# BEACH FACE PROFILE

DMF, BAY A, NO1-5



DISTANCE IN FEET

MEASURED IN OCT. 1969

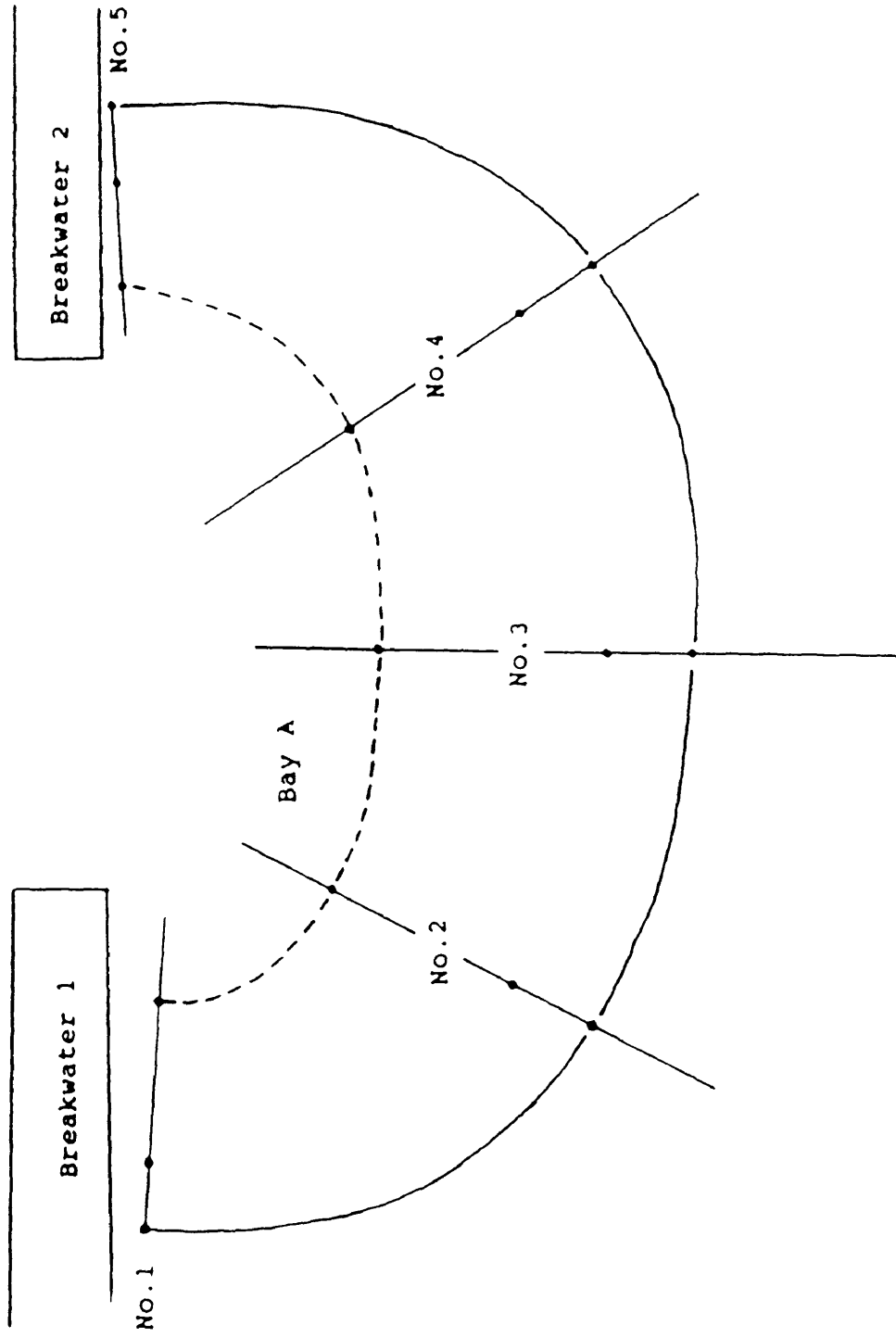
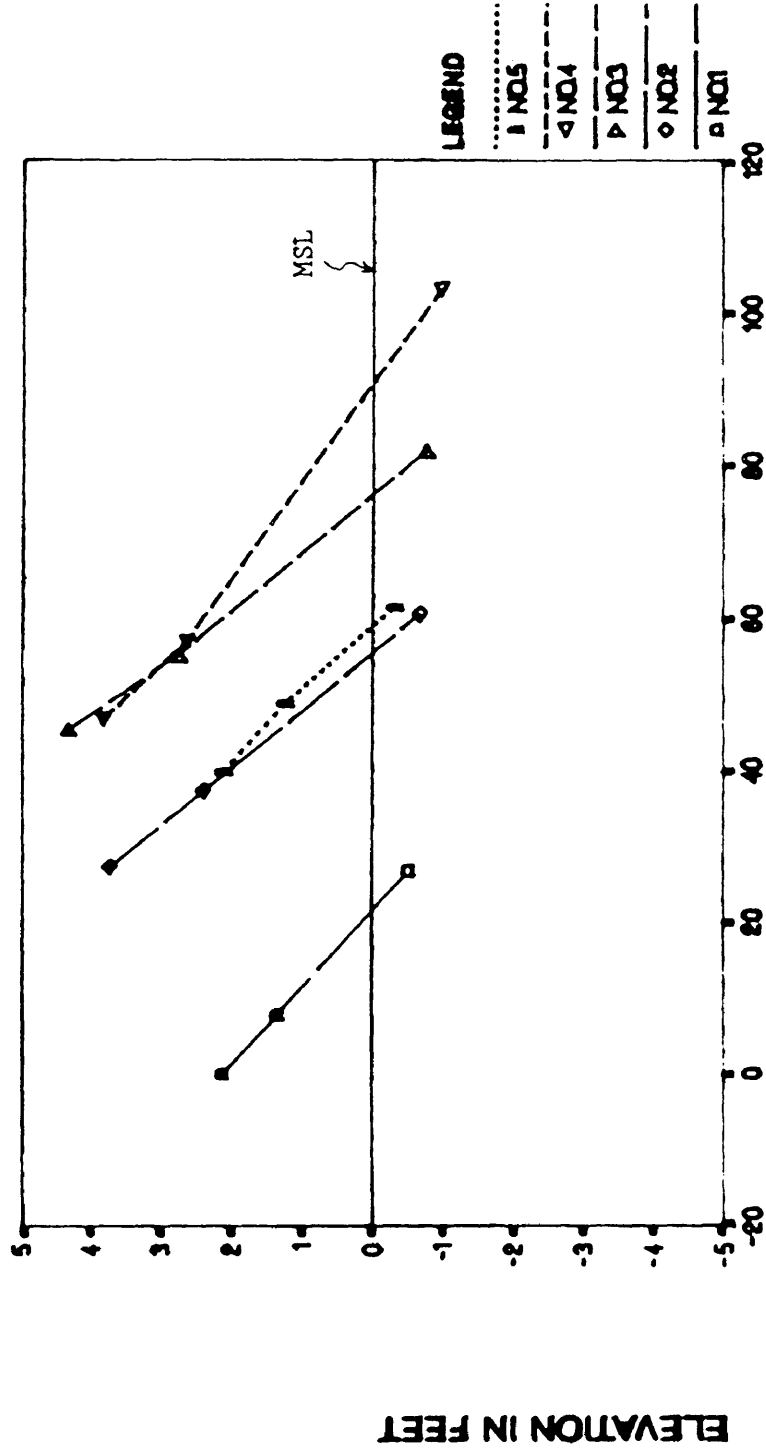


Fig. 5.14. A schematic diagram showing the measurements on bay A at WAL, Oct. 1989. No.1 through No.5 represent profiles measured, which correspond to the numbers in figures 5.15.

Fig. 5.15.

# BEACH FACE PROFILES

WALTRIP, NO.1-5



DISTANCE IN FEET

MEASURED IN OCT. 1968

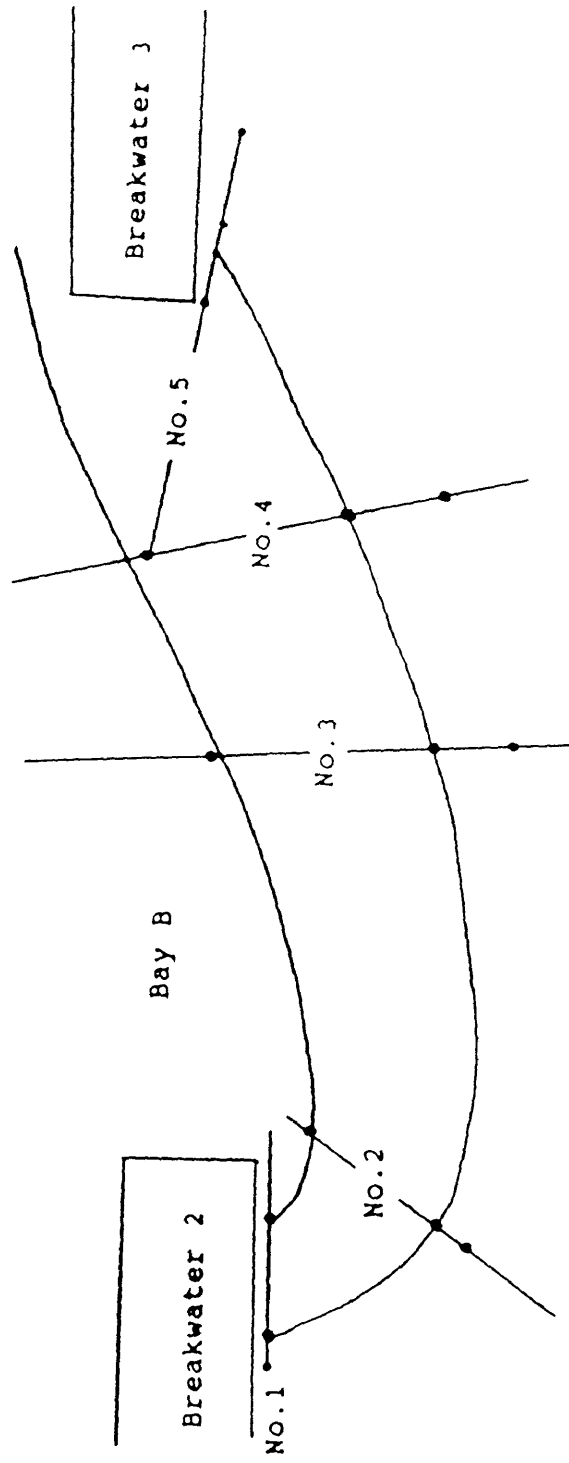
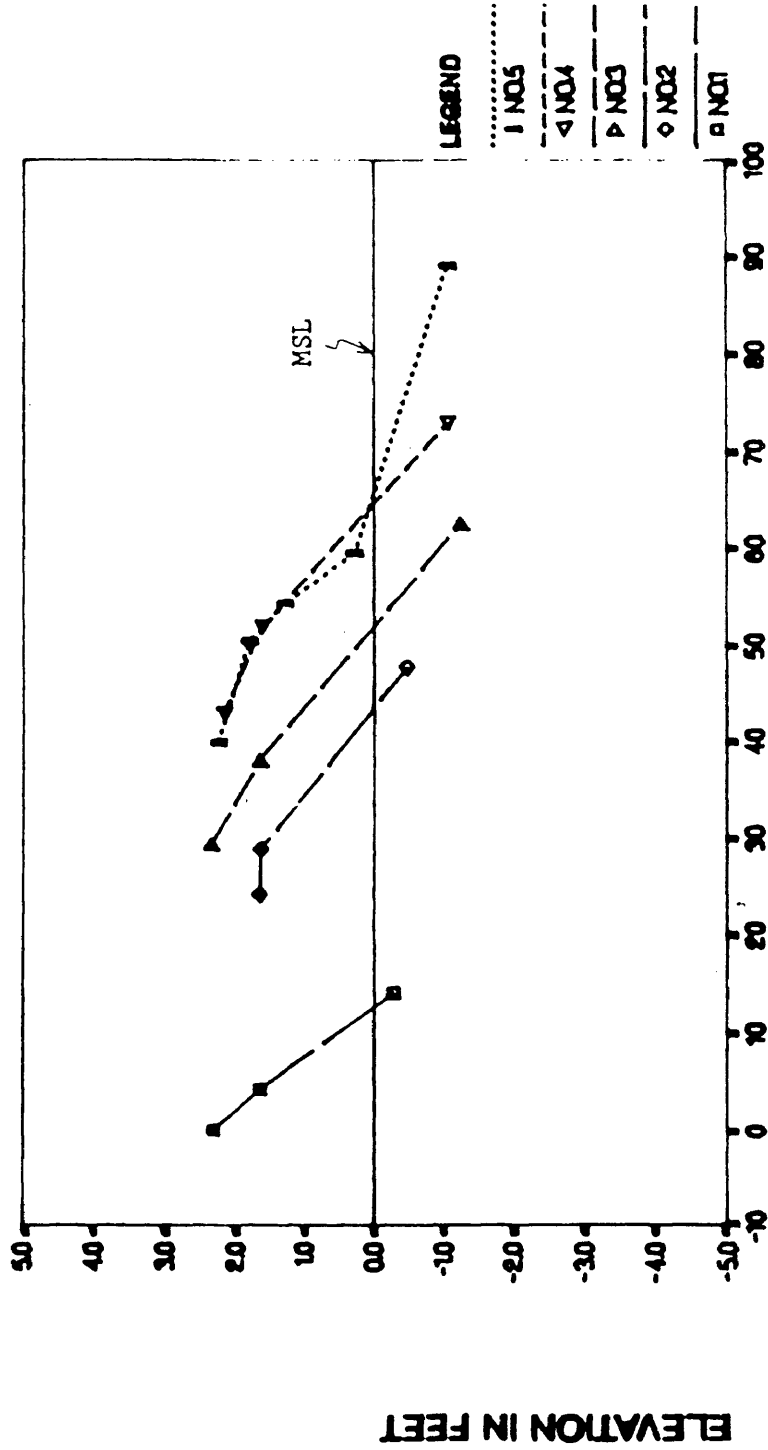


Fig. 5.16. A schematic digram showing the measurements on bay B at NPS, Oct. 1989. No.1 through No.5 represent profiles measured, which correspond to the numbers in figure 5.17.

Fig. 5.17.

# BEACH FACE PROFILES

NP8, BAY B, NO1-5



DISTANCE IN FEET

MEASURED IN OCT. 1968

## 5.2. Sediment Characteristics in the Study Area

Sediments in the study area are basically quartz based materials though sediments of some sites are more shelly (NPS, YTB and CHP). There are no great difference in the average density among the sites, being around 2.65. Beach fills/nourishments were made at HIH, HI2, DMF, WAL and YTB. The beach fill quantity is limited, this can be seen from table 6.1. Most beach fills were already completed at the beginning of this study. The average grain size of the fills are 0.40mm for HIH and HI2, 0.45 for DMF and WAL.

Sediment samples are taken along selected profiles. As pointed out by Boon (1988, p1626) when considering sediment diameter,  $D$ , as one of the environment factors the more representative sediment samples are those taken from the beach face and offshore. The sediment samples taken near the wave step were too coarse and extent limited. The representative grain diameters were taken as the average of a few sediment samples taken on different dates but from the same beach face for upper segment and nearshore for the lower profile segment. The final results of sediment analysis are also presented in Table 5.1. In this table, the Moment Measure Mean, is used when expressing average grain size resulting from a computational method (not graphical method). It gives a truer picture than the graphic method. This is because it is supposed that every grain in the sediment affects the measure in the computation. However, the median obtained graphically is merely the reading of the diameter at the 50% mark of the cumulative curve. It is not affected by the character of the rest of the curve. Table 5.2 shows the horizontal sediment size distributions along bay beaches between



breakwaters and headlands sampled in Oct.1989.

Table 5.2. Sediment Size Distribution Along Bay Beaches

		MIDDLE BAY	RIGHT BAY	SITE No.
LEFT BAY		( $\phi$ )	( $\phi$ )	
HI2	1	1.425	1.539	1.395
	2	0.281	1.479	1.036
	3	0.328	1.310	1.226
	4	1.181	1.123	1.683
	5	2.005	1.923	2.487
	MEAN	1.044	1.475	1.565
	TOTAL MEAN	= (1.044+1.475+1.565)/3 = 1.361		
CHP	1	1.513	1.441	1.267
	2	1.900	1.371	1.847
	3	1.724	1.074	1.665
	4	2.063	1.845	1.709
	5	2.570	2.474	2.207
	MEAN	1.952	1.641	1.739
	TOTAL MEAN	= (1.952+1.641+1.739)/3 = 1.777		
DMF	1	1.570	1.331	1.755
	2	1.412	0.871	1.480
	3	0.601	0.612	0.571
	4	2.424	1.991	1.106
	5	2.469	2.913	2.203
	MEAN	1.695	1.544	1.423
	TOTAL MEAN	= (1.695+1.544+1.423)/3 = 1.554		
WAL	1	1.182	0.949	0.820
	2	1.553	1.485	1.791
	3	1.075	0.908	1.261
	4	2.786	2.020	2.633
	5	2.985	3.072	3.192
	MEAN	1.916	1.687	1.939
	TOTAL MEAN	= (1.916+1.687+1.939)/3 = 1.847		
NPS	1	1.662	1.787	1.819
	2	1.714	1.708	1.541
	3	1.749	1.651	1.683
	4	2.116	2.354	2.346
	5	2.222	2.273	2.268
	MEAN	1.893	1.955	1.931
	TOTAL MEAN	= (1.893+1.955+1.931)/3 = 1.908		

(spiral part)

(tangential part)

Table continued:

SUM	1	0.114	1.003	0.391
	2	1.103	0.814	0.766
	3	0.480	-0.034	-0.252
	4	0.220	1.151	1.196
	5	0.902	1.519	1.750
	MEAN	0.564	0.891	0.770
		(spiral part)		(tangential part)
	TOTAL MEAN	= (0.564+0.891+0.770)/3 = 0.474		
YTB	1	0.696		0.786
	2	0.944		0.551
	3	0.555		0.264
	4	-0.133		0.447
	5	0.991		2.104
	MEAN	0.611		0.831
	TOTAL MEAN	= (0.611+0.831)/2 = 0.721		

---

were collected. 1 - backshore; 2 - berm; 3 - beachface; 4 - beach toe;  
5 - offshore.

## 6. DISCUSSIONS AND CONCLUSIONS - PROFILES

### 6.1. General Characteristics of Nearshore Profiles

From the data analysis in the previous chapters, a general picture of beach and nearshore profiles can be obtained: the whole profile is two segmented. The upper segment is the beach face, from the beach berm to beach toe or wave step (Dean, 1990, and refer to Komar, 1976 for the definition of beach face). This segment is more or less linear, and best represented by

$$h=M_1x \quad \text{or} \quad h=x\tan\beta_1 \quad (6-1)$$

where  $M_1$  is beach face slope,  $x$  the distance offshore from beach berm (Dean used  $h=Ay$  in his 1990 theoretical work). The lower segment is the offshore section, from beach toe waterward. This segment can be well described by either

$$h=Ax^m \quad (6-2)$$

or

$$h=M_2x \quad \text{or} \quad h=x\tan\beta_2 \quad (6-3)$$

where  $M_2$  is the nearshore profile slope. Equation 6-2 has the same mathematical form as Bruun-Dean's model, but the mechanism leading to such a profile is not totally the same. This is because that this formula was originally derived based on the assumption of uniform average wave energy dissipation rate per unit water volume ( $D_v$ ) under FULLY dissipative surf zone condition of open ocean environments. The

areas of this study are located in very fetch-limited environments. The wave climate is incomparable with those of open ocean. The surf zone width is also incomparable with that of open ocean. It is very narrow in this study area and sometimes disappears. Therefore, the mechanisms of development of profiles can not be totally the same (see section 6.2 for further discussions).

The variation of the profiles from a straight line was low, being only 0 - 4% of the total variance for beach face; and 3.5% of the total variance for lower profile. The average value of  $M_1$ , the beach face slope, is 0.12 in this study (Fig.6.1 and 6.2). The average value of  $m$ , shape factor, is 0.15, and  $A$ , the scale factor, is 0.56 (See Appendix A for the detailed calculation of these two factors). Dean's (1977)  $m$  and  $A$  ranges are [0.5,0.8] and [0.0025,6.31], respectively. The average value of  $M_2$ , the nearshore profile slope, is 0.01, which is a little bit smaller in comparison with a range of the value of this parameter [0.012, 0.020] in the study by Wright et al.(1979). The average beach width in this study is 31 feet with a range [21, 43]. The profiled distance of the lower profile waterward is variable depending on the tidal stage when profiling was made.

When talking about the fitness of a certain mathematical model to the real data, one thing that should be noticed is the "unrealistic" properties that represented by the model. For example, one of the main improvements Dean made in his 1990 work is that on the unrealistic property of the form of the equilibrium beach profile which has an infinite predicted slope at the shoreline. Other examples can be seen from the fitness of Yasso's spiral bay model, LeBlond's mathematical

Fig. 6.1.

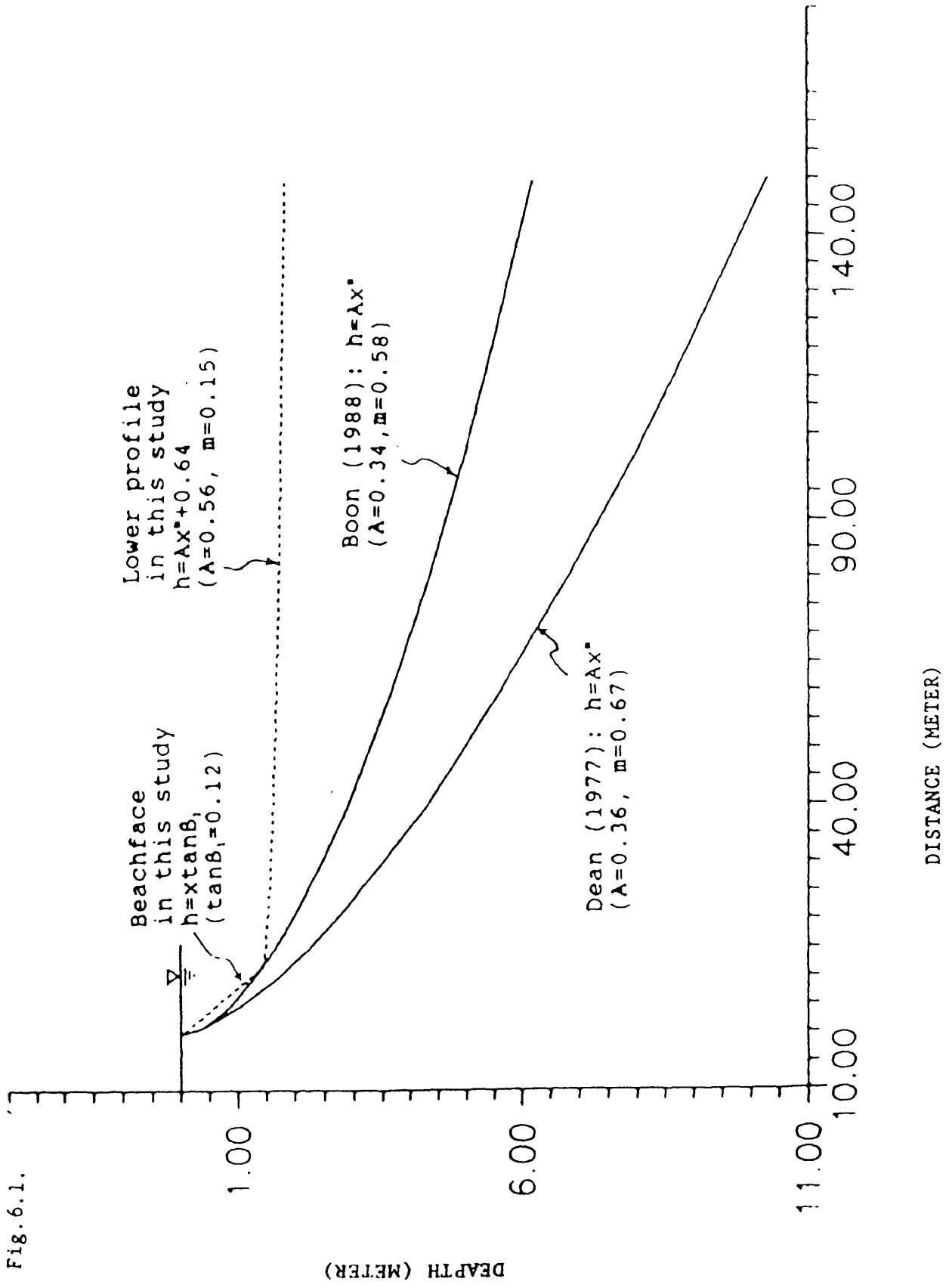
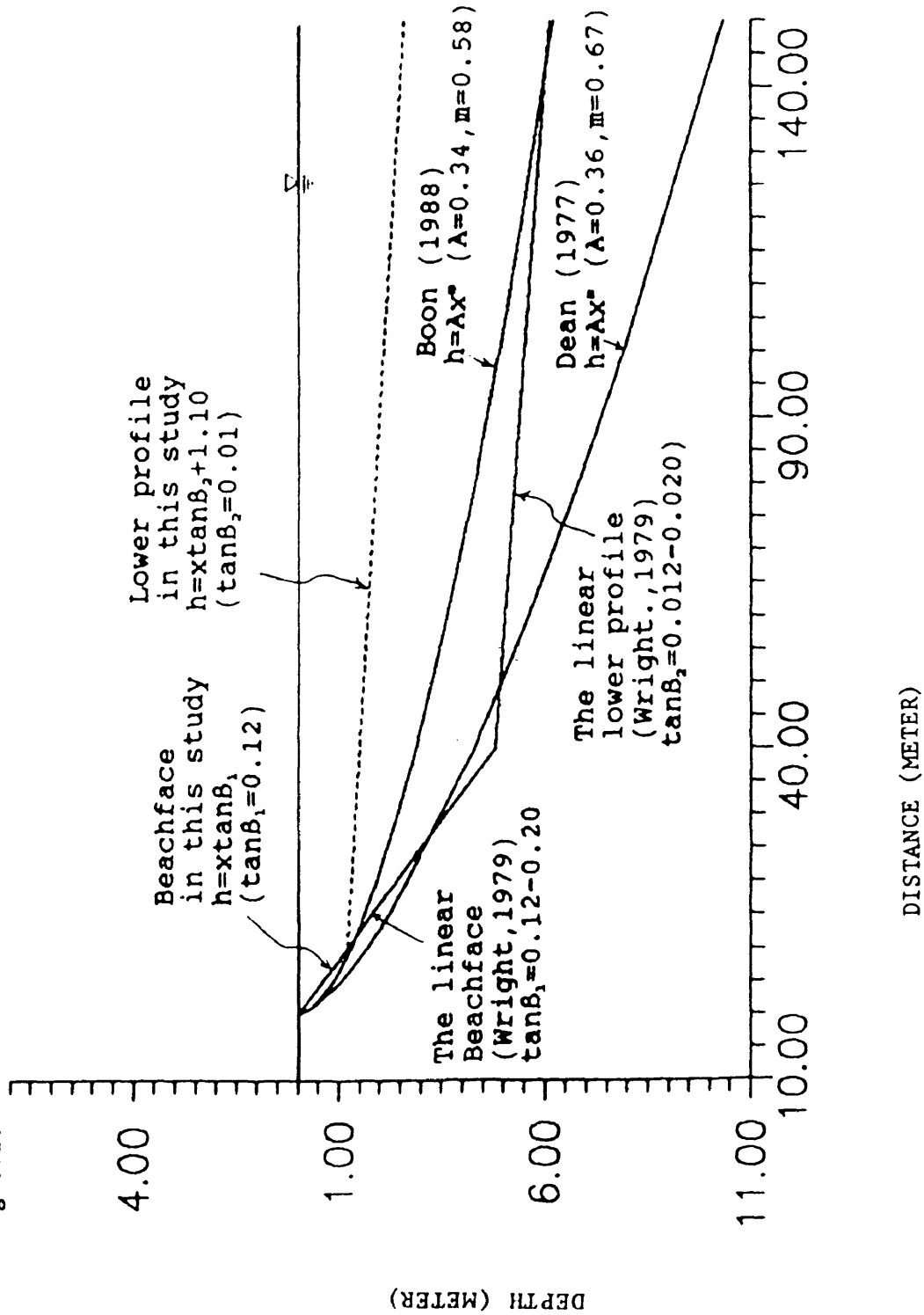


Fig. 6.2.



shoreline model (1972). The same thing is true in this study. When one connects the two linear profile segments together, the joining point/angle is unrealistic in terms of the real world profiles. There is no profiles that have a perfect mathematically described sharp angle between the two segments. However, this unrealistic property represented by the two segment model is much more reasonable than that represented by the single curve model (at least in this study).

The two segment profiles appeared in figures 6.1 and 6.2 from this study are established within the same coordinate. The starting point of the lower profile is the lower end of the beach face profile. Because of the unrealistic properties of the very beginning part of the profile represented by the lower profile model, this part does not appear in the figures of 6.1 and 6.2. Although there is no reference or method in the literature dealing with this kind of jointing of model curves, from the good fitness represented by these curves to the real profiles in the study area it can be said that this kind of method is reasonable.

Boon (1988)'s profile is different from Dean (1977)'s, being more concave upward near the beach face with a average shape factor value equal to  $1/2$ . It is probably because Boon's data was from a different environment with different beach state and carbonate based materials which response differently to the local wave climate than Dean's mostly quartz based beach materials.

According to Wright et al (1979), the steep, linear beach face and the linear gentler nearshore profile are one of the major morphological characteristics of reflective beaches (Fig.6.3). The beach profile in figure 6.3 is very similar to those in this study. The surf scaling

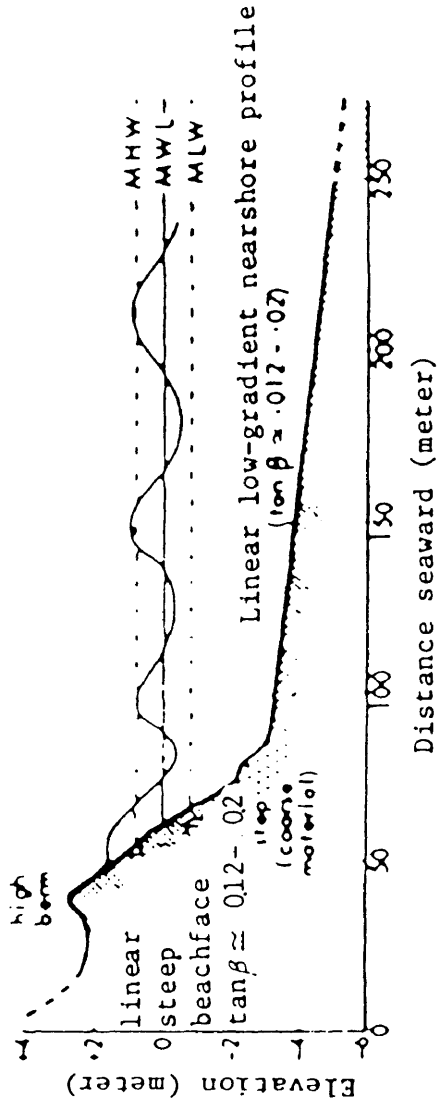


Fig.6.3. Typical cross-sectional profile of a reflective beach (after Wright 1979).



parameter,  $\epsilon$ , is one of the main standards of beach state classification (Guza and Brown, 1975; Guza and Inman, 1975, Wright 1979 and 1983). It has been shown theoretically and in the laboratory that wave breaking characteristics, runup amplitude, and the degree of inshore resonance are dependent on this parameter. Table 6.1 shows its variation in this study (refer to Table 6.3 for the parameters that are used to calculate the surf-scaling parameter).

Table 6.1. Surf scaling parameters in the study area

SITE	HIH	HI2	CHP	DMF	WAL	NPS	YTB	AVERAGE
$\epsilon$	4.03	3.64	4.23	4.76	4.14	4.03	3.47	4.04

The average  $\epsilon$  value of 4.04 should represent a situation of partial wave reflection environment, more detailed discussions on this will be presented a little bit later.

It is rather obvious that Dean (1990) made a great improvement theoretically on his previous model in his new work (Fig.6.4). It is believed that such an improvement was resulted from the fact that the mathematical formula  $h=Ax^m$  can not predict a non-monotonous curve or profile. A certain form has to be introduced to predict the two-segment characteristics of some beach profiles in nature. The early Bruun-Dean's model is only a very general theoretical one. When one goes further to apply this model to real situations, problems arise: where should be the starting modeling point on a beach? from beach berm? mean high high water? mean sea level? or mean low low water (beach toe in this study)? The beach face profile can not be excluded from the discussions and predictions of beach and nearshore profiles. It is these problems at

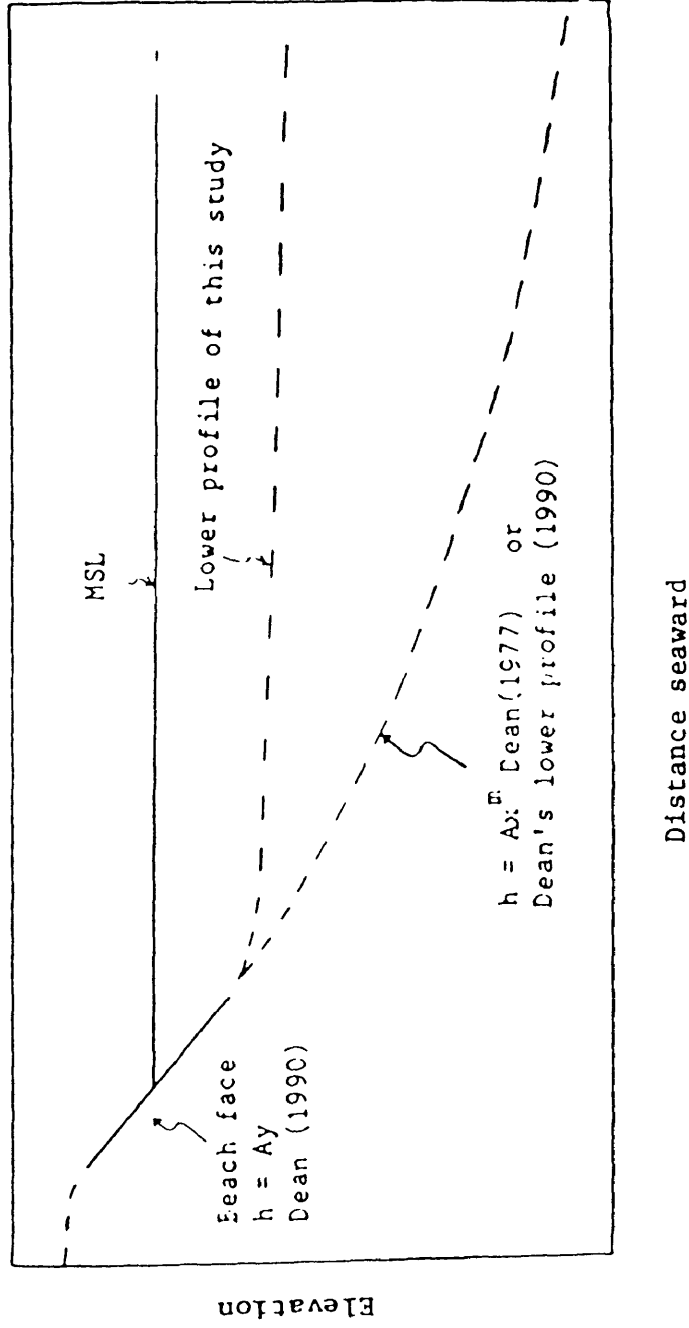


Fig.6.4. Comparisons of Dean's new work (1990) and the work in this study of beach profiles.

least partly that made Dean improve his previous work greatly. This shows again the fact that like wave prediction the state of the art of a certain model on beach processes largely depends on the increase of data collection, when data accumulates model evolves.

## 6.2. The Mechanisms of Profile Development

At present stage, there is still not a totally satisfactory explanation on the mechanisms of beach and nearshore profile development. This can be seen from various points of view in the literature and the ever changing or improvement on the previous models with the increasing accumulation of data and analysis.

The following discussions will be mainly around two groups of ideas: The first one is represented by the Bruun-Dean's model being started in 1954. The focus has been around the model form,  $h=Ax^M$ , and its origination or the mechanisms of profile development, being more heavily relied on the traditional descriptive methods. The second one is represented by the work done by Inman and Guza (1975), Wright et. al. (1979, 1982a, b, c; Short, 1979; Wright and Short 1983, 1984). In this group, the focus has been on the beach morphology and dynamics, or "morphodynamics" which is a term frequently used in the studies by Wright et al. One of the obvious characteristics of their work is the more rigorous analysis on the nearshore dynamics such as the wave behavior in surf zone. They classify beaches into dissipative and reflective extremes and the intermediate states between the extremes.

Like solving a complicated mathematical problem, there may exist a couple of ways to get the same correct answer. The co-existence of different ideas is a good way to get the final goal. The following

discussions will focus on these two groups.

(1). As briefly mentioned earlier the Bruun-Dean's model was derived theoretically from the mechanism of uniform wave energy dissipation rate per unit water volume in fully dissipative surf zone. The wave dissipation is due to breaking of waves in the surf zone in which the ratio of  $H_b/h$  is basically constant ( $k=H_b/h=0.78$ ). The bottom friction is insignificant which only occurs in the bottom boundary layer. Because of the peculiar characteristics such as the limited variable fetch size, not fully dissipative surf zone, complex shoreline configuration and bottom topography in this study, it is obvious that the mechanism of the profile development proposed by Dean can not be simply moved to this study without any change. Here some efforts are made to try to explain the mechanism of profile development in fetch limited environment.

Because there are still some similarities in the process of profile development in the environments between open ocean and fetch limited river systems, it would be helpful to give a short brief summary here on some relatively new work in this group on the mechanisms of beach profile development.

As implied in Dean's new work (1990) that the establishment of a rational physics-based prediction of equilibrium beach profiles is still difficult due to the complex force system acting on sediment particles. However, in a broad sense, it is rather obvious that sediment particles are acted on by a complex system of constructive and destructive generic "forces" acting to displace the sediment particles landward and vice versa. Constructive forces include landward directed bottom shear

stress due to the nonlinear character of shallow water waves, landward directed "streaming" velocities in the bottom boundary layer (Bagnold, 1946; Phillips, 1966), the phasing associated with intermittent suspended sediment motion, etc. The most obvious destructive force is that of gravity coupled with the destabilizing effects of turbulence induced by wave breaking. Others include the effect of seaward directed bottom undertow currents and forces due to wave set-up within the surf zone (e.g. Svendsen, 1984; Stive and Wind, 1986).

When explaining beach profile development in Caribbean area, Boon (1988) pointed out that the main processes driving nearshore sediment movements are: asymmetric waves, rips, combined wave and steady currents, downwelling and upwelling, gravity flows and "groupy" waves (Wright, 1987).

The most important factors controlling the beach processes in the fetch limited environments of Chesapeake Bay were summarized by Byrne and Anderson (1978). These factors are: the intensity of wave action, the exposure to strong tidal currents, the orientation of shorelines and sediment characteristics. The raised water level by wind set-up during storms in conjunction with the higher tides during the lunar month can enhance the beach erosion. The orientation of the tributary estuaries is also important. The most frequently happening northeast storms attack western shorelines of tributaries with fetches to the northeast and east. All these factors contribute to the development of profiles.

In Dean's new theoretical work, he considers the gravity force as one of the important destructive forces, especially in the development of beach face profiles,

$$\frac{D_*}{M} \frac{\partial h}{\partial x} + \frac{1}{h} \frac{\partial}{\partial x} (EC_g) = D_* \quad (6-4)$$

where the two terms on the left hand side consist of the destabilizing forces due to gravity (first term) and turbulent fluctuations (second term) due to wave energy dissipation.  $M$  is beach face slope,  $D_*$  is the average wave energy dissipation rate per unit water volume,  $x$  is the distance offshore from beach. Equation 6-4 can be integrated to

$$x = (h/M) + h^{3/2} / A^{3/2} \quad (6-5)$$

where  $A$  is related to  $D_*$  by equation 6-6.

$$A = [24D_*(D)/5dg^{3/2} k^2]^{2/3} \quad (6-6)$$

where  $g$  is gravity,  $D$  sediment particle size.  $k = H_b/h = 0.78$  under fully developed wave condition. In shallow water or beach face, the first term in equation 6-4 dominates, simplifying to

$$h = Mx \quad (6-7)$$

In deeper water, the second term dominates with the simplification

$$h = Ax^m \quad (6-8)$$

As stated earlier, Dean's model was derived based on the uniform wave energy dissipation rate per unit water volume under fully dissipative surf zone condition. However, in fetch-limited environment, e.g. the area in this study, the wave climate is incomparable with those of open ocean. Therefore, the mechanism of profile development differ in some aspects. In the case of open ocean, sediment particles are always actively under the influence of wave actions such as the reflection of wave energy, the turbulence from the dissipation of wave energy and the gravity effects. Sediment particles are constantly moving around toward the best equilibrium position with the ever

changing wave conditions. In fetch-limited environment with complex shoreline configurations, however, the influences on sediment particles from waves are smaller. The wave period and length can be as smaller as five to ten times than those of open ocean (wave periods are 2-3 seconds in this study comparing with the common wave period in ocean of more than 10 seconds). The scale of turbulence from waves is much small and the wave energies dissipated on the sediment particles on the bed are much less. The turbulence is only large enough to rigorously disturb sediment during severe weather condition like storm waves. The 2-3 second waves in the study areas are not strong enough to move sediment particles in a rigorous manner. This basic difference in the general dynamical background has to be considered in the application of Bruun-Dean's model when applied in fetch limited environment. The lower profiles are relict from a time when forces were actively at work, being a settling basin. Large quantities of fine sand/silt can stably stay on the bed, no much is moved to the further offshore region. The result of such a deposition of fine materials due to the low wave energy and weaker turbulence is the formation of a gentler bed topography with near linear slope.

(2). Another explanation on the mechanisms of two segment beach profile development is based on the reflective beach characteristics (Inman and Guza, 1975; Wright et al. 1979, 1982, 1983).

According to Wright et al., the steep, linear beach face and the linear gentler nearshore profile are one of the major morphological characteristics in reflective environments. The beach reflectivity is determined mainly by the incident wave amplitude near the breaker

height, wave period, acceleration of gravity and the beach slope.

$$\epsilon = a_1 \omega^2 / g \tan^2 \beta \quad (6-9)$$

Based on the value of this parameter, beaches can be classified into dissipative, reflective and intermediate domains of beach states (refer to chapter 2 for a review on this).

The average  $\epsilon$  value in this study area is 4.04 (Table 6.1) with the range [3.47, 4.76], which indicating a situation of partial reflection environment. The average beach face slope is 0.116, which means the beach angle,  $\beta$ , being greater than  $6^\circ$ , which is one of the two major factors described by Wright et al:  $e < 2.5$  and  $\beta > 6^\circ$  for strong reflective beaches. Therefore, the profiles in this study have the similar appearances as that in figure 6.4 by Wright et al (1979). One thing that should be pointed out here is that some important morphological and dynamical features commonly found in Bowen, Inman (1975) and Wright's studies are not common in this study of fetch-limited environment such as the much larger wave parameters, some well evolved rhythmic beach forms, "unlimited fetches" etc. With all these differences in the general morphodynamic background between open ocean and river water environments and the poorness of study references in the literature on nearshore processes in fetch-limited river systems, a rigorous establishment of the mechanisms on profile development in fetch-limited environment would be an interesting topic large enough for future study. Such a study would need more detailed wave data and analysis like what Wright did (1979, 1982, 1983).

Two major limitations in using the two segment model proposed in this study should be considered: (1). The two segment model is only



valid within the nearshore region. Special cautions should be exercised when using the model to predict profiles in the region beyond 200 meters from beach. This is because the model was established based only on the measured profile data within the region of 150 meters from beach. (2). The two segment model should be used only in fetch limited tributary systems.

### 6.3. Beach Slope and Sediments

Sediments around breakwaters and headlands are mostly derived from local bank erosion, either from the bank behind structures or from adjacent bank erosion. Some fine sediments such as silt and clay are moved by longshore currents, mostly tidal currents as stated by Byrne et al (1978). The coarser sediments like sands and gravel can only be moved alongshore by obliquely incident waves generated by strong winds or wind "set-up" during storm time (Byrne, 1978). It is observed in field that there are often no waves at all during calm weather conditions or weak winds (below 10 MPH) blowing in a direction from land to water. Under such conditions, longshore movement of coarser materials dose not occur.

From table 5.1 in chapter 5 and table 6.2, one can get a general picture of sediment characteristics and bank erosion rate in the study area at which the bank has been supplying materials to the water in the past century. One thing should be pointed out that the erosion rate in the table represents the average of a larger section of shore line including the study site. It dose not necessarily accurately represent the erosion rate at the site in this study in the past few years. It only serves as a general reference. For more detailed information,

refer to Byrne et al (1978).

Table 6.2 Bank Erosion History And Beach Fill

SITE	REACH #	EROSION RATE (ft/100yr)	BEACH FILL (yds <sup>3</sup> )	BEACH FILL GRAIN SIZE (mm)
HIH	197	2.8	1,000	0.40
HI2	196	1.7	1,500	0.40
CHP	189	—	—	—
DMF	305	2.4	10,000	0.45
WAL	305	2.4	—	0.45
NPS	22	0.0	—	—
YTB	25	0.7	—	0.69

Note: — means no sure data available. For detailed information on erosion rate refer to Byrne et al (1978).

Study shows that after approximately one or two years of the construction of breakwaters and/or headlands, bank erosion generally stops for most sites like those: NPS, DMF, WAL, YTB and CHP. Only two sites are still experiencing bank erosion almost three years after the construction of structures, HIH and HI2. HI2 is a site with which experiment of breakwater design and construction is ongoing. Six pairs of breakwaters were set up in June, 1987. Five pairs of those are proven not very successful due to either being constructed too close to the high bank or being undersized. High banks in between breakwaters still face erosion whenever storm surges come into the area, especially during high tide stage of the lunar month which was already stated by Byrne et al (1978). The bank erosion in between headlands at HIH is within expectation as designed in advance. The final plan geometry of this section will be two crenelate shaped embayments in between three headlands. However, the development of such a final plan shape is a slow process due to the small size of fetch, weak wave climate and hard

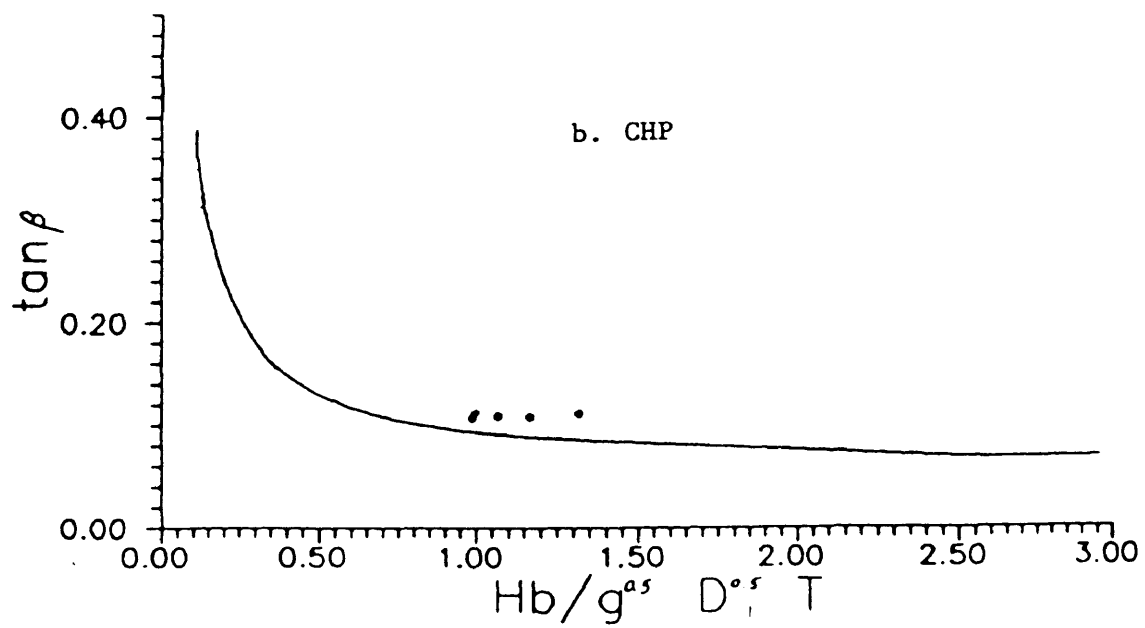
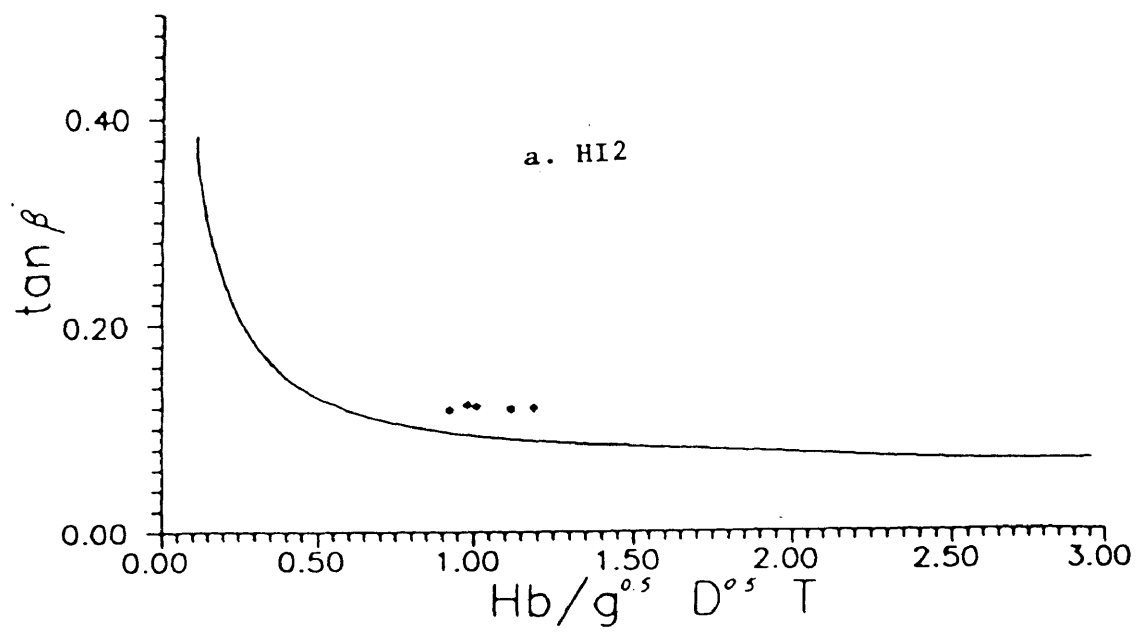
clayey erosion resistant bed.

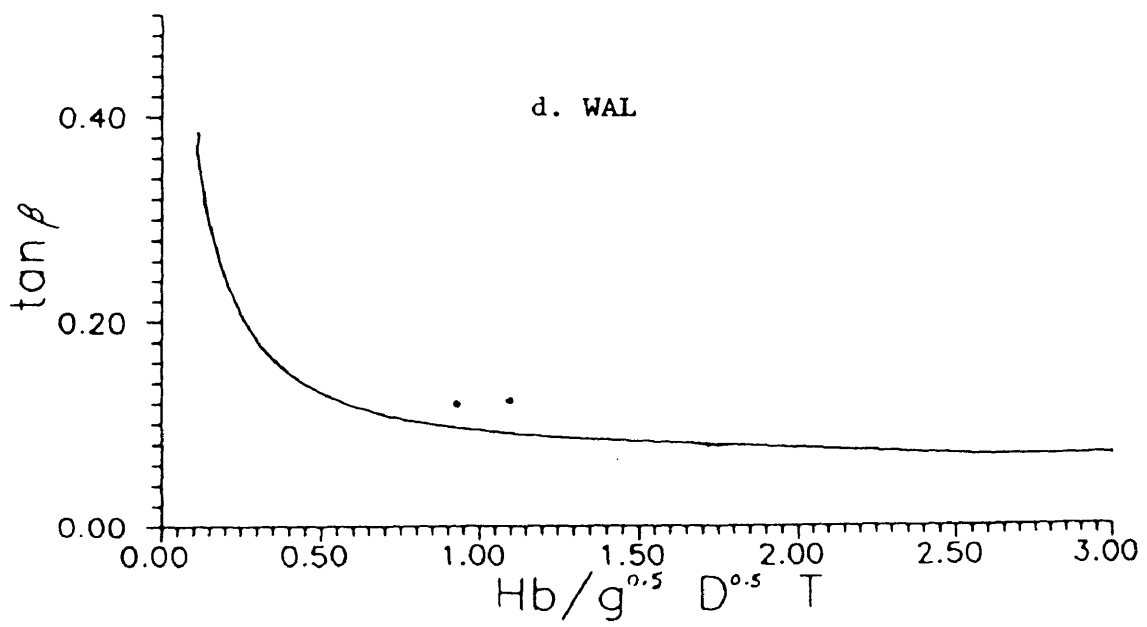
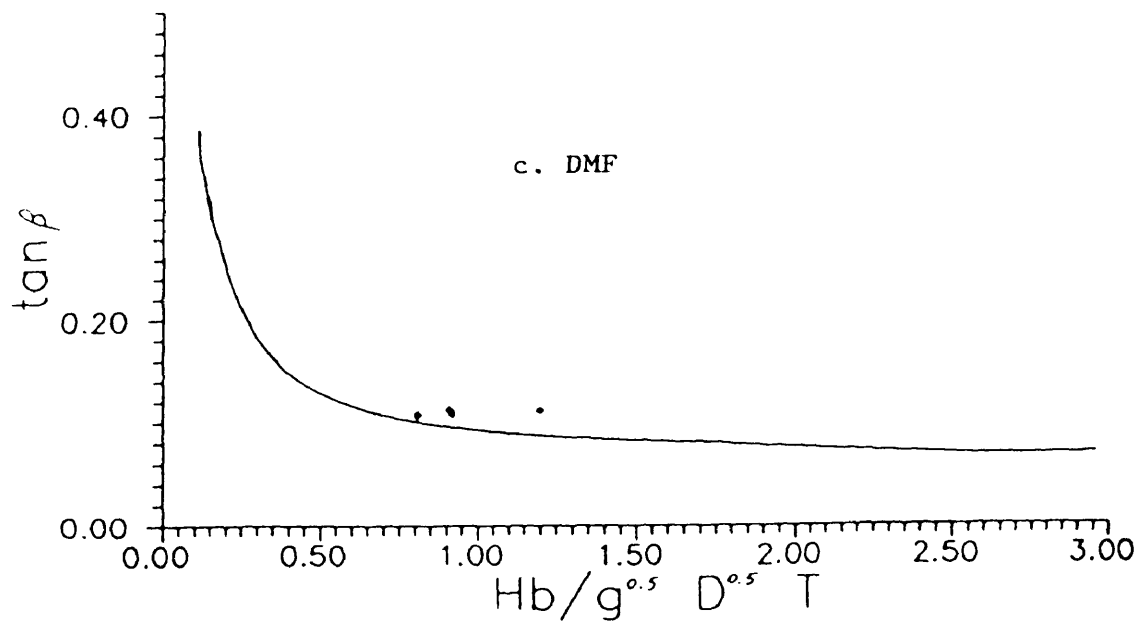
Sunamura (1984) suggested the best fit equation for beach slope prediction in field based on extensive field data (refer to chapter 2 for more detailed review) to be:

$$\tan\beta_1 = 0.12/[(H_b/g^{0.5}D^{0.5}T)]^{0.5} \quad (6-10)$$

The results of our data analysis (Fig.6.5) are reasonably fit the model suggested by Sunamura (refer to chapter 2 for Sunamura's figure). This means that the selection of the four major parameters in his model is reasonable. These parameters are also included in many other researchers' papers as important factors in the nearshore processes. The empirical constant in his model may be changed to a certain degree to predict beach slopes in different environments. However, such a serious change should be based on much more accurate data in future study. At present stage, the most difficult thing in this kind of beach slope prediction is still the collection of accurate wave data. This is mostly because of the complexity of the nearshore nonlinear wave actions coupled with many other time varying factors. However, it is expected that with the increasing of field wave data collection and the development of various wave predicting models, wave prediction in the nearshore zone will get to the point very close to the nature reality. Table 6.3 presents the field measured data and Sunamura's dimensionless parameter.

Figure 6.5.a-f. Diagrames showing the relationship among waves, sediment diameter and accelerational gravity based on Sunamura's (1984) model.





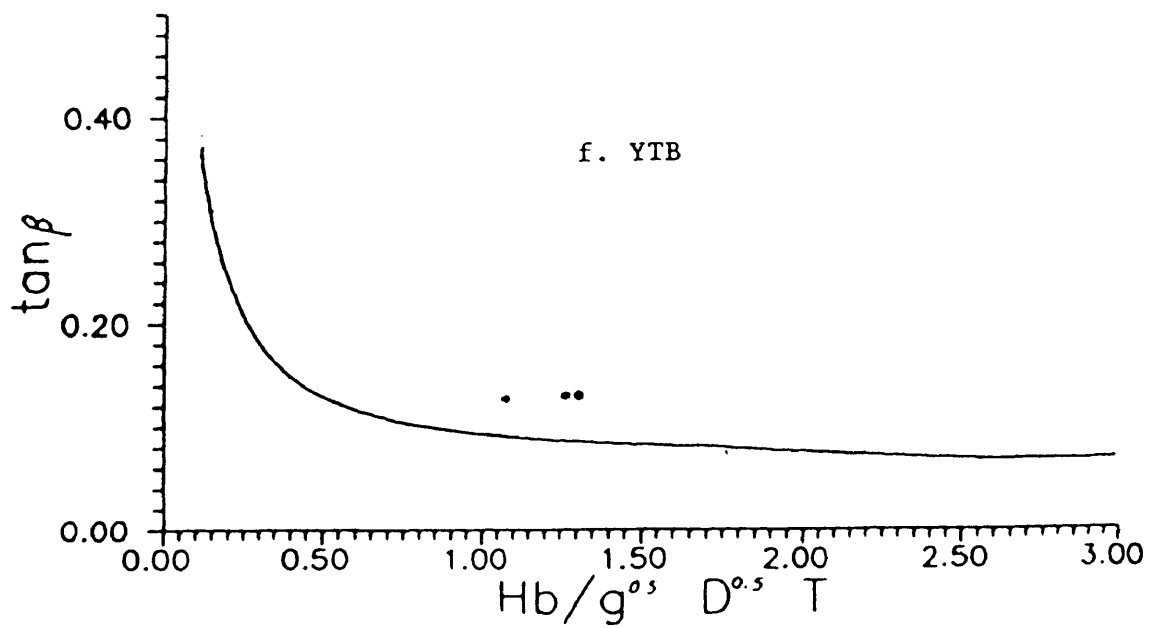
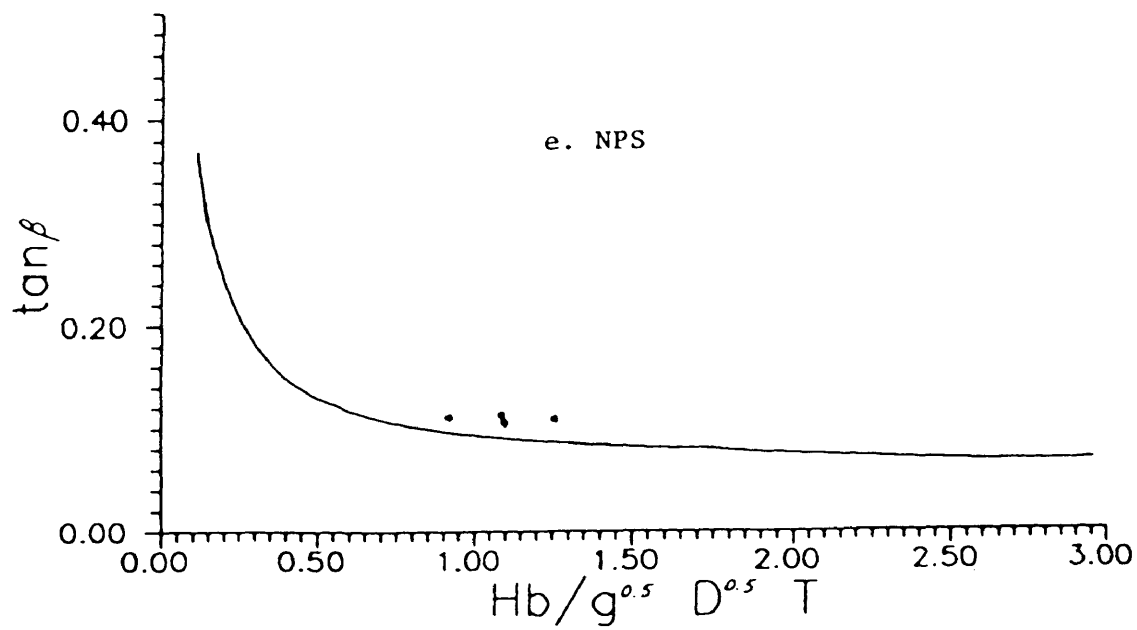


Table 6.3. Field Measured Data and Sunamura's Parameter

SITE	DATE	WAVE		GRAIN SIZE ( $\times 10^{-4}$ m)	BEACH SLOPE MEASURED	$h_b/g^{0.5}D^{0.5}T$
		MEASURED HEIGHT (m)	PERIOD (sec)			
HI2	OCT87	0.145	2.5	4.4	0.118	0.92
	MAY88	0.140	2.0	2.5	0.119	1.12
	DEC88	0.156	2.1	6.1	0.120	1.19
	JUN89	0.152	2.4	6.6	0.121	1.01
	MAY90	0.141	2.3	6.6	0.123	0.98
CHP	OCT87	0.142	2.0	5.4	0.107	0.99
	MAY88	0.140	2.1	3.9	0.109	1.07
	DEC88	0.146	2.2	4.3	0.112	1.00
	JUN89	0.153	2.0	4.4	0.108	1.17
	MAY90	0.139	2.1	2.6	0.111	1.32
DMF	OCT87	0.156	2.1	3.5	0.112	1.20
	DEC88	0.137	2.1	5.1	0.113	0.91
	APR89	0.132	2.3	4.0	0.109	0.92
	MAY90	0.158	2.3	7.7	0.108	0.81
WAL	DEC88	0.154	2.2	5.0	0.119	0.93
	MAY90	0.158	2.0	5.4	0.122	1.10
NPS	OCT87	0.155	2.2	3.1	0.109	1.26
	MAY88	0.130	2.1	3.2	0.105	1.10
	DEC88	0.131	2.4	3.5	0.111	0.92
	MAY90	0.147	2.4	3.2	0.113	1.09
YTB	OCT87	0.23	2.6	7.0	0.127	1.08
	MAY88	0.31	2.7	7.7	0.129	1.21
	DEC88	0.32	2.7	8.4	0.131	1.31
	MAY90	0.28	2.5	7.9	0.130	1.27

The bay beaches are very similar in slope for most bays in between breakwaters with smaller gaps such as these at HI2, CHP and WAL. All these bays have a near half-circle plan bay shape. However, there are variations along bay beaches for some bays with larger gaps between breakwaters with a elongated bay plan shape. The bays at DMF are the examples. Along the bay beaches, the general tendency is that slopes increases toward the central bay. The sediment size on the central



beach is coarser ( $0.85 \phi$ ), it is finer on both sides ( $1.45 \phi$ ), which is consistent with some of the traditional explanation.

#### 6.4. Profile Variations With Seasons/wave Climate

From frequently field profile measurements at fixed profile locations, it is noticed that not only short-term profile variation occurs all the time, but also systematic long-term variations. Here short-term refers to days and weeks, and long-term to seasons and years. The most significant variation is seasonal changes. A series of names have been given to profiles formed in different seasons such as summer profile (swell profile, normal profile) and winter profile (storm profile). Traditionally, summer profile is described as a profile with a wide berm and a relatively smooth offshore profile, and winter profile is described as one having almost no berm, the sand having been shifted offshore to form a series of bars parallel to the shore. In our very fetch-limited environments with breakwaters and headlands, these traditional descriptions seem to be not sufficiently inclusive, because all data from the seven study sites do not fit the traditional descriptions of the mechanisms for winter and summer profile development. There were no significant bars forming during winter due to the sand shifting from beaches at all seven sites (see all profile plots for the seven sites in Appendixes) and therefore there were no bars to disappear in summer time. However, sand does shift from beaches to offshore insignificantly during winter though no bars were formed. This kind of sand shifting or on/offshore motion can be seen commonly from the data plots in Appendixes.

#### 6.5. Patterns of Sediment Distribution Along Profiles

The patterns of grain size distribution along profiles are believed to be one of the reflectors of dynamical strength exerting on nearshore region. The average grain size at a certain point on a profile represents the particle size that is in a relatively dynamical equilibrium with the forces in fluids and its own gravity. If the grain size is too big to be moved by fluid forces, it simply stays there. If the grain size is too small than what it should be for an equilibrium state it will be suspended in the water column or moved to other places where the environment is suitable for it to settle out. Sediments with different sizes are always being sorted by mainly fluid forces and gravity. The general tendency is that every particle on the very surface of a profile moves around to a location where it could be settle down more stably, which depends on its own size, density, local slopes, the strength of fluid forces and hence its incipient motion velocity. The final consequence of such a process is the zonation of sediment sizes, or sediment sorting.

Based on many field observations and the results of sediment analysis in VIMS' sediment laboratory, a general pattern of sediment distribution was obtained along profiles (Fig.6.6). This pattern divides the nearshore region into five general zones:

- 1). Bank zone - from the line between backshore and bank landward, which provides most of the beach and nearshore material.

- 2). Backshore zone - This is the zone where both water and winds act. It usually consists of well sorted sands.

- 3). Beach face zone - This is the zone where sediments most actively adjust themselves to the tidal and wave actions. A narrow

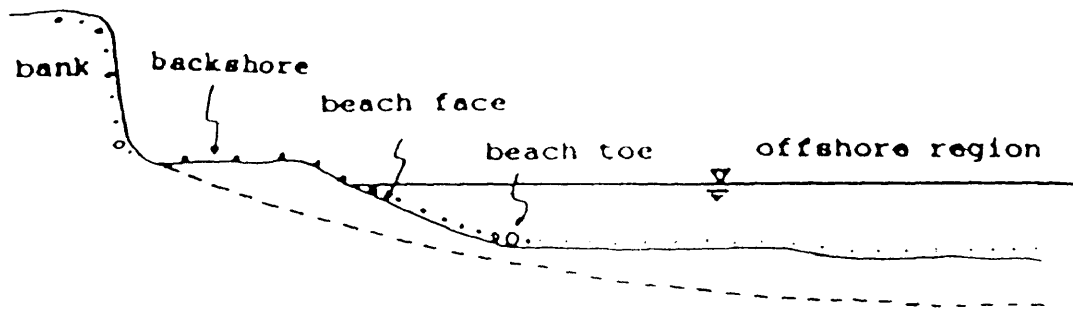


Fig.6.6. A schematic diagram showing a general pattern of sediment distributions along a profile.

strip of coarse material (mostly gravel) was found to move up and down with the instantaneously changing water level, being basically consistent with the colliding zone between backwash and incident waves.

4). Beach toe zone - this is a zone where particles most poorly sorted (The particles great than 2 mm are excluded in the results presented in Chapter 5). Particles larger than the gravel size are very common in this zone. These large particles are mostly from the bank material and sorted by mainly gravity and turbulence. As mentioned earlier the nearshore profile is broken here. According to the field observations during storms, this is also the zone where waves break during severe weather conditions.

5). Offshore zone - from the beach toe offshore. This is the zone where sediments are the finest and best sorted. Fine sands/silt dominate. They are mostly from the fine part of the bank material and adjacent shore sections.

## 7. RESULTS OF PLAN-VIEW BEACH FORM MEASUREMENTS

Four basic plan-beach forms can be generally recognized based on: (1) low aerial photographs; (2) frequent profiling; (3) records from field observations; (4) detailed measurements of selected bays. The four types are as follows:

### 7.1. Circular Bay Beach Forms

This type of bay beaches generally evolves in regions well sheltered by breakwaters. This type of bay beaches is found at four of the study sites: HI2, CHP, DMF and WAL. They represent the most stable beach forms along shorelines sheltered by breakwaters, but they also are the most expensive to install.

Breakwater systems with circular bays generally have smaller gaps between breakwaters and are larger in relative sizes than other breakwater systems with irregular bays. Fig. 7.1 shows the details of the arrangement of breakwaters at CHP. The closely spaced breakwaters provide good shelter to the bay beaches. In Fig. 7.2, we can see a variety of beach forms. The original purpose of HI2 is to examine the effects of breakwaters of varying lengths, heights, and offshore distances. From this figure, we can see that the best evolved circular bay is formed between the two largest breakwaters, 11 and 12. Two other circular bays are also formed in relatively well sheltered areas, bays between breakwaters 2 and 3, 10 and 11. Figure 7.3, 7.4 and 7.5 exhibit

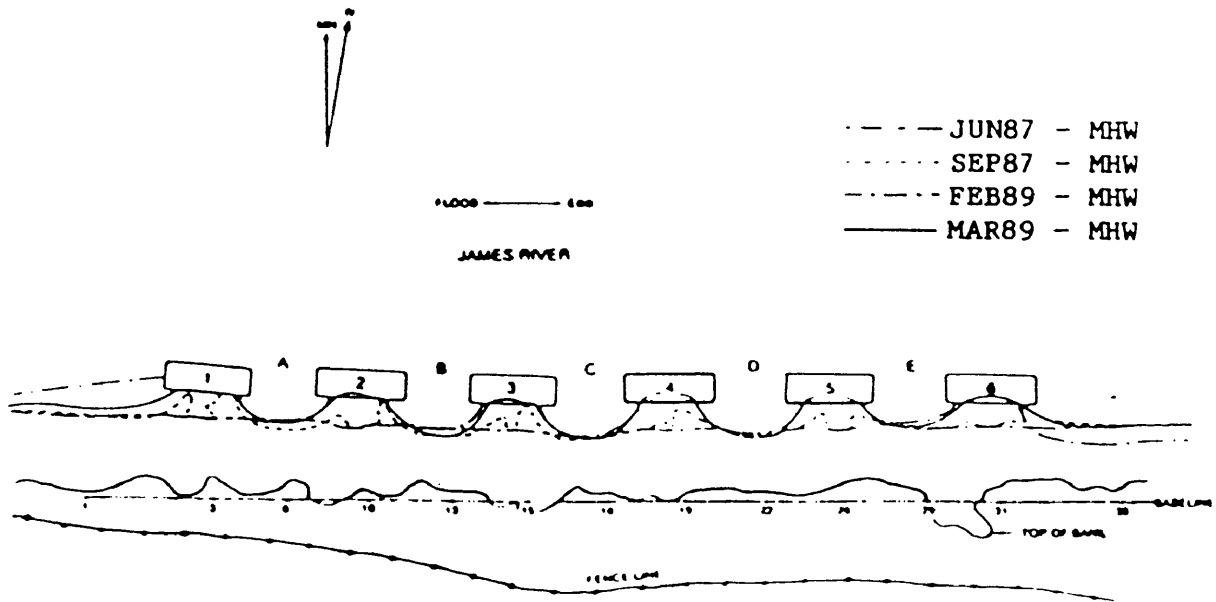


Fig.7.1. Breakwater system and its embayments at CHP.

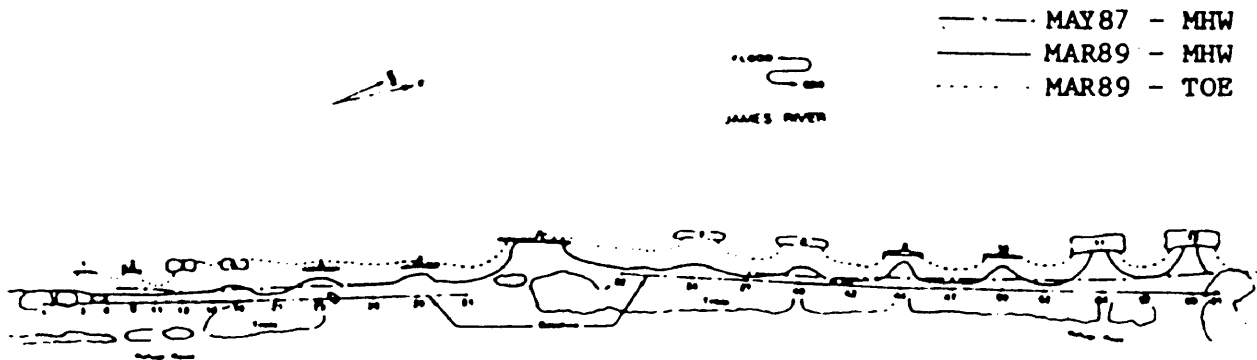


Fig.7.2. Breakwater system and its embayments at HI2.

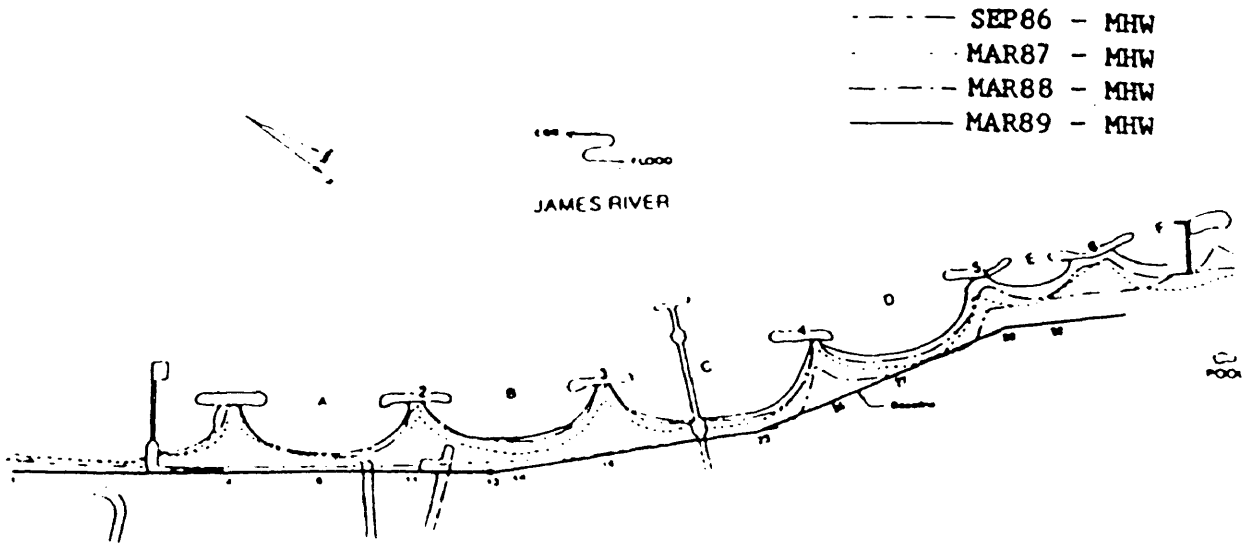


Fig.7.3. Breakwater system and its embayments at DMF.

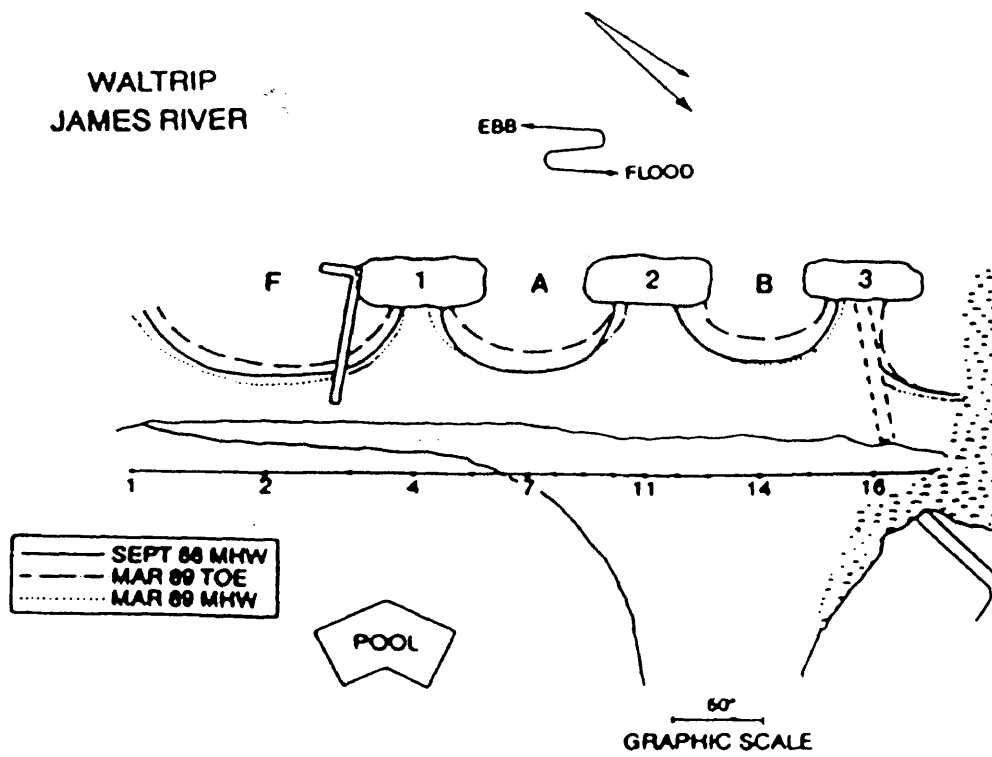


Fig.7.4. Breakwater system and its embayments at WAL.

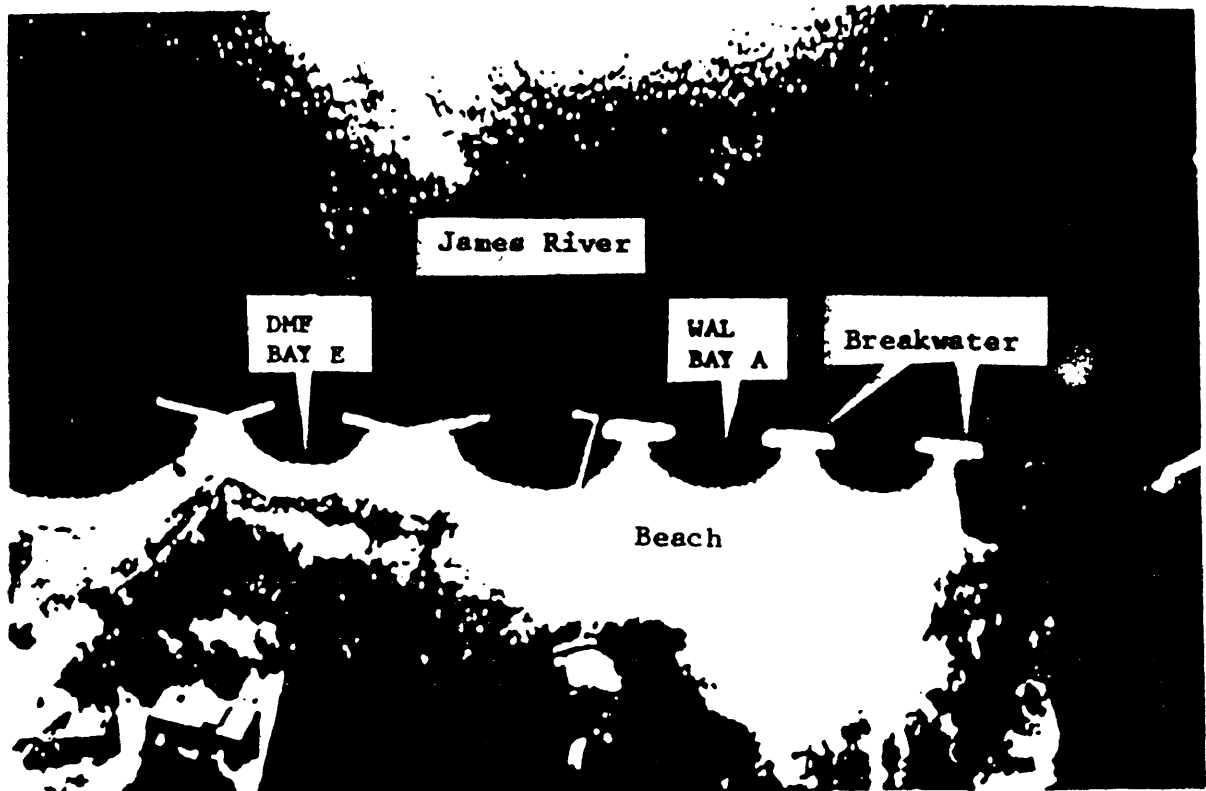


Fig.7.5. A photo showing the Breakwaters and embayments.



some other circular bay beaches at DMF and WAL. Because of the smaller ratio of breakwater crest length to gap, the bay beaches at DMF are formed not as regularly as those at CHP, WAL and some at HI2.

## 7.2. Spiral Bay Beaches

Spiral bay beaches are well evolved only at these sites with higher energy levels and obliquely incident waves. The only well evolved spiral bay is found at site SUM (Fig.7.6 and 7.7), the site with the highest energy in the study area. This bay retains its spiral plan form all the year round. A couple of other spiral bays are not well evolved at site NPS and YTB. Especially at NPS (Fig.7.8), the spiral bays are sensitive to the variations in seasonal wave climate. They can not retain their spiral form well year around. Spiral bays can only be formed during winter storm season. During summer, the tangential sections of the bays are likely destroyed by the southeastly wave climate. The YTB site (Fig.7.9 and 7.10) is the most dynamically complicated site in the study area. The beach forms are not only dependent as heavily on the seasonal wave climate as other sites, but also on the general characteristics of the geological setting. The east wave climate is not as important to beach forms at other sites, but at YTB with a horn-shape shorelines at the lower York River and a more than 20 nautical mile fetch from the east all the way to the eastern shore of Chesapeake Bay, east wave climate plays a more important role than waves from other directions in influencing beach forms at YTB. The nearly east facing of the tangential sections at this site clearly indicates this.

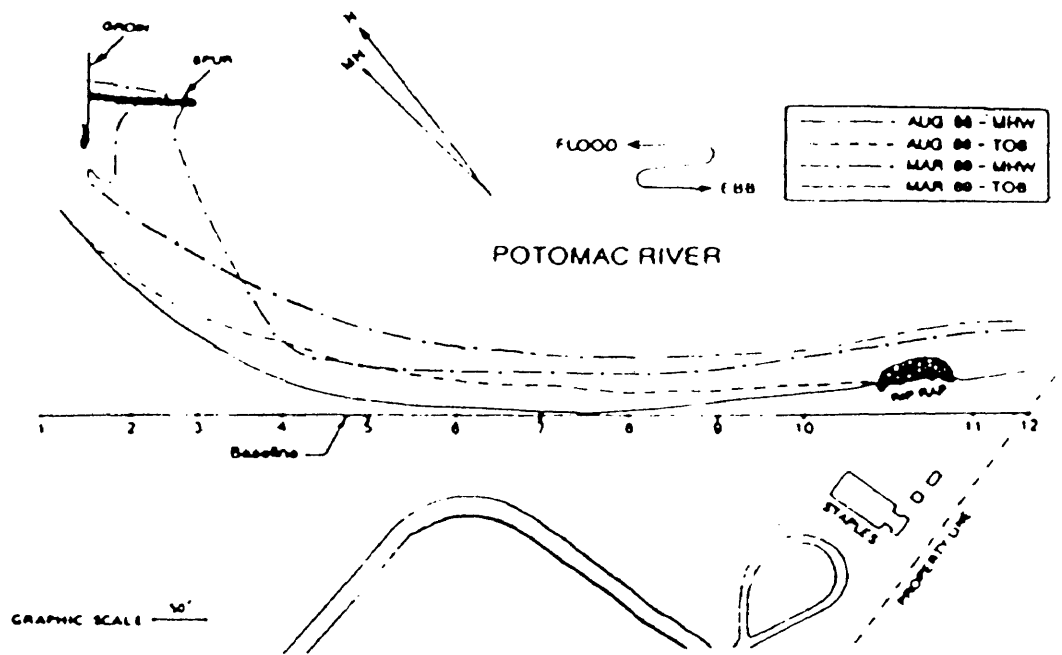


Fig.7.6. The spiral bay at SUM.

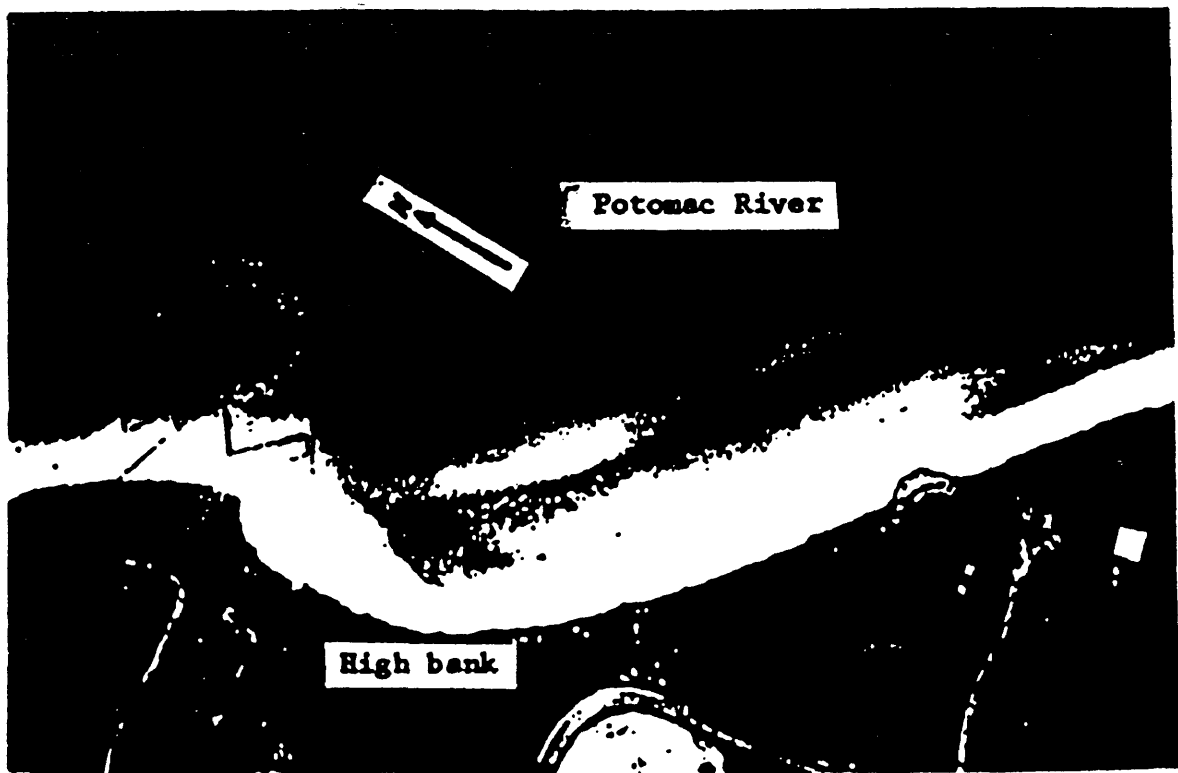


Fig.7.7. A photo showing the general spiral bay shape at SUM.

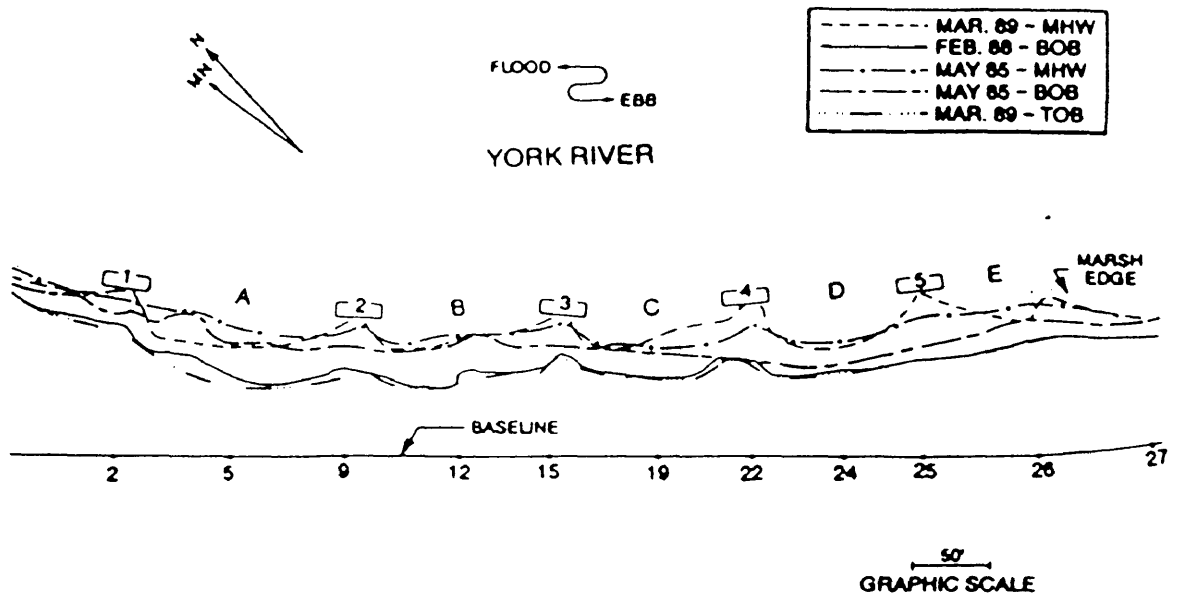


Fig.7.8. Breakwater system and its embayments at NPS.

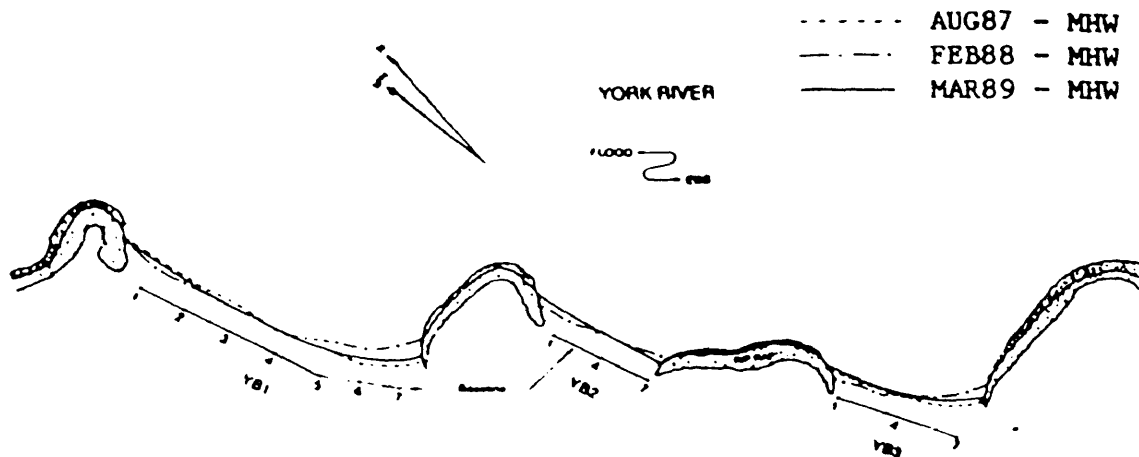


Fig.7.9. Headlands and their bays at YTB.

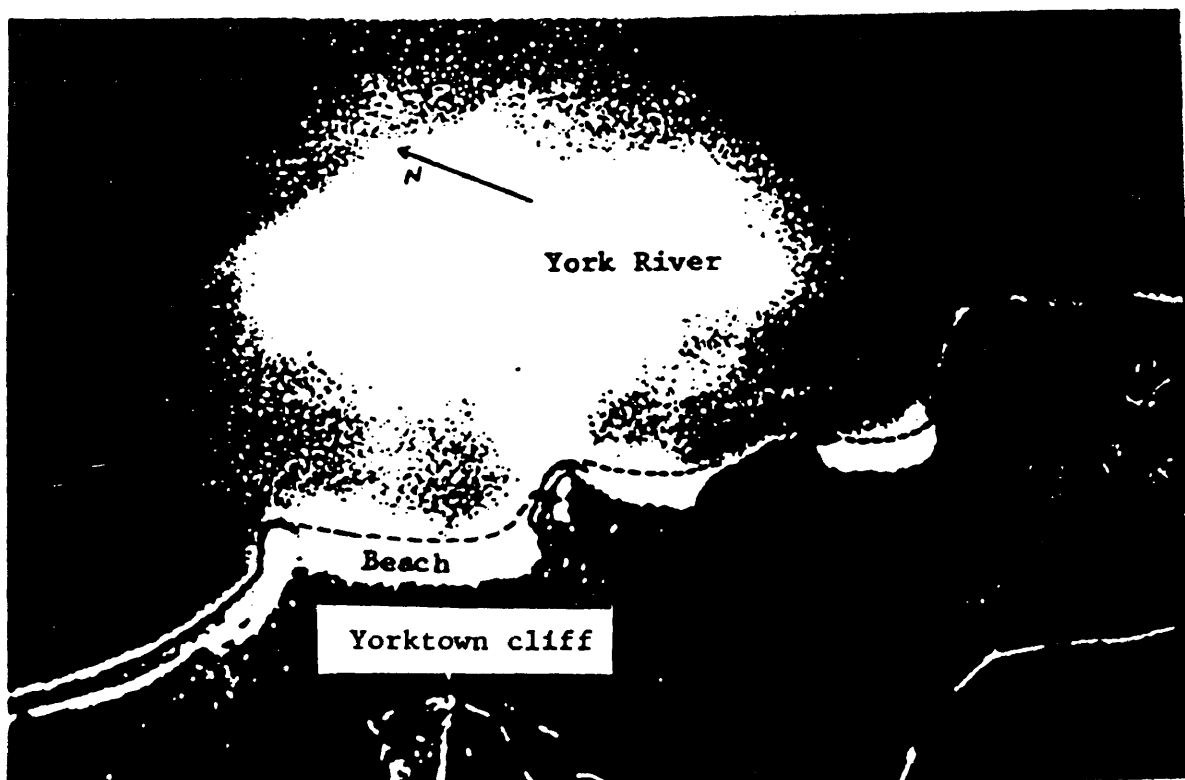


Fig.7.10. Photo showing the Headlands at YTB.

### 7.3. Irregular Bay Beach forms

The word "irregular" may be improperly used here. It only means these beach forms between circular and spiral. The beach forms of this type are mostly transitional. They may finally evolve into either circular or spiral bay beaches. Some of the bay beaches which appears to be irregular may just due to erosion-resistant spots within the bay such as the stiff hard clayey bed or tree roots.

Part of the plan beach forms at HIH belongs to this type (Fig.7.11). It is located within a fetch-limited environment. The very stiff, hard clayey bed and bank material is erosion resistant. The progress of the beach adjustment to the local wave climate is a fairly slow and long term process. Other irregular beach forms can also be found at HI2 (Figure 7.2). More detailed discussions will be addressed in chapter 8.

The straight beach form is an insignificant characteristic for all study sites.. Only a small section at HIH between headland 2 and 3 is found to be somewhat straight. This kind of straight beach is similar to other regular straight beaches out of the structure systems, because the two headlands on each end were originally installed on a basically straight section of shore, and far apart, the middle straight section needs more time to adjust itself to the installation of headland structures. An embayment will be expected in future though it is a slow process.

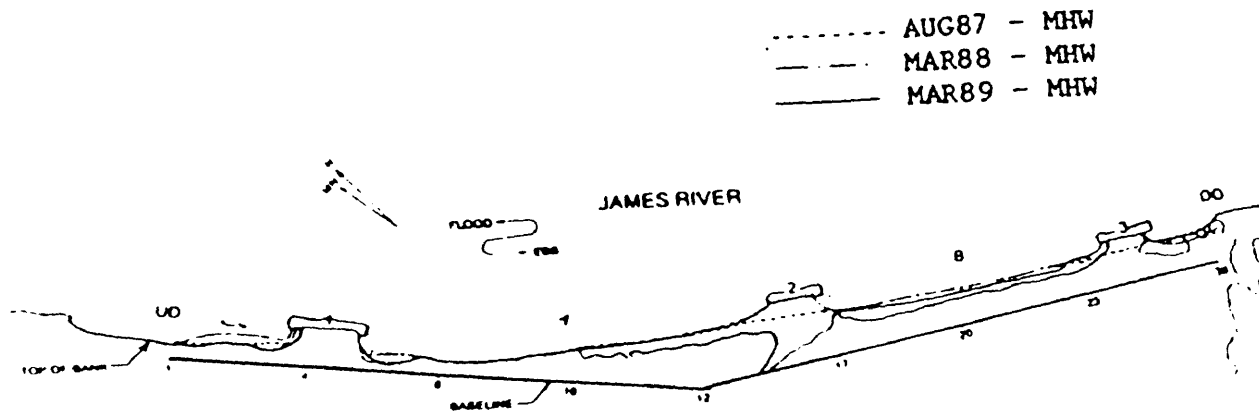


Fig.7.11. Three headlands and the plan beach forms at HIH.

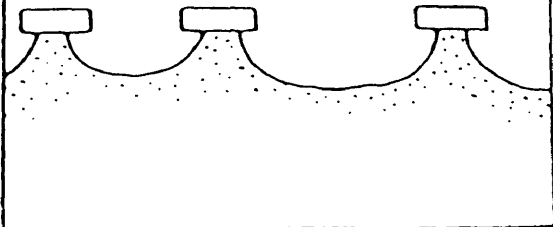
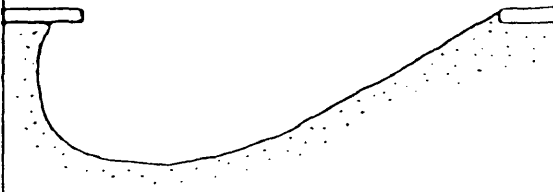
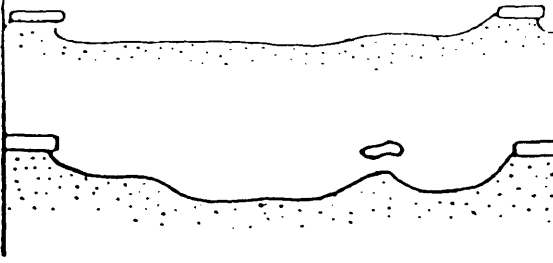
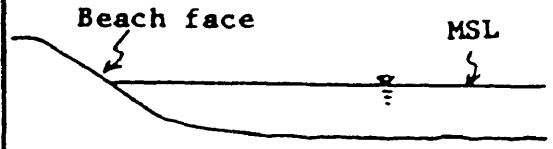
## 8. DISCUSSIONS AND CONCLUSIONS - PLAN BEACH FORMS

### 8.1. General characteristics

As mentioned in section 7, the plan beach forms can be generally classified into four broad groups in the study area: 1). Circular bay beaches such as those at CHP, DMF, WAL and some at HI2; 2). Spiral bay beaches like these at SUM and some at NPS and YTB; 3). Straight beach form like the small section between the headlands 2 and 3 at HIH; 4). Irregular bay beaches such as those at HIH and some at HI2 (Table 8.1).

The general rule is that whenever there is a breakwater or headland system installed along a sand beach, bay beaches will be formed immediately, either spiral or circular, depending on the local wave climate, sediment characteristics and the geological setting of the site. Circular bay beach forms are usually formed at these sites with closely spaced breakwaters; the main incident wave direction is nearly normal, especially during storm seasons there are no significant obliquely incident waves from a particular direction. In contrast, spiral bay beaches are usually formed at those sites with wider spaced breakwaters or headlands; the overall energy level is relatively higher (e.g. the sites SUM, NPS and YTB all have higher energy level); the incident wave direction during severe storms is oblique relative to the general site orientation. Sediment characteristics are not crucial factors in determining the plan beach forms.

Table 8.1 Summary Table of Beach Forms

FORMS	TYPE	DESCRIPTIONS	GENERAL SHAPE/EXAMPLE
P L A N  B E A C H  F O R M S	Circular Bay Beaches	This type of bay beaches are generally formed due to one or more of the following reasons: (1). low energy level; (2). small gap between BWs. (3). normally incident waves; (4). sediment supply plenty.	
	Spiral Bay Beaches	Spiral bay beaches may be evolved due to the following reasons: (1). higher energy levels; (2). obliquely incident waves; (3). headlands; (4). sandy beaches.	
	Irregular Bay Beaches	This type of bay beaches are mostly in a transitional phase. The irregular shapes may be eventually evolved into circular or spiral bay beaches, depending on the local environmental factors.	
	Straight Beach	This is a very insignificant beach form in the study area. It is only found in between headlands at MH.	
P R O F I L E		Profiles in the study area are two-segmented: Beach face profile: $h=Mx$ ( $M=0.11$ ); The lower profile: $h=Ax^m$ , ( $A=0.56$ , $m=0.15$ ).	



The mechanisms of the formation of various plan beach forms are not only related to the general geological and physical characteristics as briefly mentioned above, but also are closely related to other subsequent wave related dynamics such as wave refraction, diffraction and reflection in the vicinity of structures. Wave refraction, diffraction and reflection are three of the most basic mechanisms in shaping beaches into various forms around coastal structures. The following are discussions on these mechanisms based on field observation data.

## 8.2. Plan Forms and Wave Refractions

Waves are subject to refraction as they enter shallow water. Wave orthogonals change direction with decreasing water depth in such a way that the crests tend to parallel the depth contours.

A spreading or convergence of wave orthogonals/wave rays can be caused by wave refraction, which also means the spreading or convergence of wave energy. That is, when the wave rays spread out as the shore is approached, the wave energy per unit wave length is reduced. The wave energy flux (or wave power),  $P$ , between the rays is constant. The spreading due to the refraction causes the same amount of  $P$  to be distributed over a longer wave crest as shown in figures 8.1 a and b. The conservation of wave energy flux can be expressed by a relationship (Komar, 1976)

$$P = E C_n L_s = E C_n L_{s0} \quad (8-1)$$

where  $E$  = wave energy (or energy density);  $C$  = phase velocity;  $n = \left( \frac{1+2kh}{\sinh(2kh)} \right)^{1/2} = C/C_0 \rightarrow 1$  (in nearshore shallow water);  $C$  here is

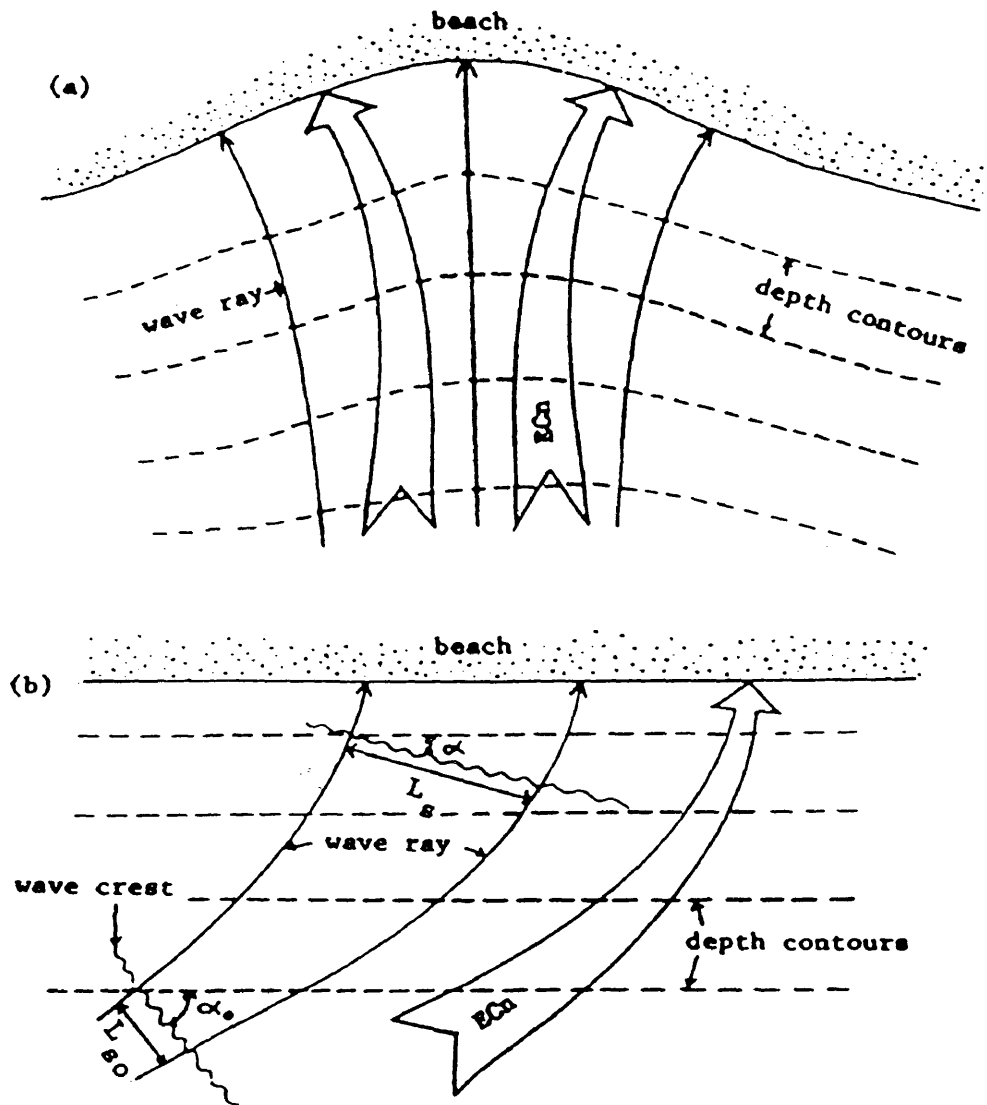


Fig.8.1. Wave refractions in waters with curved shorelines(a) and straight shoreline(b). Big arrows represent schematically the decreasing of energy flux,  $EC_n$ , per unit wave length as waves approaching the beach.

the group velocity;  $L$  is the width between wave rays, the subscript  $o$  represents the deep water condition. In Fig.8.1a, the shoreline is not straight. As waves enter into the depression, wave rays are refracted so that the rays could be as perpendicular to the depth contours as possible. Figure 8.1b is an example of straight shoreline with almost parallel depth contours. In this case, as waves enter into the shallow water, wave crests tend to parallel to the depth contour. Wave energy is reduced on approaching the beach due to the widening/ spreading of wave rays. Figures 8.2 and 8.3 are examples showing wave refractions around coastal breakwaters.

In the case of circular bays formed between breakwaters (figure 8.2), wave energy is reduced as waves approach the bay periphery due to wave refraction, while wave energy is increased at the ends of breakwaters due to the converging of wave rays. This kind of method of making wave rays spreading and converging at desired points is actually one of the principles that is used for shoreline protection using structures like breakwaters. Figure 8.2 is a schematic diagram that represent the bays formed in between breakwaters at the study sites such as those of Chippokes State Park, Drummonds Field, Waltrip and Hog Island West.

In the case of spiral bays, refraction patterns are more complex, as can be seen from figure 8.3. This complexity is basically due to the more complex bottom topography, which is, in turn, closely related to wave diffraction as will be discussed later. Figure 8.3 is schematically drawn based on field observations during a northeast storm in Feb. 1989 at national park service beach site.

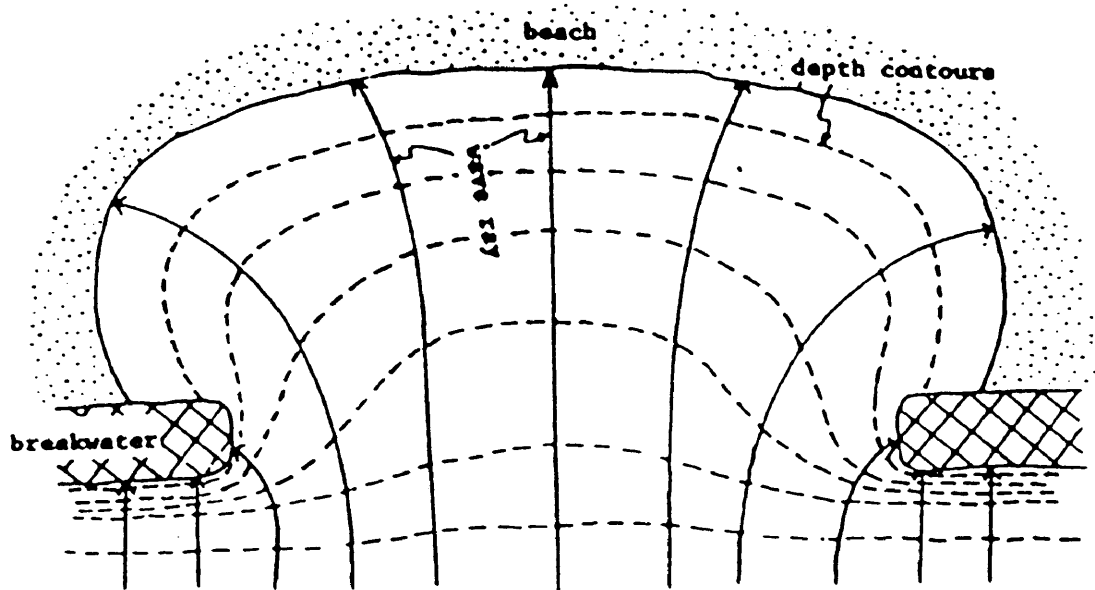


Fig.8.2. A schematic diagram showing wave refractions in a semi-elliptical/round bays in between breakwaters, which represents the situations of some of our study sites such as Chippoke State Park, Drummonds Field, And Hog Island West. The wave rays are drawn based on field observations.

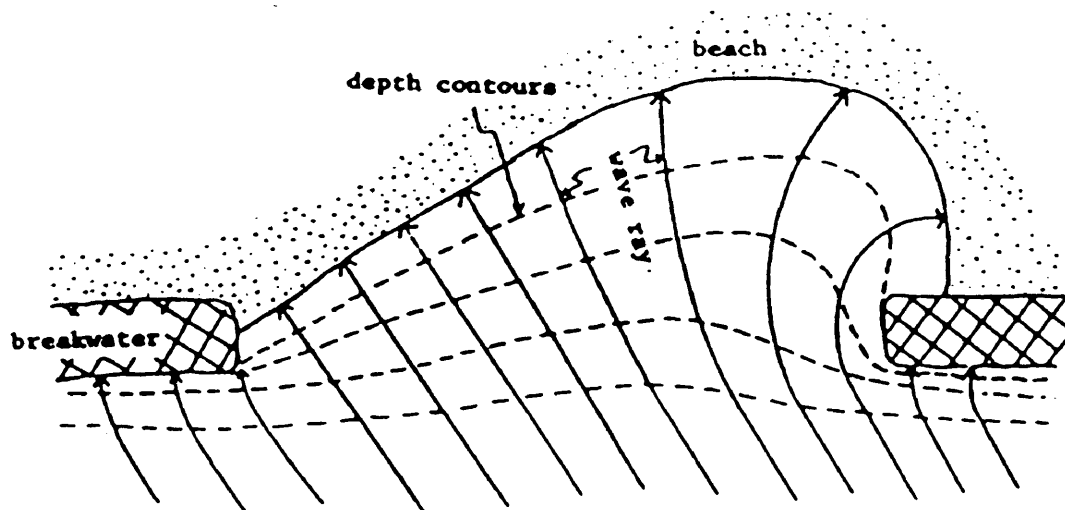


Fig.8.3. A schematic diagram showing wave refractions in a half-heart or spiral bay formed in between breakwaters at National Park Service beach site. The construction of this diagram is based on field observations in Feb.,1989 during a storm. The unit is arbitrary.

The situation is likely that waves from offshore arriving in the vicinity of structures at most of the river sites have been subjected to refraction while travelling over the very shallow and wide terraces (often upto thousands of feet in distance). Wave energy is also greatly reduced due to friction of the shallow bed. These waves will be refracted more severely in the bays and other regions near structures in a much shorter distance and time (Figs.8.2 and 8.3).

### 8.3. Plan Forms and Wave Diffraction

As mentioned earlier, the phenomenon of wave diffraction is very common along coasts with various manmade or natural structures. In this process, wave energy is transferred laterally along wave crests from where the wave height is large to where it is small. The result of wave diffraction is the re-distribution of wave energy, which is manifested in the variation of wave height. The wave diffraction is best expressed by the patterns of wave diffraction coefficient,  $K'$ , which is defined as the ratio of a wave height,  $H_d$ , in the area affected by diffraction to the incident wave height,  $H_1$ , in the area unaffected by diffraction:

$$K' = H_d/H_1 \quad (8-2)$$

There is a whole set of steps in applying the diffraction diagrams to actual problems. The following example shows the steps in calculating and constructing a diffraction diagram.

1). Location: SUM (Fig. 8.4), one of the study sites located on the west shore of Potomac River near its mouth.

2). Wave condition: Significant wave parameters were observed during a spring north east storm in April, 1988. Wave period( $T$ ) = 2.9 sec, wave length ( $L$ ) = 33 feet. Incident wave height,  $H_1$  = 3 feet.

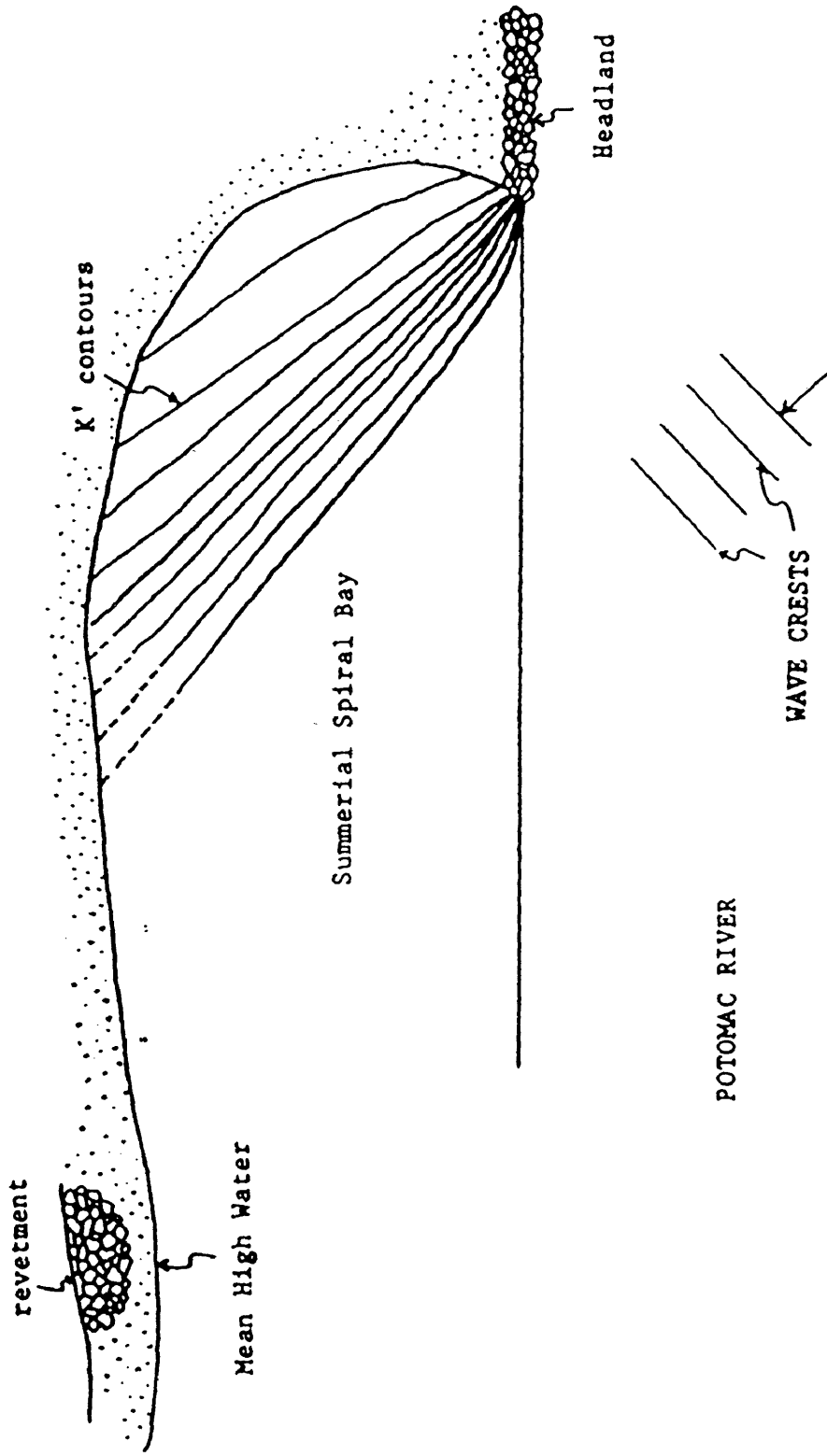


Fig. 8.4. Wave diffraction diagram for Summerial, Potomac River, showing the patterns of distributions of diffraction coefficient,  $K'$ , by which wave height can be estimated more accurately. This diagram is constructed based on field observation data.

3). Wind direction = NE, approximately 135 in Wiegel and SPM's system.

4). The water depth at the tip of the spur,  $d_s=4$  feet.

5). Purpose: construct diffraction diagram, understand the patterns of wave height distribution and get a general picture about the interrelationship between the beach equilibrium shape and the process of wave diffraction.

The first step is to find the wave length in the area affected by wave diffraction, because the wave length will be used as the unit for the space/span between arcs. The diagram can not be constructed without this wave parameter and the accuracy of the diagram is also dependent on this parameter. In our case, the wave length was measured directly at site during the storm as stated in 2) above. However, if wave length was not given, it must be calculated based on a simple relation

$$d_s/L_0 = d_s/5.12 T \quad (8-3)$$

and use a previously prepared table C-1 in SPM to find the ratio  $d_s/L$ , then deviding  $d_s$  by  $d_s/L$  will give the shallow water wave length,  $L$ .

The value of the ratio in this case is

$$d_s/L = 4/33 = 0.1212$$

$$L = d_s/(d_s/L) = 4/0.1212 = 33 \text{ feet}$$

The second step is to make the scale of working chart as the same as the standard diffraction diagram or vice versa.

The third step is to transfer the contours of  $K'$  onto the working chart.

In the fourth step, the wave height at any point in the lee of the structure can be found very easily from the relationship

$$H_d = K'H_i \quad (8-4)$$

For instance, if the wave height at point A is concerned, simply measure A in units of wave length in the rectangular coordinate system. Find the value of K' at that point. Then use equation 8-3 to find the wave height at that point.

#### 8.4. Wave Reflection

Waves impinging on natural or manmade barriers will reflect either partially or totally depending on the incident direction and wave parameters such as wave height, steepness etc. Obviously, this process can not be negligible when considering equilibrium beach forms around structures. This is because beach forms are closely related to the patterns of wave energy distribution, while wave reflection implies reflection of wave energy. Therefore, various processes in the nearshore region are not isolated, but closely related each other.

The wave reflection can be expressed by a ratio of the reflected wave height,  $H_r$ , to the incident wave height,  $H_i$ . This ratio is called reflection coefficient,  $K_r$ , having the form

$$K_r = H_r/H_i \quad (8-5)$$

$K_r$  changes from 1.0 for complete reflection to zero for no reflection.

When the concern is focused on permeable structures like most of the breakwaters in the study sites (Fig.8.5), another ratio termed transmission coefficient,  $K_t$ , is used which is defined as the ratio of transmitted wave height,  $H_t$ , to incident wave height,  $H_i$ , i.e.

$$K_t = H_t/H_i \quad (8-6)$$

The magnitude of transmitted wave height,  $H_t$ , is variable depending on the permeability of structures. The higher the permeability, the



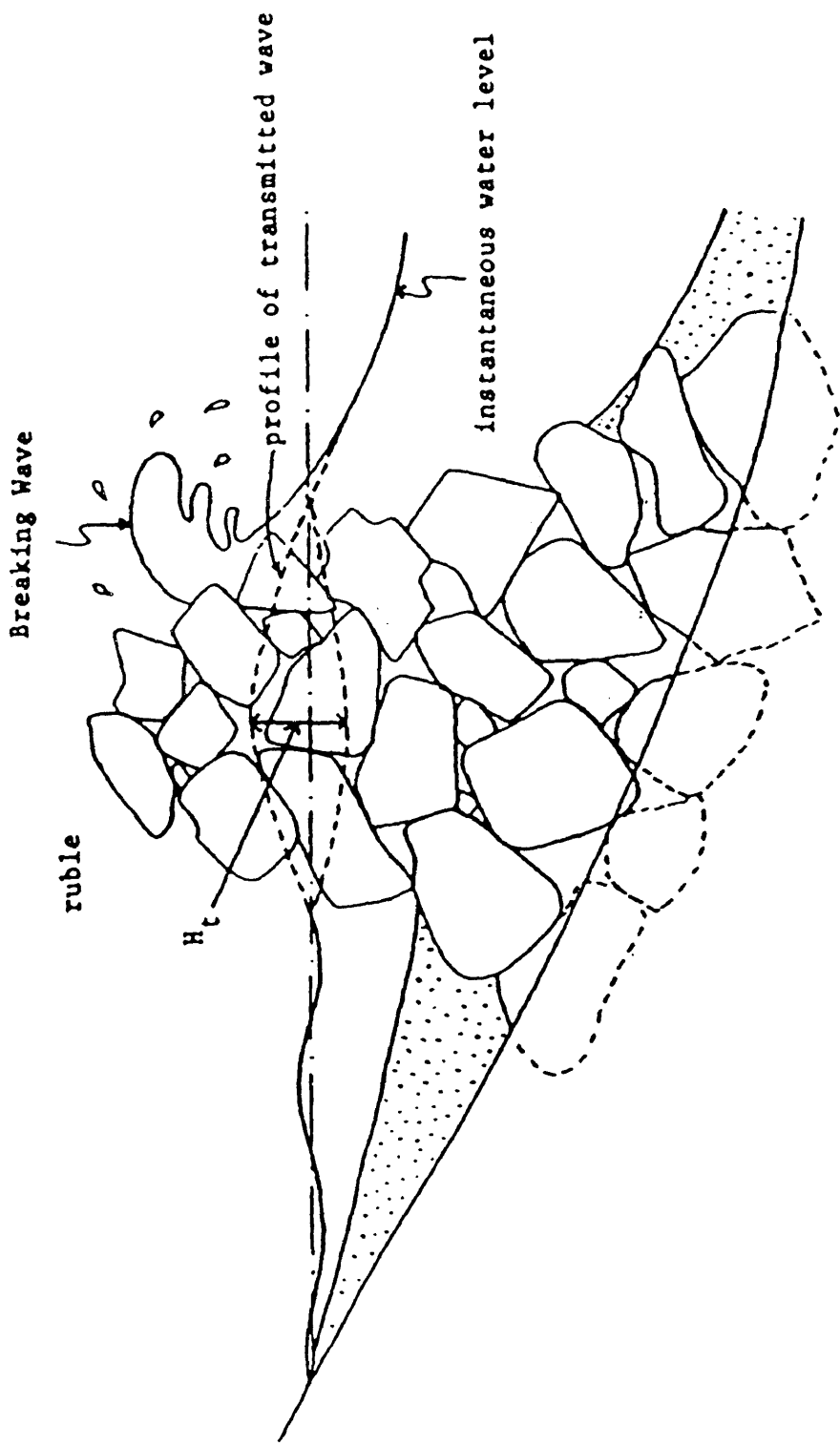


Fig. 8.5. A schematic diagram of the transsection of a breakwater which represents the very permeable type of structures like those at all of our study sites. Water level fluctuates within the structure in response to incident waves that are partially transmitted through the structures. Wave energy is dissipated by: 1). partial reflection; 2). breaking; 3). transmitting through the structure.

larger the  $H_t$  value, and the more wave energy that can be transferred through. The space volume within rubble-mound structures in our study sites is estimated approximately 20% of the whole gross volume of structures. This large volume of space within structures helps dissipate wave energy by transmission. Figure 8.5 shows a typical transect through rubble-mound structures in our study sites.

As shown conceptually in figure 8.5, breakwaters can also dissipate wave energy by breaking waves. This kind of breaking as shown in the figure is not common in the study areas during average weather conditions according to the field observation data. This is because almost all of our study sites are located in the low energy river systems. It is, however, a common phenomenon during severe weather conditions.

Wave reflection from breakwaters almost always occurs when the incident wind speed is over 30 MPH based on field observation. In addition to wave breaking and transmission through the breakwaters, reflection can account for most of the remaining energy redistribution from breakwaters. The short waves are usually dissipated or "absorbed" by breakwaters, long waves are partially reflected.

## 9. FUTURE STUDY CONSIDERATIONS

The followings are considered as the future study problems:

1. The more detailed morphodynamic characteristics of fetch-limited environments in the tributary systems as a general topic need to be further studied. The fetch-limited environment should be treated separately as one of the major domains in nature in contrast to the open water environment that has its own characteristics in morphology and dynamics. The differences in some primary aspects such as in morphology, waves and current patterns between open and fetch-limited environments need to be more clearly defined.

2. The relationship between longshore drift/transport and profile development need to be further studied, though Bruun (1962) pointed out that the gradient in longshore sediment transport is not important in influencing the profile development.

3. Studies on the physics-based mechanism of profile variation and development around structures and bays in between structures should be further addressed in future, which is involved many factors. One of which is the wave characteristic that needs more accurate measurement and analysis.

## APPENDIX A

### Calculations

of

the scale parameter,  $A$ , Shape parameter,  $m$ ,

and the Root-Mean-Square error,  $e_r$

### 1. Procedures in Calculating Shape and Scale Factors, m and A:

The calculation of "best fit" values of scale and shape factors, A and m, in Bruun-Dean's model  $h=Ax$  can be carried out by using the least square procedures which can be found in Dean's report (1977). The two equations resulted from the usual method of least squares are:

$$m = [S_{1,n}S_{4,n} - I S_{3,n}] / [(S_{1,n})^2 - I S_{2,n}] \quad (A-1)$$

$$A = e^{Vn} \quad (A-1)$$

where

$$Vn = [S_{1,n}S_{3,n} - S_{2,n}S_{4,n}] / [(S_{1,n})^2 - I S_{2,n}] \quad (A-3)$$

and

$$S_{1,n} = \sum_{i=1}^I \ln x_{i,n} \quad (A-4)$$

$$S_{2,n} = \sum_{i=1}^I (\ln x_{i,n})^2 \quad (A-5)$$

$$S_{3,n} = \sum_{i=1}^I (\ln x_{i,n})(\ln h_m) \quad (A-6)$$

$$S_{4,n} = \sum_{i=1}^I \ln h_m \quad (A-7)$$

where the subscripts n and i denote the nth profile and distance index across the profile, respectively, I represents the total data points on the profile.  $h_m$  is the water depth measured in field. Two examples below show how these equations work.

## Example 1.

Site: NPS, Profile 12, Dec.6, 1988

x	ln x	(ln x)	$h_m$	$\ln h_m$	$(\ln x)(\ln h_m)$
0.00			0.00		
23.0	3.14	9.86	0.32	-1.14	-3.58
66.0	4.19	17.56	0.34	-1.08	-4.53
146.0	4.98	24.80	0.80	-0.22	-1.10
216.0	5.38	28.94	1.01	0.01	0.05
299.0	5.70	32.49	1.19	0.17	0.97
total	23.39	113.65		-3.30	-8.19
	(S <sub>1</sub> )	(S <sub>2</sub> )		(S <sub>4</sub> )	(S <sub>3</sub> )

hence  
 $m = 0.21$   
 $V_n = -1.36$   
 $A = e^{V_n} = 2.718^{-1.36} = 0.26$

## Example 2. Site: WAL, profile 7, May 26, 1989

x	ln x	ln(x)	$h_m$	$\ln h_m$	$(\ln x)(\ln h_m)$
0.00			0.00		
19.0	2.94	8.64	0.40	-0.92	-0.18
55.0	4.01	16.08	0.80	-0.22	-0.09
131.0	4.88	23.81	1.08	0.08	0.05
total	11.83	48.53		-1.06	-0.23

hence  
 $m = 0.21$   
 $V_n = -0.90$   
 $A = e^{V_n} = e^{-0.90} = 0.41$

## Example 3:

Site: CHP, profile 13, Mar., 1989

x	ln x	(lnx) <sup>2</sup>	h <sub>m</sub>	ln h <sub>m</sub>	(lnx)(lnh <sub>m</sub> )
0.00			0.0		
16.0	2.77	7.67	0.80	-0.22	-0.61
38.0	3.64	13.25	1.13	0.12	0.44
77.0	4.34	18.84	1.11	0.10	0.43
144.0	4.97	24.70	1.07	0.07	0.35
317.0	5.76	33.18	1.50	0.41	2.36
total	21.48	97.64		0.48	2.97

hence

$$m = 0.06$$

$$V_n = -0.16$$

$$A = e^{V_n} = 0.85$$

## Example 4.

Site HI2, Mar.16, 1989, Oct., 1989

x	ln x	(ln x) <sup>2</sup>	h <sub>m</sub>	ln h <sub>m</sub>	(lnx)(lnh <sub>m</sub> )
0.0					
6.0	1.79	3.20	0.54	-0.62	-1.11
18.0	2.89	8.35	1.19	0.17	0.49
24.0	3.18	10.11	1.28	0.25	0.80
39.0	3.66	13.40	1.57	0.45	1.65
78.0	4.36	19.01	1.92	0.65	2.83
132.0	4.88	23.81	2.02	0.70	3.12
total	20.76	77.88		1.60	7.78

hence

$$m = 0.19$$

$$V_n = -0.32$$

$$A = e^{V_n} = 0.7$$

## 2. Calculation of Root-Mean-Square (RMS) Error, $e_r$ :

When evaluating the Goodness-of-Fit of the data points RSQ (R Squared) is a good method (see section 3 for the explanation of the method) like the results as presented in Section 5 and Appendix C. Another method evaluating the goodness-of-fit of data points to a certain model line is the calculation of RMS  $e_r$  (Root Mean Square Error). The Table below lists the average  $e_r$  value distribution for this study.

### Root-Mean-Square Error in this study

RMS $e_r$ (ft)	DECIMAL PERCENTAGE (BEACHFACE)	DECIMAL PERCENTAGE (LOWER PROFILE)
0.0-0.1	0.00	0.00
0.1-0.2	0.00	0.10
0.2-0.3	0.50	0.20
0.3-0.4	0.30	0.40
0.4-0.5	0.10	0.10
0.5-0.6	0.10	0.10
0.6-0.7	0.10	0.10
0.7-0.8	0.00	0.00
0.8-0.9	0.00	0.00
0.9-1.0	0.00	0.00



The followings are the procedures showing how these  $e_r$  values are obtained. It is not possible to list all calculations for all profiles due to the space limitation, here only two examples are shown. In the following tables,  $h_m$  represents field measured water depth,  $h_p$  represents the predicted water depth by the model:  $h=0.56x^{0.15} + 0.64$ .

1. Site: DMF;

Jun.1989, Profile 8, beach face profile:

x	$h_m$	$h_p$	$(h_m-h_p)^2$
0	0.00	0.00	0.00
5	-1.00	-0.55	0.20
15	-2.06	-1.65	0.17
23	-2.98	-2.53	0.20
33	-4.46	-3.63	0.69
46	-6.31	-5.06	1.56
Total			2.82

Using equation 3-10:

$$e_r = 0.69 \text{ feet}$$

2. DMF, Mar.1989, Profile 8, Lower profile:

x	$h_m$	$h_p$	$(h_m-h_p)^2$
0	0.00	0.00	0.00
25	-0.85	-1.55	0.49
51	-2.04	-1.65	0.15
73	-1.20	-1.71	0.26
100	-1.35	-1.76	0.17
Total			1.07

Using equation 3-10:

$$e_r = 0.46 \text{ feet}$$

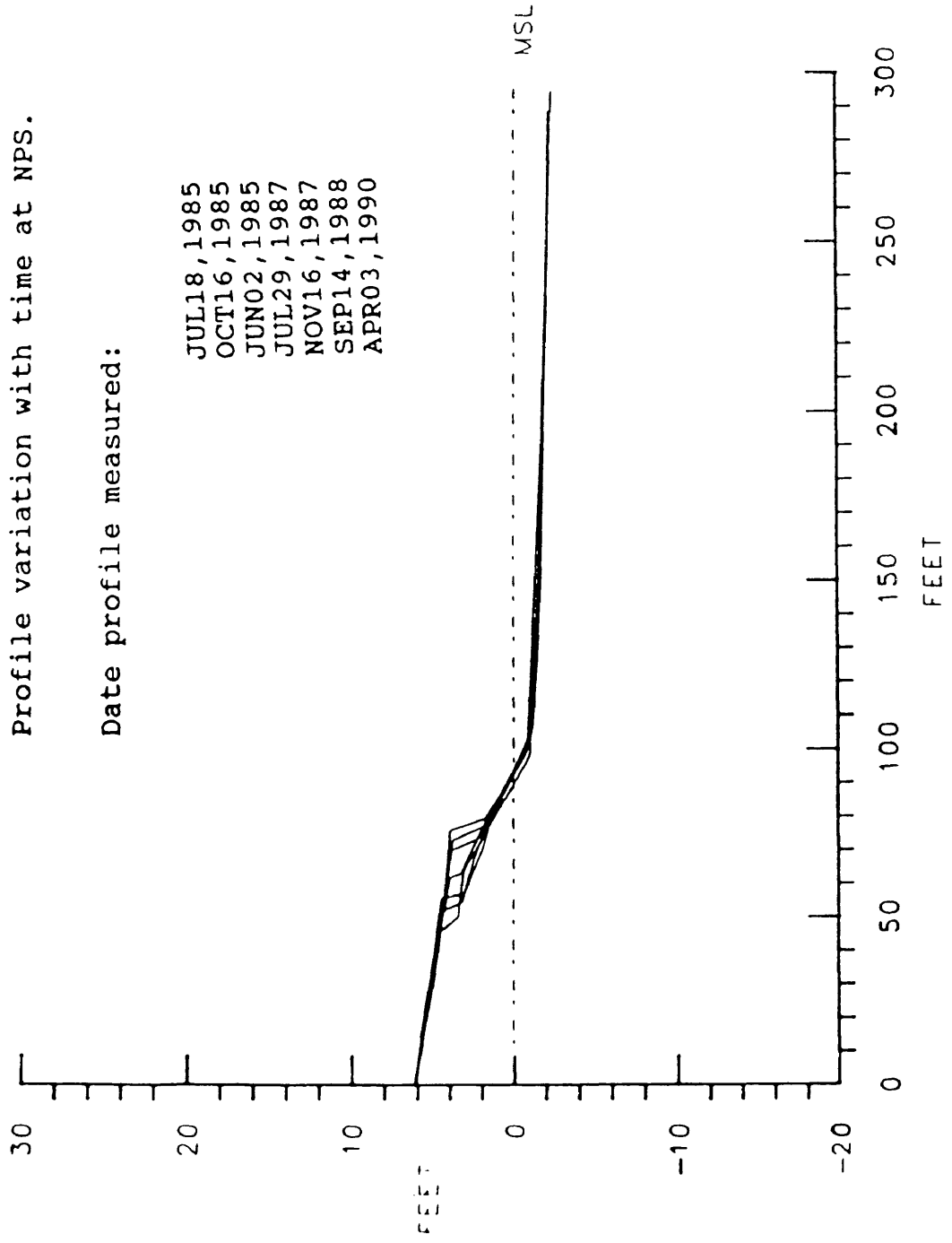
APPENDIX B

Time varying and enlarged beach profiles

Profile variation with time at NPS.

Date profile measured:

- JUL18, 1985
- OCT16, 1985
- JUN02, 1985
- JUL29, 1987
- NOV16, 1987
- SEP14, 1988
- APR03, 1990

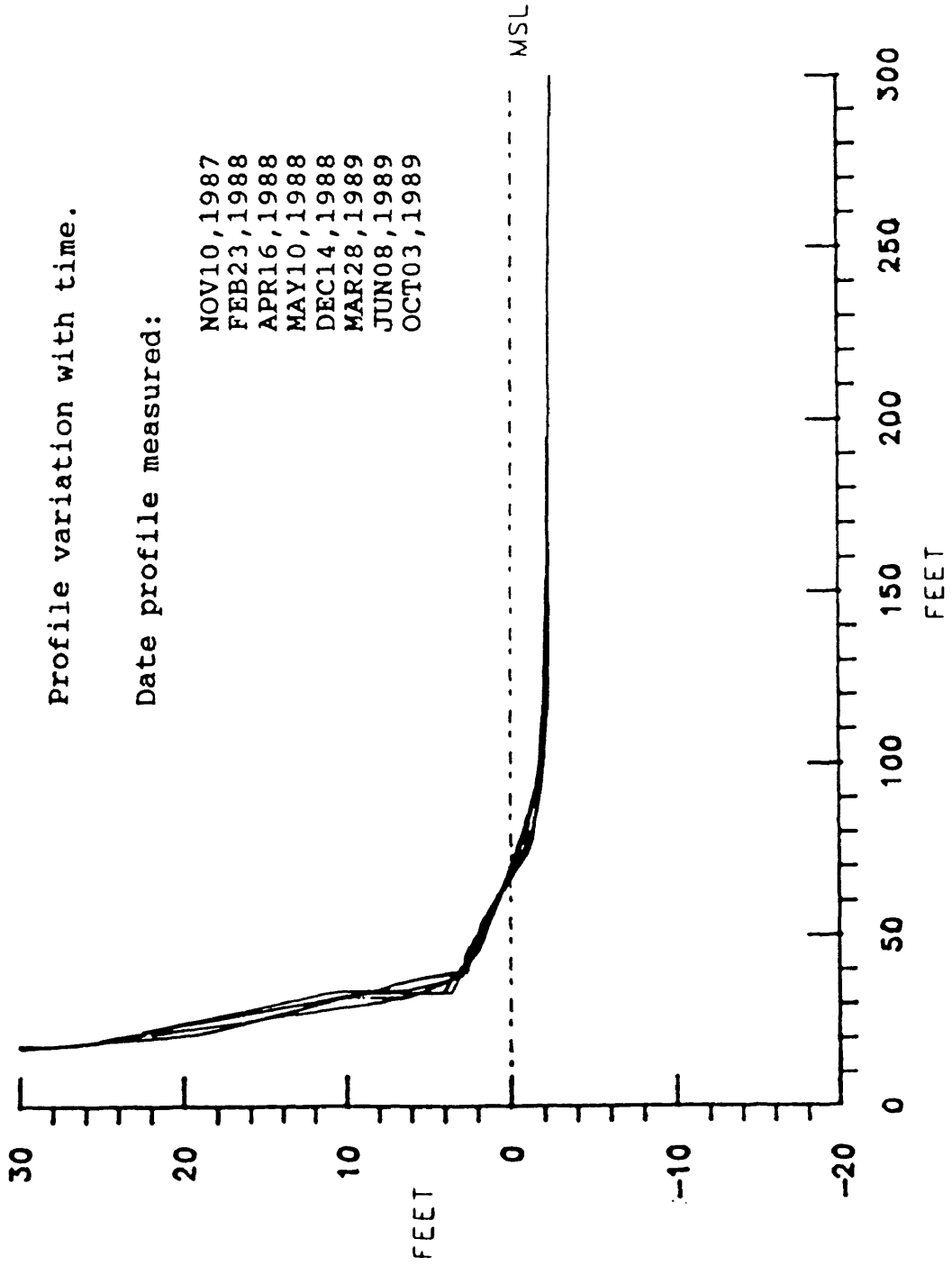


CHP PROFILES  
PROFILE NO. 13

Profile variation with time.

Date profile measured:

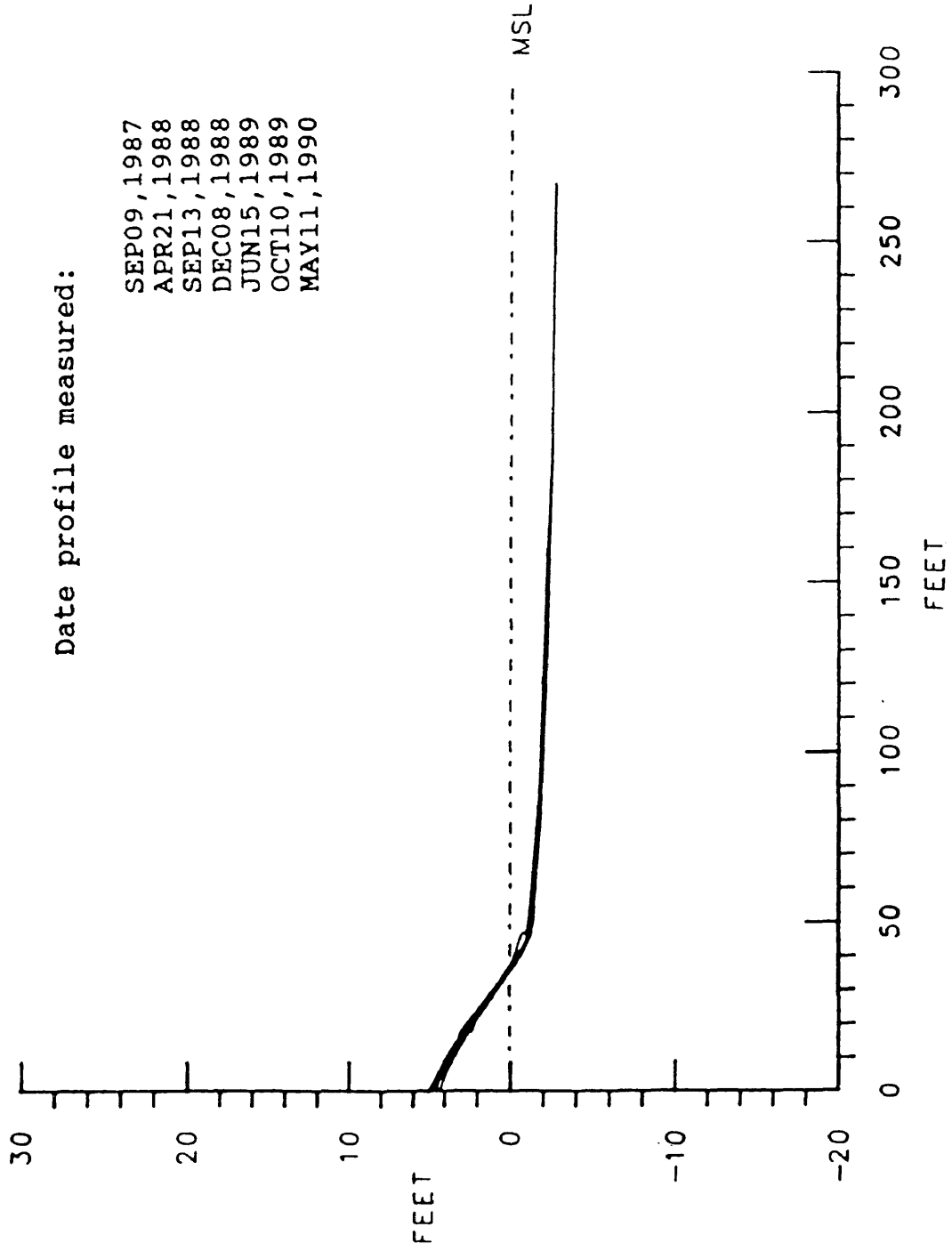
- NOV10, 1987
- FEB23, 1988
- APR16, 1988
- MAY10, 1988
- DEC14, 1988
- MAR28, 1989
- JUN08, 1989
- OCT03, 1989



Profile variation at DMF.

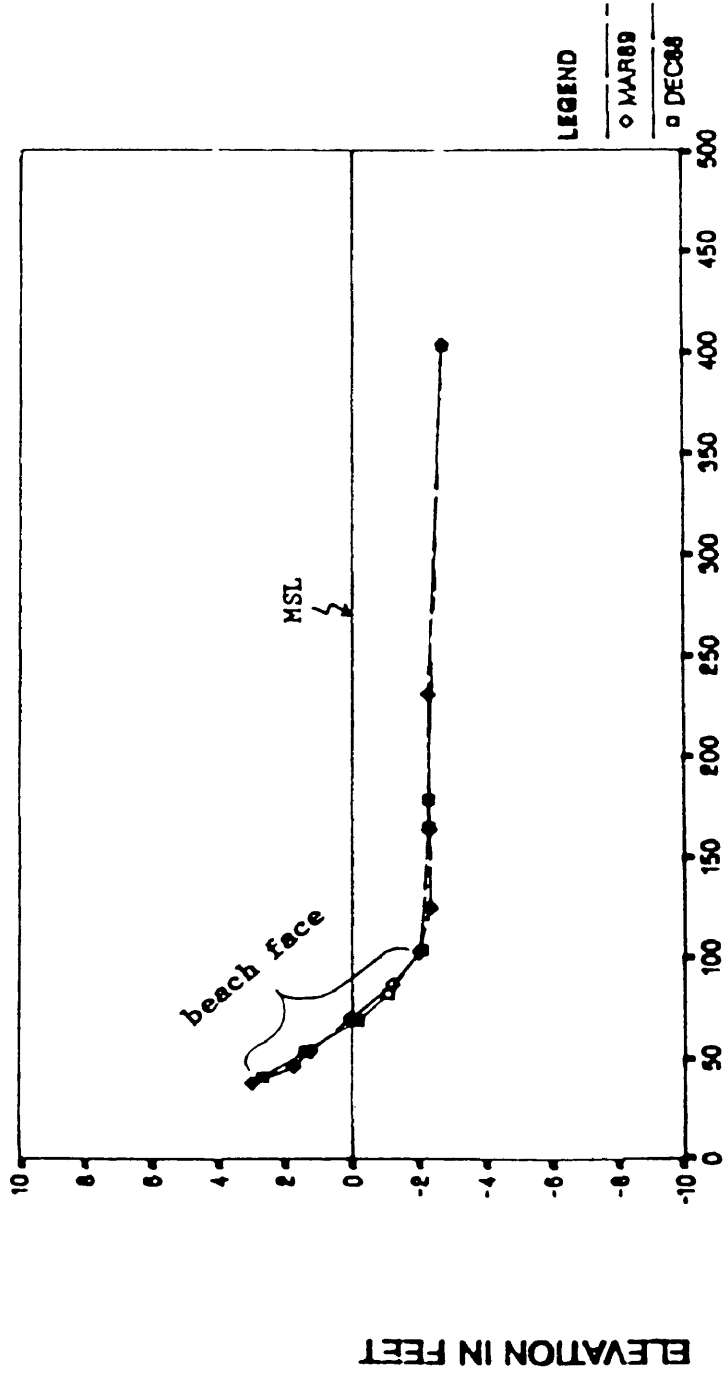
Date profile measured:

- SEP09, 1987
- APR21, 1988
- SEP13, 1988
- DEC08, 1988
- JUN15, 1989
- OCT10, 1989
- MAY11, 1990



# BEACH PROFILES AT CHP

PROFILE 13

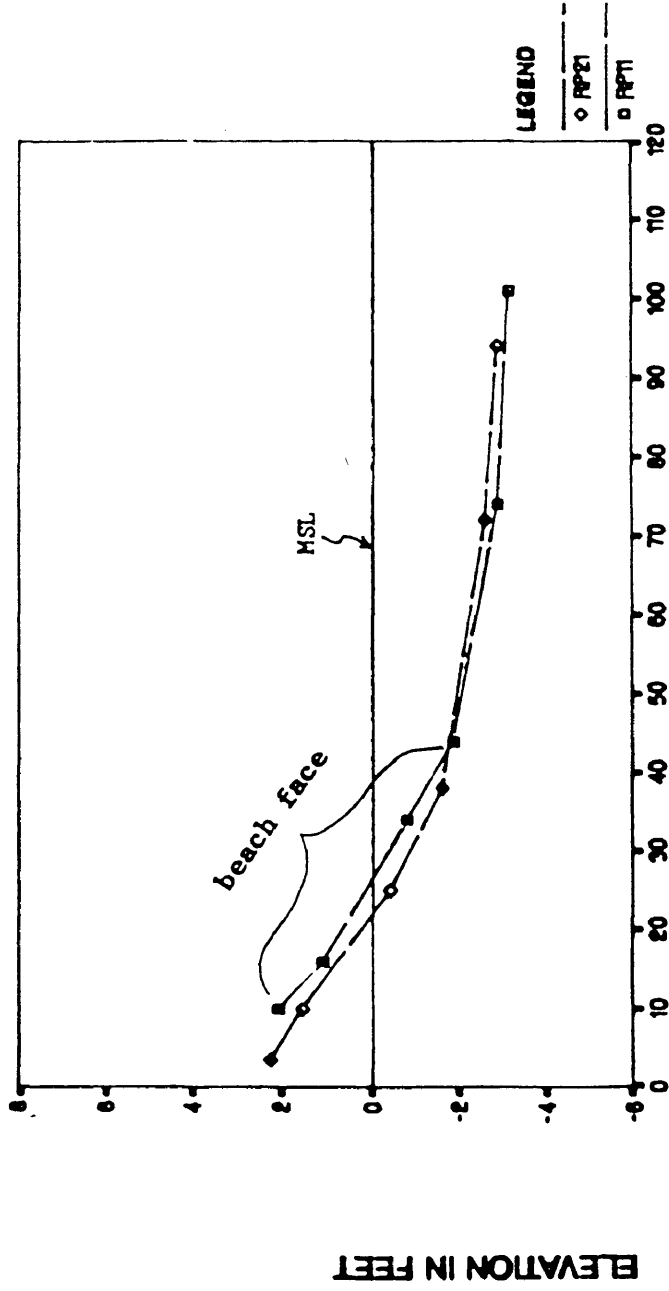


DISTANCE IN FEET

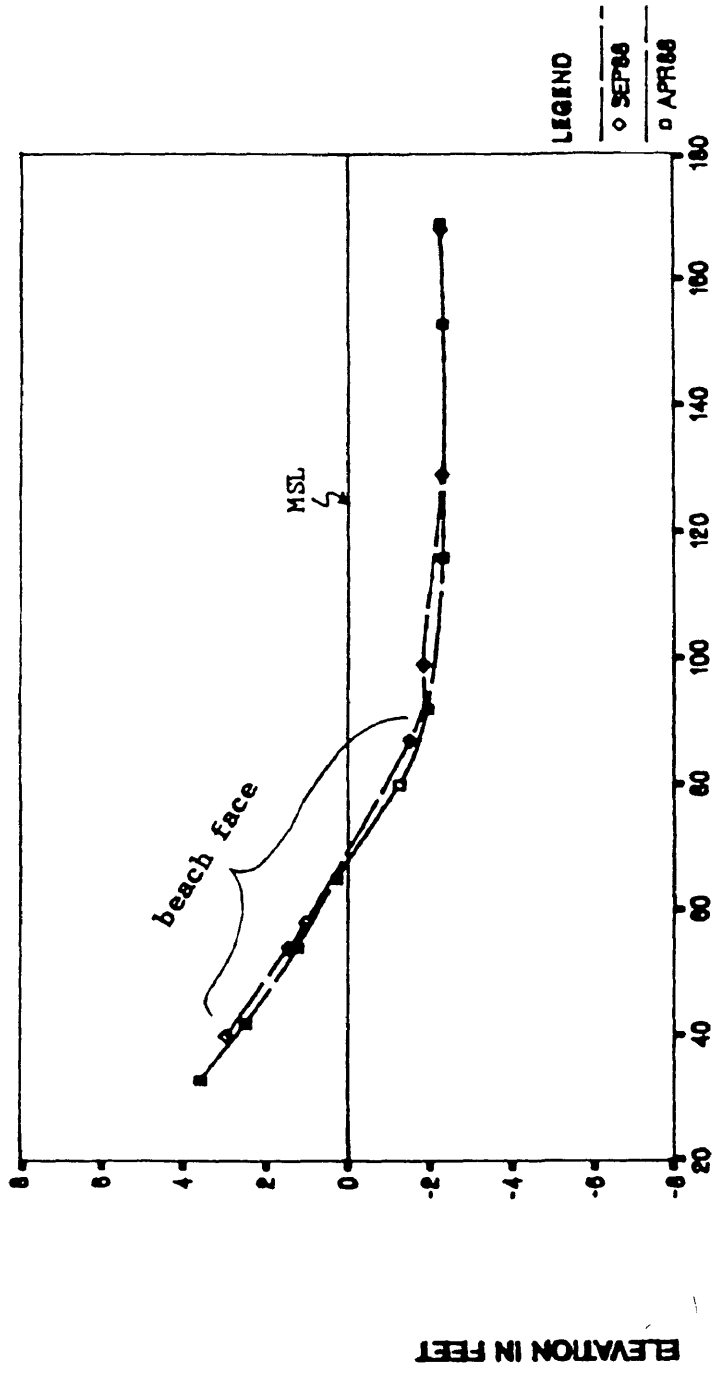
DEC1488 MAR1989

PROFILES AT HI2, PROFILES 11 AND 21

OCT. 4, 1989



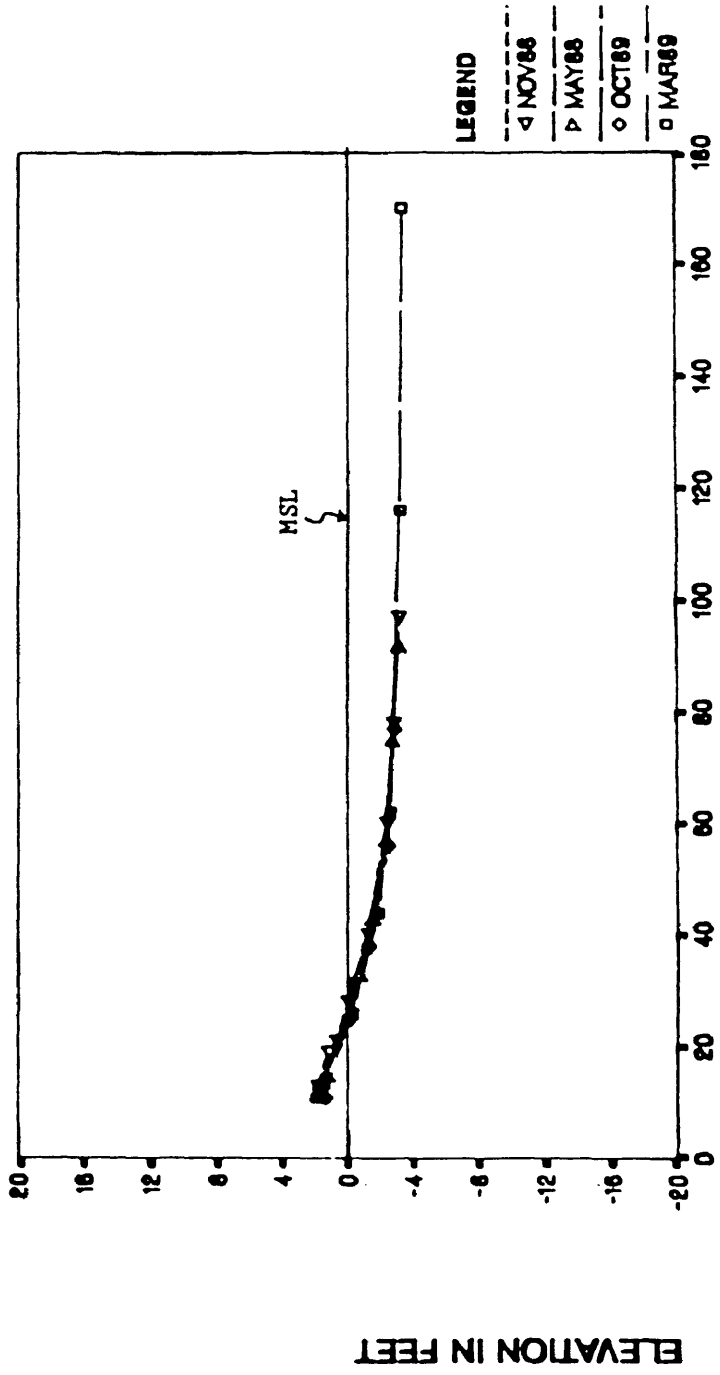
# PROFILES AT CHP APR.16,1988 AND SEP.21,1988





# BEACH PROFILES AT HI2

PROFILE 28



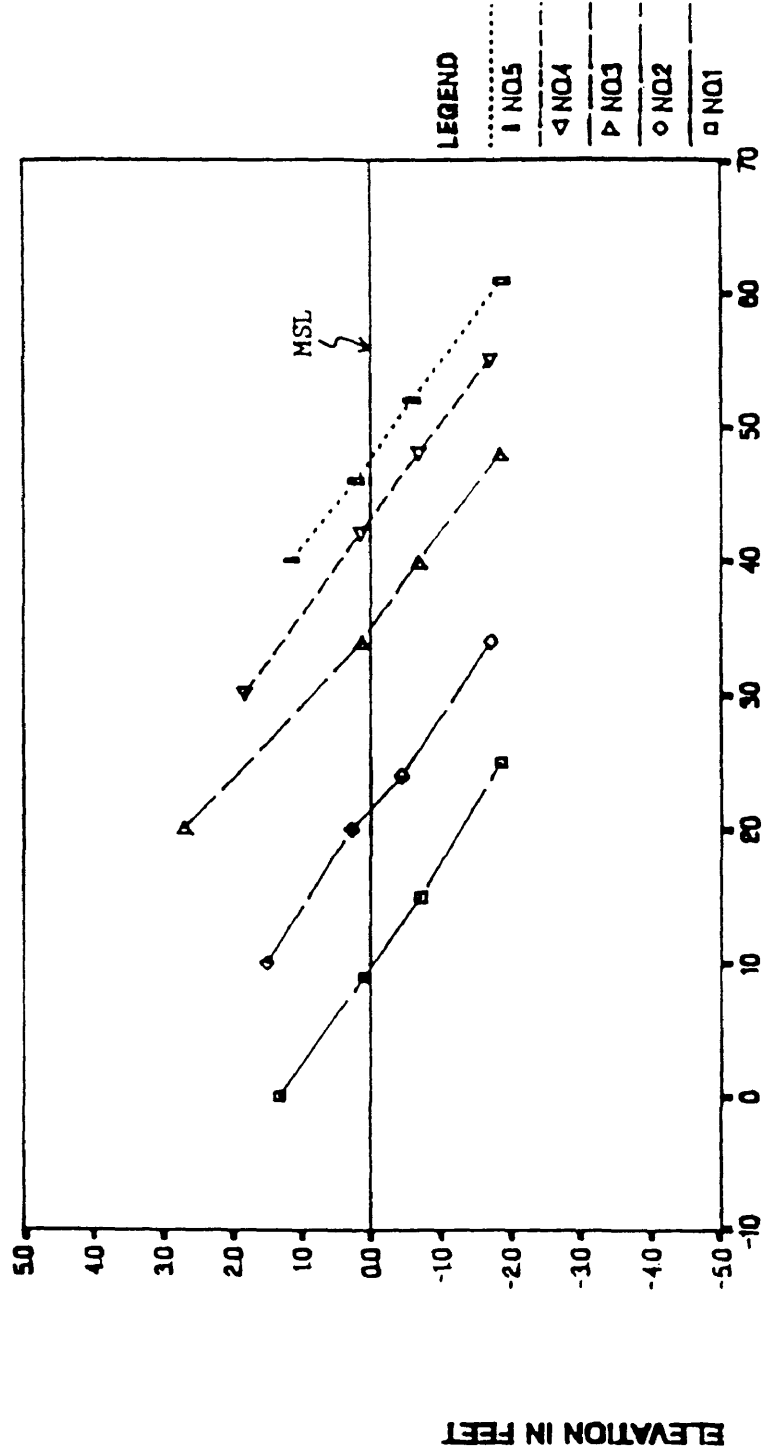
DISTANCE IN FEET

APPENDIX C

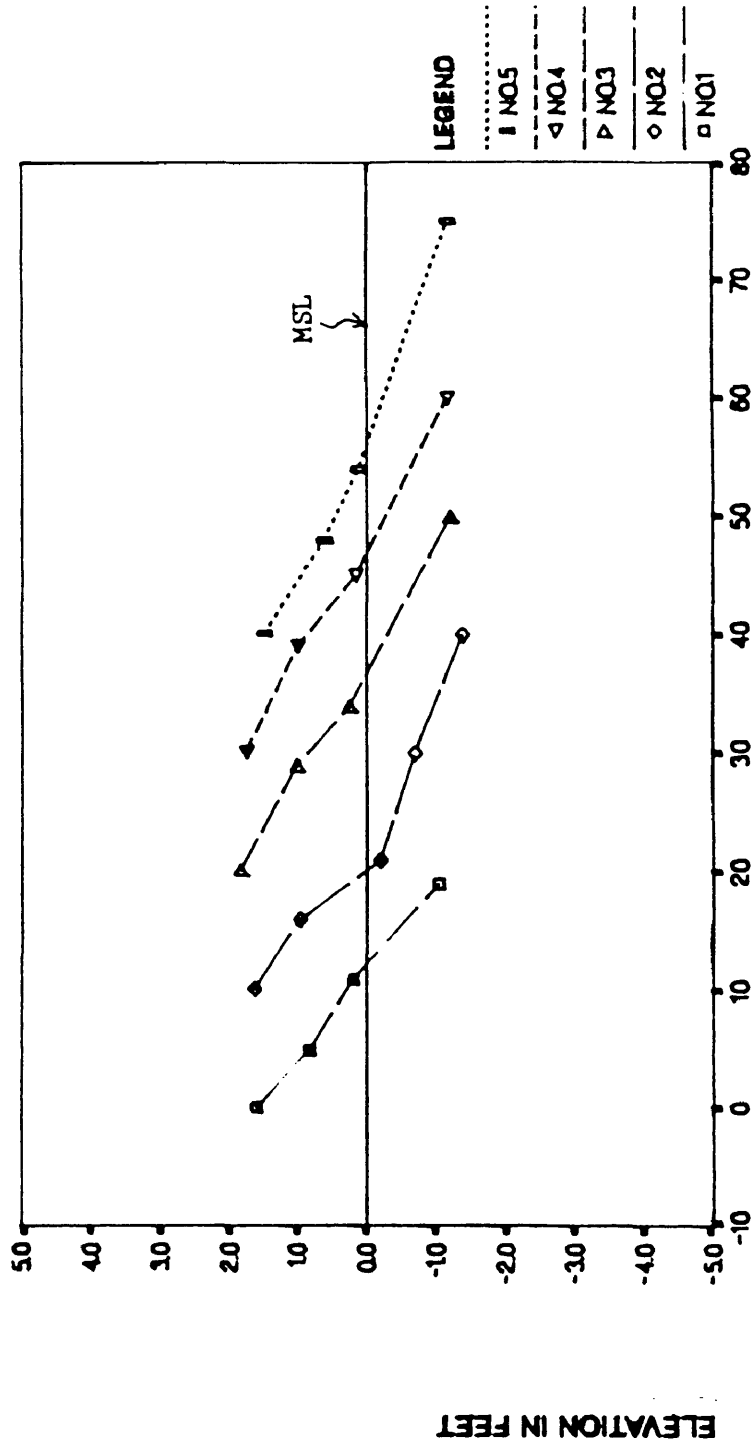
Bay beach profiles

Measured in Spring of 1990

# BAY BEACH SLOPES HI2 BAY L, MAY 1990.

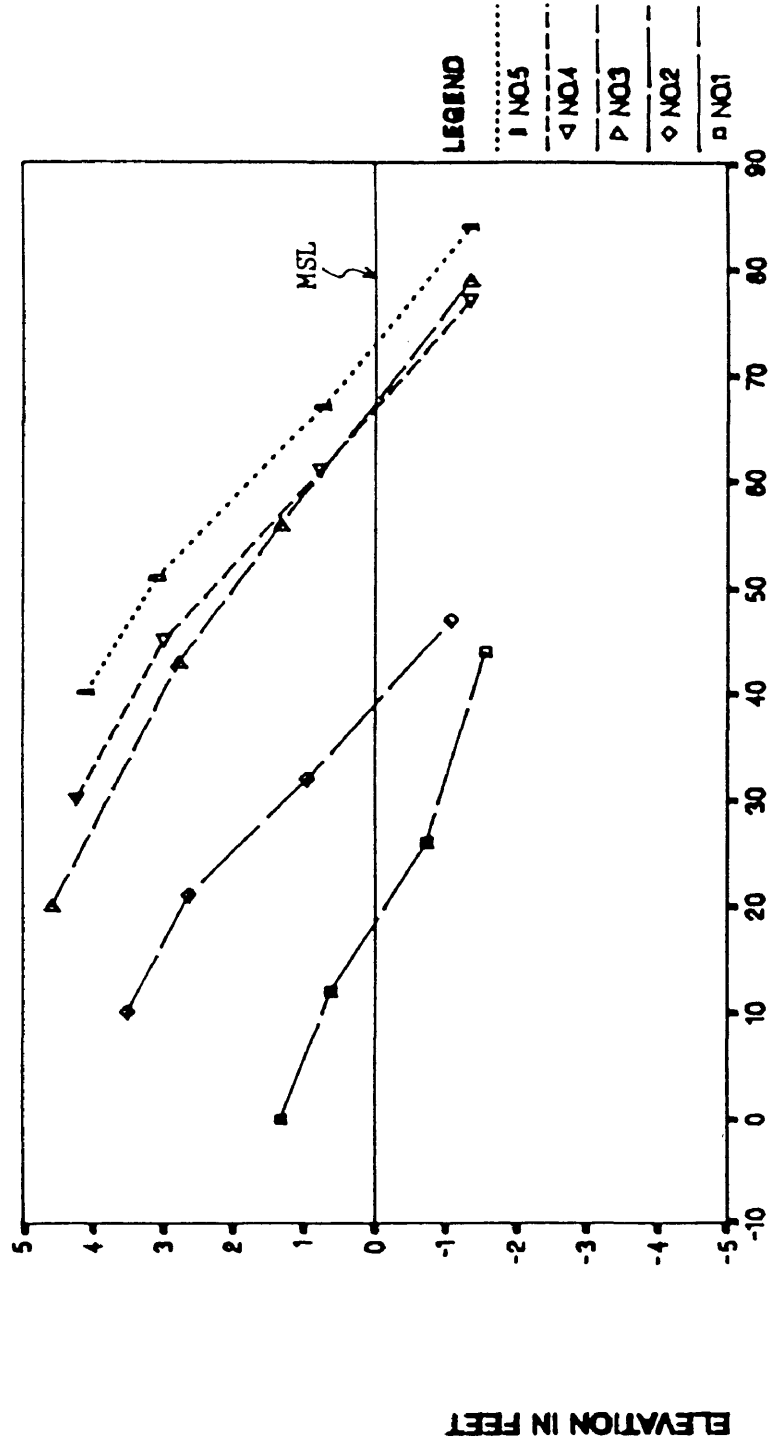


BAY BEACH SLOPES  
 CHP, BAY B, 8 MAY, 1990



DISTANCE IN FEET

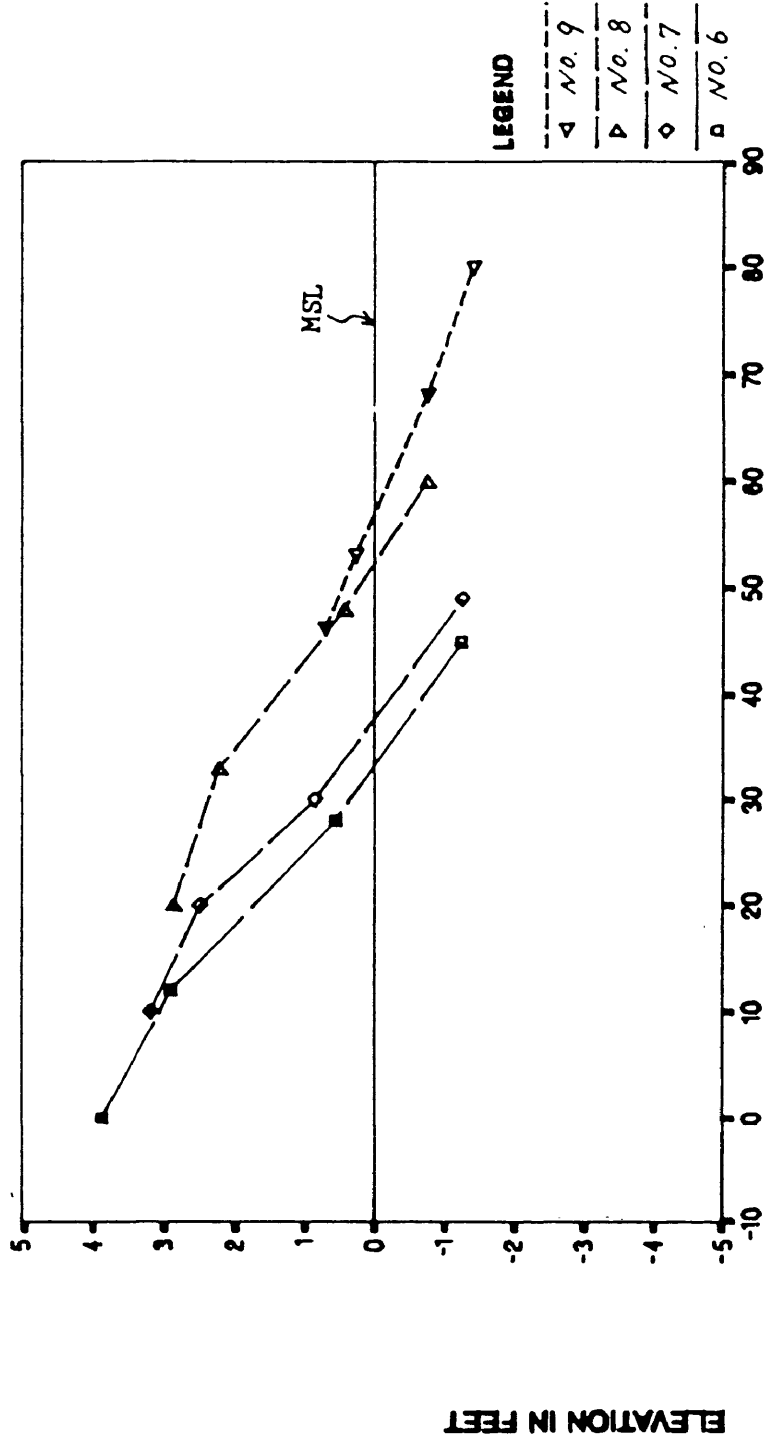
# BAY BEACH SLOPES DMF BAY A, MAY 11, 1990



DISTANCE IN FEET

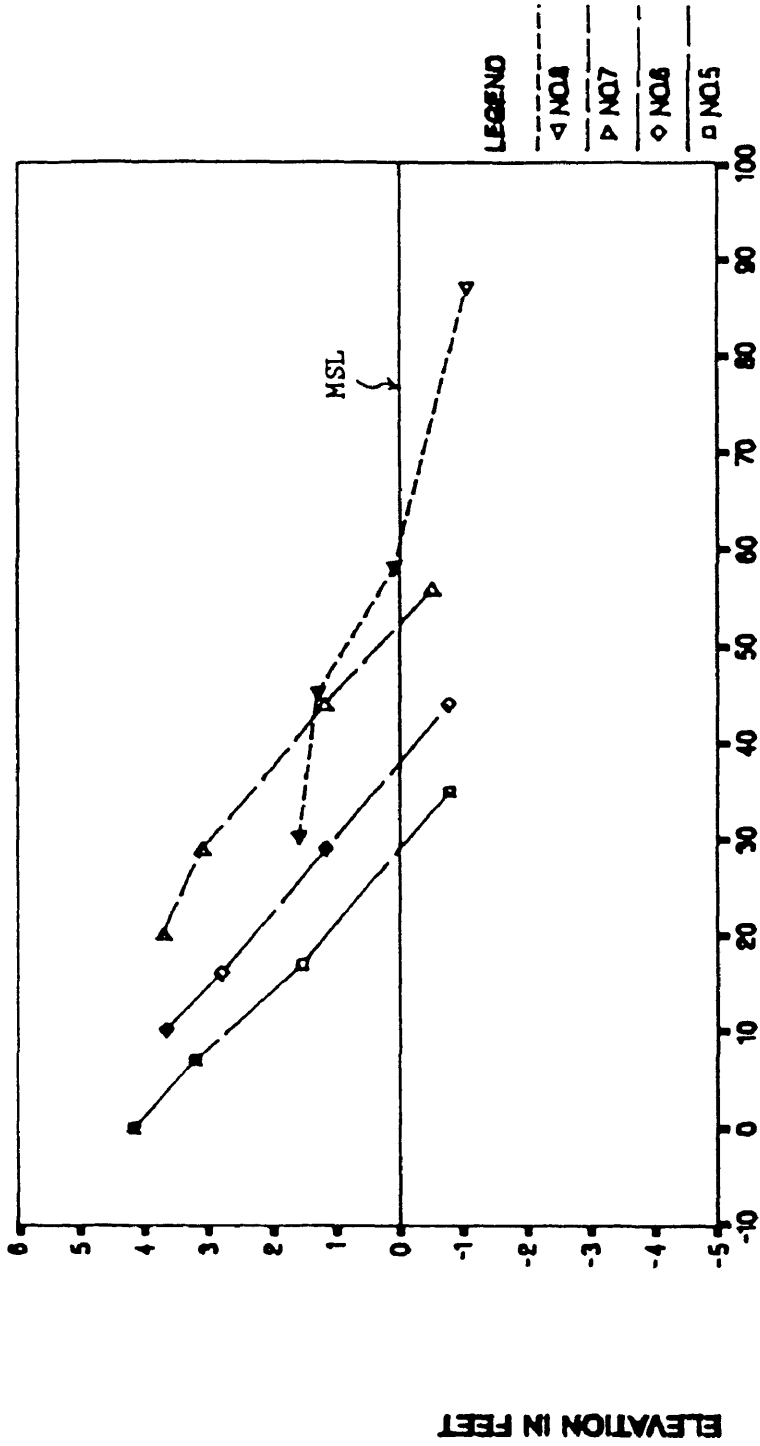
ELEVATION IN FEET

# BAY BEACH SLOPES DMF BAY A, MAY 11, 1990



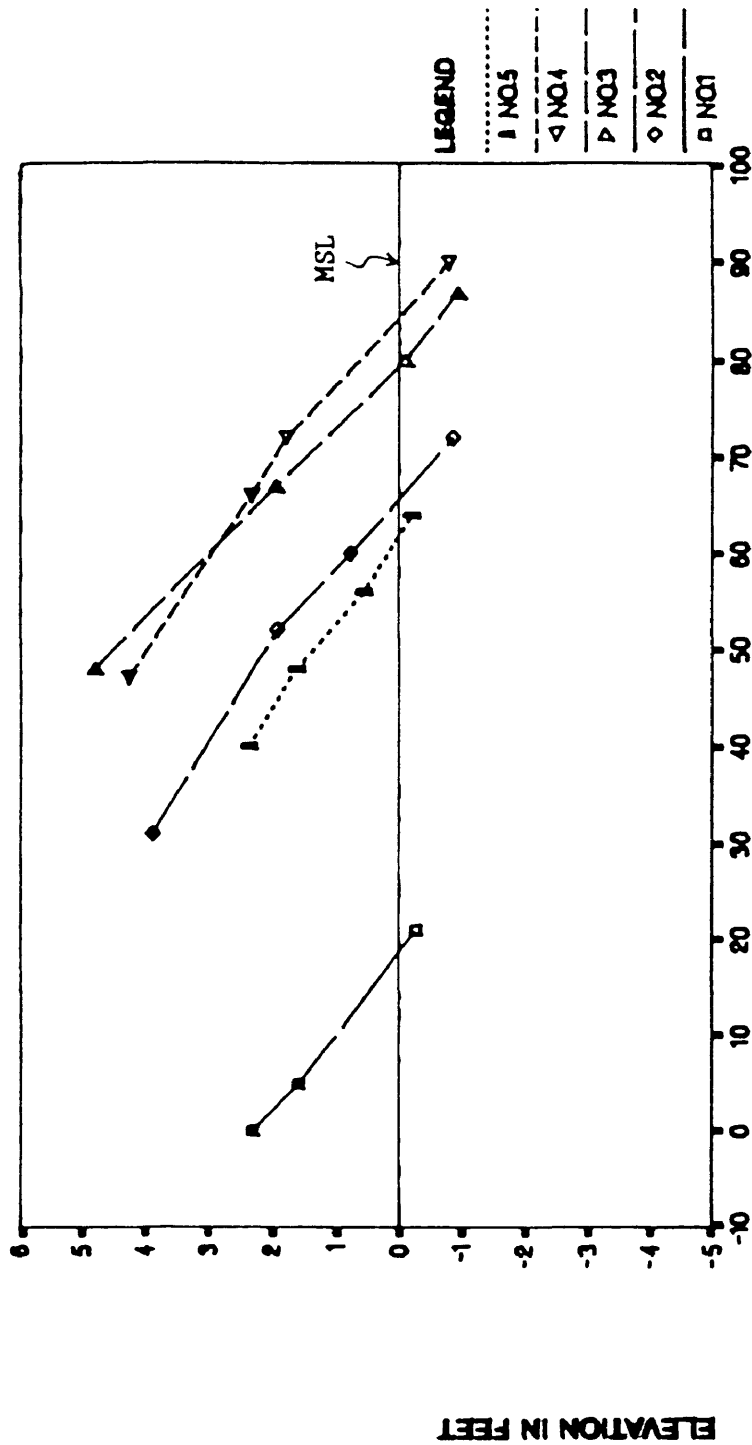
# BAY BEACH SLOPES DMF BAY D, PROFILES 5-8.

MAY 11, 1990



# BAY BEACH SLOPES WALTRIP BAY B, PROFILES 1-5

MAY 13, 1990

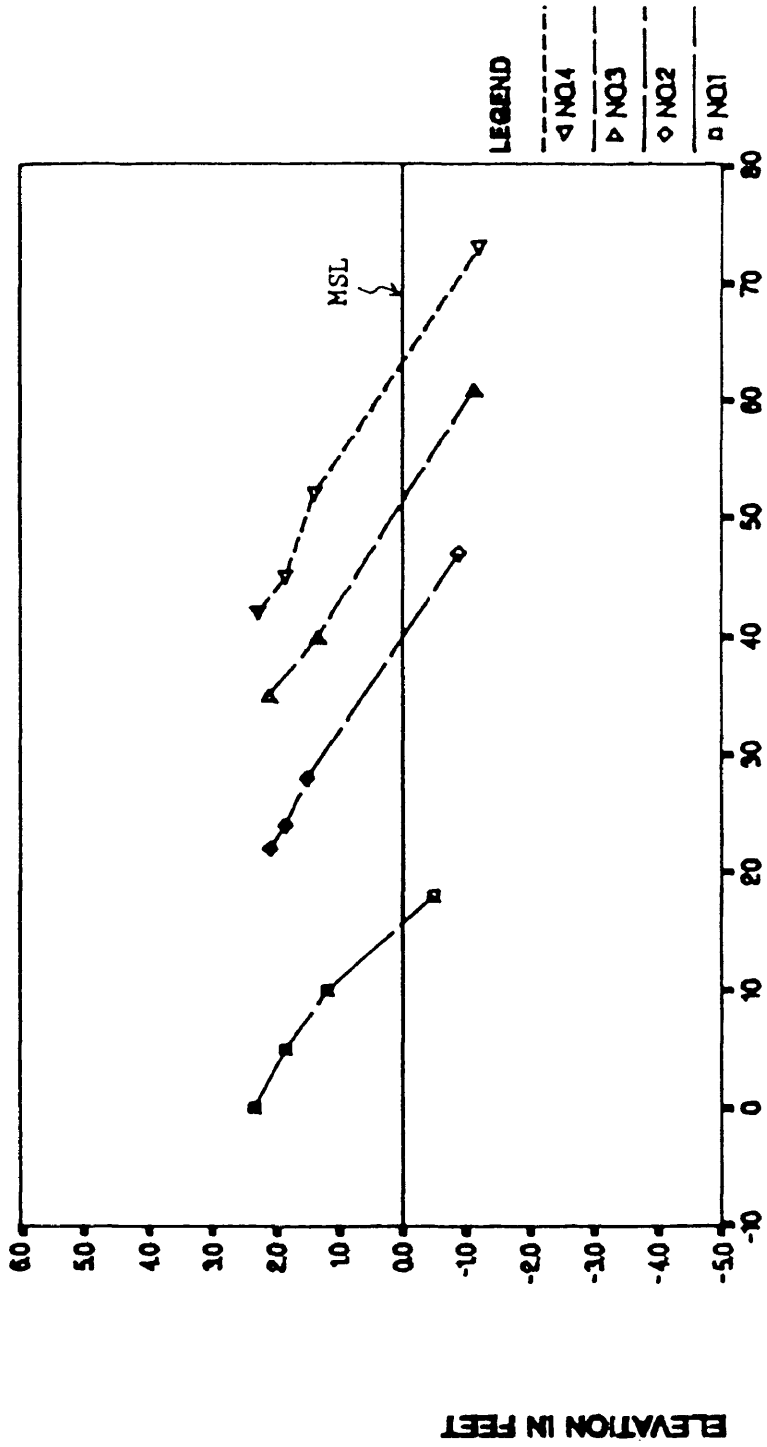


DISTANCE IN FEET



# BAY BEACH SLOPES NPS BAY B, PROFILES 1-4.

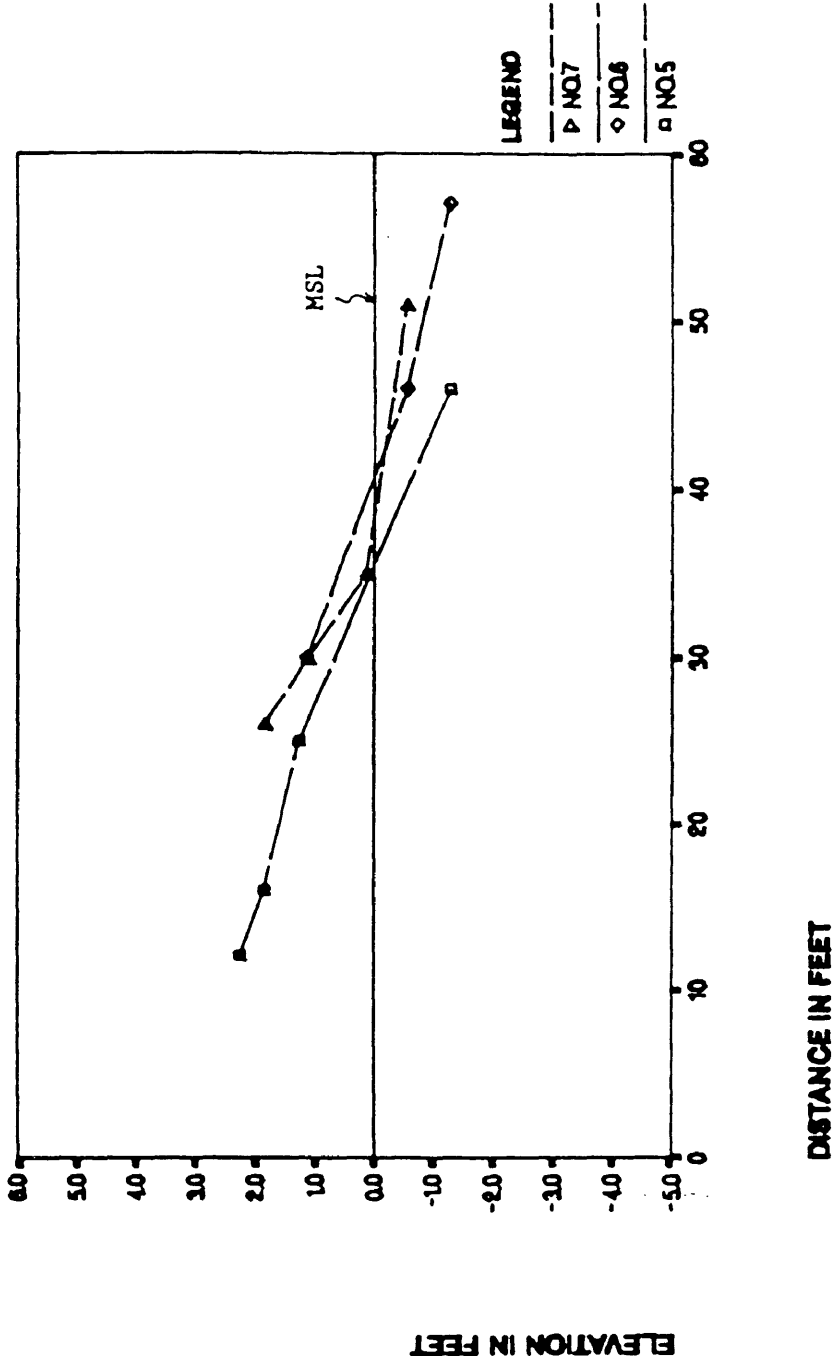
APR 6, 1990



DISTANCE IN FEET

# BAY BEACH SLOPES NPS BAY B, PROFILES 5-8

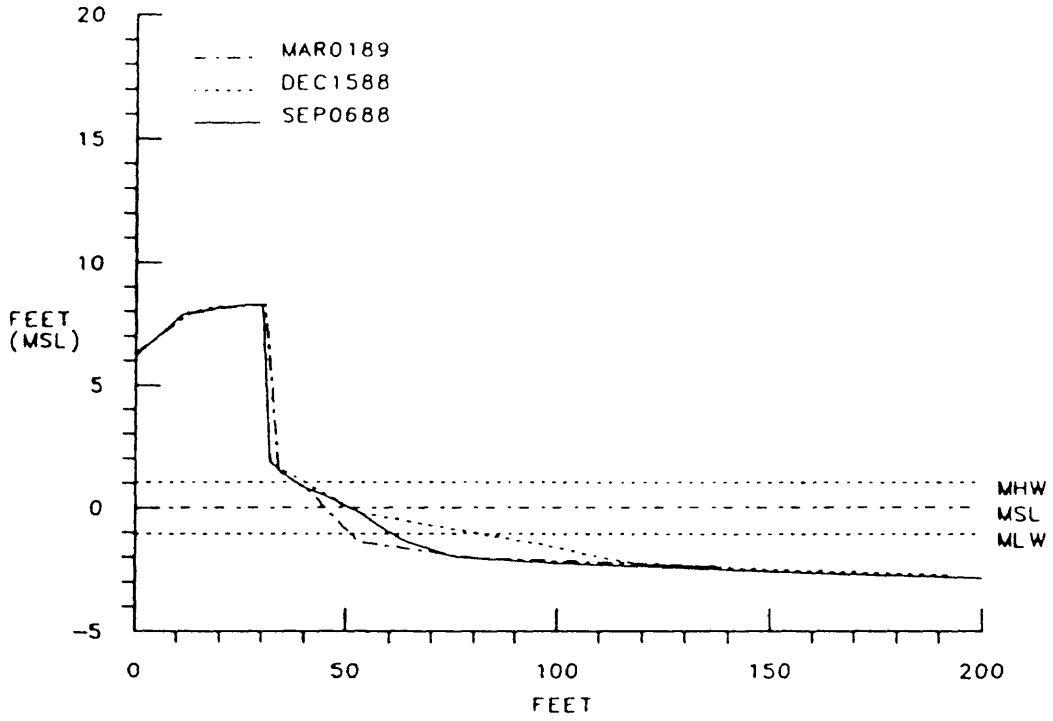
APR 6, 1990



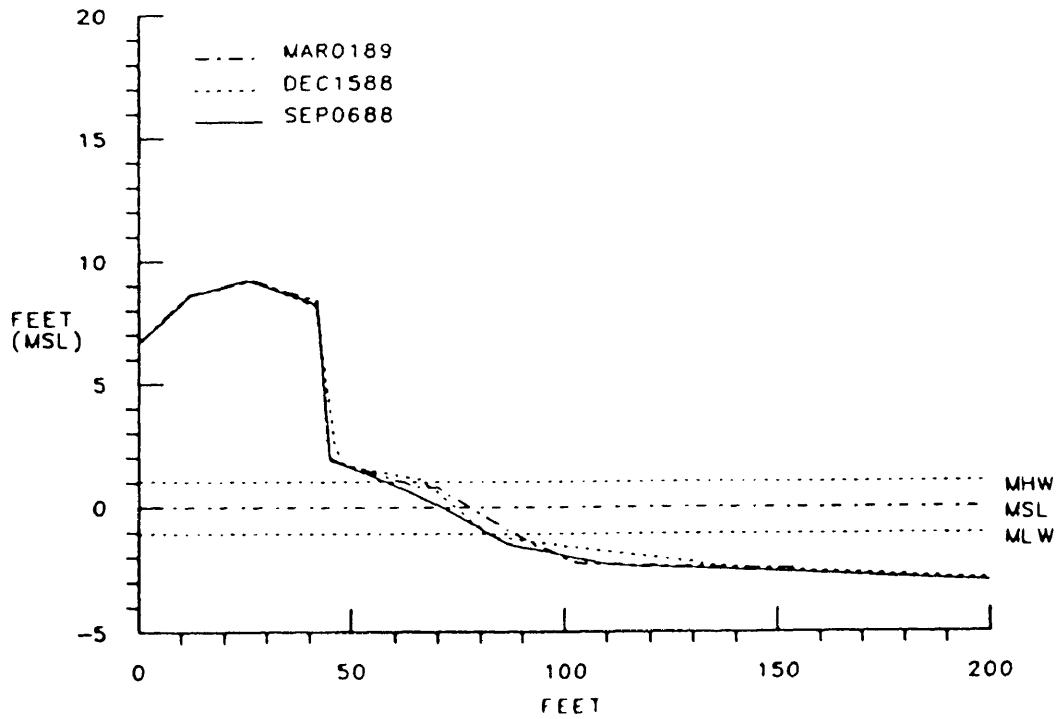
APPENDIX D

Plots of beach profiles

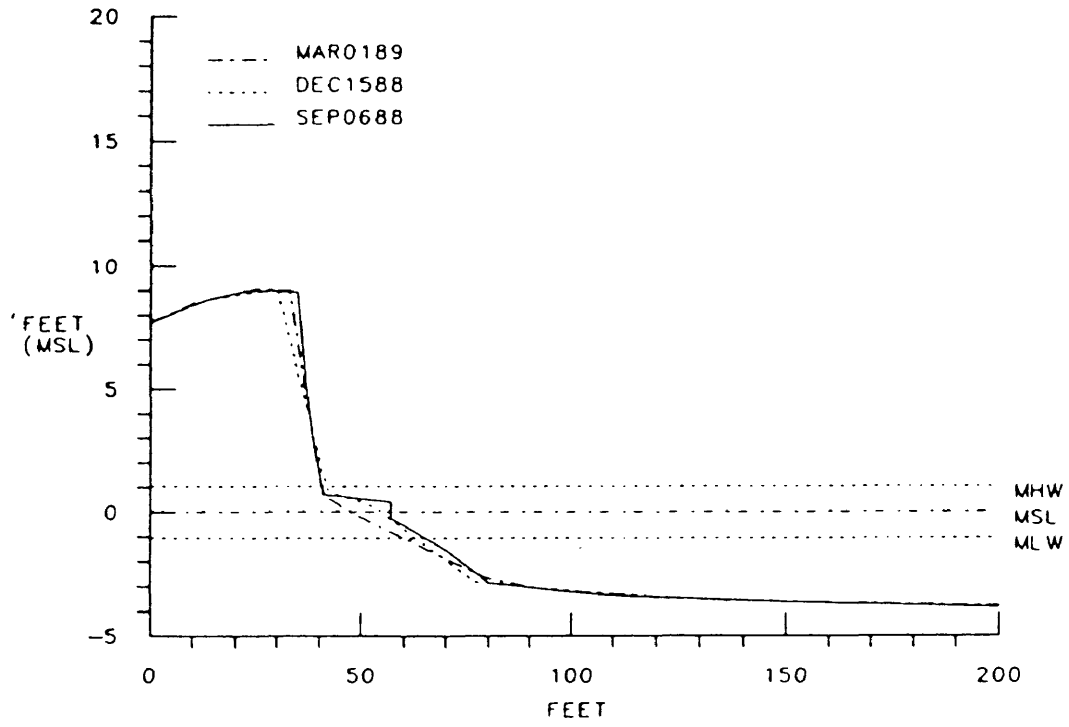
HOG ISLAND HEADLANDS  
PROFILE NO 01



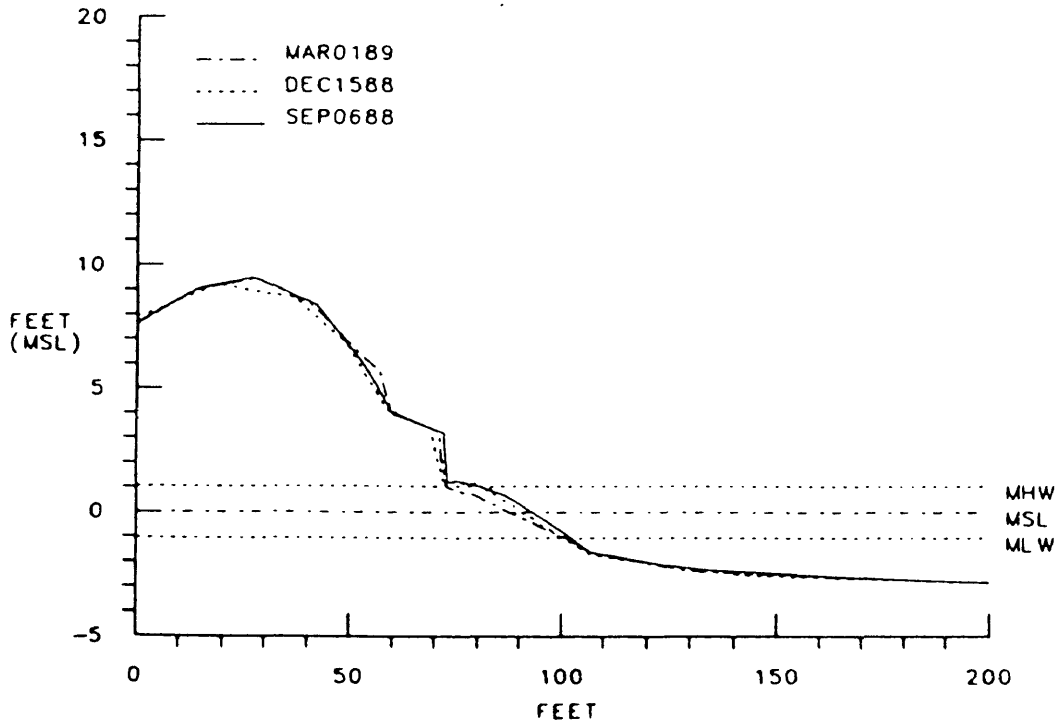
HOG ISLAND HEADLANDS  
PROFILE NO. 02



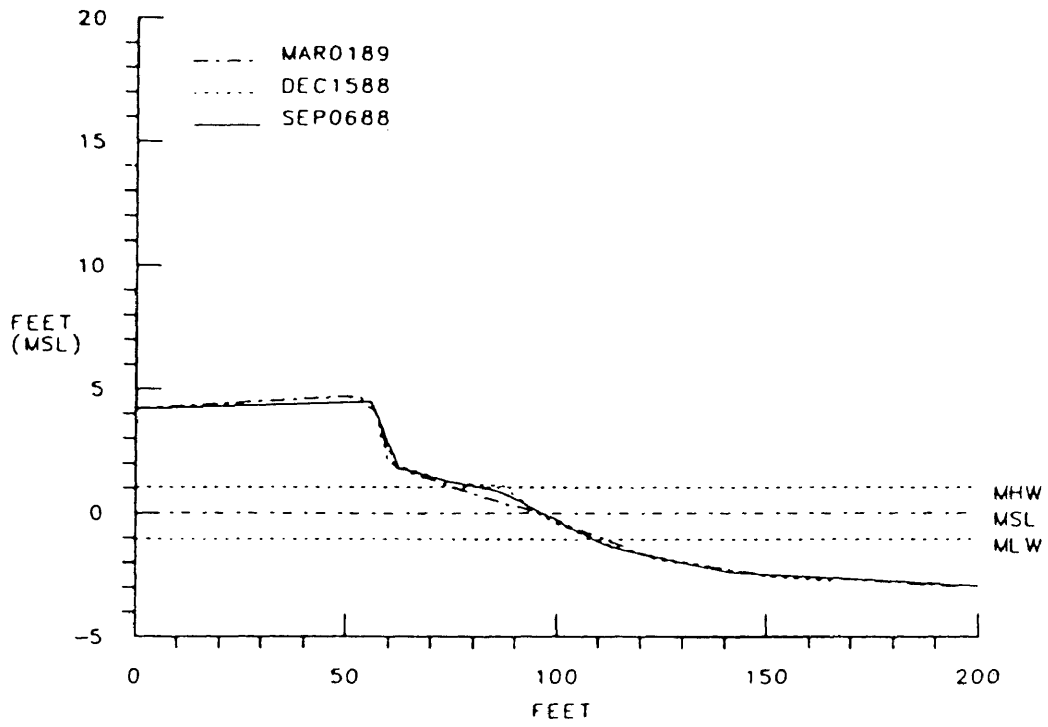
HOG ISLAND HEADLANDS  
PROFILE NO. 09



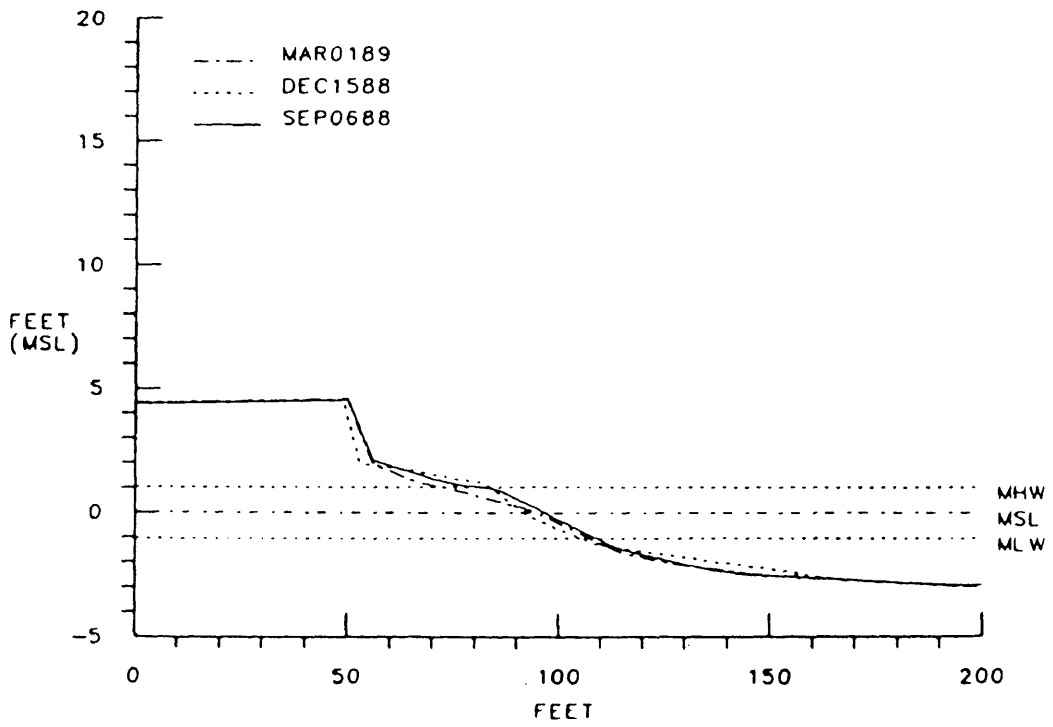
HOG ISLAND HEADLANDS  
PROFILE NO 10



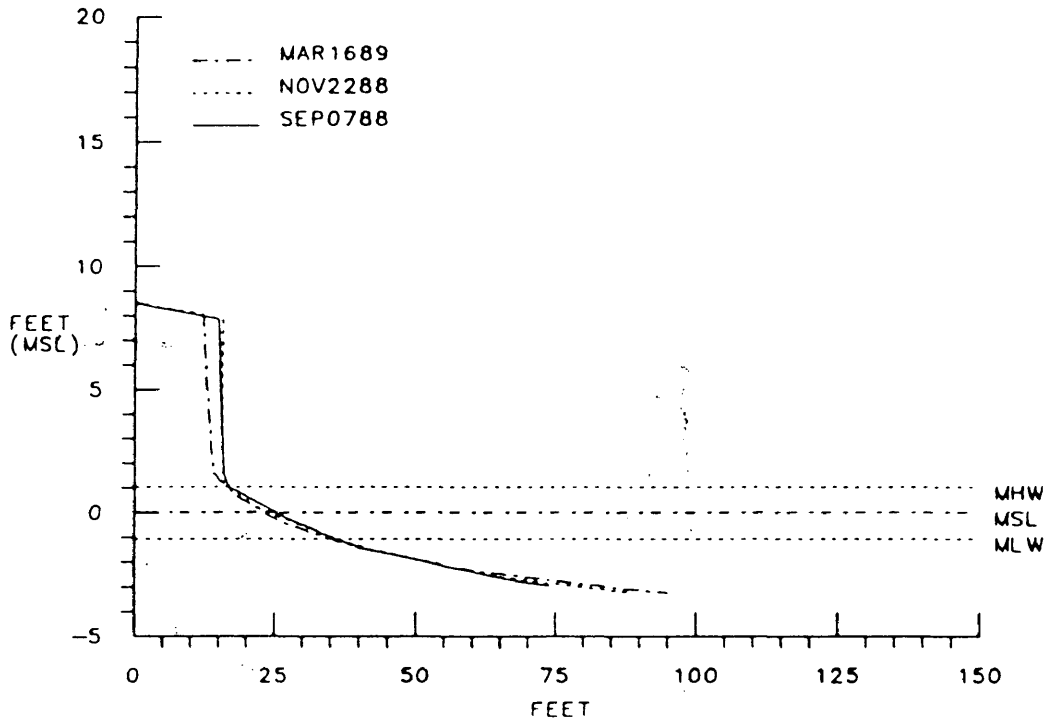
HOG ISLAND HEADLANDS  
PROFILE NO. 20



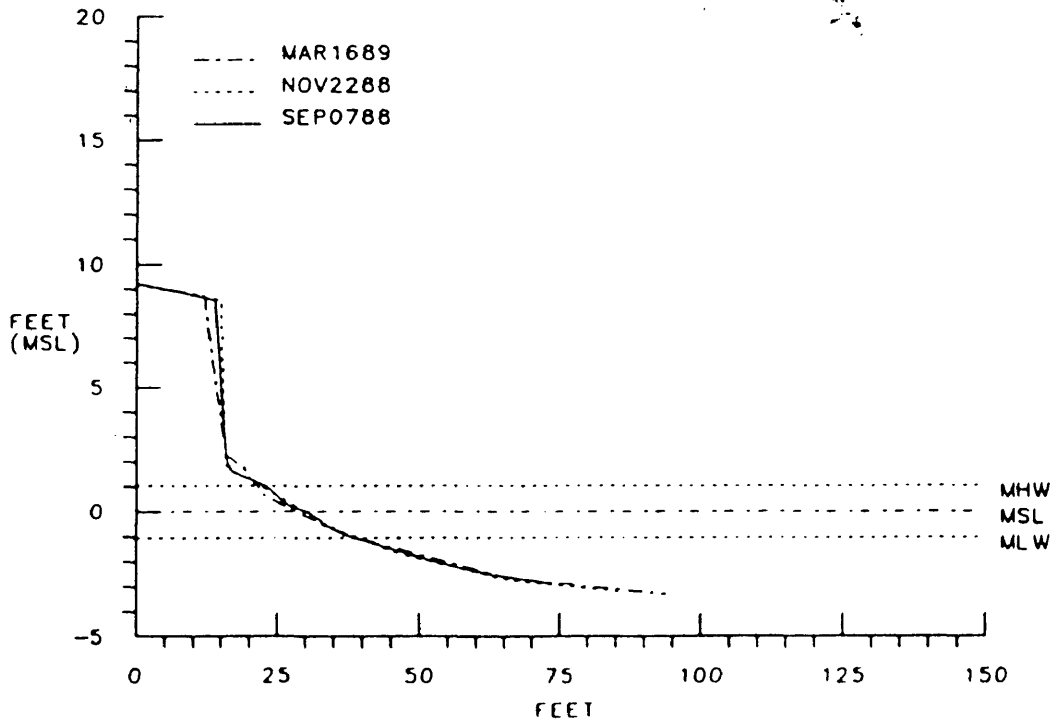
HOG ISLAND HEADLANDS  
PROFILE NO. 21



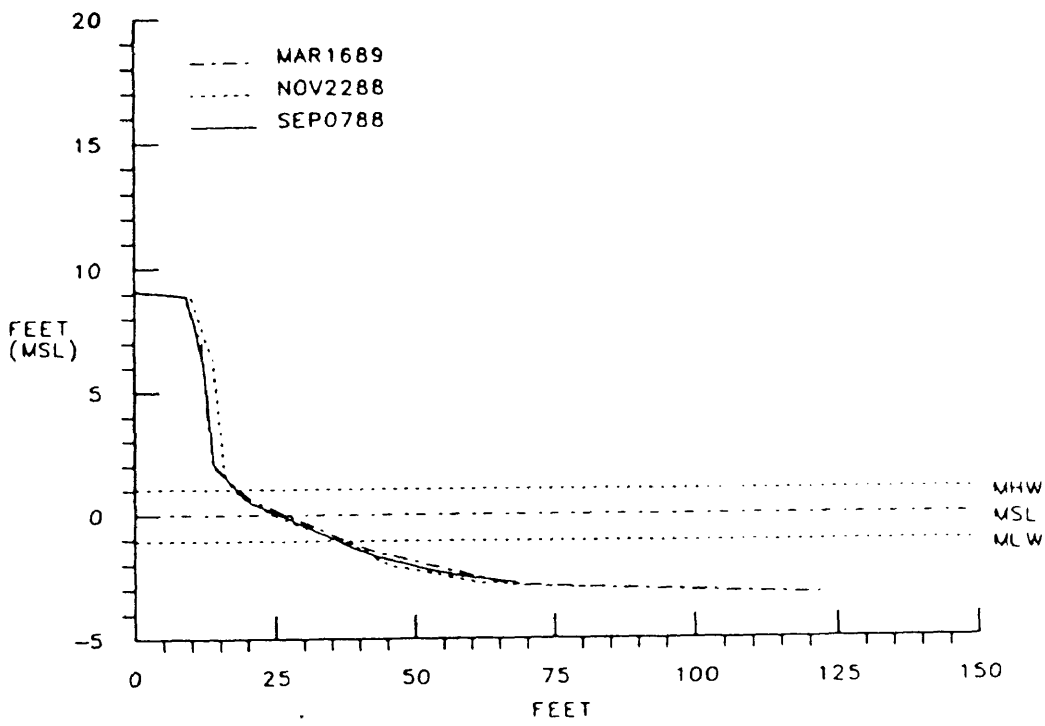
HOG ISLAND BREAKWATERS  
PROFILE NO. 01



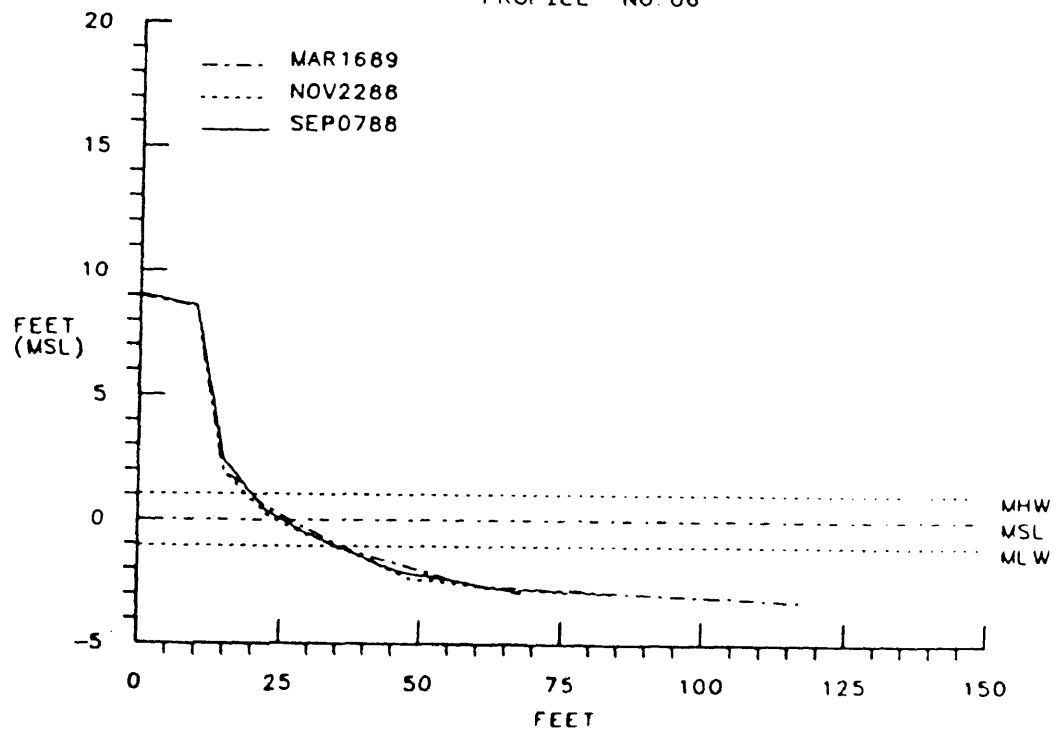
HOG ISLAND BREAKWATERS  
PROFILE NO. 02



HOG ISLAND BREAKWATERS  
PROFILE NO. 05

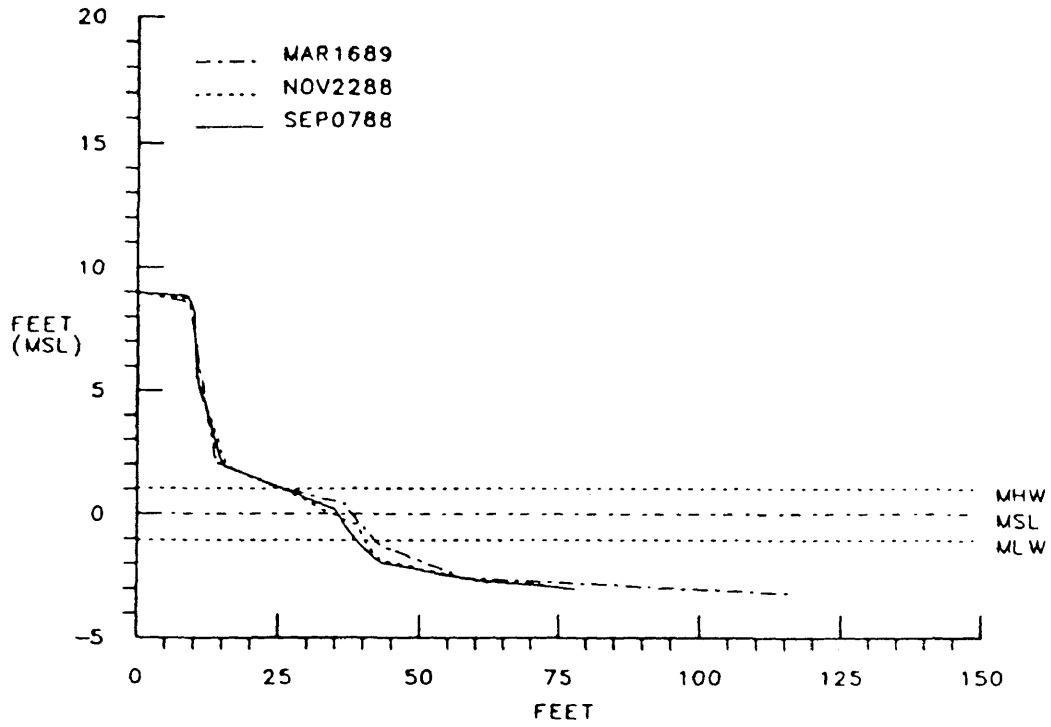


HOG ISLAND BREAKWATERS  
PROFILE NO. 06

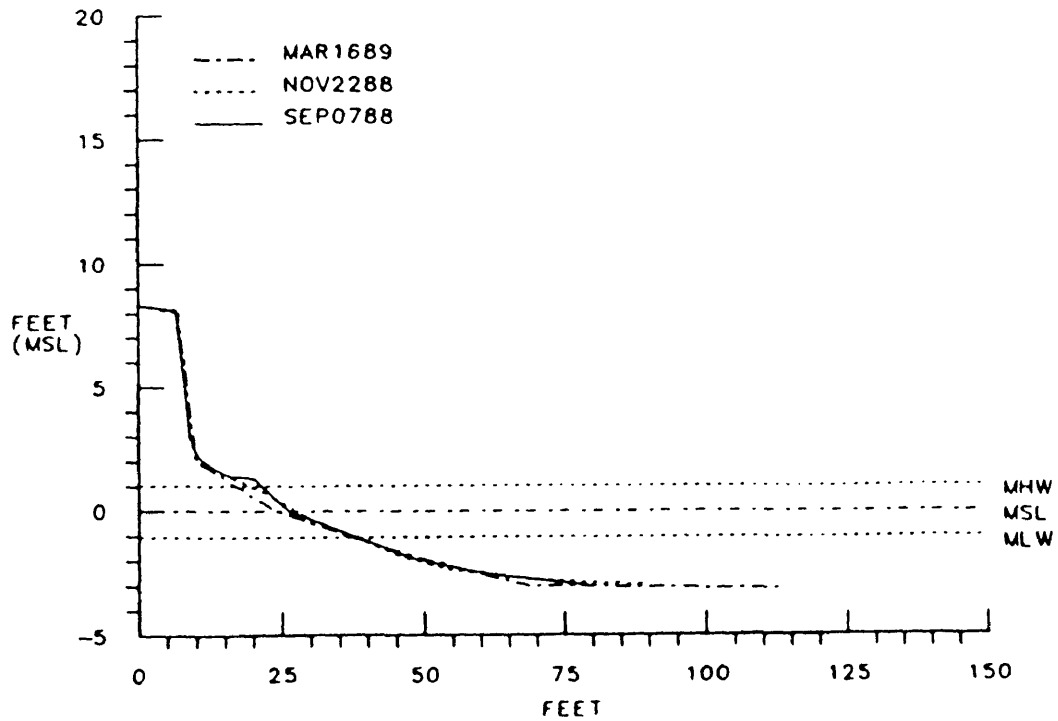




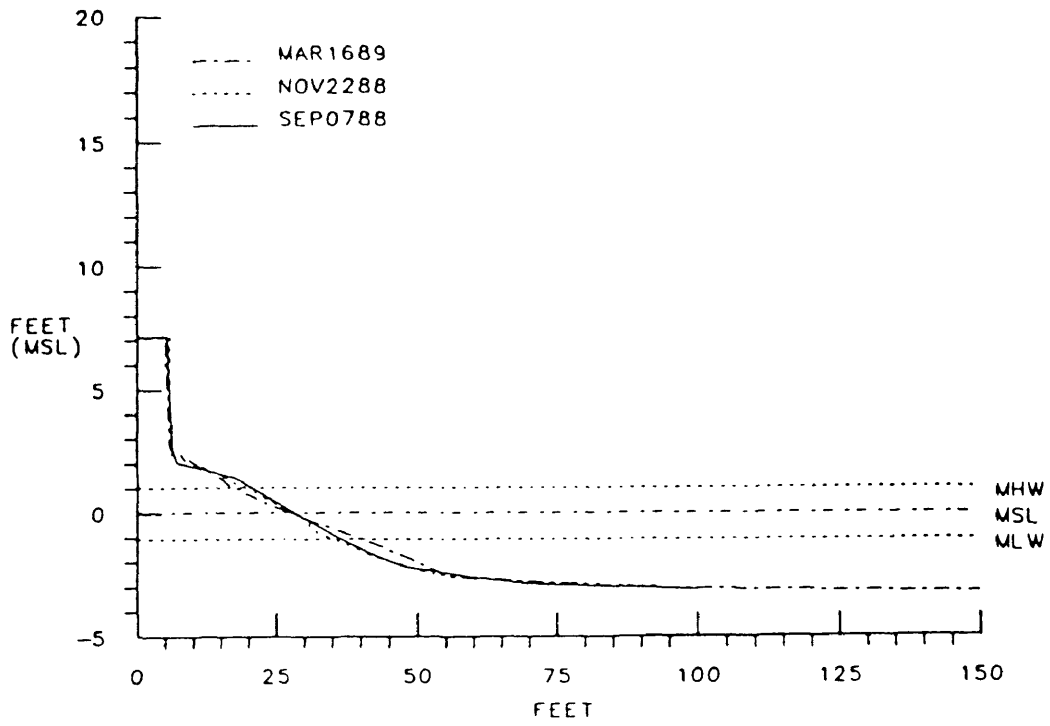
HOG ISLAND BREAKWATERS  
PROFILE NO. 09



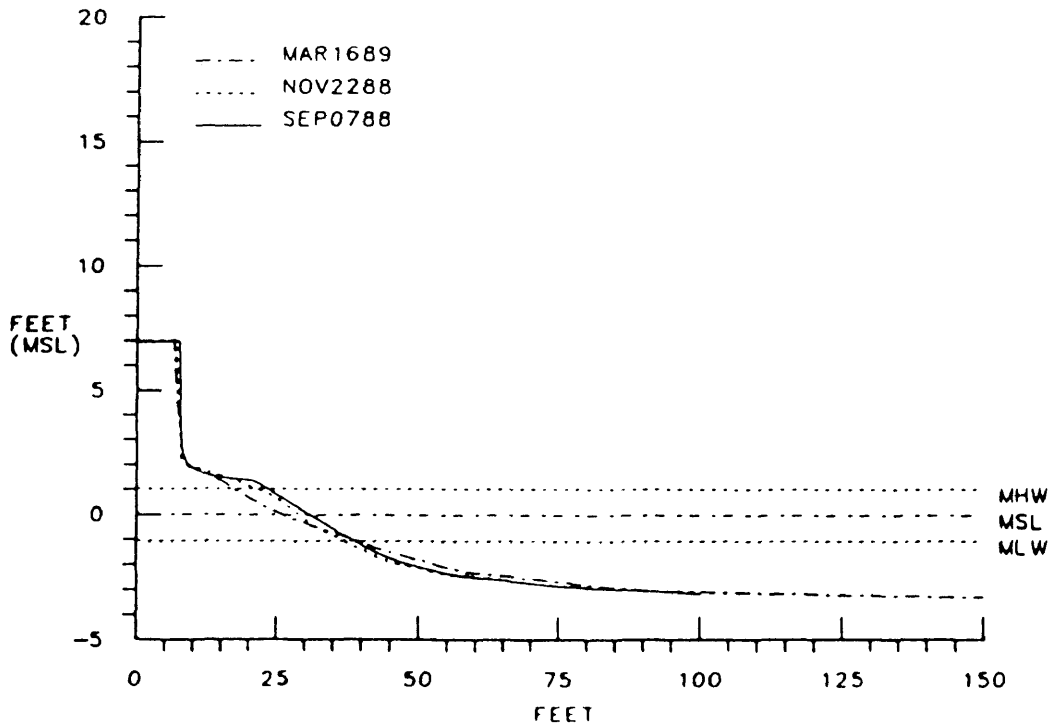
HOG ISLAND BREAKWATERS  
PROFILE NO. 12



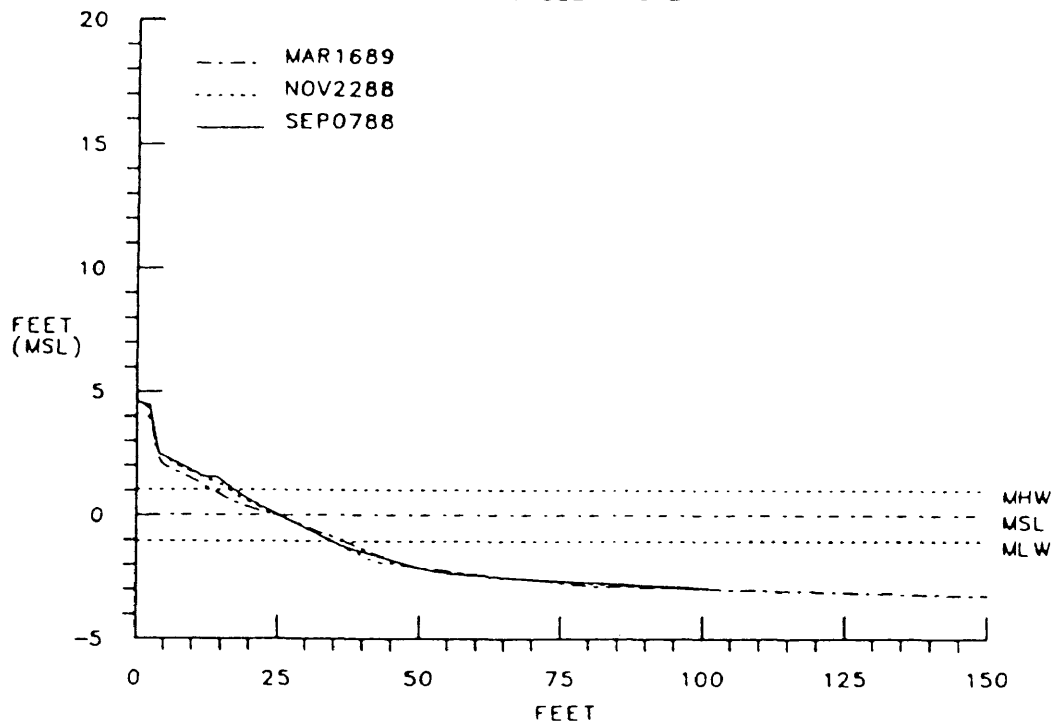
HOG ISLAND BREAKWATERS  
PROFILE NO 17



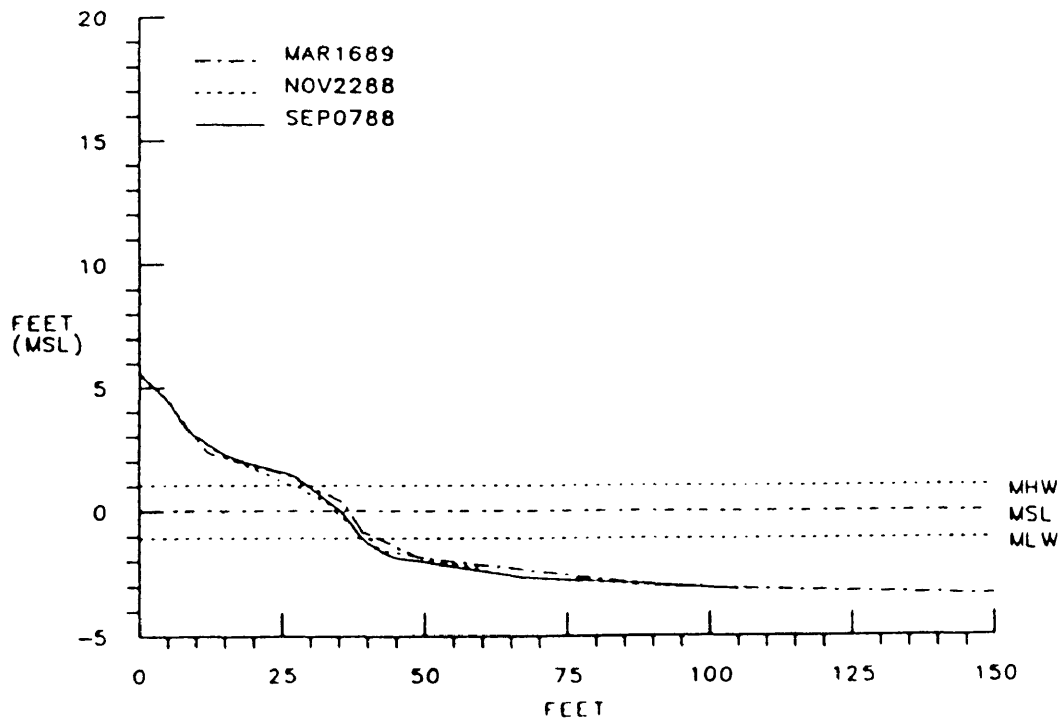
HOG ISLAND BREAKWATERS  
PROFILE NO 18



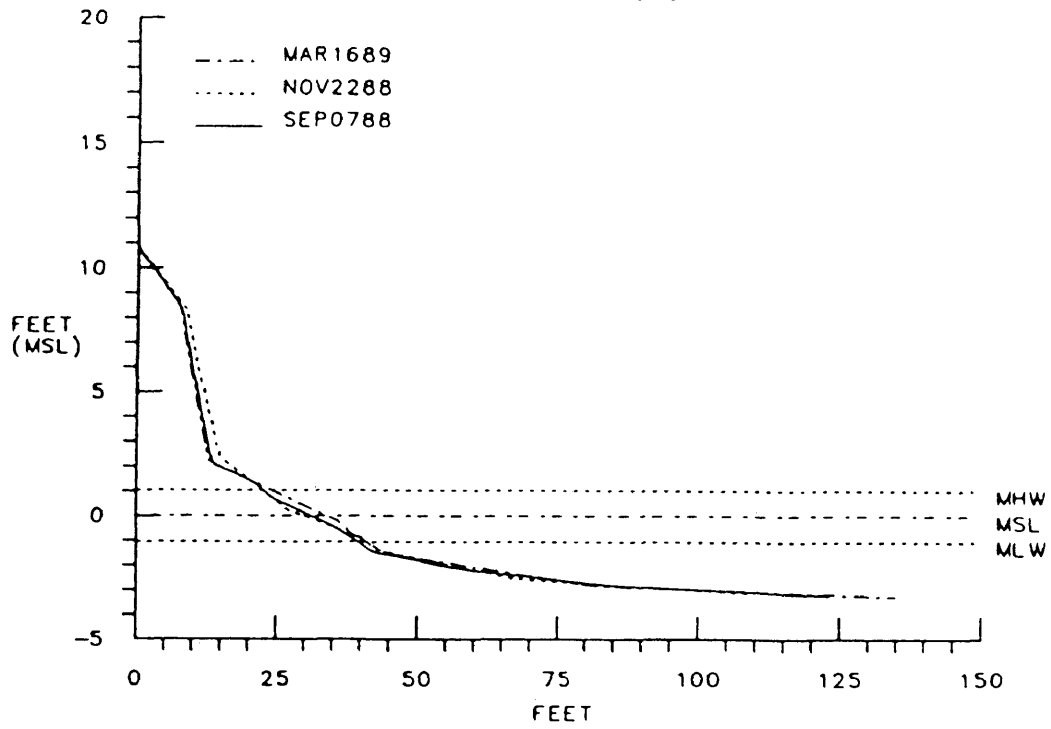
HOG ISLAND BREAKWATERS  
PROFILE NO. 21



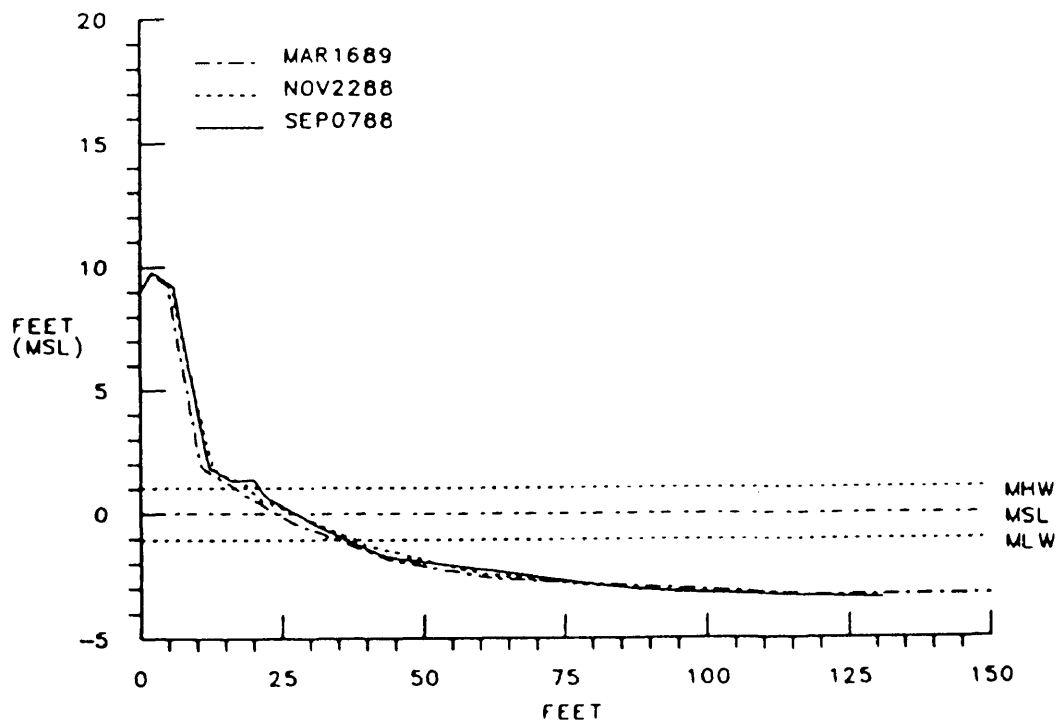
HOG ISLAND BREAKWATERS  
PROFILE NO. 23



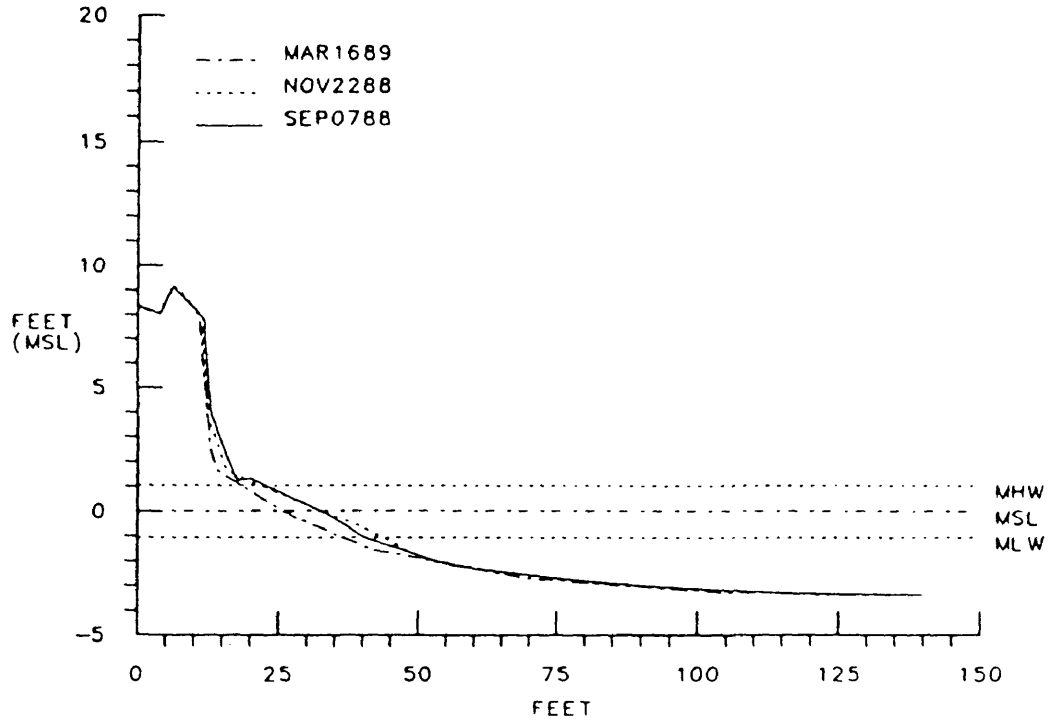
HOG ISLAND BREAKWATERS  
PROFILE NO. 24



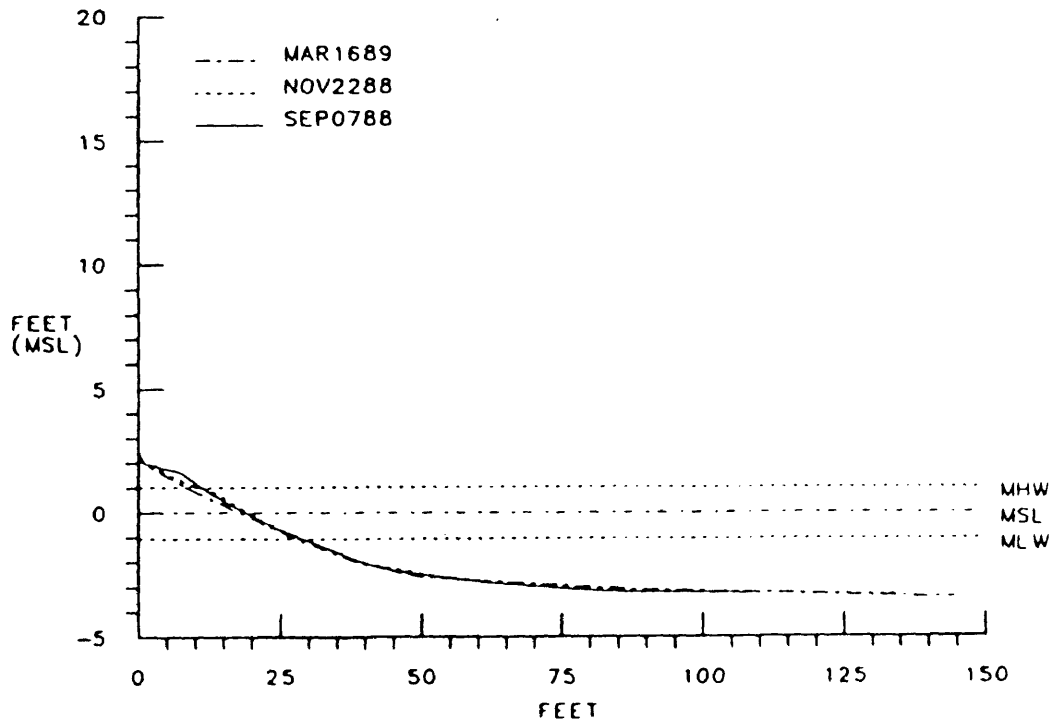
HOG ISLAND BREAKWATERS  
PROFILE NO. 26



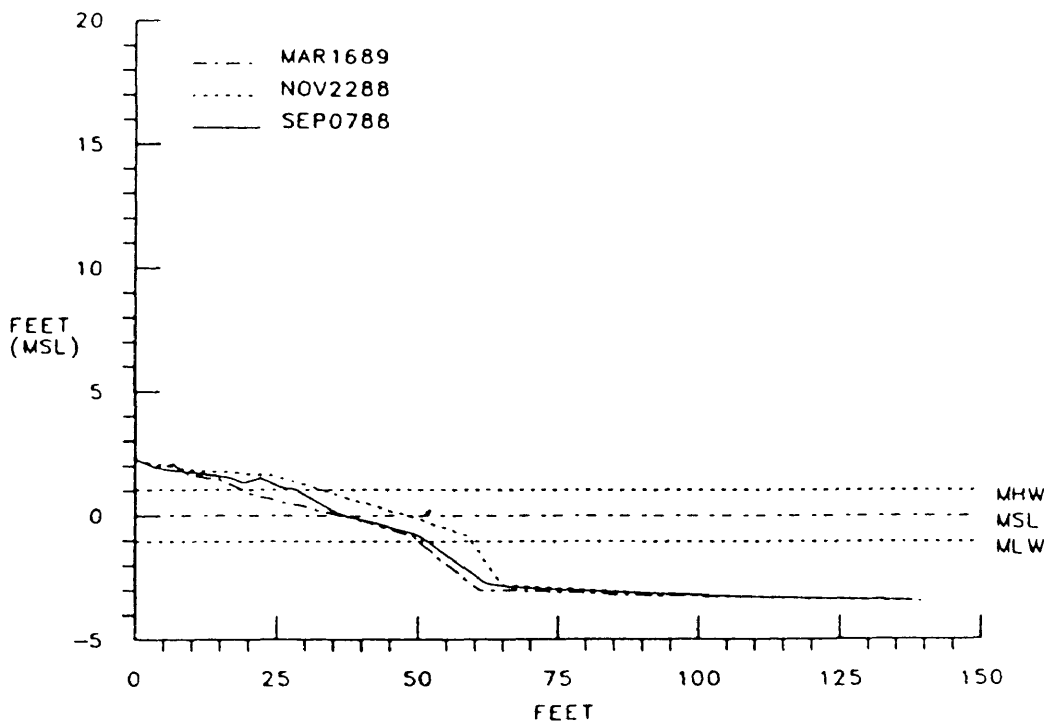
HOG ISLAND BREAKWATERS  
PROFILE NO. 31



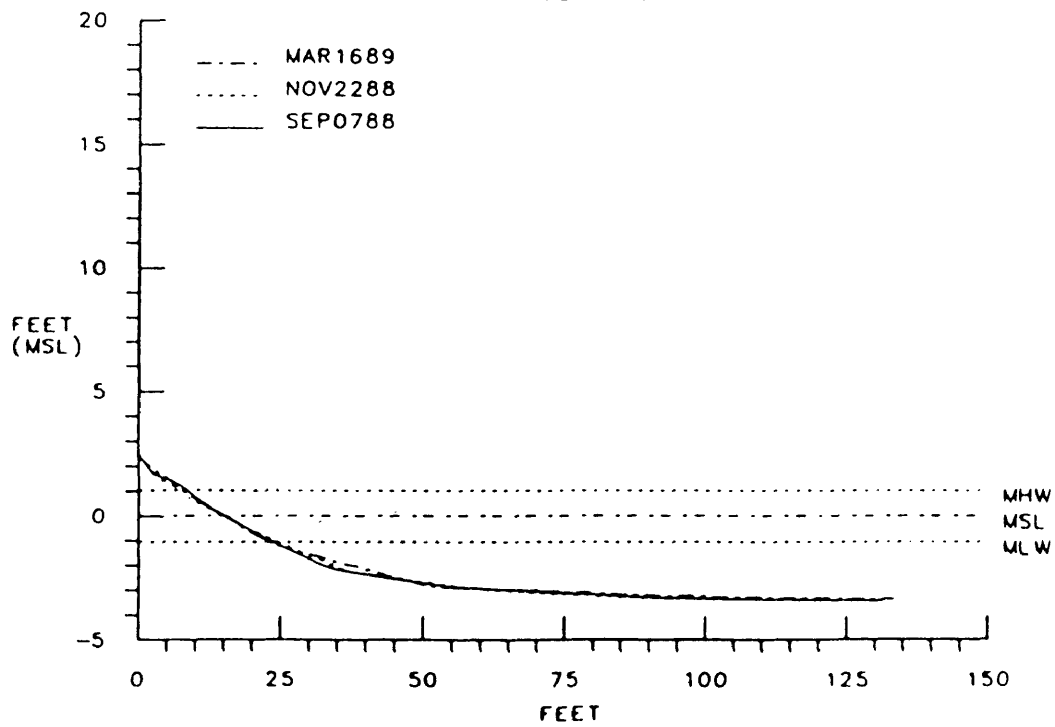
HOG ISLAND BREAKWATERS  
PROFILE NO. 32



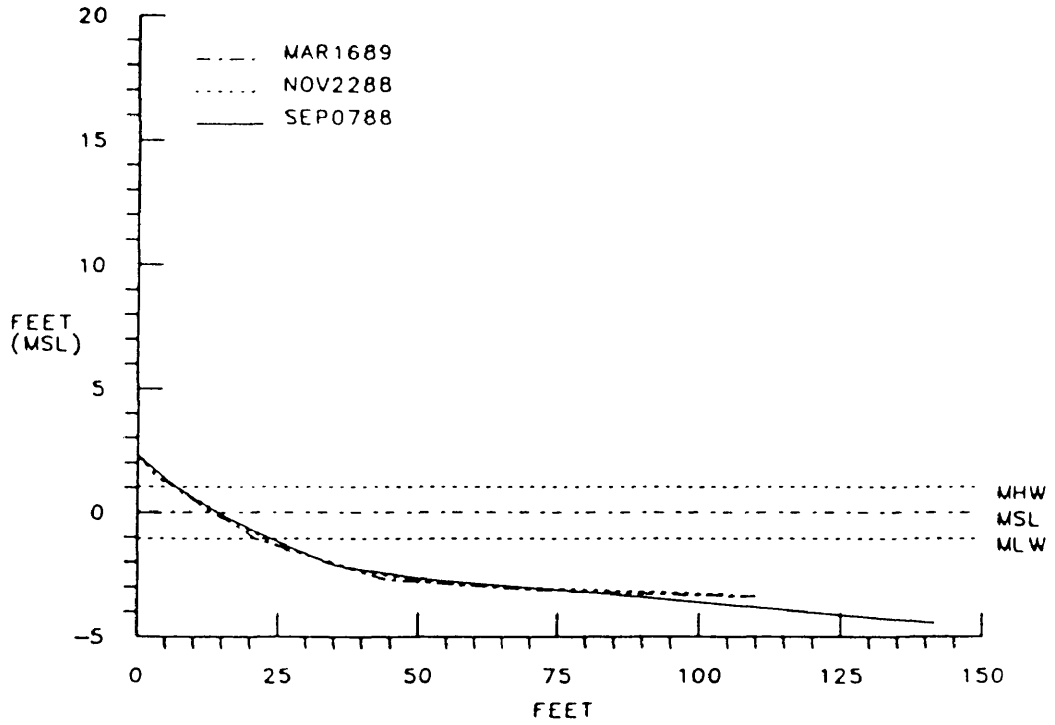
HOG ISLAND BREAKWATERS  
PROFILE NO 34



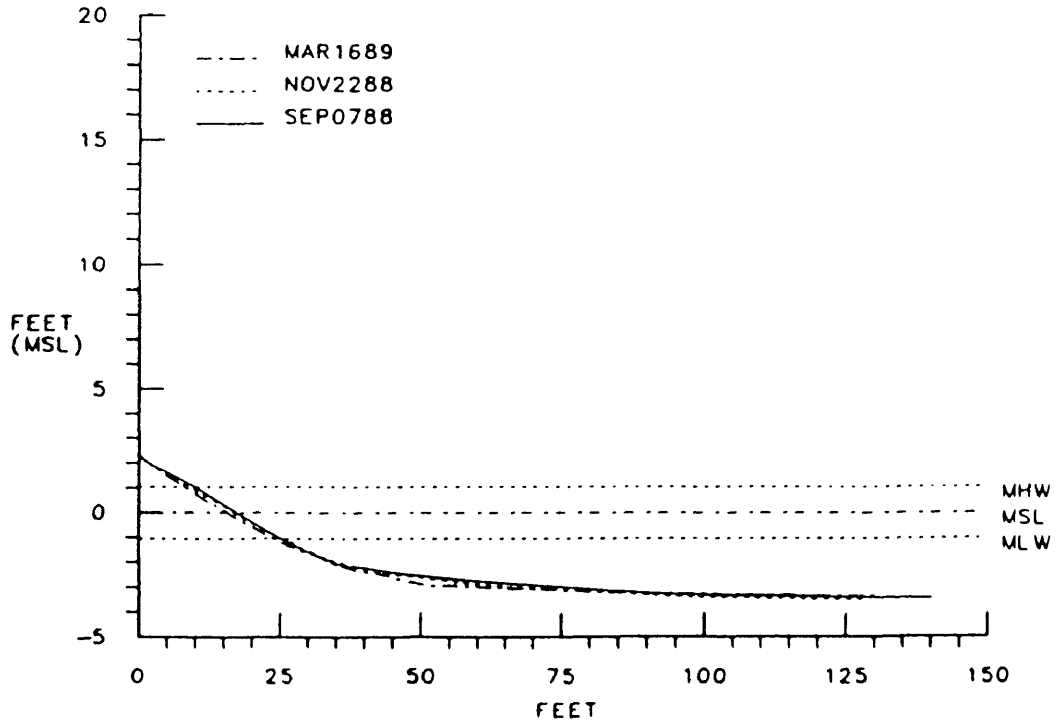
HOG ISLAND BREAKWATERS  
PROFILE NO. 36



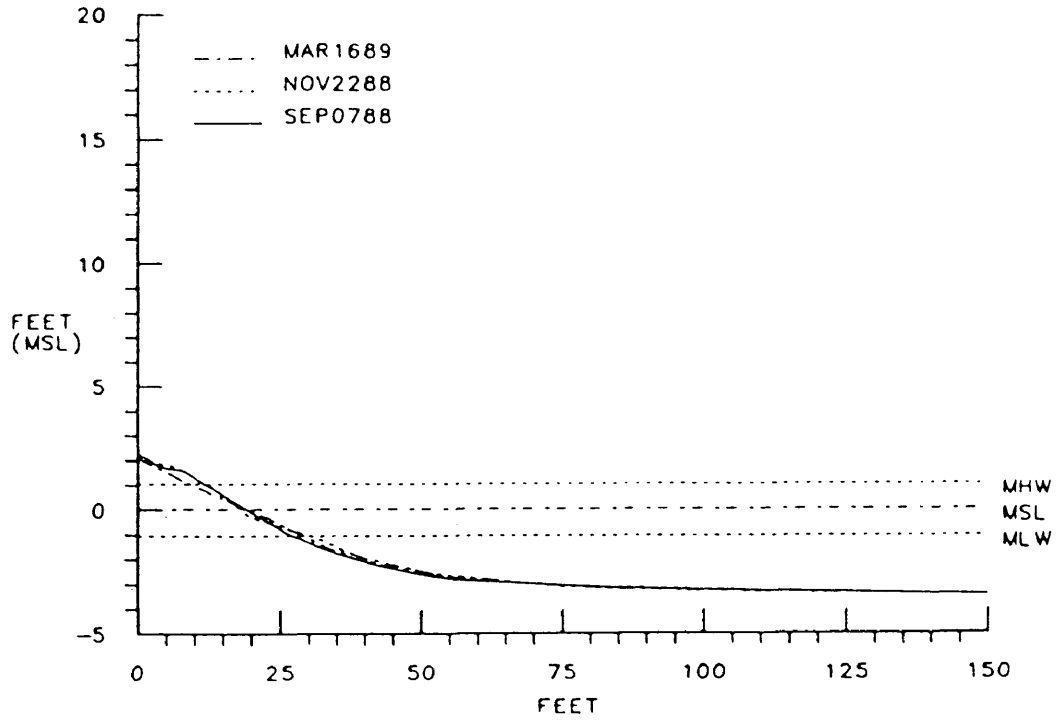
HOG ISLAND BREAKWATERS  
PROFILE NO. 37



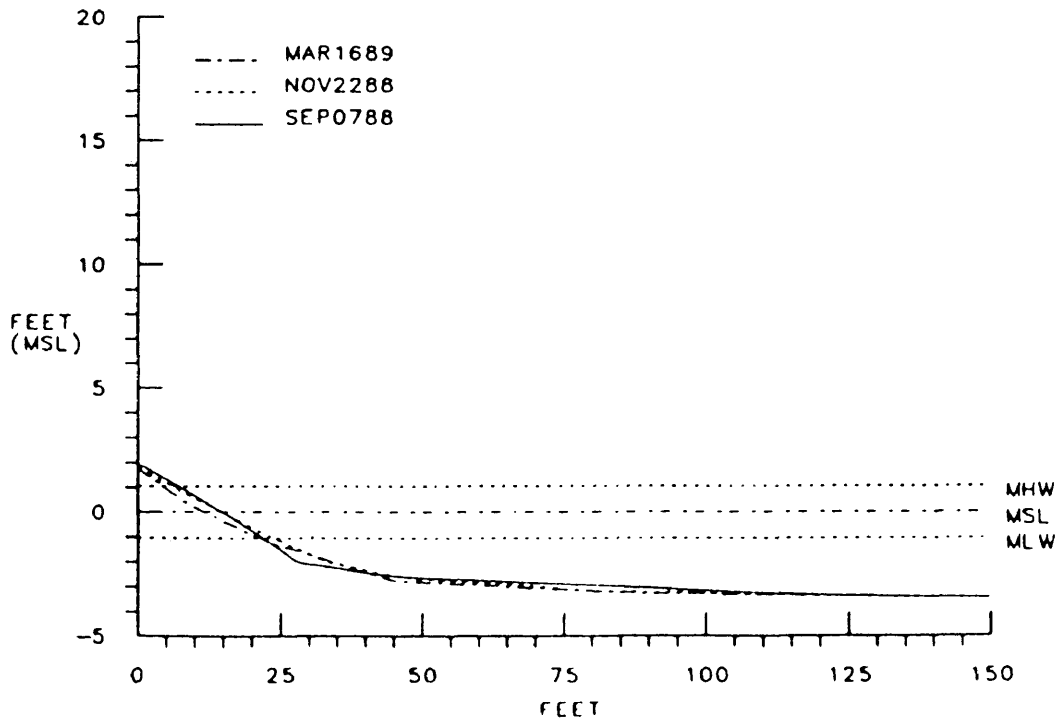
HOG ISLAND BREAKWATERS  
PROFILE NO. 38



HOG ISLAND BREAKWATERS  
PROFILE NO 41

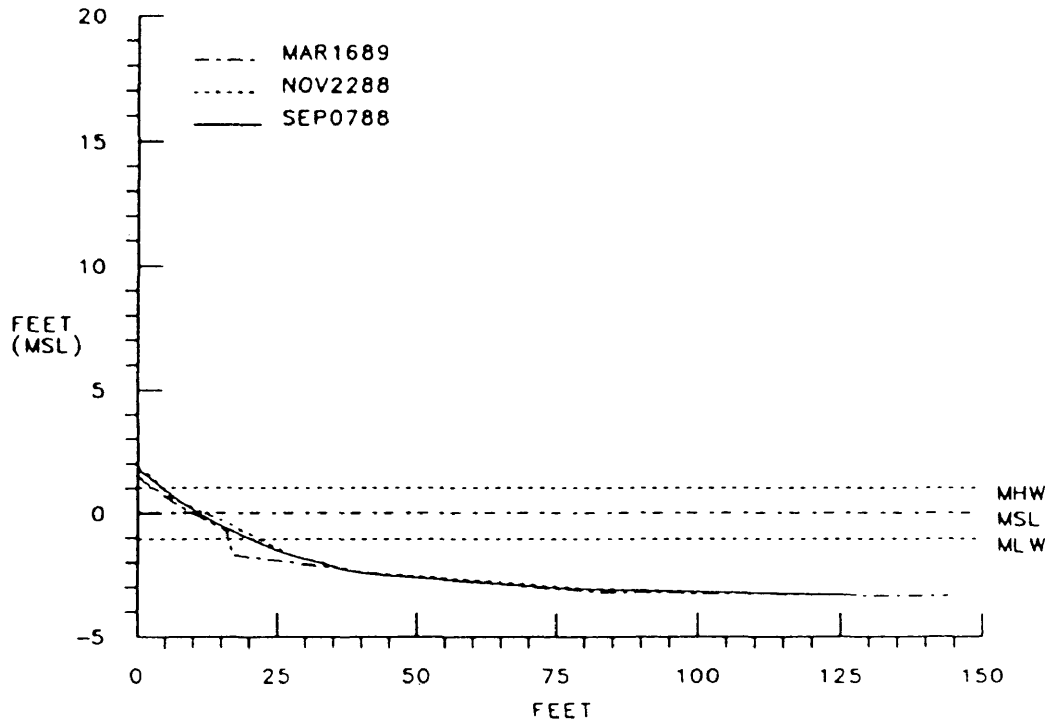


HOG ISLAND BREAKWATERS  
PROFILE NO 42

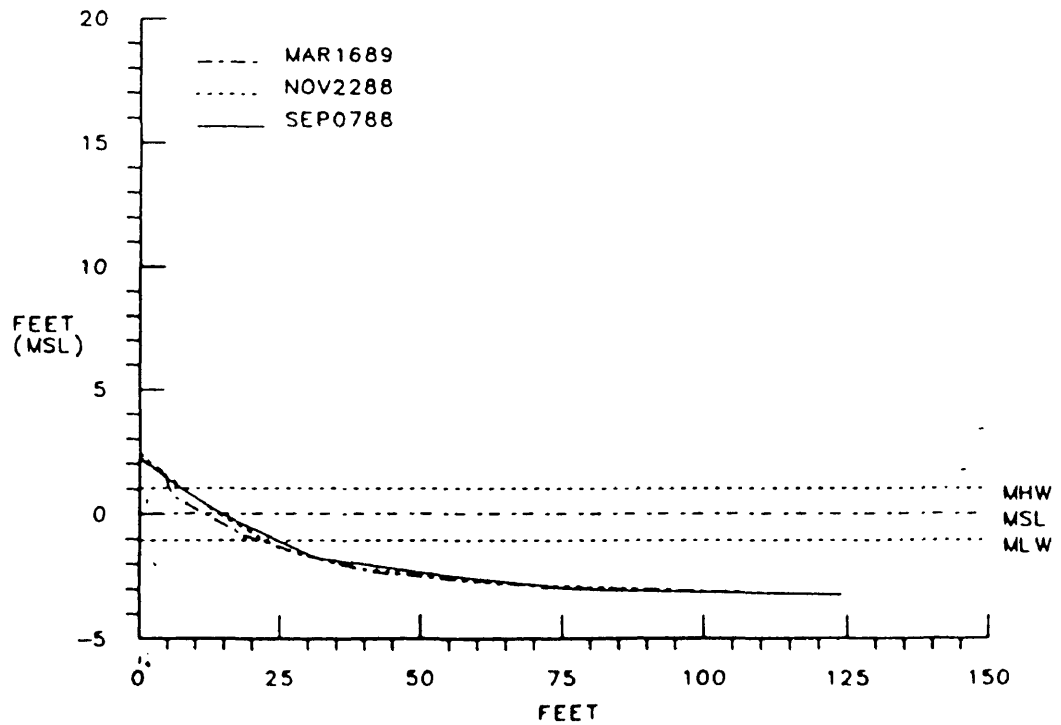




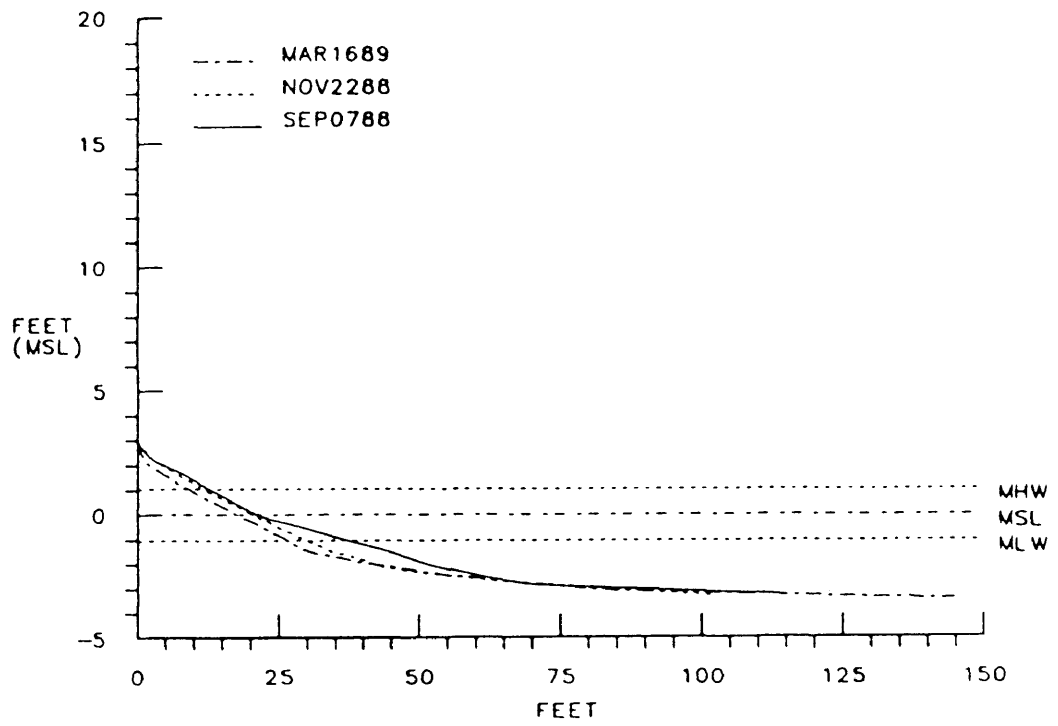
HOG ISLAND BREAKWATERS  
PROFILE NO. 47



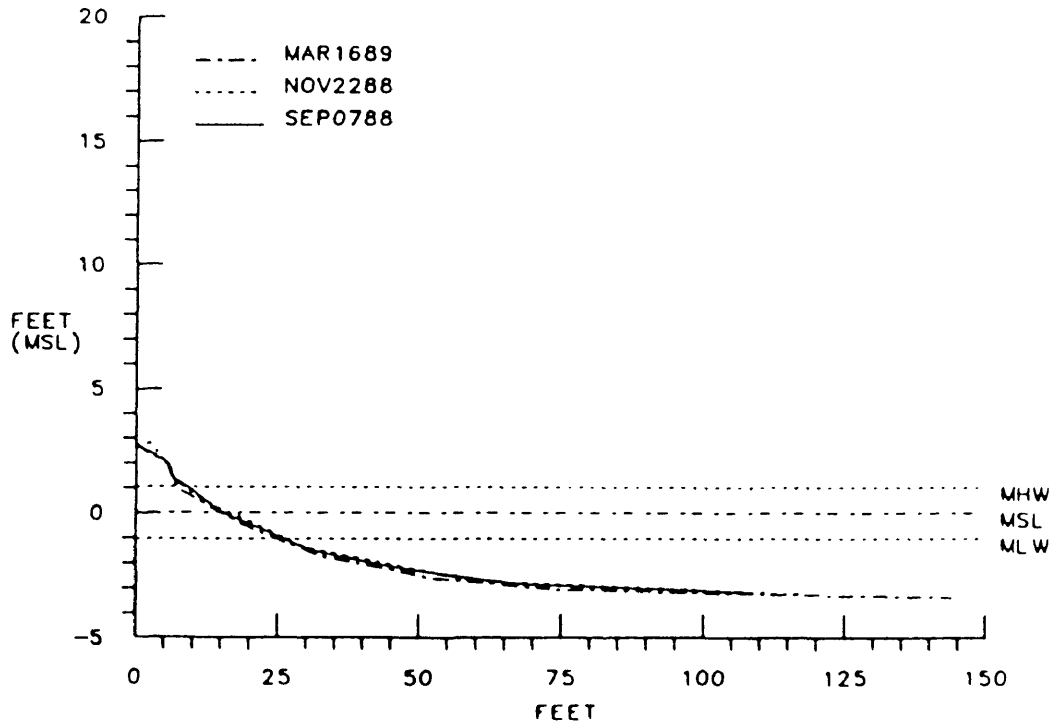
HOG ISLAND BREAKWATERS  
PROFILE NO. 48



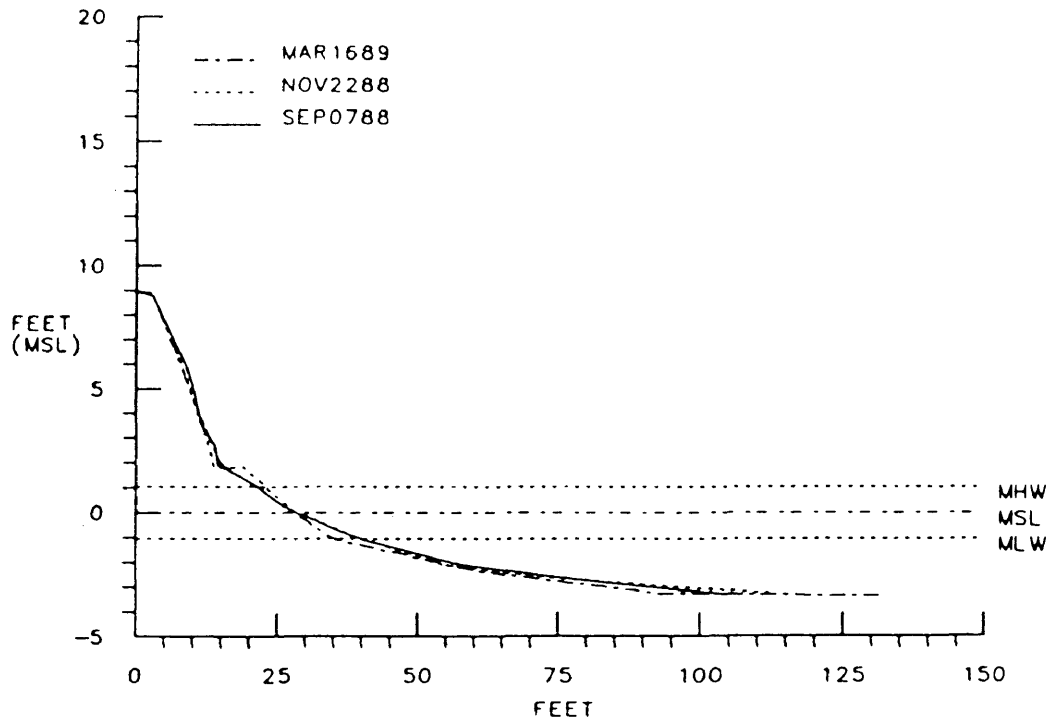
HOG ISLAND BREAKWATERS  
PROFILE NO. 51



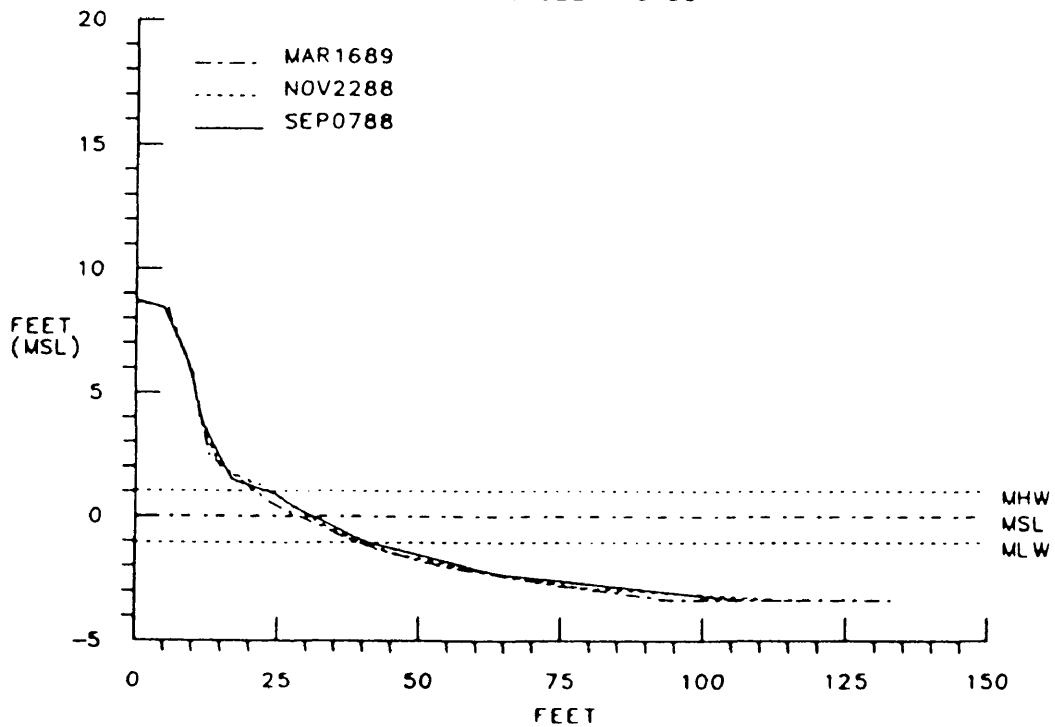
HOG ISLAND BREAKWATERS  
PROFILE NO. 52



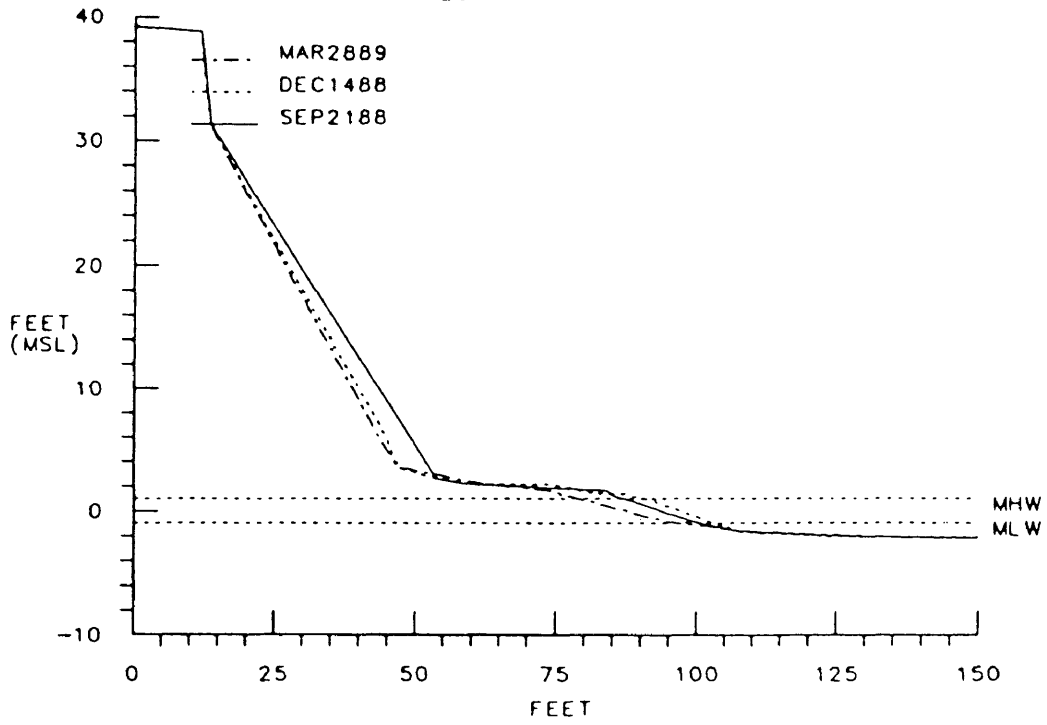
HOG ISLAND BREAKWATERS  
PROFILE NO 57



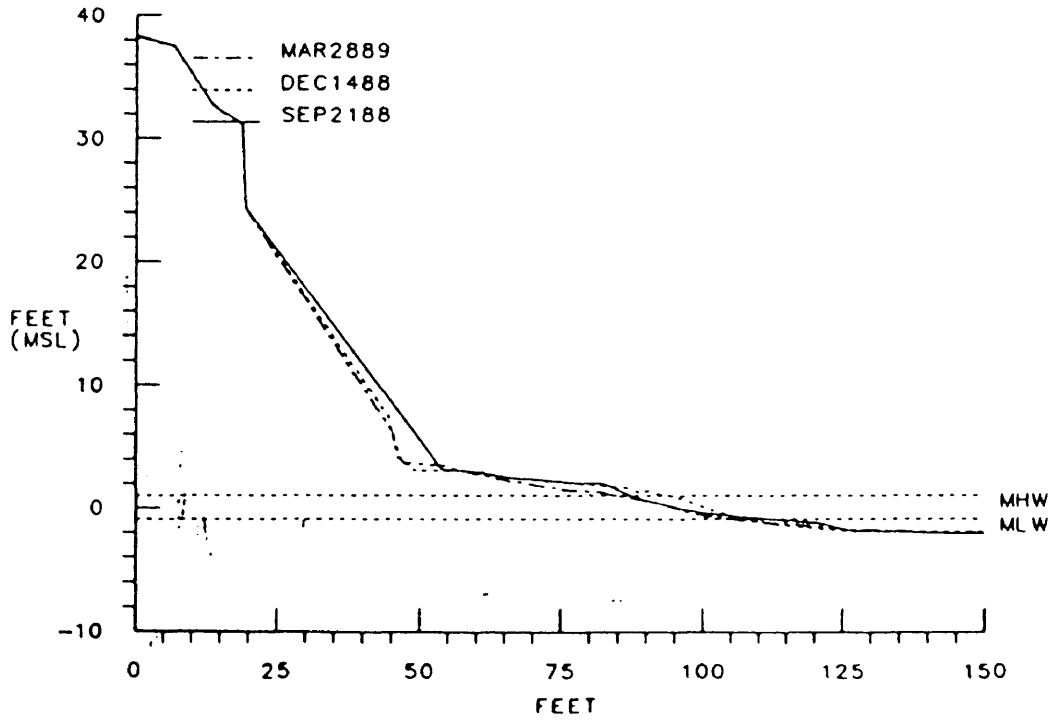
HOG ISLAND BREAKWATERS  
PROFILE NO 58



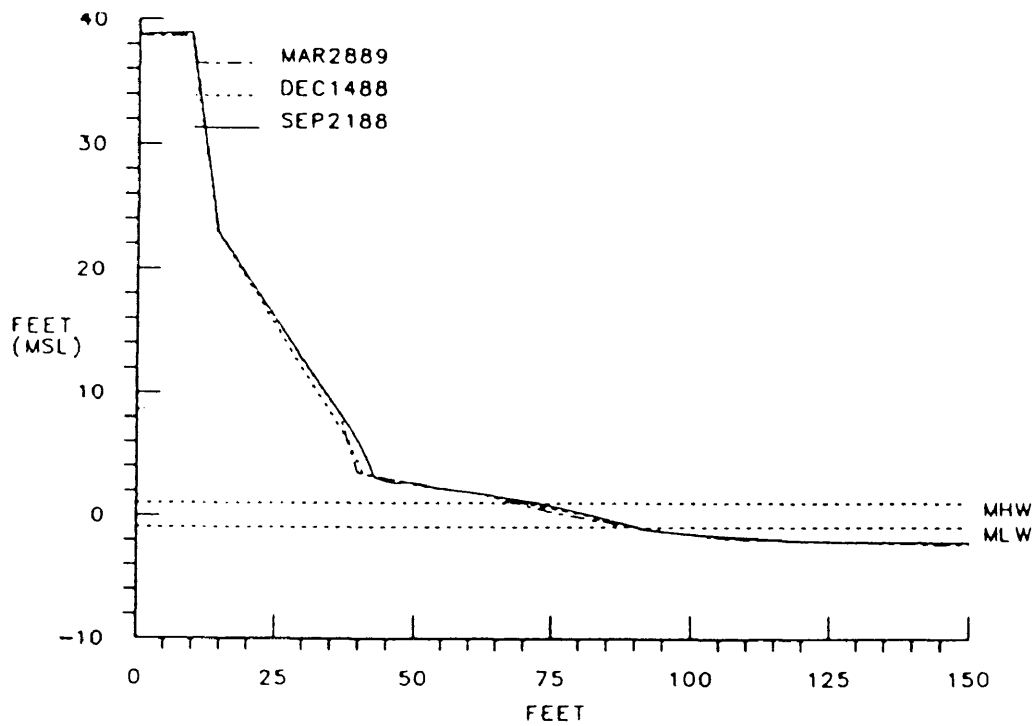
Chippokes state park  
Profile No.01



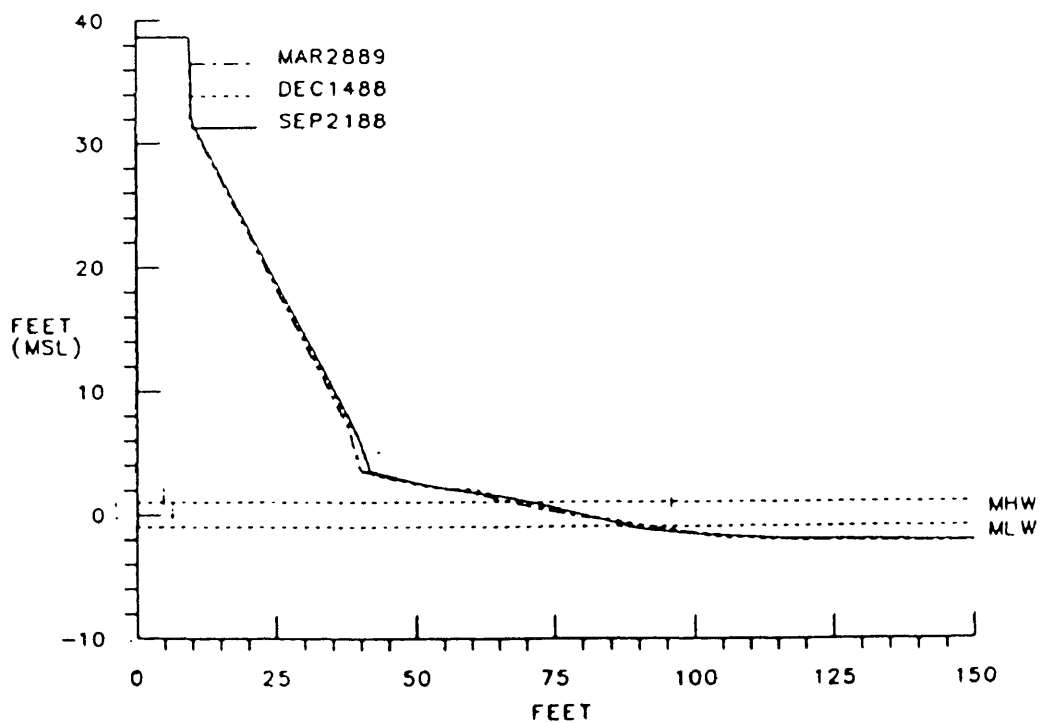
CHIPPOKES STATE PARK  
PROFILE NO. 02



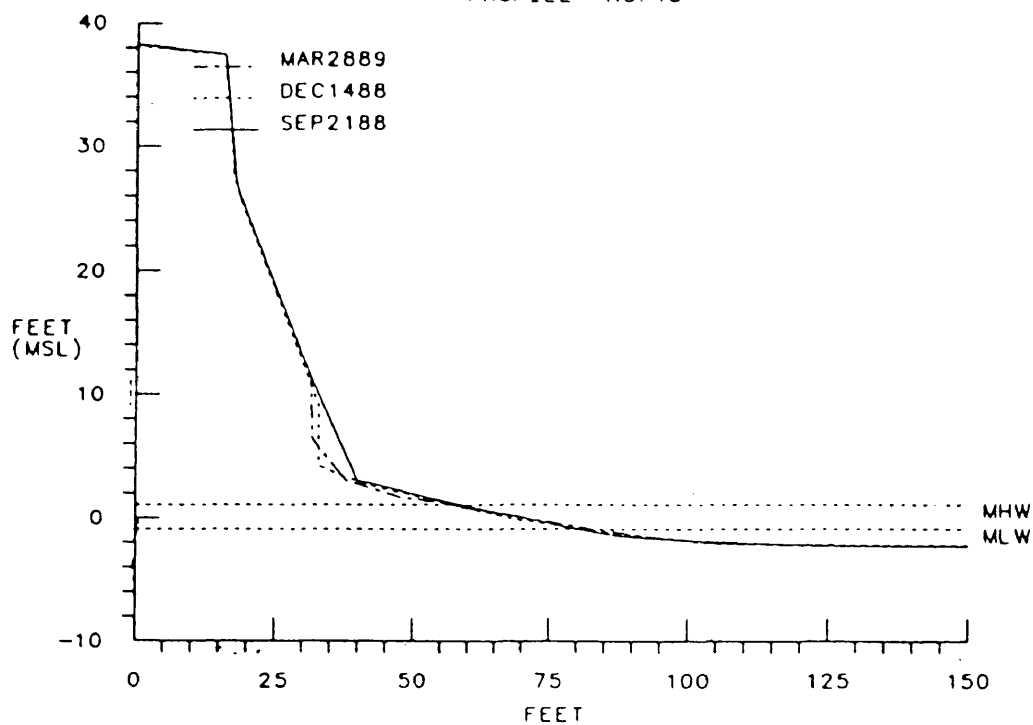
CHIPPOKES STATE PARK  
PROFILE NO. 05



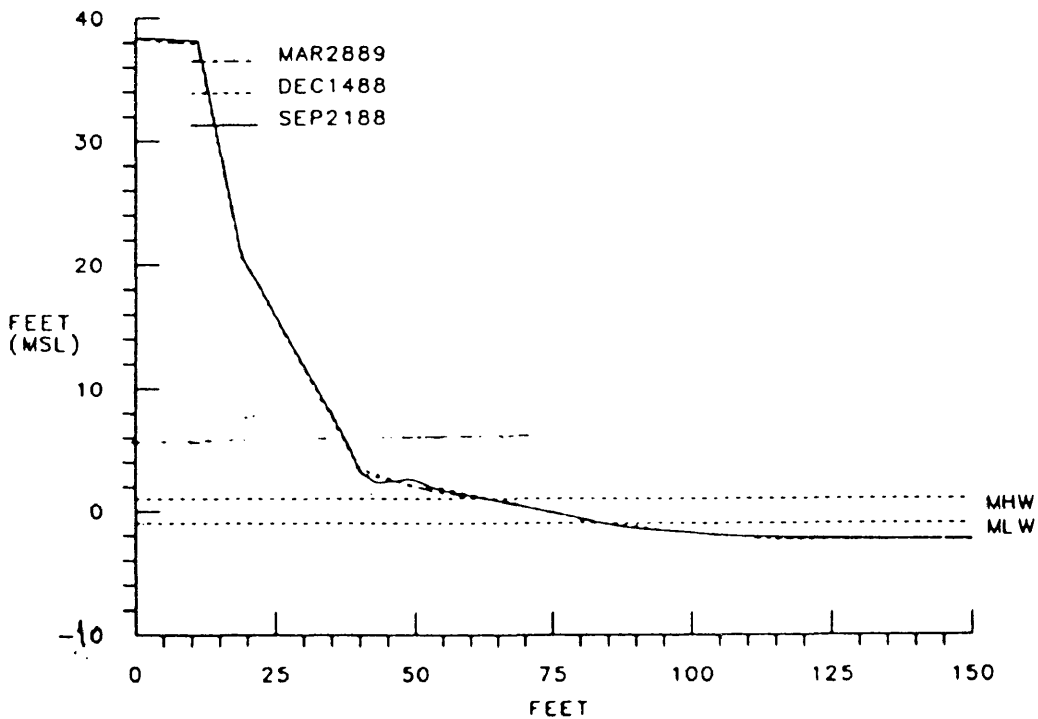
CHIPPOKES STATE PARK  
PROFILE NO. 06



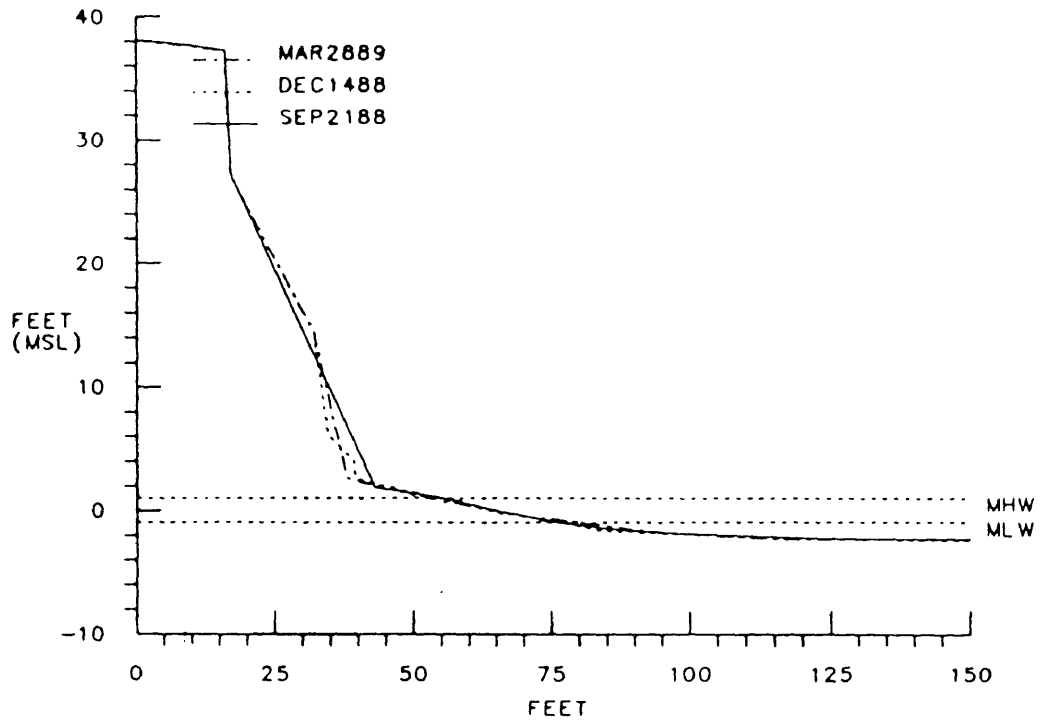
CHIPPOKES STATE PARK  
PROFILE NO. 13



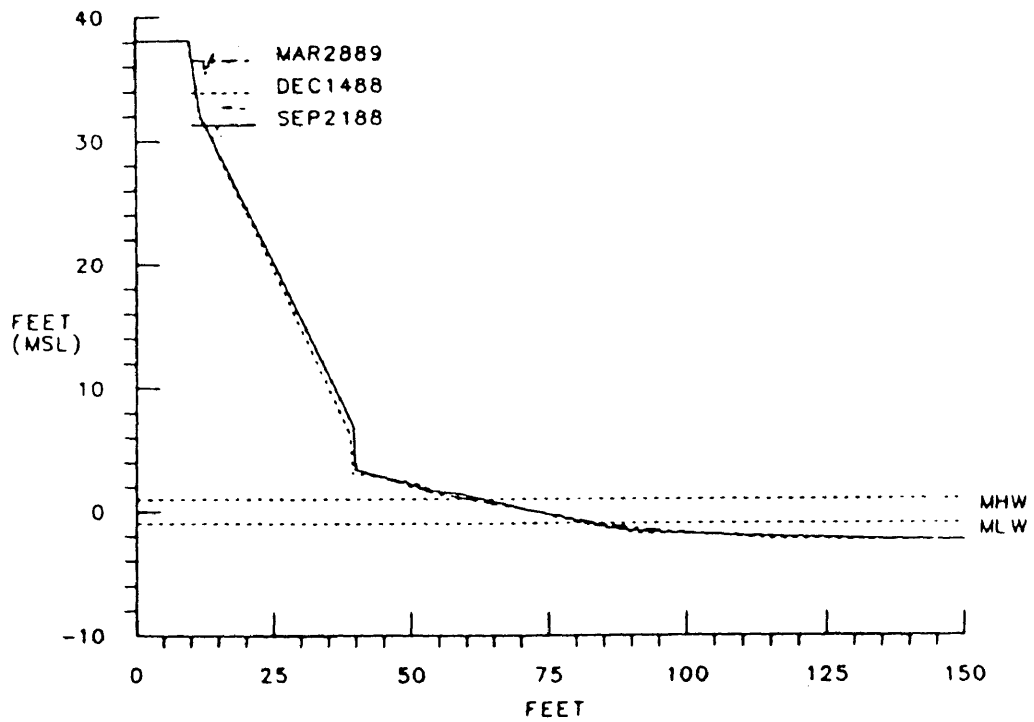
CHIPPOKES STATE PARK  
PROFILE NO. 14



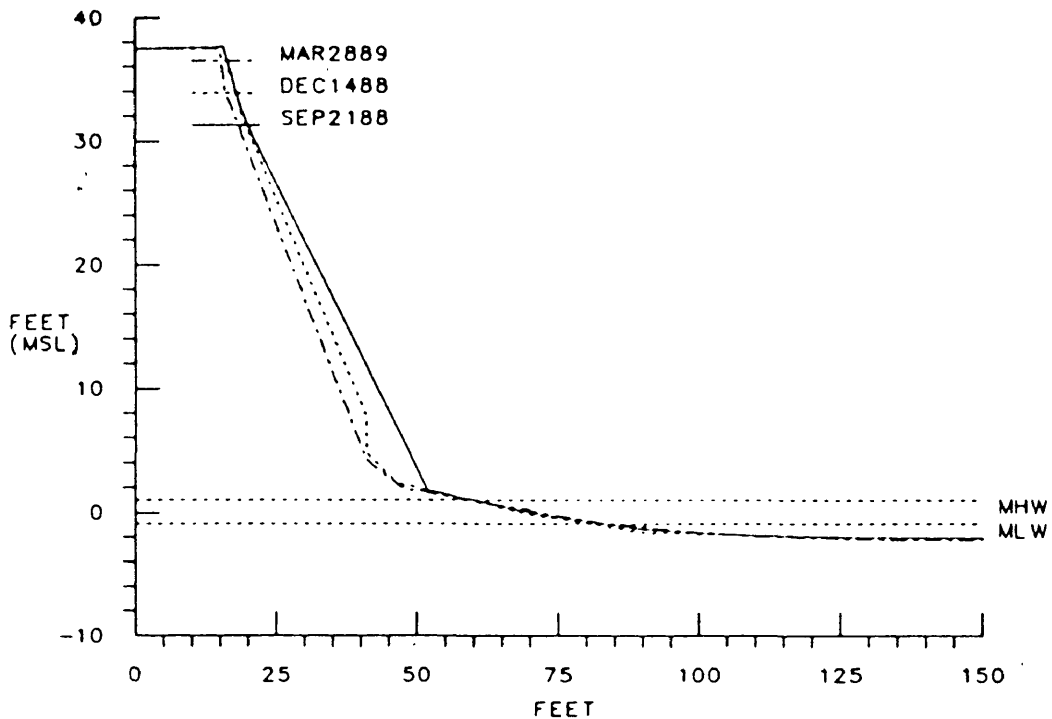
CHIPPOKES STATE PARK  
PROFILE NO. 17



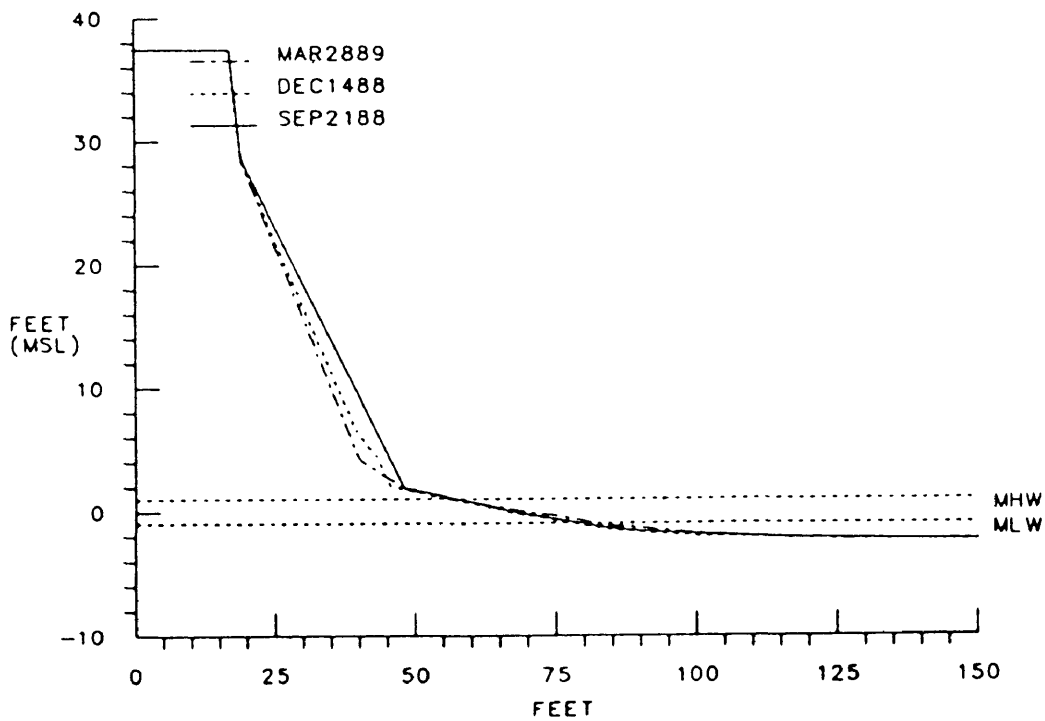
CHIPPOKES STATE PARK  
PROFILE NO. 18



CHIPPOKES STATE PARK  
PROFILE NO 21

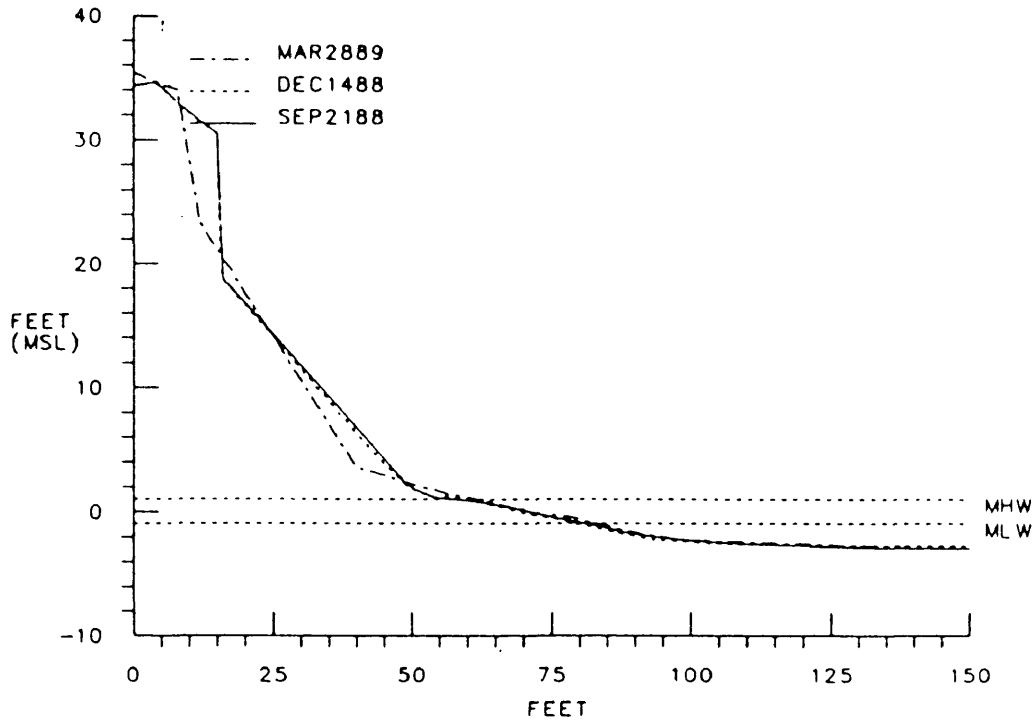


CHIPPOKES STATE PARK  
PROFILE NO 22

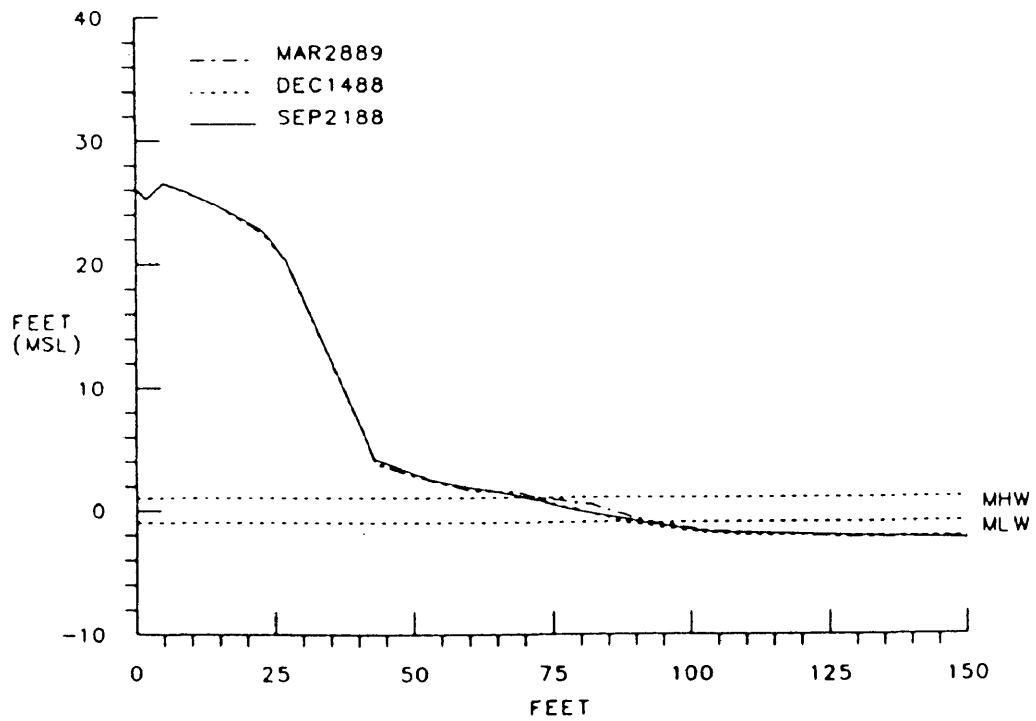




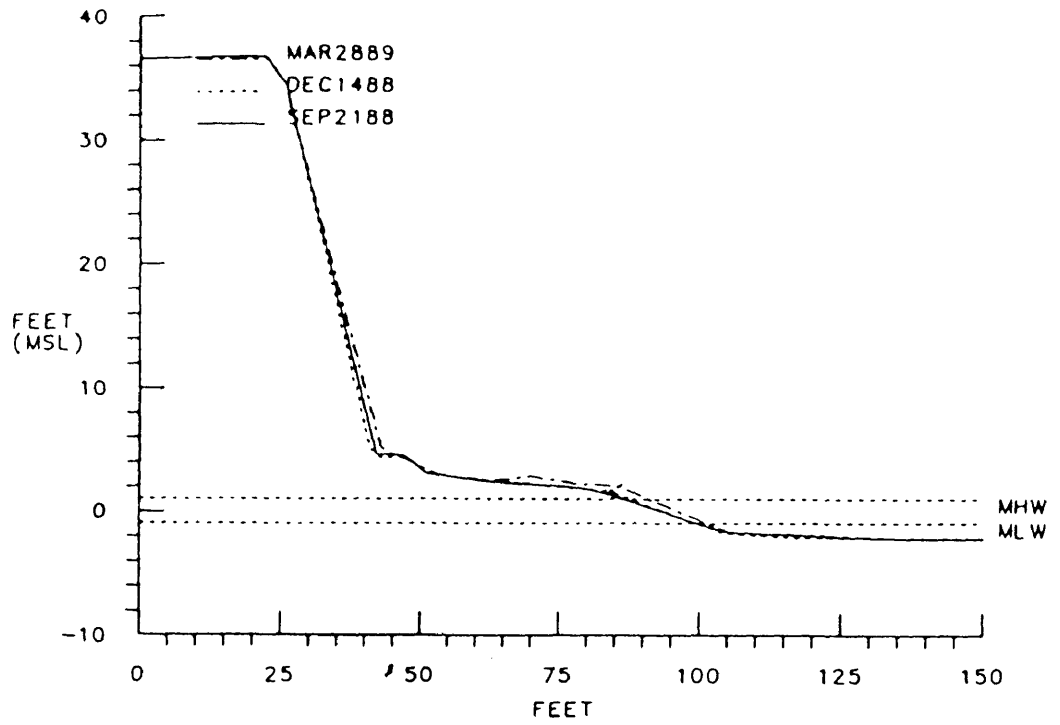
CHIPPOKES STATE PARK  
PROFILE NO. 29



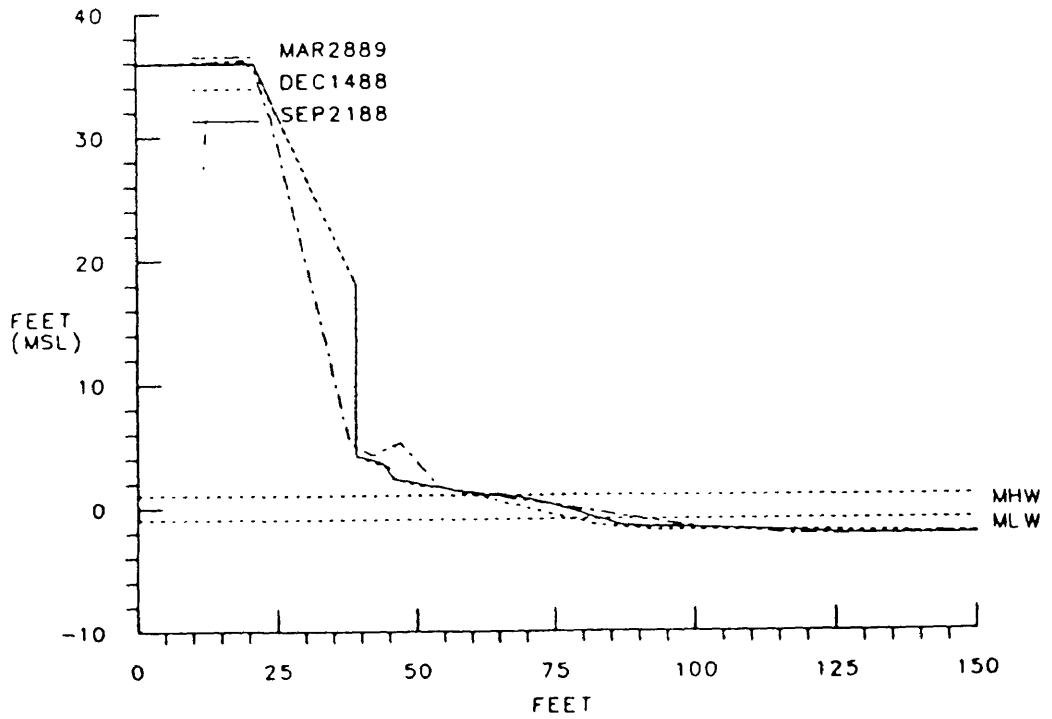
CHIPPOKES STATE PARK  
PROFILE NO. 30



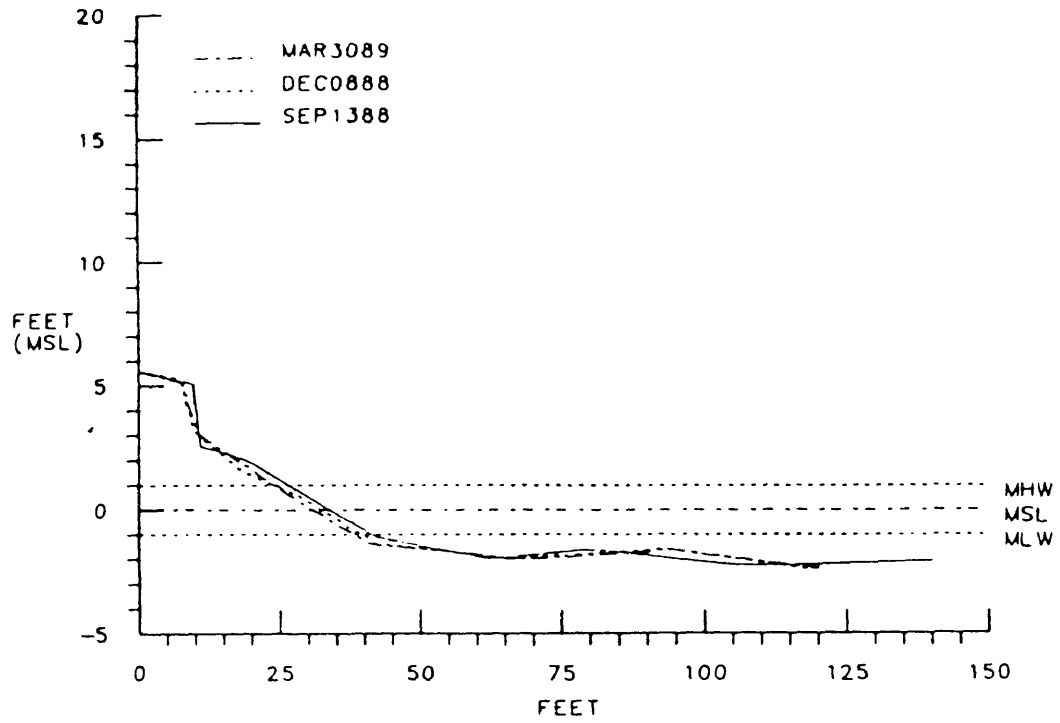
CHIPPOKES STATE PARK  
PROFILE NO 31



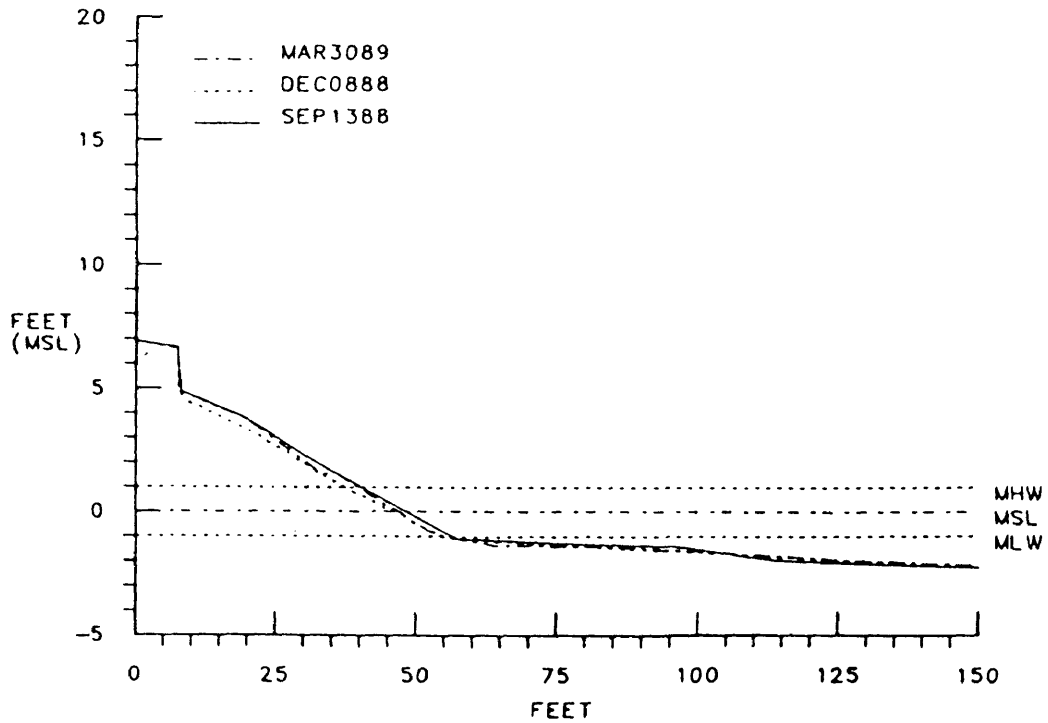
CHIPPOKES STATE PARK  
PROFILE NO. 33



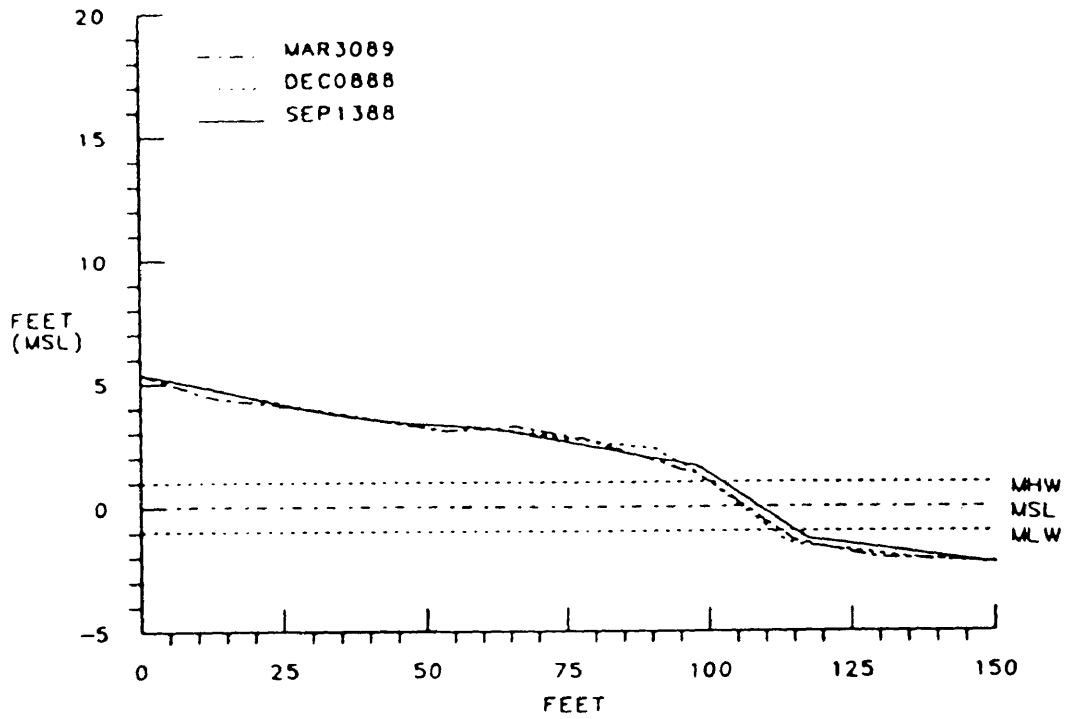
DRUMMONDS FIELD  
PROFILE NO 01



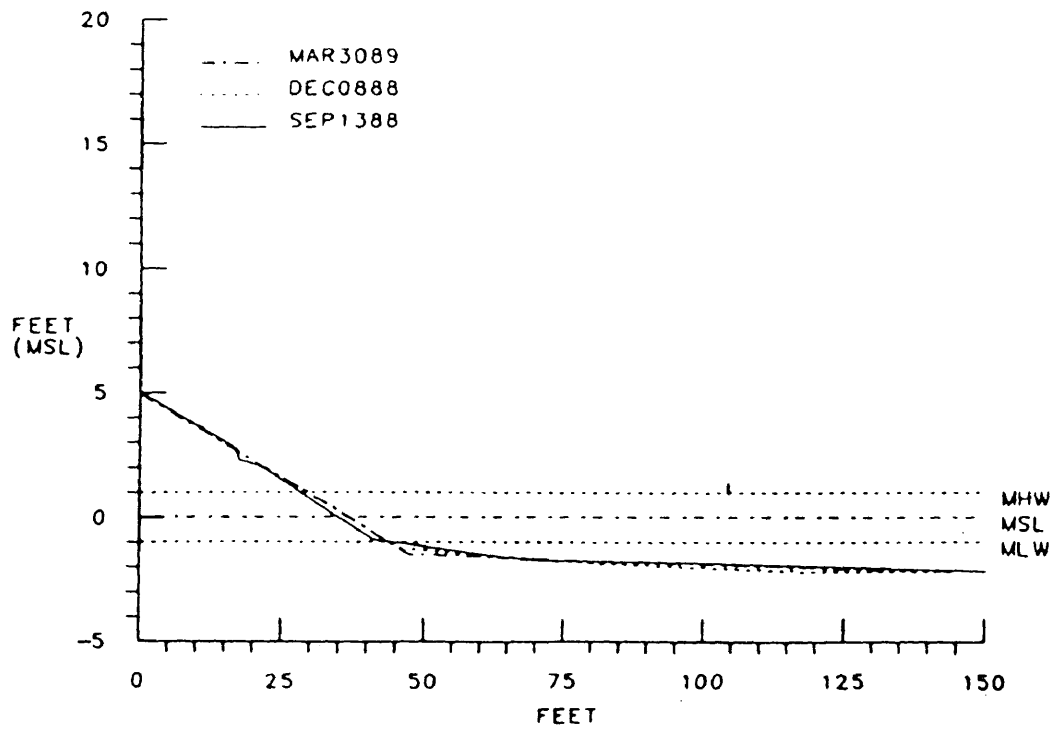
DRUMMONDS FIELD  
PROFILE NO. 02



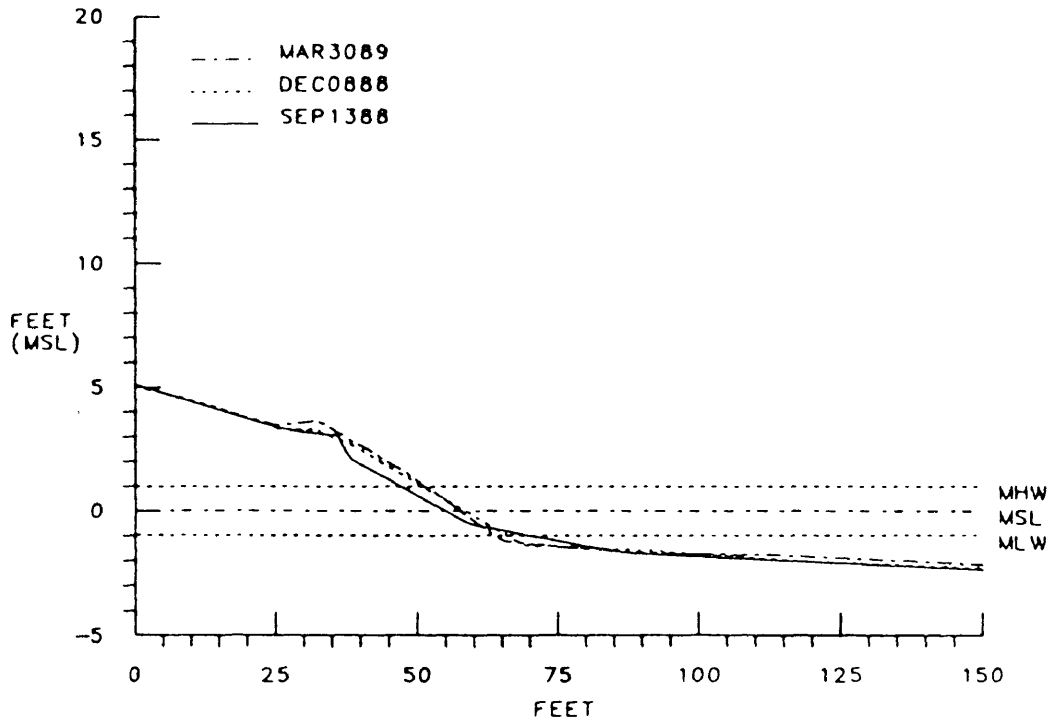
DRUMMONDS FIELD  
PROFILE NO 04



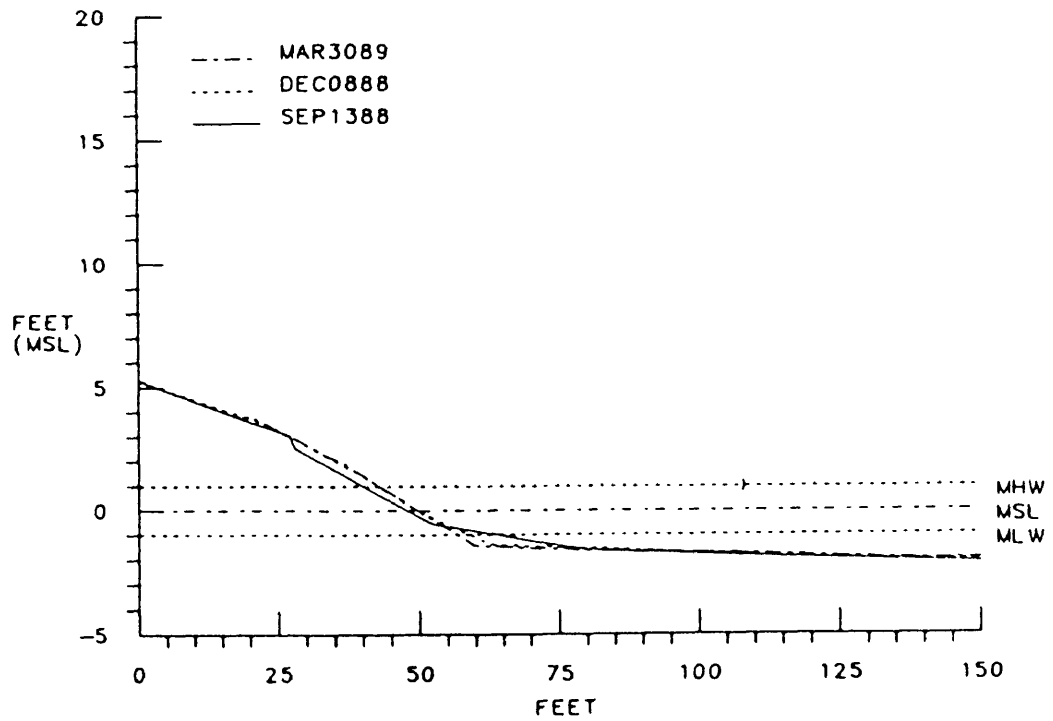
DRUMMONDS FIELD  
PROFILE NO 08



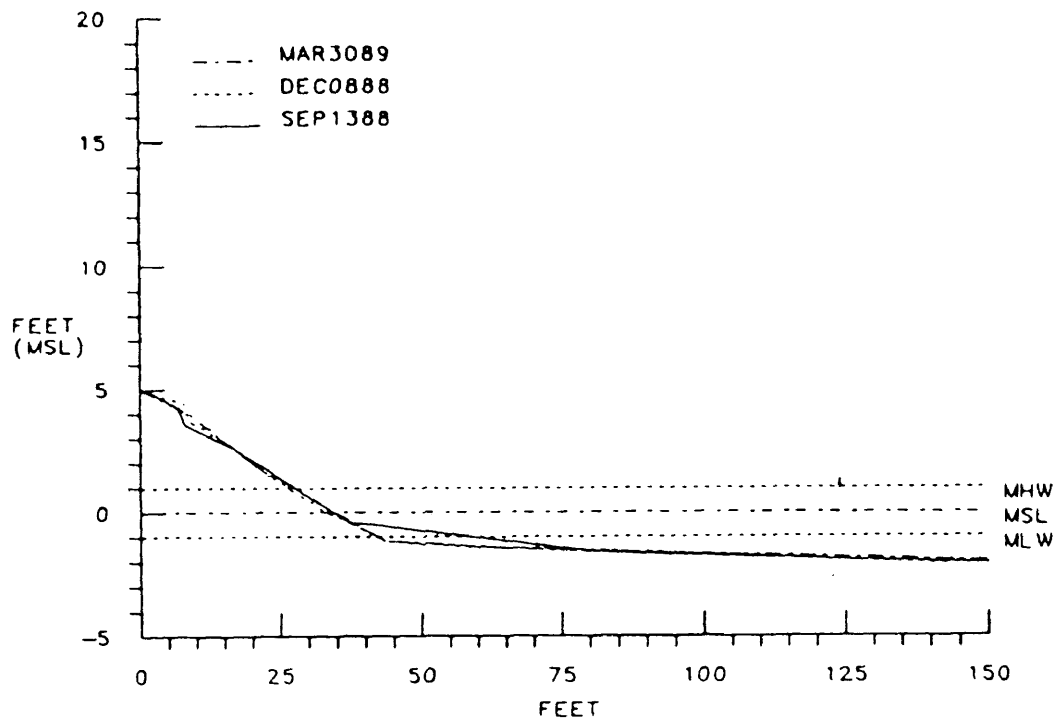
DRUMMONDS FIELD  
PROFILE NO 13



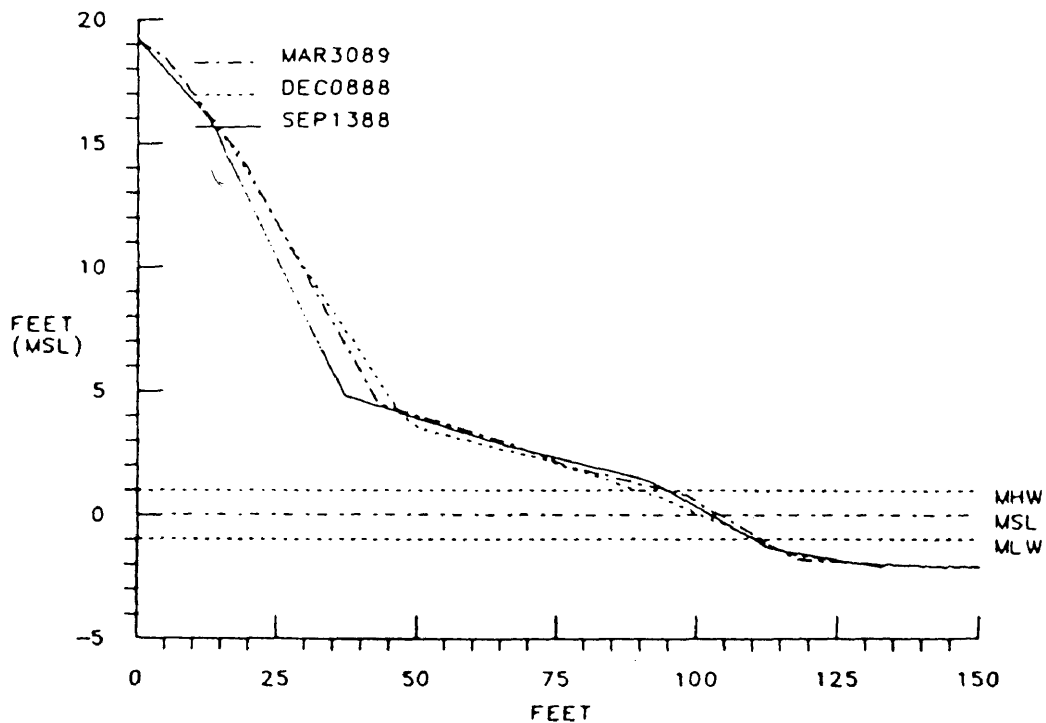
DRUMMONDS FIELD  
PROFILE NO. 14



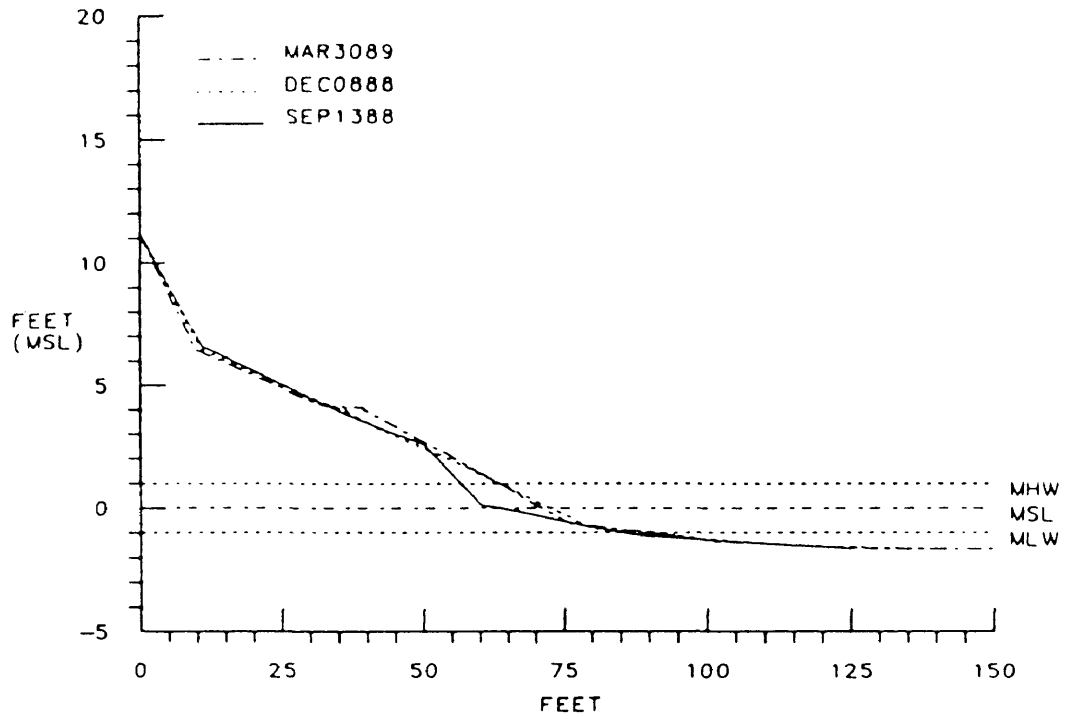
DRUMMONDS FIELD  
PROFILE NO 23



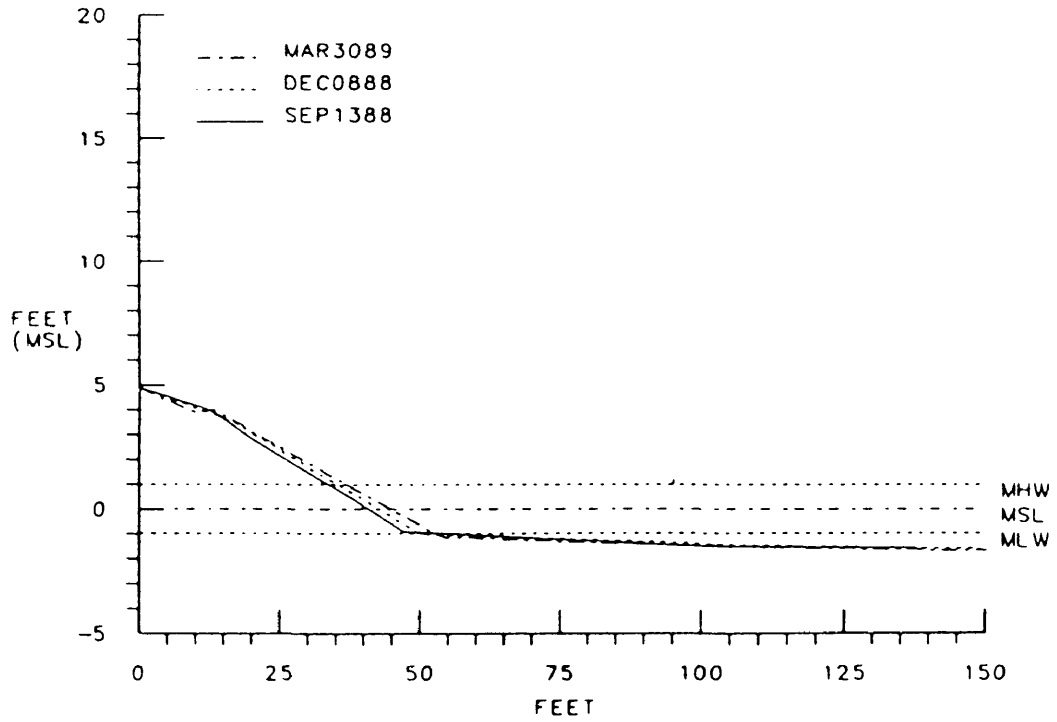
DRUMMONDS FIELD  
PROFILE NO 25



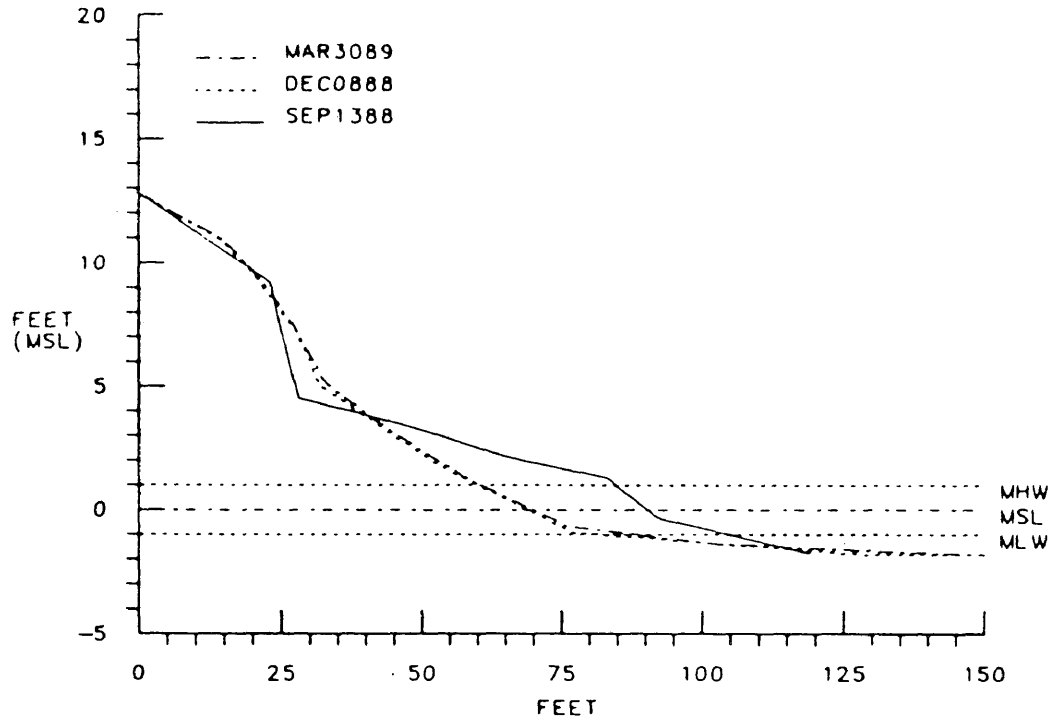
DRUMMONDS FIELD  
PROFILE NO 26



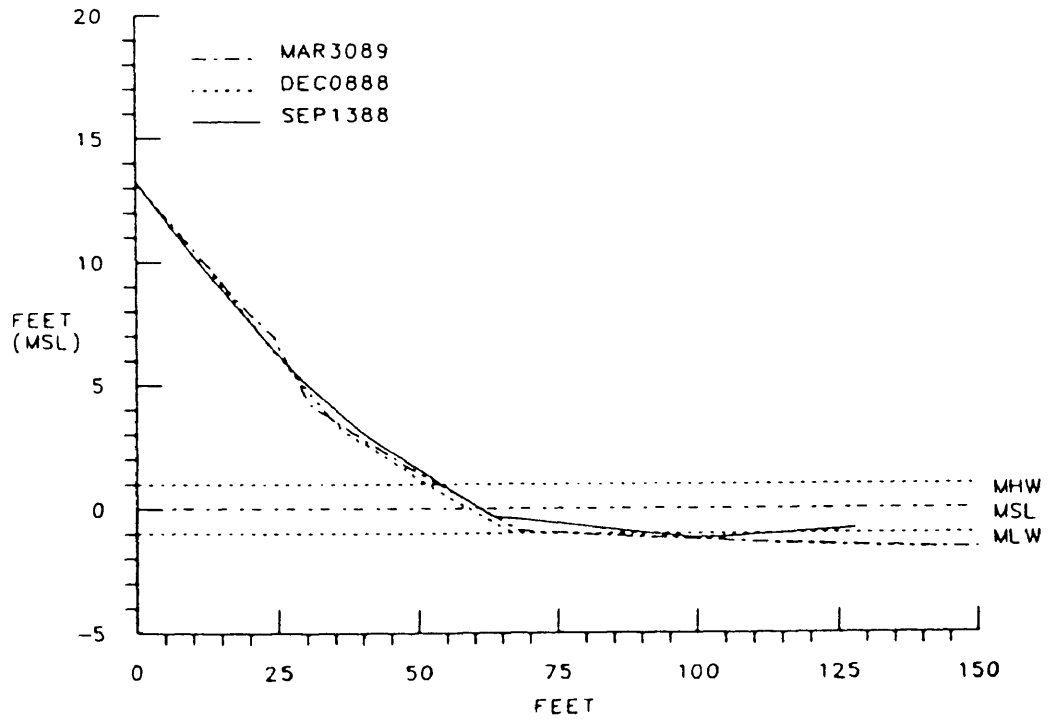
DRUMMONDS FIELD  
PROFILE NO 27



DRUMMONDS FIELD  
PROFILE NO 30

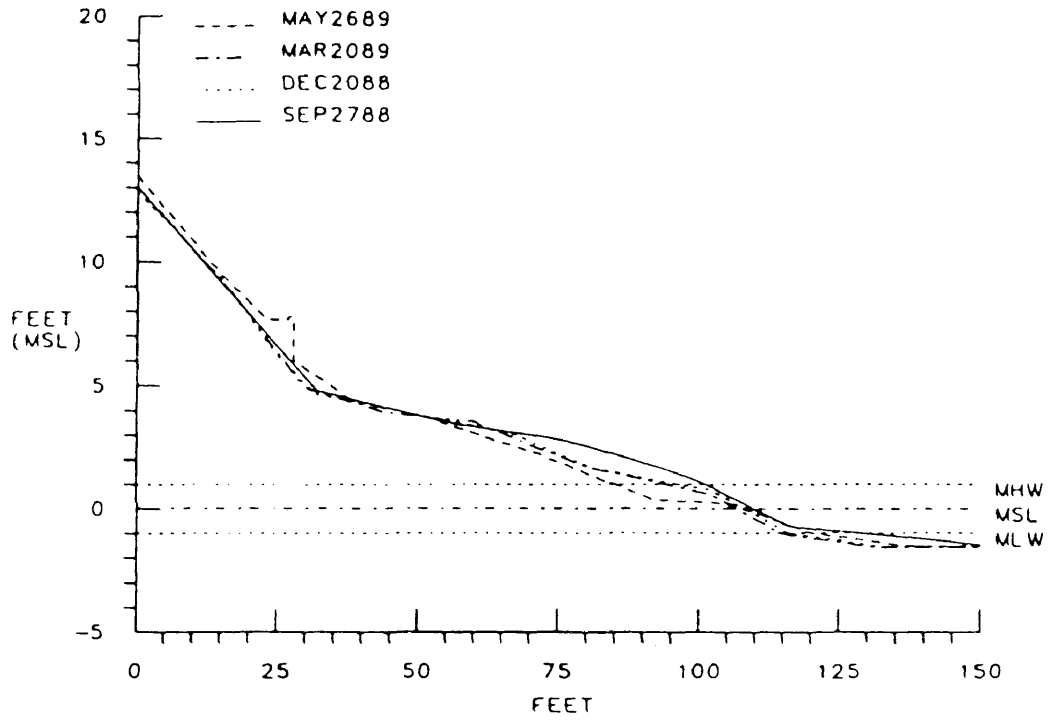


DRUMMONDS FIELD  
PROFILE NO 31

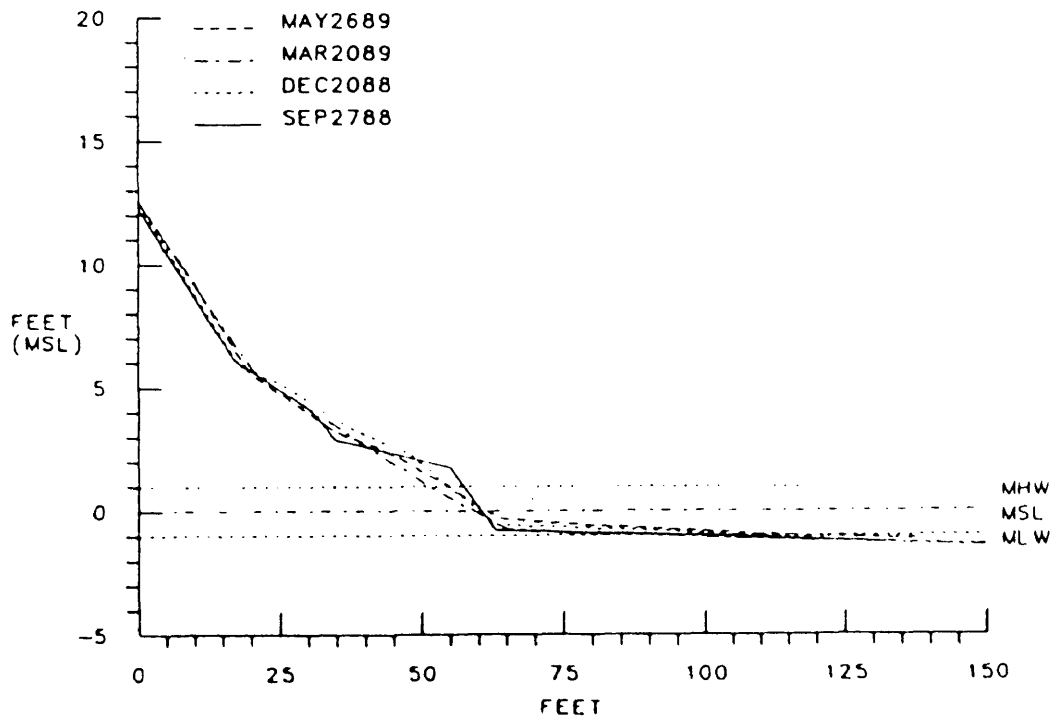




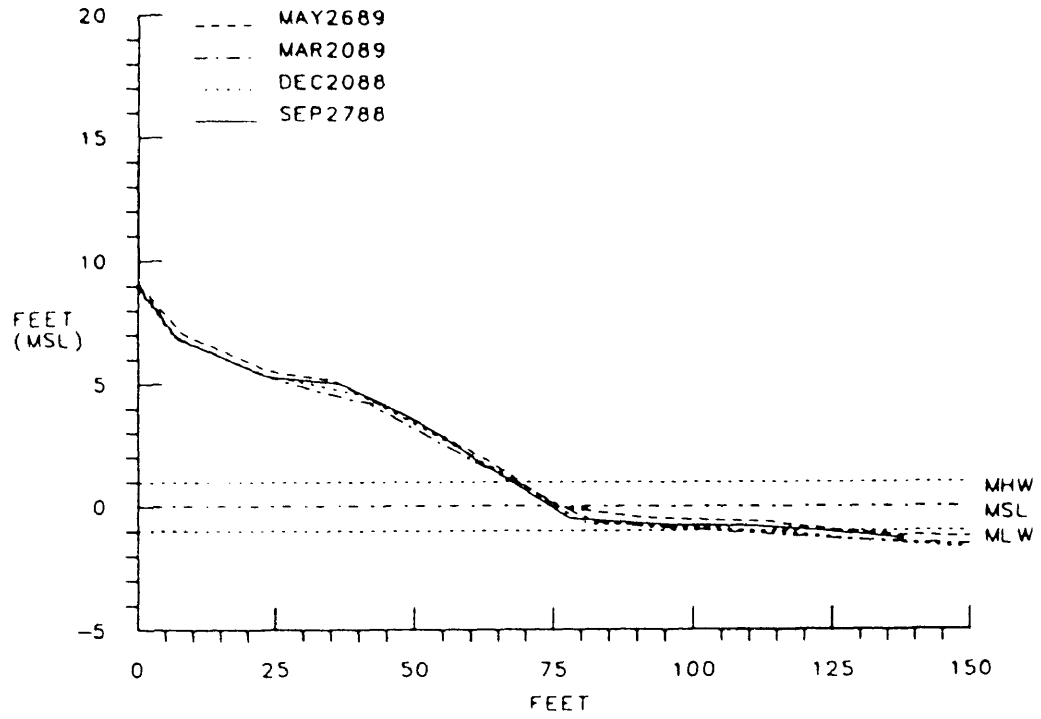
WALTRIP  
PROFILE NO 01



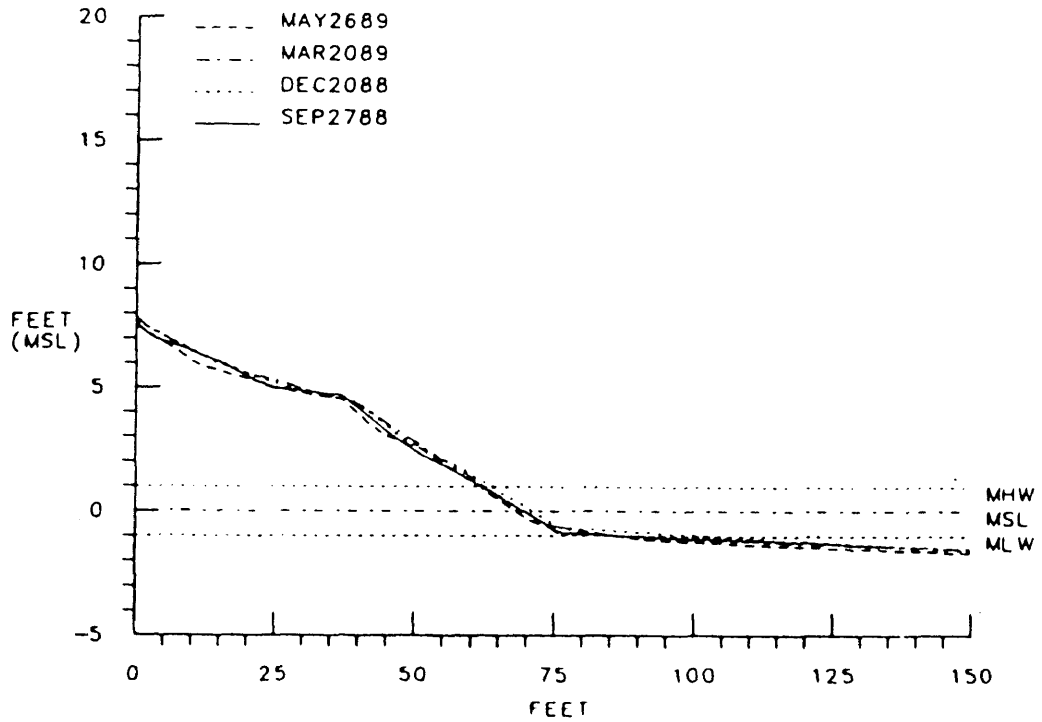
WALTRIP  
PROFILE NO 02



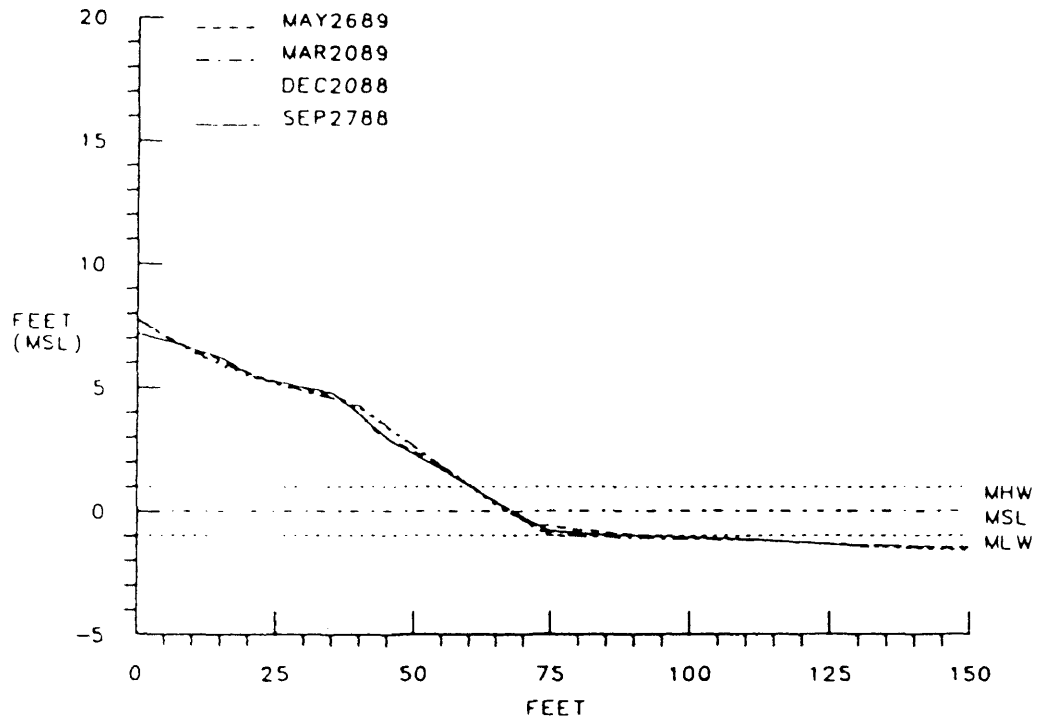
WALTRIP  
PROFILE NO 05



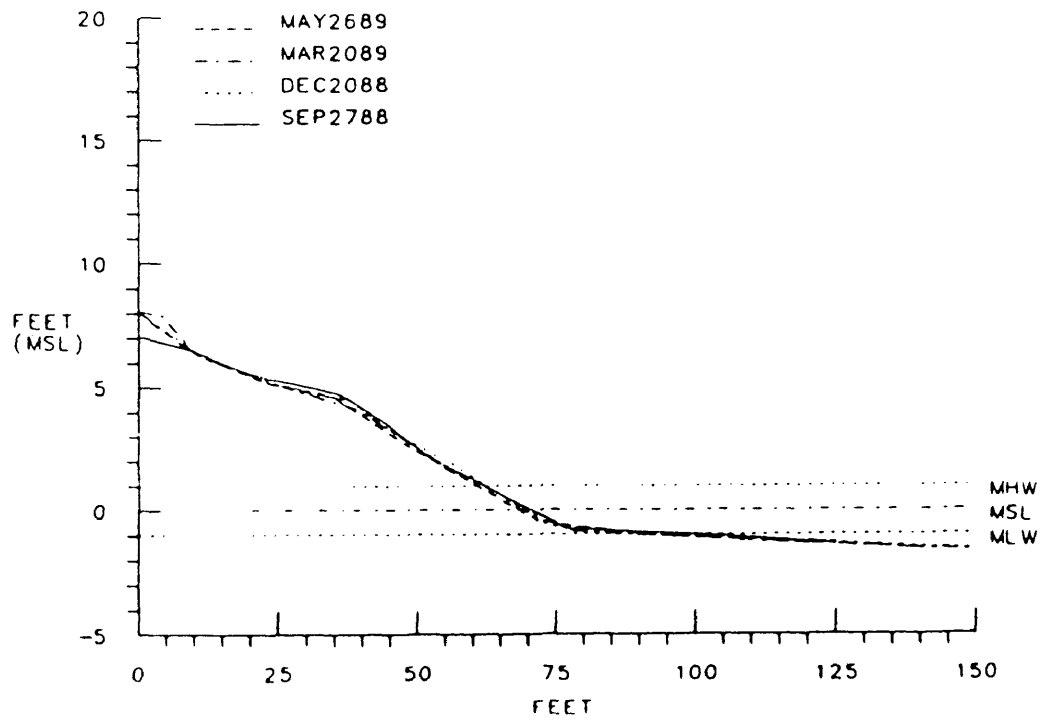
WALTRIP  
PROFILE NO. 06



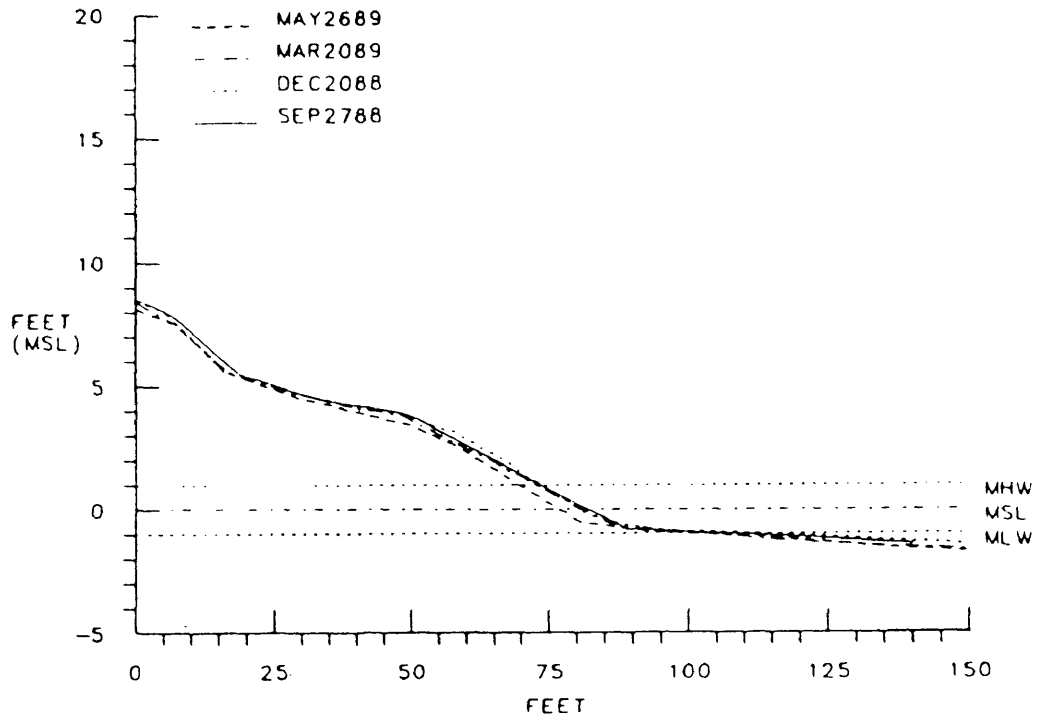
WALTRIP  
PROFILE NO 07



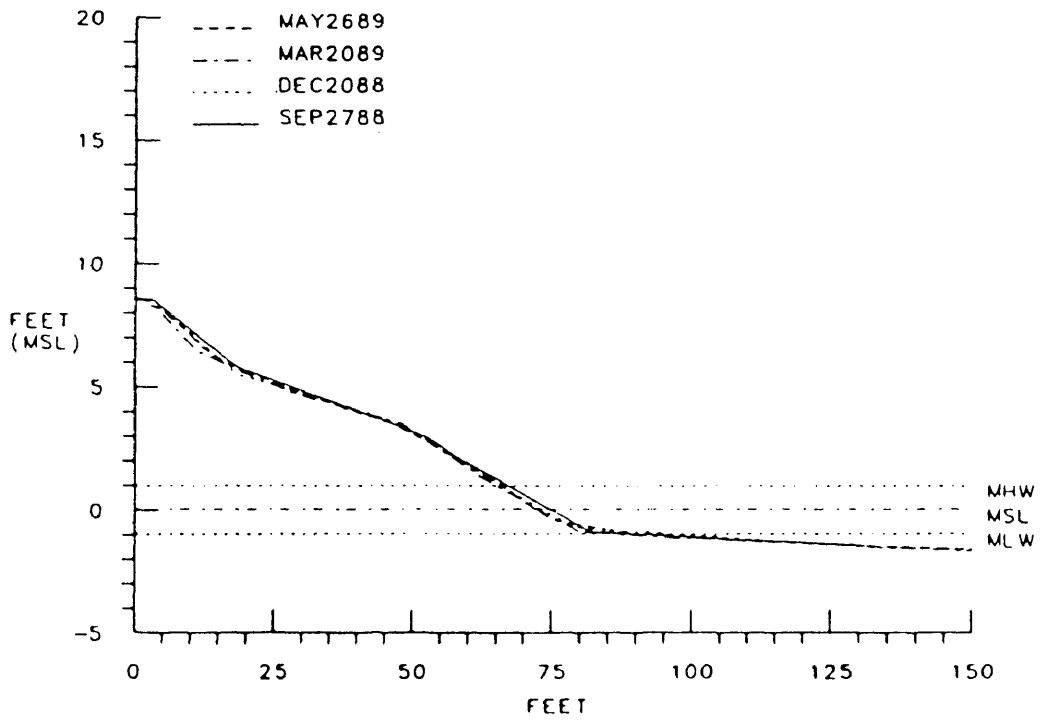
WALTRIP  
PROFILE NO. 08



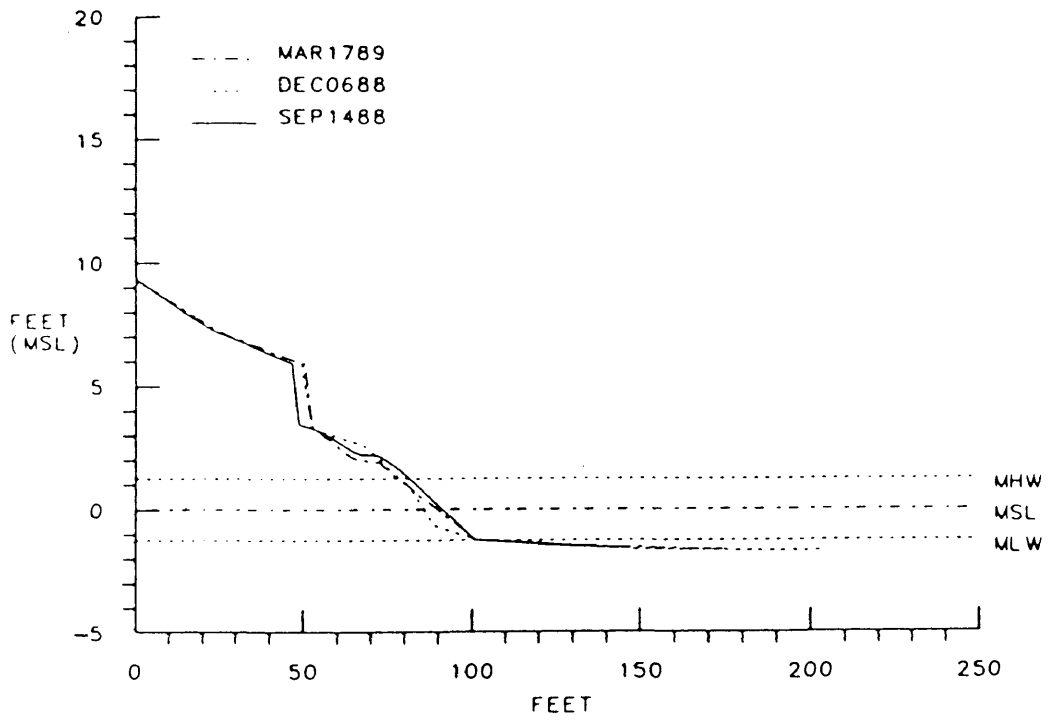
WALTRIP  
PROFILE NO 13



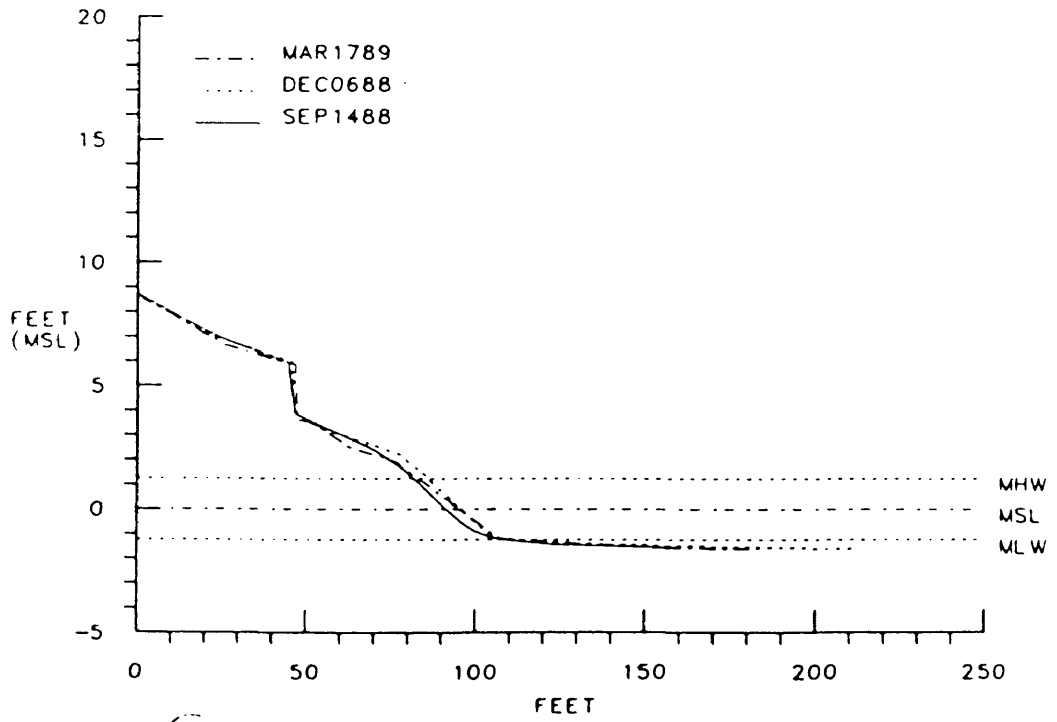
WALTRIP  
PROFILE NO 14



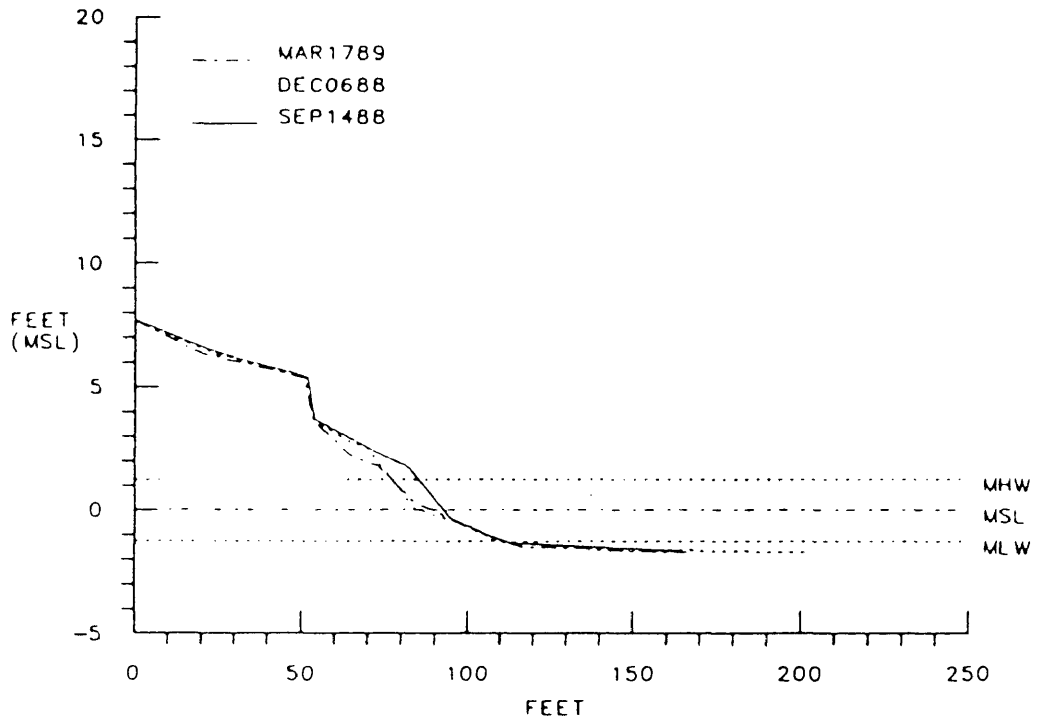
PARKWAY BREAKWATERS  
PROFILE NO. 05



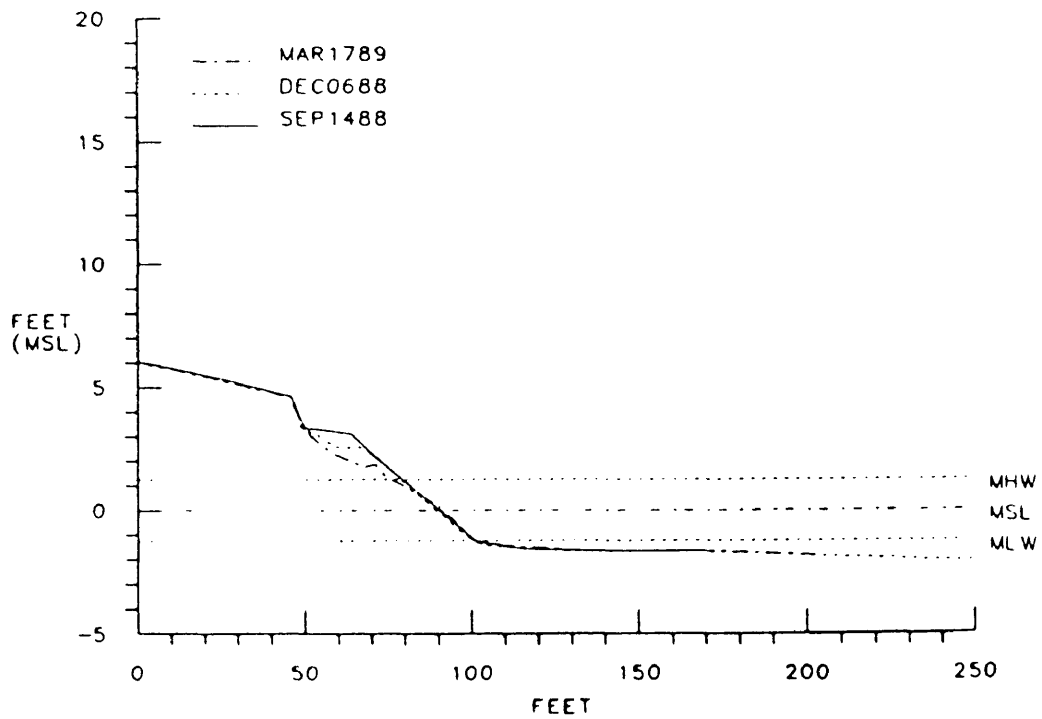
PARKWAY BREAKWATERS  
PROFILE NO 06



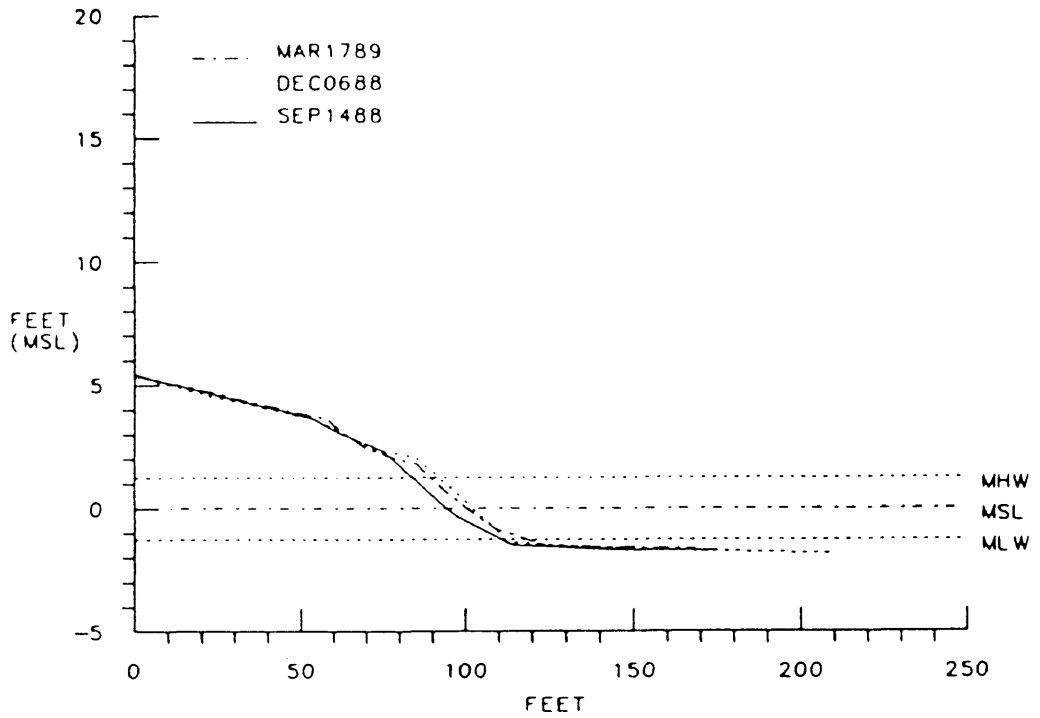
PARKWAY BREAKWATERS  
PROFILE NO 11



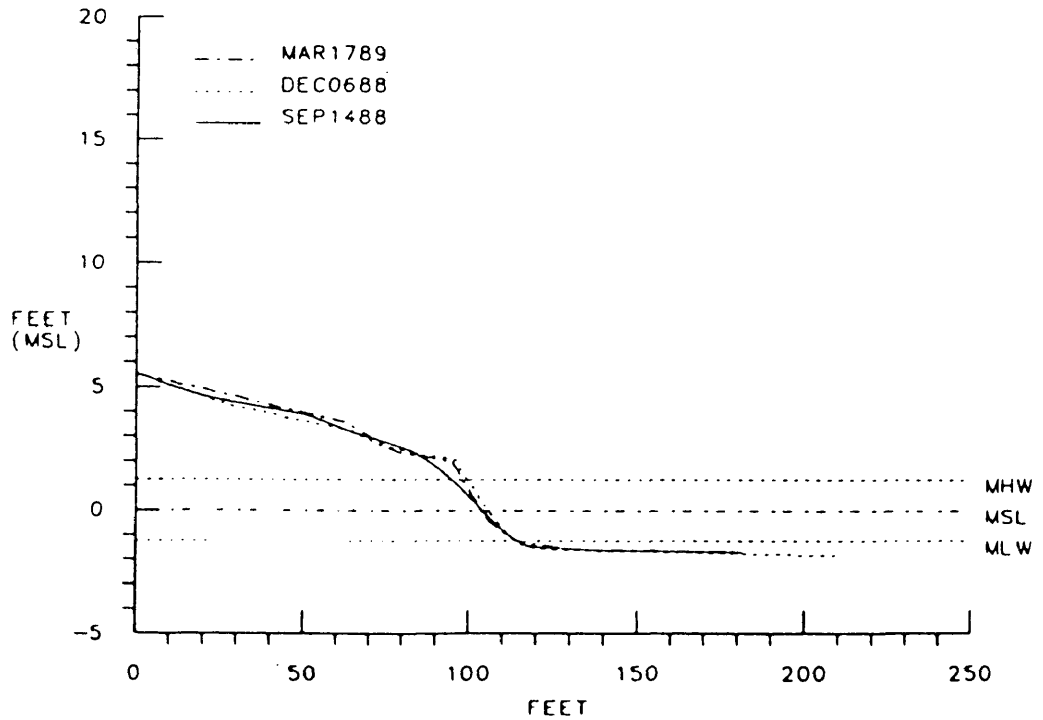
PARKWAY BREAKWATERS  
PROFILE NO 12



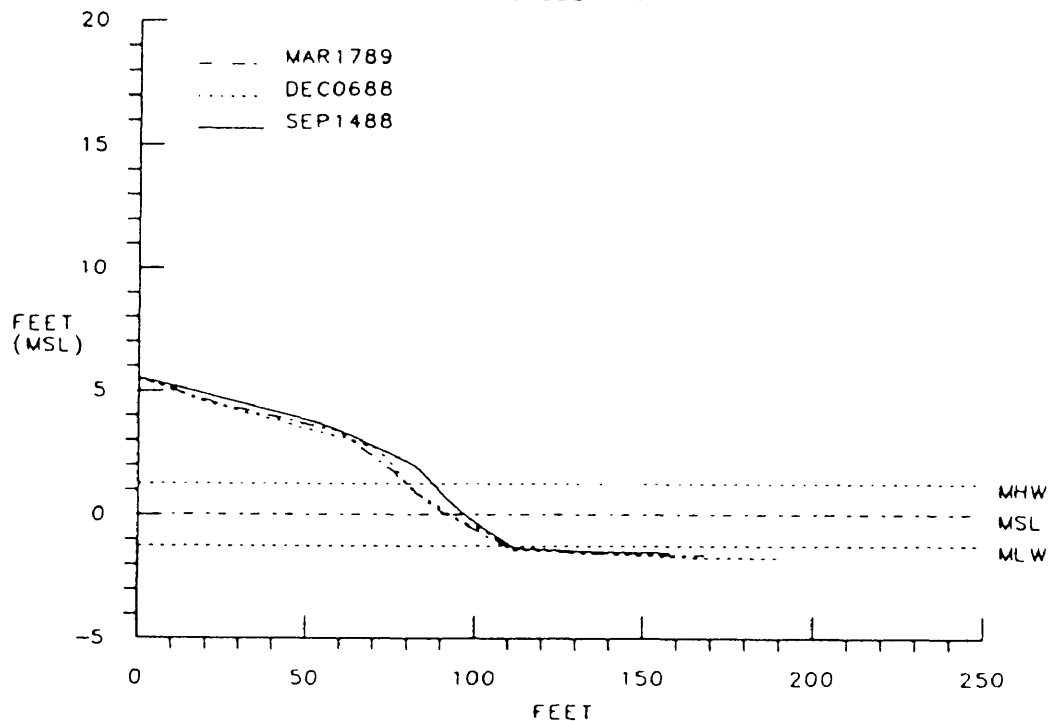
PARKWAY BREAKWATERS  
PROFILE NO 13



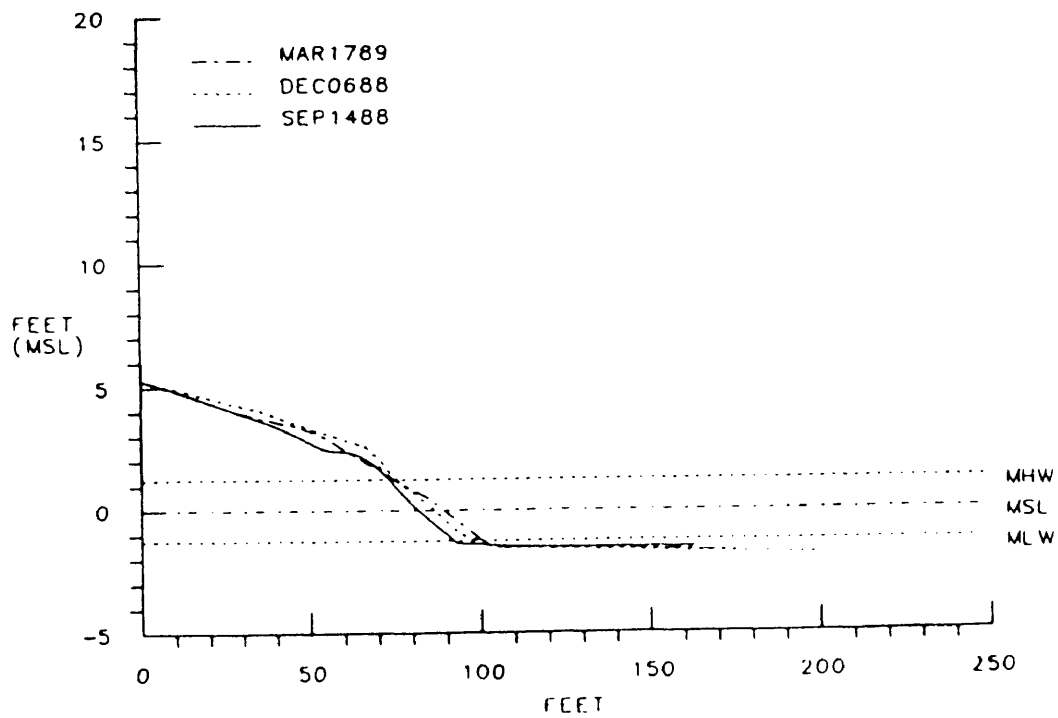
PARKWAY BREAKWATERS  
PROFILE NO 14



PARKWAY BREAKWATERS  
PROFILE NO 17

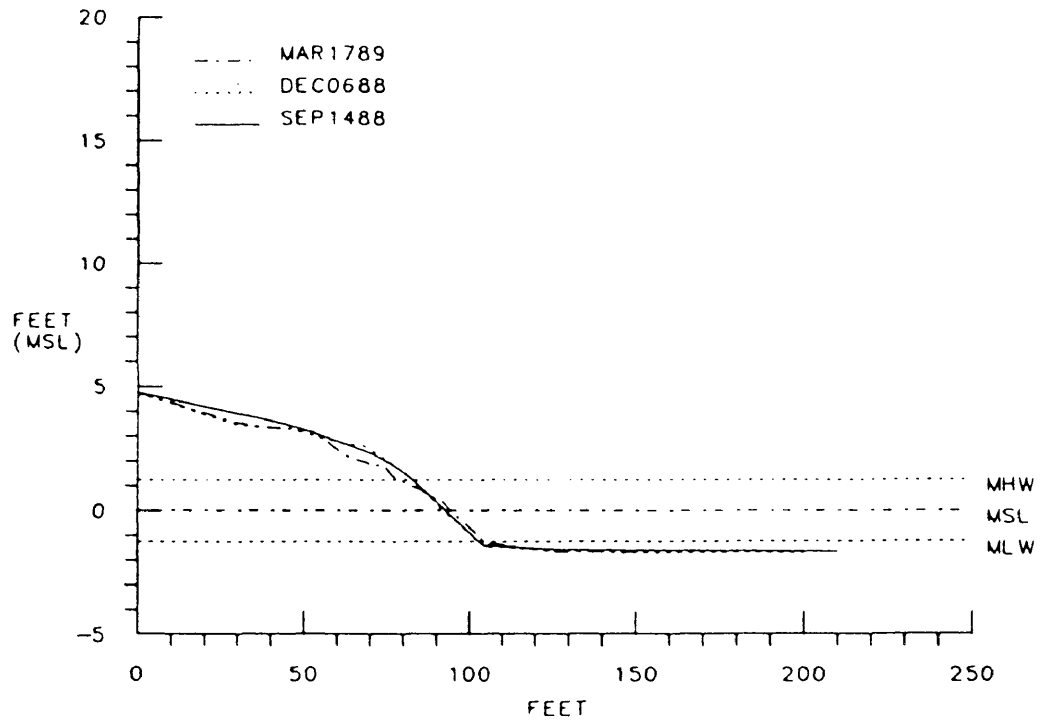


PARKWAY BREAKWATERS  
PROFILE NO. 18

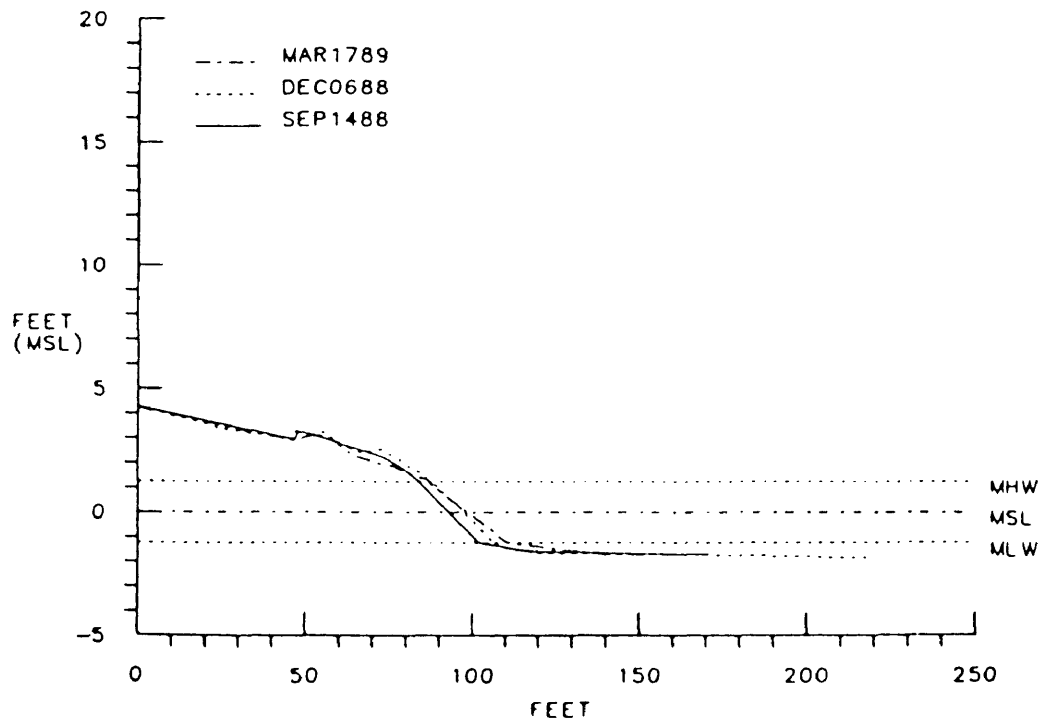




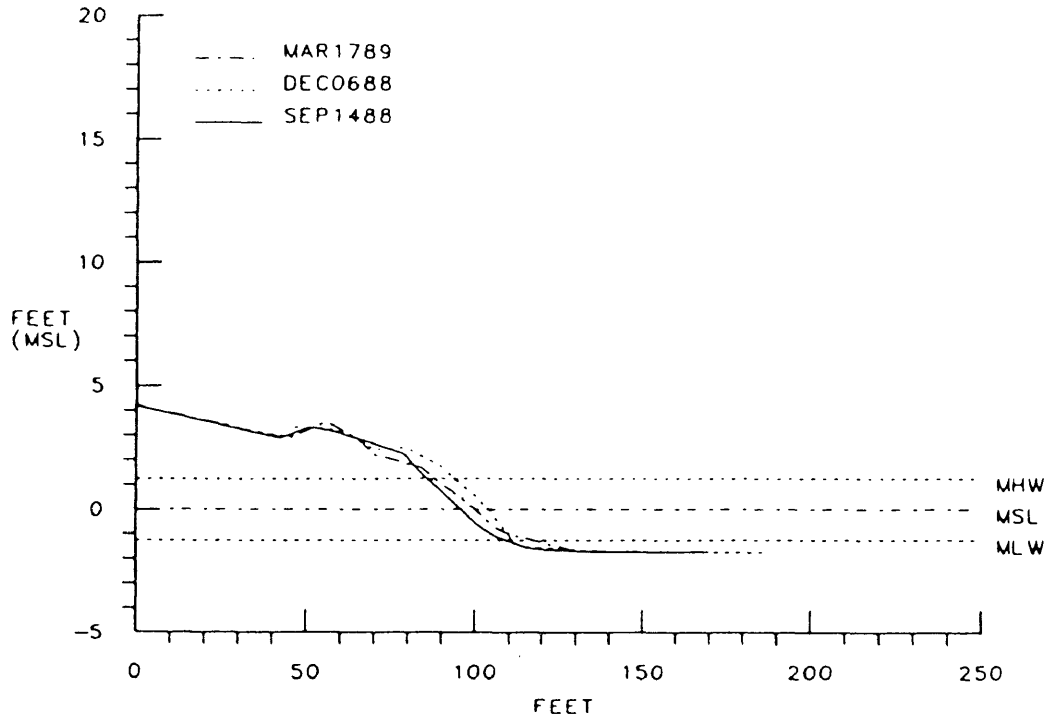
PARKWAY BREAKWATERS  
PROFILE NO 19



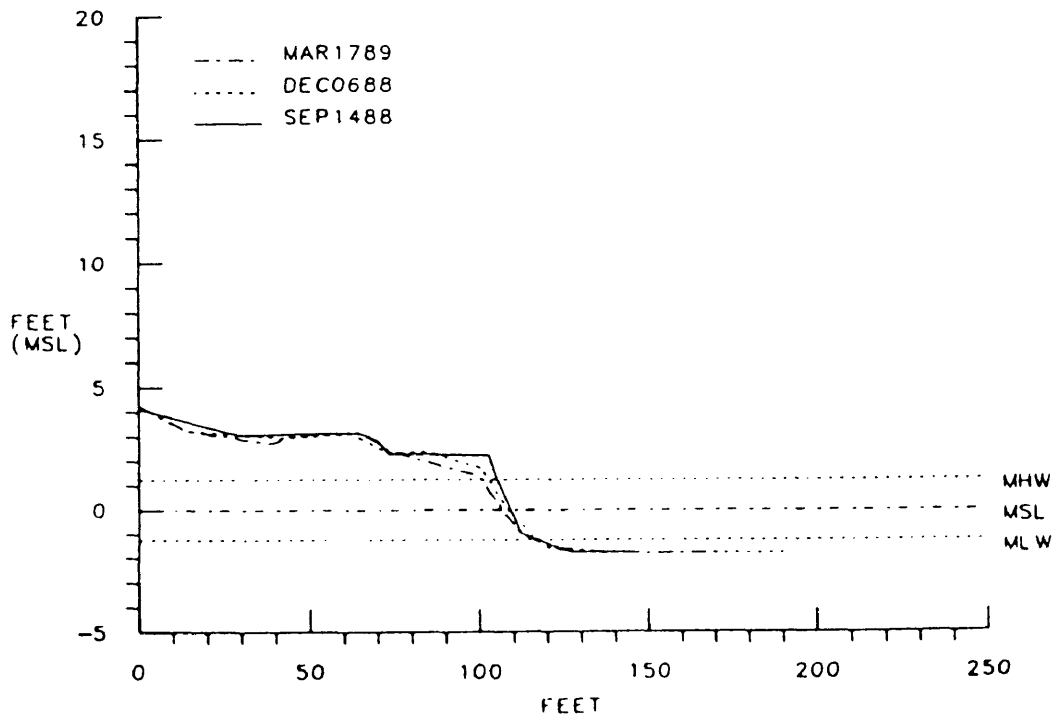
PARKWAY BREAKWATERS  
PROFILE NO 20



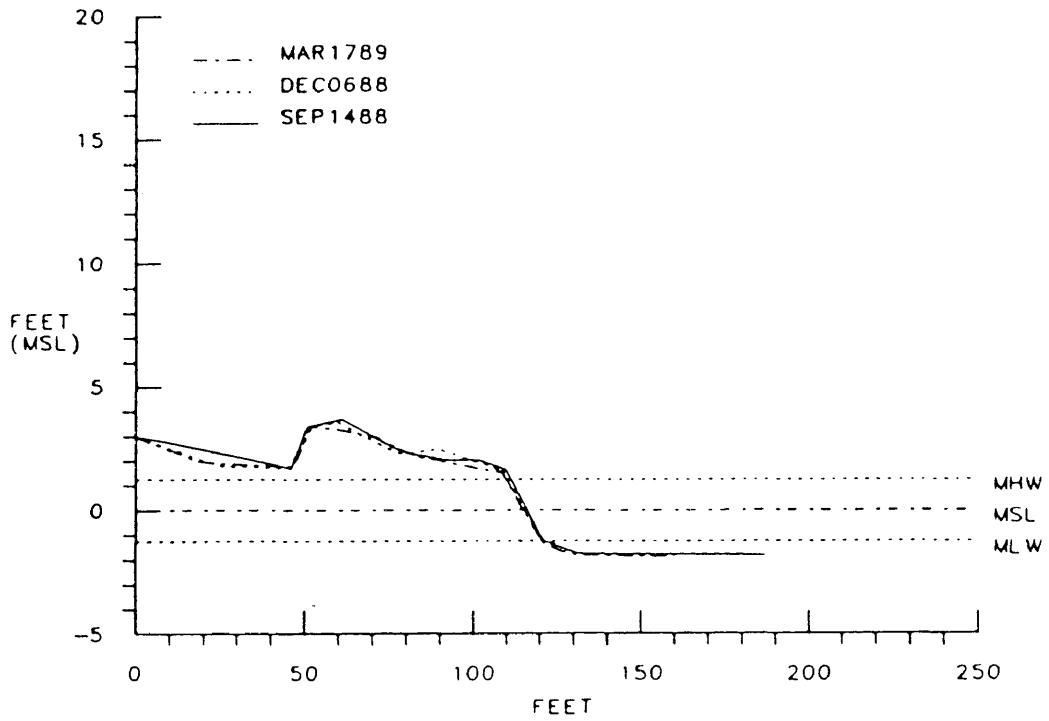
PARKWAY BREAKWATERS  
PROFILE NO 21



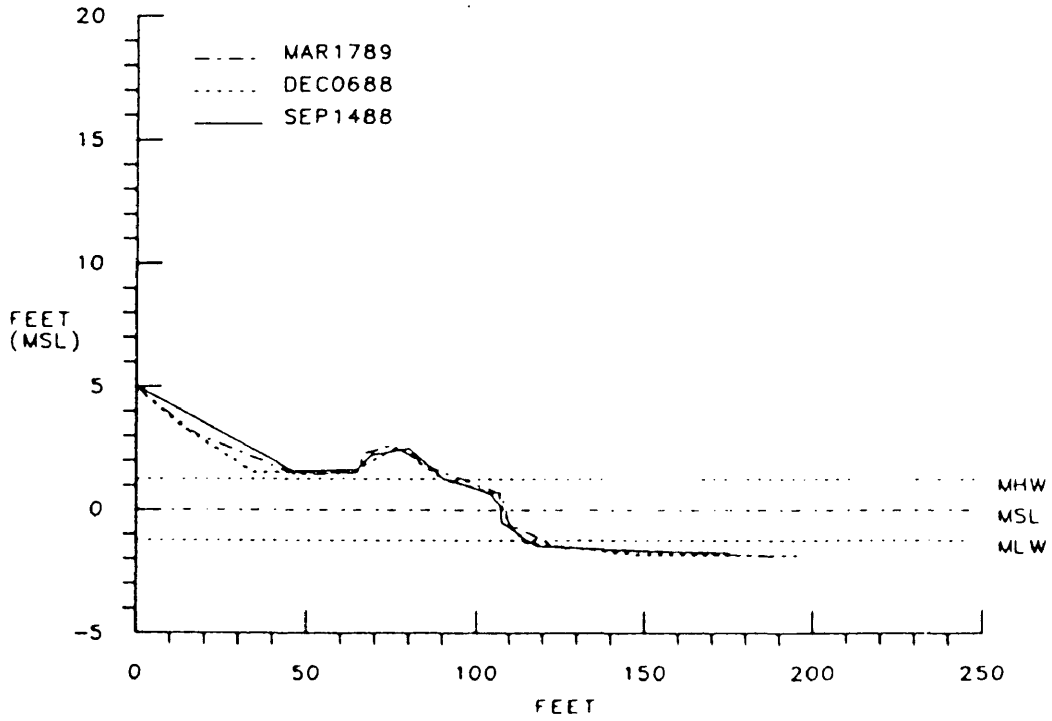
PARKWAY BREAKWATERS  
PROFILE NO 22



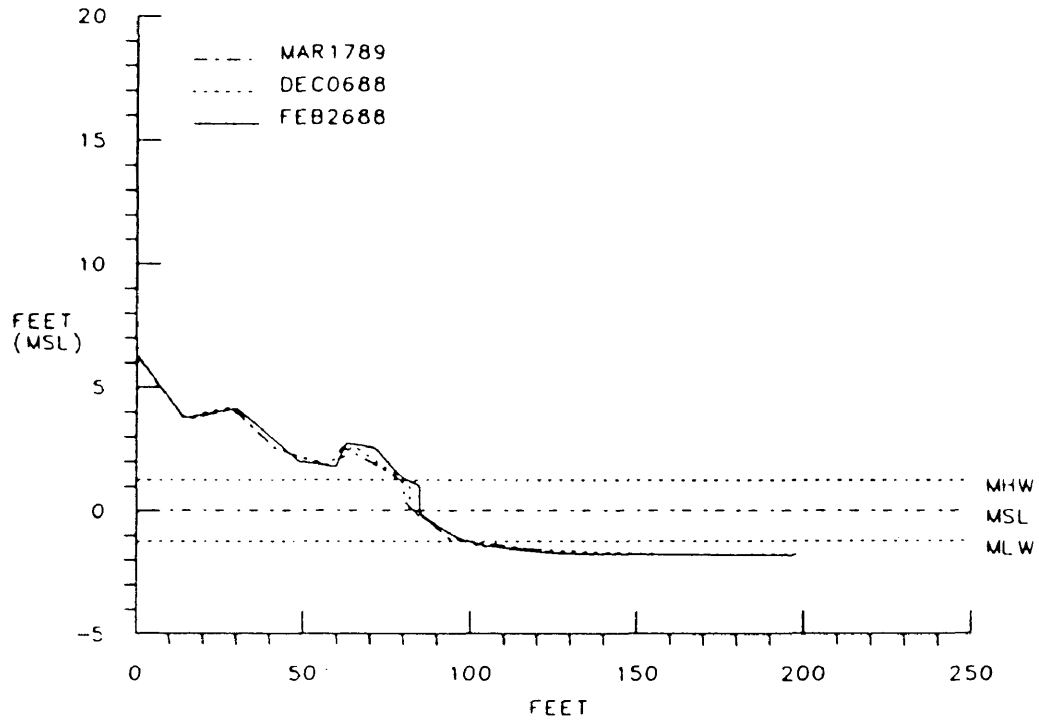
PARKWAY BREAKWATERS  
PROFILE NO 25



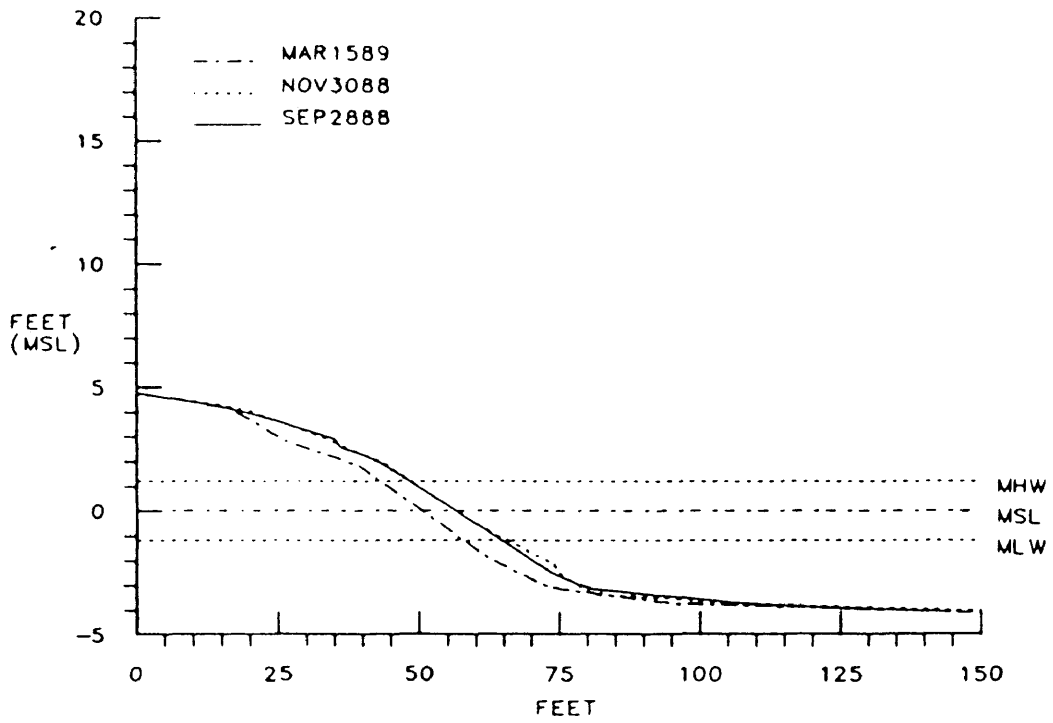
PARKWAY BREAKWATERS  
PROFILE NO 26



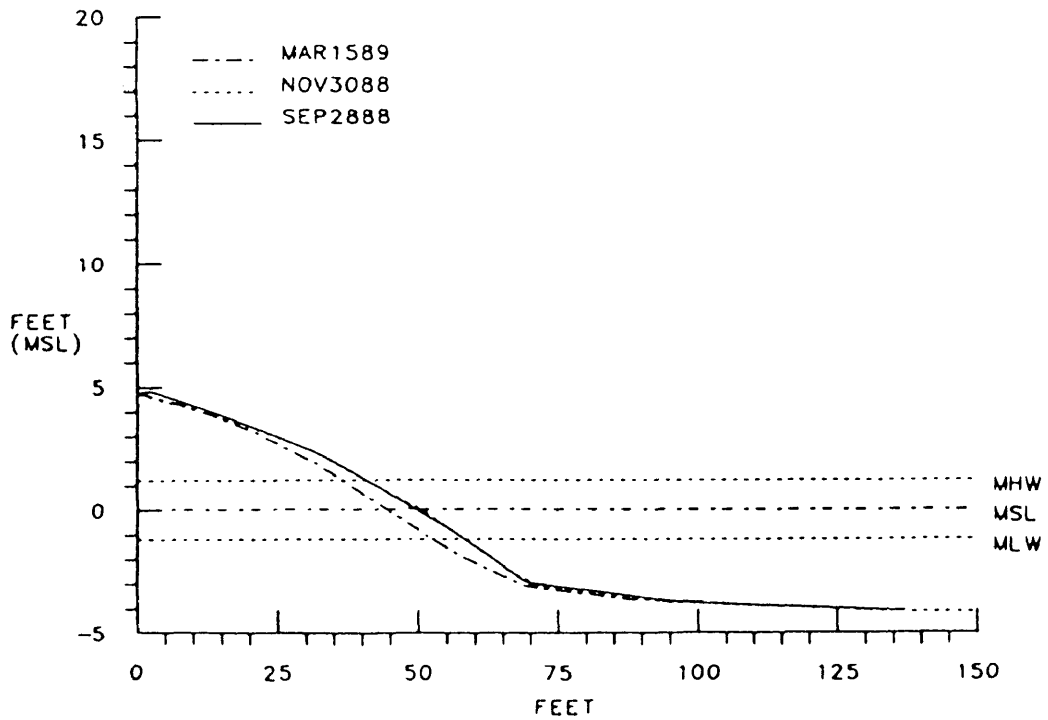
PARKWAY BREAKWATERS  
PROFILE NO 27



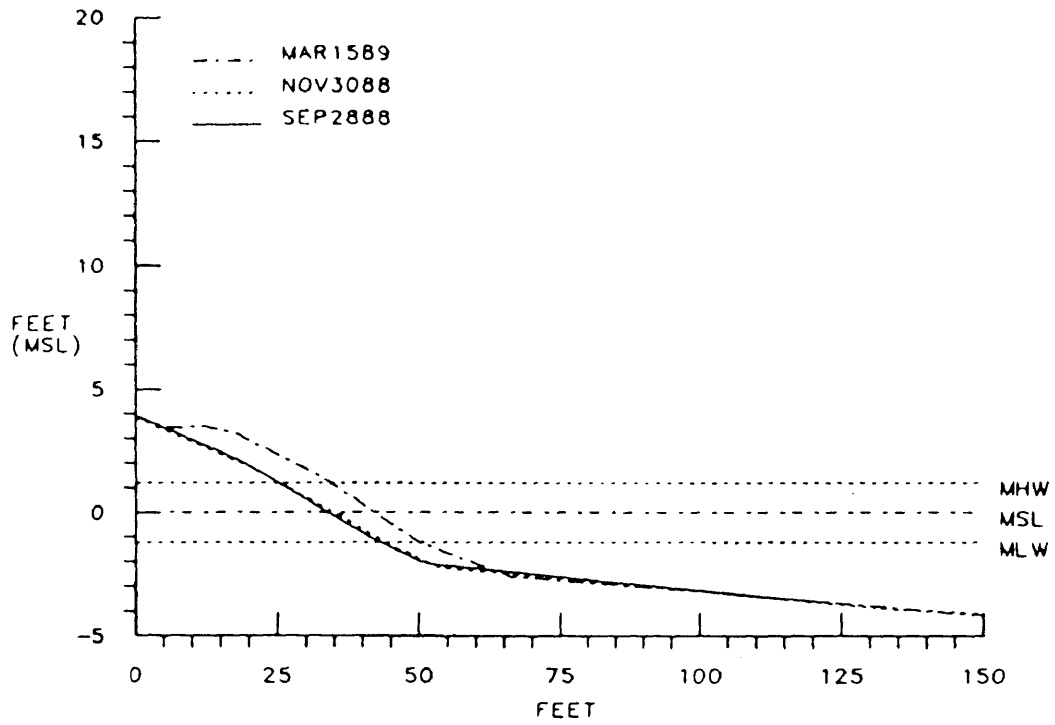
YORKTOWN BAY 1  
PROFILE NO 01



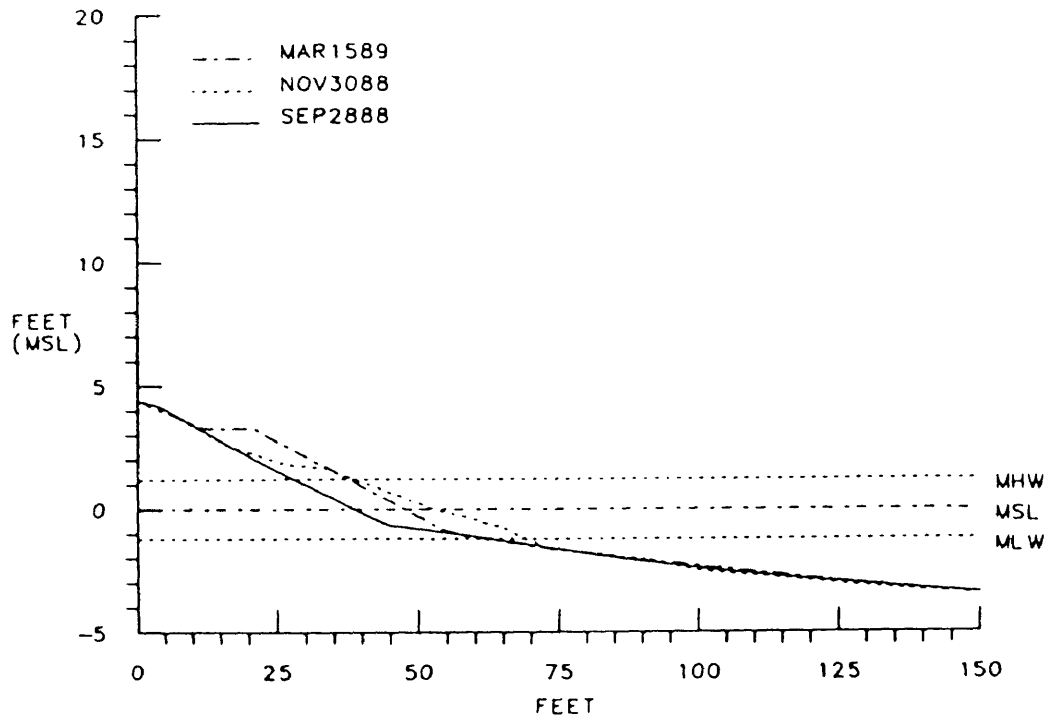
YORKTOWN BAY 1  
PROFILE NO 02



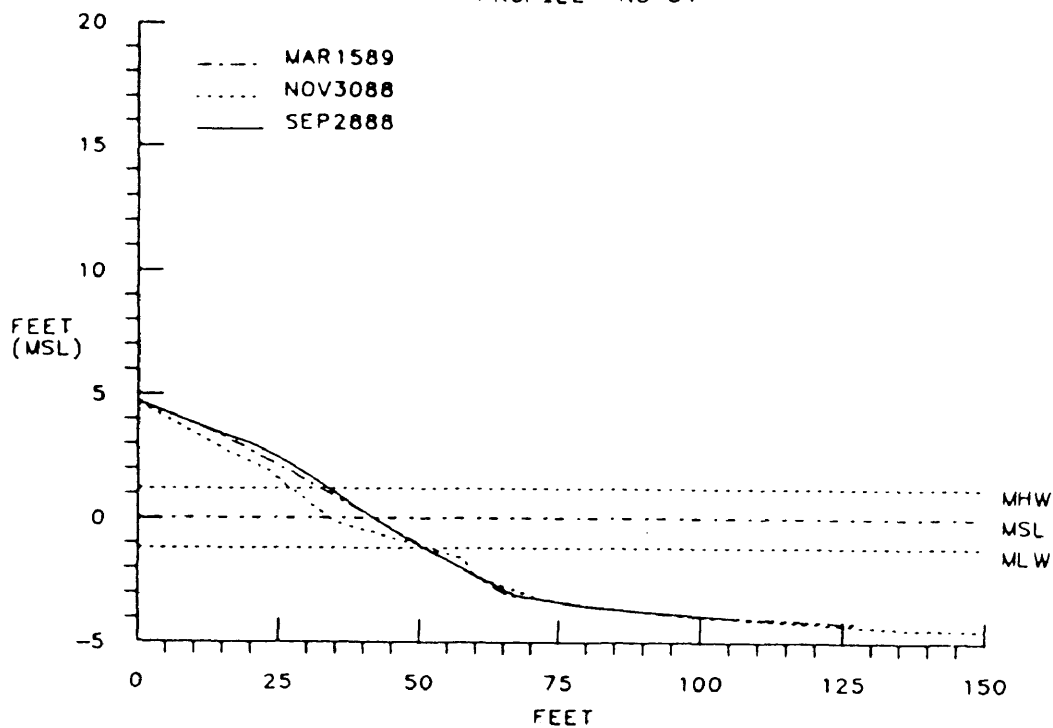
YORKTOWN BAY 1  
PROFILE NO 06



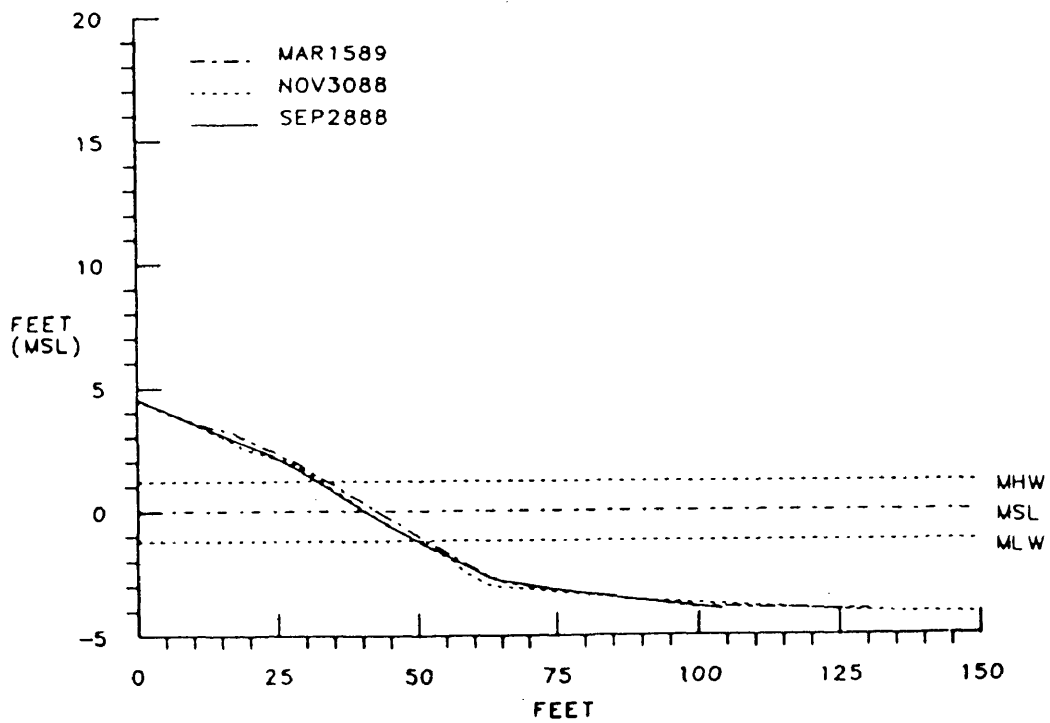
YORKTOWN BAY 1  
PROFILE NO 07



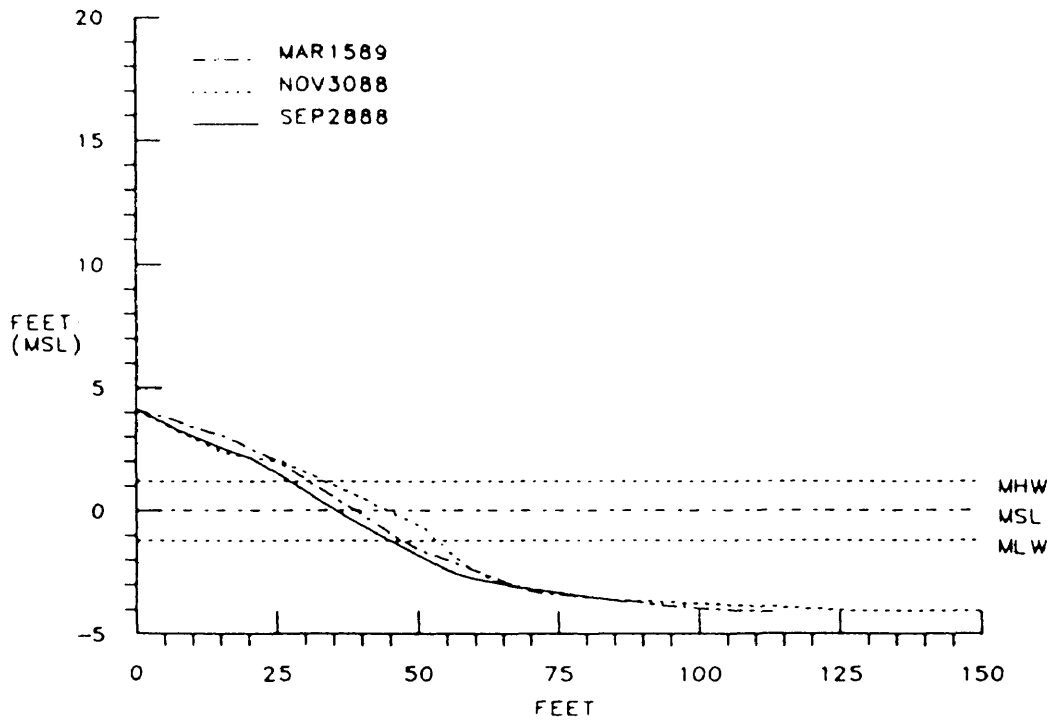
YORKTOWN BAY 2  
PROFILE NO 01



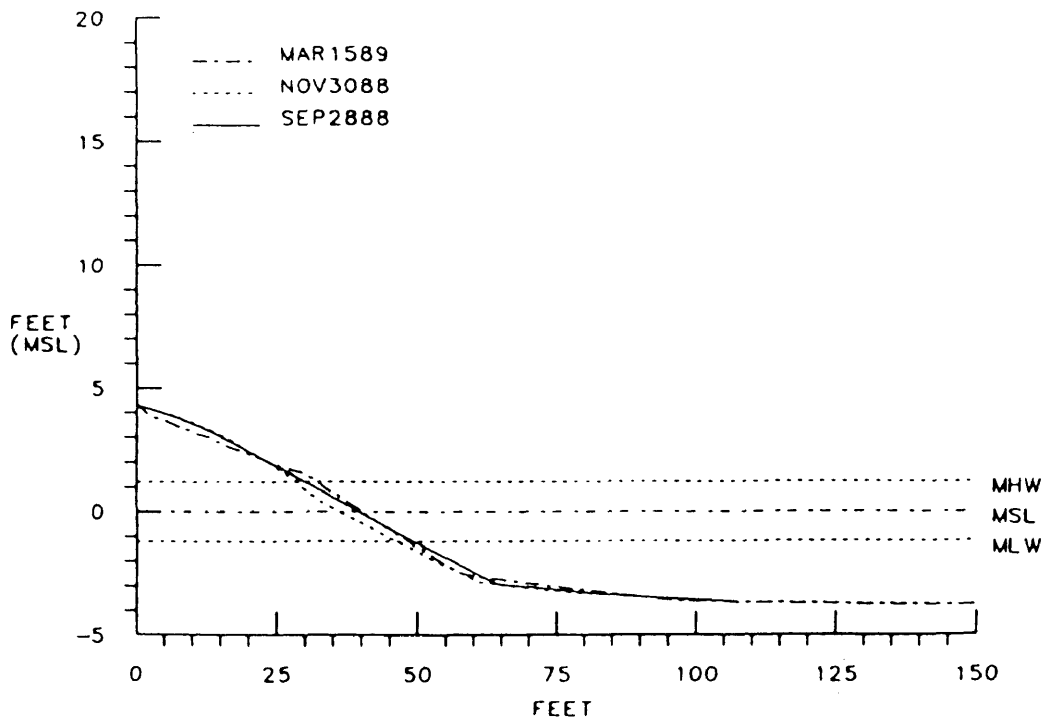
YORKTOWN BAY 2  
PROFILE NO 03



YORKTOWN BAY 2  
PROFILE NO 07

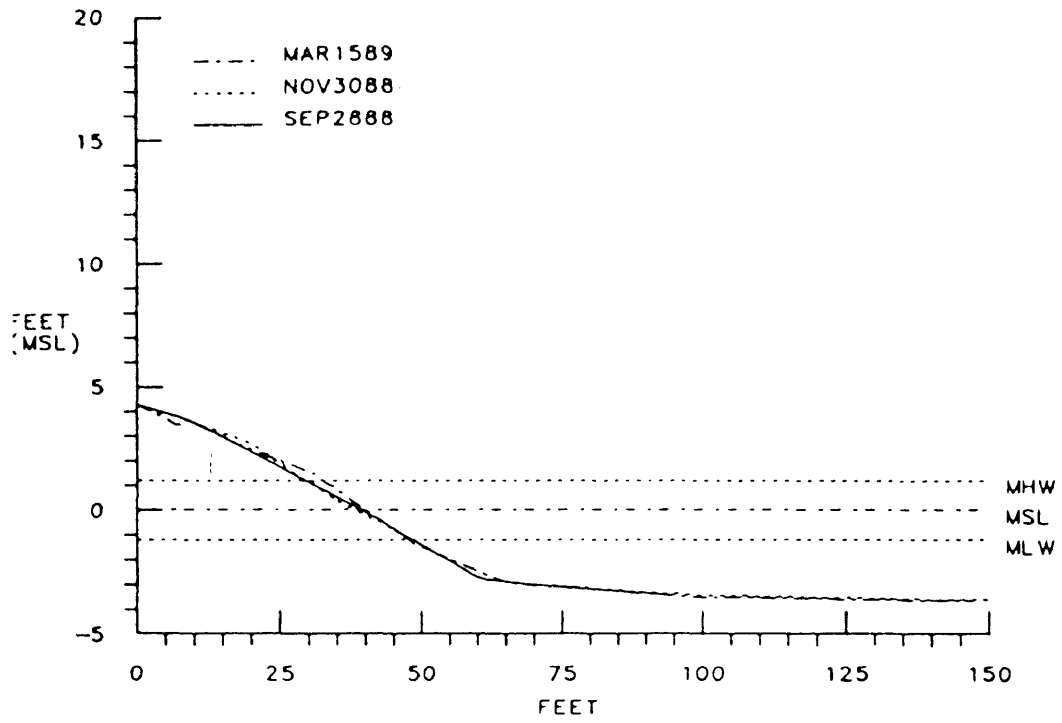


YORKTOWN BAY 3  
PROFILE NO 01

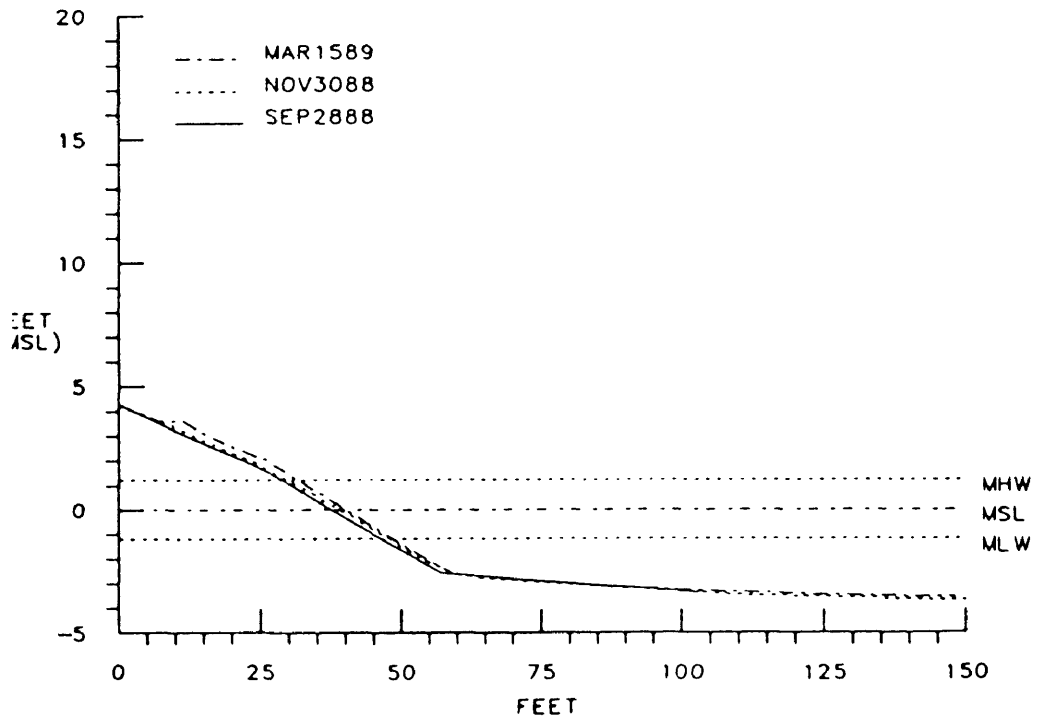




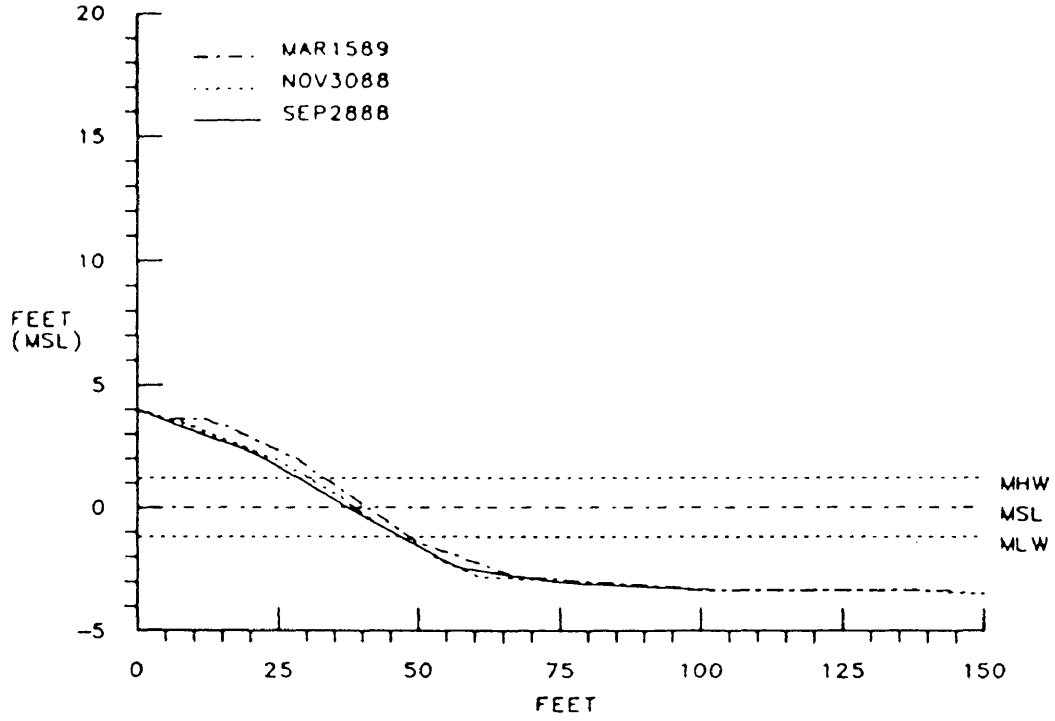
YORKTOWN BAY 3  
PROFILE NO 02



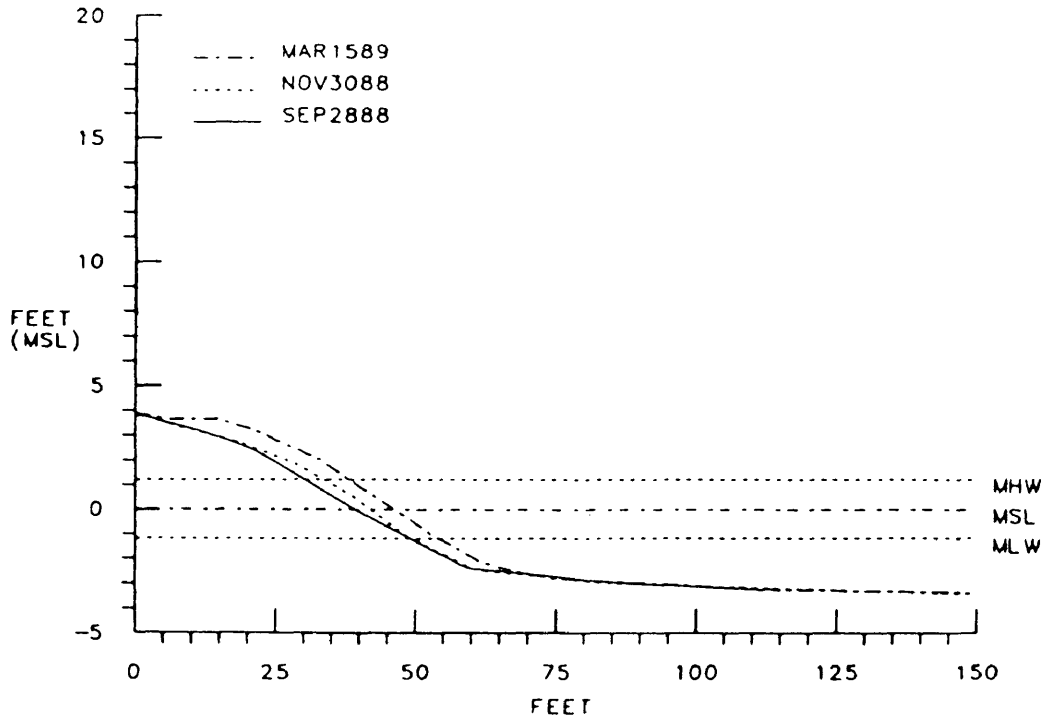
YORKTOWN BAY 3  
PROFILE NO. 03



YORKTOWN BAY 3  
PROFILE NO 04



YORKTOWN BAY 3  
PROFILE NO 05



### References cited

- Athearn, W.D., G.L. Anderson, R.J. Byrne, C.H. Hobs, III, and J.M. Zeigler, 1974, Shoreline situation report: SRAMSOE No. 54, Virginia Institute of Marine Science, College of William & Mary, 153p.
- Bagnold, R.A., 1940, Beach formation by waves; some model-experiments in a wave tank: J. Inst. Civ. Eng., V. 15, n. 1, pp. 27-52
- Biggs, R.B., 1962, Modern sediments of Chesapeake Bay (abs.) in Proceedings First National Coastal and Shallow Water Research Conference, p. 166.
- Biggs, R.B., 1970, Sources and distribution of suspended sediment in northern Chesapeake Bay, Mar. geol., Vol. 9, pp. 187-201
- Boon, J.D., C.S. Welch, et. al., 1978, A Storm Surge Model Study, Vol. I, Storm surge height-frequency analysis and model prediction for Chesapeake Bay. A report to the Federal Insurance Administration, Dept. Housing and Urban Development under Contract No. H-4508. Special report No. 189 in applied marine science and ocean engineering.
- Boon, J.D., Green, M.O., 1988, Caribbean beach-face slopes and beach equilibrium profiles, 21st Coastal Engineering Conference, CERC/ASCE.
- Bowen, A.J., 1980, Simple models of nearshore sedimentation; beach profiles and longshore bars, Geological Survey of Canada, paper 80-10, p. 1-11.
- Bretschneider, C.L., 1959, Hurricane surge predictions for Ches. Bay, Beach erosion board Misc. paper 3-59, U.S. Corps of Engineers, Washington D.C., 51p.
- Bruun, P., 1985, Analytical predictions of beach profile change in response to a sea level rise.
- Bruun, P., 1986, Sedimentary balances (land and sea) with special reference to the Icelandic south coast. River nourishment of shores - practical analogies on artificial nourishment. Coastal Engineering, 10, 193-210.
- Bruun, P., 1962, Sea level rise as a cause of shore erosion: Am. Soc. Civ. Eng. Proce., Jour. Waterways and Harbors Div., Vol. 88, pp. 117-130
- Byrne, R.J., G. L. Anderson, and A. Sallenger, 1972, Shore erosion in tide water, Virginia, pp. 216-229 in Ches. Research Consortium, Inc., Ann. Rpt., June 1971- May 1972, VIMS, 754 p.

- Byrne, R.J., G.L. Anderson, 1973, Shoreline erosion in Virginia's tidal rivers and Chesapeake Bay (abs): VA Jour.Sci., V.24,n.3,p.158.
- Byrne R.J. and G.L. Anderson, 1978, Shoreline Erosion in Tide water Virginia, VIMS, Special Report in Applied Marine Science and Ocean Engineering, No.111, 102 pp.
- Byrne, R.J., Thomas G.R. and Gammisch R.A., 1980, Tidal prism inlet area relations for small tidal inlets: Proceedings, 21st coastal engineering conference, American society of civil engineers, New York, pp.2517-2533.
- Carron, M.C., 1979, The Virginia Chesapeake Bay; Recent Sedimentation and paleodrainage: unpublished Ph.D. dissertation, School of Marine Science, College of William & Mary, 83p.
- Carter, R.W.G., 1987, Coastal Environments.
- Chappell, J. 1978, Surfzone resonance and coupled morphology, Proc. 16th Coastal Eng. Conf., ASCE, 1978.
- Davis, R., E. Seibel, W. Fox, 1973, Coastal erosion in eastern lake Michigan: Causes and effects: Proc. 16th conf. Great lakes Res., pp.404-412.
- Dean, R.G., 1973, Engineering Dynamics of the Coastal Zone, 1st Australian Conference on Coastal Engineering. p208-213.
- Dean, R. G., 1977, Equilibrium beach profiles: U.S. Atlantic and gulf coasts, Tech. Rep. No.12, University of Delaware, Newark.
- Dean, R. G., 1976, Beach erosion: causes, Processes and remedial measures, CRC Crit. Rev. Environ. Control, 6(3), 259.
- Dean, R. G., 1982, Models for beach profile response, Tech. Rep. No. 30, University of Delaware, Newark. Dubois, R. N., 1975, Support and refinement of the Bruun rule on beach erosion, J. Geol., 83, 651.
- Dean, R.G., 1983, Principles of Beach Nourishment, Chp.11 of CRC hand Book of Coastal Processes and Erosion, PP.217-231.
- Dean, R.G., 1990, Equilibrium beach profiles: characteristics and applications.
- Dubois, R. N., 1976, Nearshore evidence in support of the Bruun rule on shore erosion, J. Geol., 84, 485.
- Dubois, R. N., 1977, Predicting beach erosion as a function of rising sea level, J. Geol. 77, 470.
- DuBois, R.N., 1975, Support and refinement of the Bruun rule on beach erosion: Jour. Geol., V.83, pp651-657.

- Dillon, W.P., and Oldale, R.N., 1978, Late Quarternary Sea-level Curve: Reinterpretation based on glaciotectionic influence: geology, V.6, p56-60.
- Duncan, J.R., 1964, The effects of water table and tide cycle on swash-backwash sediment distribution and beach profile development: Marine Geology, V.2, n.1, pp.186-197.
- Eagleson, P.S., Glenne, B., 1963, Equilibrium Characteristics of sand beaches, Proceedings of ASCE. p35-57.
- Emery, K.O., 1961, A simple method of Measuring Beach Profiles: Limmology & Oceanography, V.6, pp.90-93.
- Emery, K.O., J.F. Foster, 1948, Water tables in marine beaches: Jour. Marine Research, V.7, n.3, pp.644-654
- Farrell, K.M., 1979, Late Pleistocene stratigraphy and morphology of the lower northern Neck, Virginia: Unpublished M.A. thesis, School, of Marine Science, College of William & Mary, 107p.
- Feuillet, J. -P., and Fleischer, P., 1980, Estuarine circulation: controlling factor of clay mineral distribution in James River estuary, Virginia: Journal of sedimentary Petrology, V.50, p.267-279.
- Frey, D.G., 1946, Oyster bars of the Potomac River: U.S. fish and widelife service, Special Scientific Report 32, 93p.
- Glaser, J.D., 1971, Geology and mineral resources of southern Maryland: Maryland Geological Survey, Report of Investigation 15, 85p.
- Guza, R.T. and Bowen, A.J., 1975, The resonant instabilities of long waves obliquely incident on a beach. J. Geophys. Res., 80: 4259-4534.
- Guza, R.T. and Inman, D.L., 1975, Edge waves and beach cusps. J. Geophys. Res., 80(21): 2997-3012.
- Hack J.T., 1957, Submerged river system of Chesapeake Bay: Geological Society of America Bulletin, V.68, P.817-830.
- Hallermeier, Robert J. 1983, Sand transport limits in coastal structure designs, Coastal Structure'83, p704-716.
- Hardaway, C.S., Gunn, J.R., 1989, Elm's beach breakwater project - St. Mary's County, Maryland.
- Harrison, W., Malloy R.J., 1965, Possible Late Pleistocene uplift Chesapeake Bay Entrance. Jour. Geology 73: 201-229

- Hallermeier, R.J., 1977, Calculating a yearly limit depth to the active beach profile, U.S. Army coastal Eng. Res. Cent. Tech. Pap., No.77-9.
- Hobbs, C.H. III., Byrne, R.J., Kerns, W.R., Baker, N.J., 1981, Shore line erosion: A problem in environmental management. Coastal zone management journal, Vol.9, No.1, pp.89-105.
- Hsu, J.R.C., Silvester, R. and Xia, Y.M., 1989, generalities on static equilibrium bays. Coastal Engineering ,12(1989) 353-369.
- Johnson, G.H. 1972. Geology of Yorktown, Poquoson West, and Poquoson East Quadrangles, Virginia: Virginia Division of Mineral Resources Report of investigations 30, 57p.
- Johnson, G.H., 1976, Geology of the Mulberry Island, Newport News north, and Hampton quadrangles, Virginia: Virginia Div. Min. Res. Report No. 41, 72p.
- Knebel, H.J., 1981, Sedimentary framework of the Potomac River Estuary, Maryland. G.S.A.Bull., Pt.1, V.92, p578-589.
- Kim, Chang.S., Wright,L.D., 1987, Longshore bars and mass transport induced by long waves. Coastal Hydrodynamics, Proceedings of a Conference sponsored by the Waterway, Port, Coastal and Ocean Division of the American Society of civil Engineers.
- Komar, P.D., 1976, Beach processes and sedimentation.
- Komar,P.D., 1983, Beach processes and erosion - an introduction: Chp.1 of CRC Hand Book of Coastal Processes and Erosion, pp. 1-20.
- Komar P.D., 1983, Computer Models of Shoreline changes, Chp.10 of CRC Hand Book of Coastal Processes and Erosion, pp.205-217.
- Komar, P.D., 1983, Coastal Erosion in Response to the construction of jetties and Breakwaters, Chp.9 of CRC Hand Book of Coastal processes and Erosion, pp.191-204.
- Kraft, J.C., 1971, Sedimentary facies patterns and geological history of a Holocene marine transgression: Geo. Soc. Ameri. Bull., V.82, p.2131-2158.
- Lippson, A.J.,Haire, M.S.,Holland, A.F., Jacobs, F., Jensen, J., Moran-Johnson, R., 1980, Environmental Atlas of the Potomac estuary: Washington D.C., Williams and Heintz Map Corporation, 279p.
- Meisburger, E.P., 1972, Geomorphology and sediments of the Chesapeake Bay entrance: U.S. Army Corps of Engineers, Coastal engineering research center tech. memo. 38, 61p.

- Mitchell, M.L. 1984, Geologic responses to late Cenozoic marine transgressions in the Pototank river estuary, Virginia: M.A. thesis, School of marine science, College of William & Mary.
- Milici, R.C., Spiker, C.T., et al, 1963, Geologic Map of Virginia, Division of mineral resources, scale 1:50,000, 1 sheet.
- Peebles, P.C., 1984, Late Cenozoic landforms, stratigraphy and history of sea level oscillations of southeastern Virginia and northeastern North Carolina: Ph.D. Dissertation, School of Marine Science, College of William & Mary, 127p.
- Rosen, P.S., 1978, A regional test of the Bruun rule of shoreline erosion, Mar. Geol., 26, M7.
- Rosen, P.S., 1978, Predicting Beach erosion as a function of rising water level: Discussion, J. Geol., 86, 763
- Rosen, P.S., 1976, The morphology and processes of the Virginia Chesapeake Bay Shoreline: Ph.D. Dissertation, School of Marine Science, College of William & Mary, 313p.
- Ryan, J.D., 1953, The sediments of Chesapeake Bay: Maryland Department of geology, mines, and water resources bulletin 12, 120p.
- Schubel, J.R., 1968, Turbidity Maximum of the northern Chesapeake Bay: Science, V.161, p.1013-1015.
- Schubel, J.R., and Hirschberg, D.J., 1977, pb-210 determined sedimentation rate, and accumulation of metals in sediments at a station in Chesapeake Bay: Chesapeake Science, V.18, p.379-382.
- Schubel, J.R., 1972, A Pleistocene River Chennel connects the lower reaches of the Chester, Miles, and Choptank Estuaries: Special report 24, Chesapeake Bay Institute, The Johns Hopkins University, 12p.
- Schwartz, M.L., 1965, Laboratory study of sea-level rise as a cause of shore erosion, J. Geol., 73, 528.
- Schwartz, M.L., 1967, The Bruun theory of sea-level rise as a cause of shore erosion, J. Geol., 75, 76.
- Shattuck, G.B., 1906, The pliocene and Pleistocene deposits of Maryland: Maryland Geological Survey, Pliocene and pleistocene, 291p.
- Silberhorn, G.M., 1975, Northumberland County tidal marsh inventory: Special report No.58 in Applied Marine Science and Ocean Engineering, Virginia Institute of Marine Science, Gloucester Point, VA23062, 96p.

- Singewald, J.T., and Slauphter, T.H., 1949, Shore erosion in tide water Maryland: Maryland Dept. of geology, mines and water resources bulletin 6.141p.
- Stive, M.J.F. and H.G. Wind, 1986, Cross-Shore mean flow in the surf zone, Coastal Engineering, Vol.10, No.4, p.325-340.
- Swain, A., 1989, Beach profile development. Applications in Coastal Modeling.
- Swart, D.H., 1974, A schematization of onshore-offshore transport, Proc. 14th Int. Conf. Coastal Eng., ASCE:884-900.
- Sunamura, Tsuguo, 1989, Sandy beach geomorphology Elucidated by Laboratory Modeling. Applications in Coastal Modeling, p215-231.
- Sunamura, Tsuguo, 1984, Quantitative predictions of beach face slopes. Geological Society of American Bulletin, V.95, p242-245.
- Svendsen, I.A., 1974, Mass flow and undertow in the surf zone, Coastal Engineering, Vol.8, P.347-365.
- Teifke, R.H., 1973, Stratigraphic Units of lower Cretaceous through Miocene and paleogeology of early Cretaceous through Miocene time. Va. Dev. Min. Res. Bulletin 83(parts 1&2), p.1-101.
- U.S. Water Resources Council, 1966, Instruments and reports for fluvial sediment investigations, in a study of methods used in measurement and analysis of sediment loads in streams: Minneapolis Federal Inter-agency Sedimentation project, St. Anthony Falls Hydraulic Laboratory, 67p.
- Wark, J.W., and Keller, F.J., 1963, Preliminary Study of sediment sources and transport in the Potomac river basin, 28p.
- Ward, L.W., Blackwelder B.W., 1980, Stratigraphic revision of upper Miocene and lower Pliocene beds of the Chesapeake group - middle Atlantic Coastal plain. U.S.G.S. Buul. 1482- D, 61p.
- Wiegel, Robert L., 1964, Oceanographical Engineering.
- Wright, L.D. J. Chappl, B.G. Thom, M.P. Bradshaw and P Cowell, 1979, Morphodynamics of reflective and dissipative beach and inshore systems: Southeastern Australia, Marine Geology, 32, p.105-140.
- Wright, L.D., 1980, Beach cut in relation to surf zone morphodynamics, Ch.61, proc. 17th Int. Coastal Eng. Conf., ASCE, 1980.
- Wright, L.D., P. Nielsen, A.D.Short and M.O.Green, 1982, Morphodynamics of a macrotidal beach: Marine Geology, 50(1982)97-128.



- Wright, L.D., Nielsen, P., Short, A.D. and Green M.O., 1982, Nearshore and surf zone morphodynamics of a storm wave environment: Eastern Bass Strait, Australia. Coastal Studies Unit Technical Report, No.82/3.
- Wright, L.D. and Short, A.D., 1983, Morphodynamics of beaches and surf zones in Australia, Chapter 2 of the CRC handbook of Coastal Processes and erosion, p.35-64.
- Wright, L.D., May, S.K. et al., 1984, beach and surf zone Equilibria and response time, proc. 19th Int. Conf. Coastal Eng., ASCE.
- Wright, L.D. and A.D. Short, 1984, Morphodynamic variability of surf zones and beaches: a synthesis: Marine Geology, 56(1984)93-118.
- Wright, L.D., A.D. Short and M.O. Green, 1985, Short-term changes in the morphodynamic states of beaches and surf zones: an empirical predictive model: Marine Geology, 62(1985)339-364.
- Wright, L.D., Nielsen, P., Shi, N.C. and List, J.H., 1986, morphodynamics of a bar-trough surf zone, Marine Geology, 70(1986)251-285.
- Wright, L.D., 1987, Shelf surf zone coupling: Diabathic shoreface transport, Coastal Sediments'87, p24-40.
- Zeigler, J.M., Tuttle, S.D. et al., 1964, Residence time of sand composing the beaches and bars of outer Cape Herry. Proceedings of 9th Conference on Coastal Engineering.
- Zellmer, L.R., 1979, Development and application of a pleistocene sea level curve to the coastal plain of southeastern Virginia: M.A. thesis, School of marine science, College of William & Mary, 85p.

## VITA

Jian Hua Li

Born in Shandong, China, February, 1955. Graduated from the Department of Marine Geology, Shandong College of Oceanography (now Ocean University of Qingdao) in 1979, and joined the faculty of the same college soon after his graduation. He engaged in both teaching and researching in Micropaleontology and marine geology. He was the first author of a couple of papers on the studies of microfossils and surface sediment types of East China Sea, and the second author of the Report of the Studies of Mineral Resources and Sediment of the East China Sea and Yellow Sea which was a central government funded project from 1982 to 1984. He has been focused on the studies of beach forms around coastal structures since the fall of 1986 at VIMS.